UNIVERSITY OF CAPE TOWN
IYUNIVESITHI YASEKAPA • UNIVERSITEIT VAN KAAPSTAD

Microalgae flocculation and sedimentation by physico-chemical property exploitation

Reay Gary Dicks

Submitted to the University of Cape Town in partial fulfilment of the requirements for the degree of

MSc, Master of Science Engineering

September 2011

Supervisor: Professor Susan T.L. Harrison

PLAGIARISM DECLARATION

1. I know that plagiarism is wrong. Plagiarism is to use another's work and to pretend that it is one's own.
2. I have used the Harvard system for citation and referencing. Each significant contribution to, and quotation in, this report from the work, or works, of other people has been attributed, and has been cited and referenced.
3. This report is my own work.
4. I have not allowed, and will not allow, anyone to copy my work with the intention of passing it off as his or her own work.

Synopsis

In addition to the potential role of microalgae in high-value products, market trends and fuel demands have initiated renewed interest in microalgae for bioenergy. The harvesting and recovery of microalgae are a major bottleneck, contributing 20 to 40% to the total cost of production, thereby limiting its potential for commodity products. This challenge can be attributed to small cell size, dilute suspensions, low specific gravity, variable surface properties and sensitivities to the environment and growth conditions. An effective, low energy dewatering technique is therefore required to realise value from algal biomass whilst allowing recycle of spent media and water. Harvesting of biomass requires one or more solid-liquid separation techniques, selected to exploit the natural physico-chemical properties of microalgal cells. The purpose of this research was to characterise the physical properties of microalgae, as a function of growth and suspension conditions, to enable exploitation of these characteristics for improved separation whilst allowing for water recycle. Two freshwater green microalgae were studied, namely *Scenedesmus sp.* and *Chlorella vulgaris.* These were cultured in 3.2 L airlift photobioreactors. Particle size, pH, conductivity, zeta potential, hydrophobicity, carbon accumulation and growth rate were recorded for a 13 day period in laboratory scale bioreactors. Each parameter and its inter-relation with other parameters were then investigated to determine the effect on sedimentation.

Scenedesmus sp. and *Chlorella vulgaris* reached a maximum biomass concentration of 3.22 ± 0.01 and 2.26 ± 0.01 $g.L^{-1}$ respectively in the airlift photobioreactors when cultured on 2900 ppm CO_2 and 750 $mg.L^{-1}$ $NaNO_3$. At these concentrations, cells entered stationary phase due to nutrient depletion, light limitations and autoflocculation on day 11 and 8 of growth respectively. Microalgae reactors were sterilised prior to inoculation and operated hygienically; however were found to contain a range of different co-cultured bacteria. The *Scenedesmus sp*. and *Chlorella vulgaris* cultures were contaminated predominantly by *Nocardioides aromaticivorans* and *Microbacterium chocolatum* respectively. The *Chlorella* grown *Microbacterium chocolatum* increased to a maximum of 5.45 x 10^{10} $cells.L^{-1}$ and 2.76 x 10^{-2} $g.L^{-1}$ on day 13 whilst the *Scenedesmus* grown *Nocardioides aromaticivorans* reached a maximum on day 5 at 2.67 x 10^{9} $cells.L^{-1}$ and 1.28 x 10^{-1} $g.L^{-1}$ in the co-cultured airlift photobioreactors. Zeta potential, pH, conductivity, extracellular organic material (EOM) and average particle size were found to vary significantly during growth; however the hydrophobicity index and sedimentation rates remained constant irrespective of harvesting time during the growth phase but changed on an increase in autoflocculation during the stationary phase. This was attributed to increased EOM, pH and a minimum zeta potential in the presence of ion-chelated cells. *Chlorella vulgaris* and *Scenedesmus sp*. remained electronegative throughout the growth curve and showed isoelectric points at pH 1.03 ± 0.15 and 4.34 ± 0.17 respectively. At this point colloid stability is at a minimum.

Settling rates were found to be dependent on conductivity and pH due to increased colloidal instability. Flocculation was chosen as a method to increase particle size and hydrophobicity to increase sedimentation rates and efficiencies. This technique is energy efficient with minimal chemical requirements. The bioflocculation of microalgae is a novel harvesting technique and exploits cell surface charge to induce attraction between cells. *Chlorella vulgaris* and *Scenedesmus sp*. were bioflocculated with *Bacillus sp., E. coli* BL2 (DE3),

Microbacterium chocolatum RW56 and *Nocardioides aromaticivorans* SB10005. Autoflocculation was also investigated by adjustment of pH and conductivity only. These techniques were compared to traditional chemical flocculation techniques and mechanistic explanations were investigated. Zeta potential and hydrophobicity were investigated as a function of pH and conductivity. Maximum hydrophobicity indices and flocculation efficiencies were observed near the isoelectric points, at pH regions where cells were exceedingly oppositely charged or where cells were electronegative and present in a high ionic strength solution. This colloid instability led to inter cell-cell, cell-salt-cell and cell-wall adhesions due to patching or bridging mechanisms based on van der Waals attractions.

Scenedesmus sp. bioflocculated with *Chlorella vulgaris* produced the most promising bioflocculation results with 81% cell recovery in 20 minutes at pH 2.55. The pH, conductivity, zeta potential and hydrophobicity index were all found to have a large impact on sedimentation efficiencies with recovery efficiencies of up to 100% in 20 minutes via autoflocculation.

This research suggests that autoflocculation near the PZC occurs via charge neutralisation and cell patching whilst autoflocculation at extreme alkaline conditions occurs via bridging adsorption of saturated cations between microalgal cells. Bioflocculation occurs initially via particle attraction through oppositely charged ionic attraction and then by adsorption via bridging of cells (algae-bacteria-algae) at pH values where microalgae and bacteria have opposite surface charges. Increased suspension starting conductivity and pH were found to inhibit growth thus requiring neutralisation of the effluent water to be recycled if a flocculation technique at an adjusted pH were to be considered. Ionic strength above 3 $S.cm^{-1}$ was found to be the upper tolerance limit of both species with respect to growth with *Scenedesmus sp.* and *Chlorella vulgaris* having a greater tolerance towards alkaline and acidic conditions respectively. The microalgal species were found to acclimatise and neutralise the pH to a certain extent and this, combined with a purge and freshwater blending could allow for recycle of the effluent water for microalgal cultivation.

Viscosity profiles were investigated as a function of algal concentration to determine the maximum concentration at which suspensions may be transported. *Scenedesmus sp.* was found to behave as a dilatant (shear thickening) fluid when concentrated above 205 $g.L^{-1}$ dry weight ($\tau = 0.0008\gamma^{1.52}$ for 218 $g.L^{-1}$) whilst *Chlorella vulgaris* remained Newtonian up to 275 $g.L^{-1}$ dry weight ($\tau = 0.0035\gamma$ for 275 $g.L^{-1}$). Flocculation increased the apparent viscosity for both species of microalgae and bacteria. For industrial purposes the rheology of the two strains investigated poses no design problems as only microalgal concentrations below 200 $g.L^{-1}$ are required for further downstream processing, where Newtonian rheology is present.

This work defines the significance of understanding the physical properties of microalgae to improve and develop new dewatering techniques. Flocculation followed by sedimentation appears a viable method in terms of energy, chemical and time requirements as well as recovery efficiency for both *Scenedesmus sp*. and *Chlorella vulgaris*.

ACKNOWLEDGEMENTS

First and foremost I would like to thank my father Raymond Dicks for his support in every aspect of my career and personal life making this masters dissertation possible for me.

Thank you to The Department of Science and Technology and the National Research Foundation through the SARChI Research Chair in Bioprocess Engineering and the University of Cape Town Post Graduate Funding Office for my research project finances, without which I would not have been able to complete my masters in engineering.

I would like to thank Melinda Griffiths for her explanations on many topics related to my project and for her expert demonstrations and teachings of equipment in the laboratory. Special thank you to Dr. Caryn Fenner for her isolation and donation of *Bacillus sp.* and Clive Garcin for his time and effort contributions to my project.

Thank you to Nathan van Wyk for his contributions and help in my bacteria sequencing and general conversations around my project. Special thanks to Frances Pocock for all her efforts on a daily basis in the laboratory making my life a bit easier.

I thank all the CeBER staff and friends in the department for making my masters an enjoyable experience.

Thank you to my sole supervisor, Professor Sue Harrison for her guidance in all of my work and for her support and tolerance towards trying novel technique approaches and freedom to define the direction of my study.

Table of Contents

LIST OF FIGURES

LIST OF TABLES

ABBREVIATIONS

Aq.	Aqueous
Ca.	Circa
CF	Concentration factor
CHN	Carbon, hydrogen, nitrogen
Cv	*Chlorella vulgaris*
DOC	Dissolved organic carbon
DLVO	Derjaguin and Landau, Verwey and Overbeek theory
EBF	Extracellular biopolymeric flocculants
E. coli	*Escherichia coli*
EOM	Extracellular organic matter
EPS	Extracellular polymeric substances
M	Molar concentration
MBFs	Microbial flocculants
NOM	Non-organic material
OD	Optical density
PBS	Phosphate buffered saline
PE	Photosynthetic efficiency
PZC	Point of zero charge
Rpm	Revolutions per minute
RE	Recovery efficiency
Sc	*Scenedesmus sp.*
SOP	Standard operating procedures
Sp.	One unknown species
Spp.	Many unknown species
STP	Standard temperature and pressure
TIC	Total inorganic carbon
TOC	Total organic carbon
TSS	Total suspended solids
Viz.	That is to say
VRF	Volume reduction factor

NOMENCLATURE

Notation	Description	Units
C	Concentration	$mg.dm^{-3}$
d	Cell diameter	µm
D	Dielectric constant	$C.V^{-1}cm^{-1}$
E_m	Electrophoretic mobility	$cm^2.V^{-1}s^{-1}$
g	Gravimetric constant	$J.mol^{-1}K^{-1}$
h	Depth/height	m
k	Viscosity constant	mPa.s
K''	Shape factor	
m	Mass flowrate	$g.s^{-1}$
M	Molar mass	$g.mol^{-1}$
OD	Optical density (adsorbance)	AU
Q	Volumetric flowrate	m^3h^{-1}
R	Internal radius of the reactor	mm
u_c	Settling velocity	$m.s^{-1}$
V'	Volume of liquid	m^3
X	Biomass concentration	$g.L^{-1}$
Z_p	Zeta potential	mV
η	Viscosity	$g.cm^{-1}s^{-1}$
γ	Shear rate	s^{-1}
µ	Dynamic viscosity	Pa.s
$\emptyset$	Volume fraction	
ρ	Density	$kg.m^{-3}$
τ	Shear stress	Pa

Main data markers	Description
	Bacillus sp.
	E. coli BL2 (DE3)
	Microbacterium chocolatum or *Chlorella vulgaris* grown on air
	Nocardioides aromaticivorans or *Scenedesmus sp.* on air
	Chlorella vulgaris on 2900 ppm CO_2
	Scenedesmus sp. on 2900 ppm CO_2

GLOSSARY

Adsorption	Adhesion of atoms, ions, biomolecules or molecules of gas, liquid, or dissolved solids to a surface
Aggregation	Agglomeration of colloids, known as coagulation or flocculation via van der Waals forces, electrostatic forces and forces due to macromolecules(Coulson and Richardson, 2002)
Amphoretic	Molecule or ion that can react as an acid as well as a base
Autotrophic	Organism capable of synthesizing its own food from inorganic substances
Chelation	Formation of two or more separate bindings between a cell and a single central atom
Coagulation	Chemical destabilisation of suspensions whereby electrolytes are added to reduce the charge on particles and allow agglomeration (Svarovsky, 1985). Coagulation produces microflocs
Colloid	Mixture in which one substance is dispersed evenly throughout another
Cyanophyta	Blue-green algae
Electrokinetic	The motion of charged particles
Eukaryote	Single-celled or multicellular organism whose cells contain a distinct membrane-bound nucleus
Flagellate	Organisms with one or more whip-like organelles for motion
Floc	Particles that have agglomerated, precipitated or flocculated into larger clumps of mass. The density of these clumps is between the fluid and the solid
Flocculation	Flocculation follows initial coagulation, a gentle mixing stage, and increases the particle size from submicroscopic microflocs to visible suspended particles (Svarovsky, 1985)
Gibbs free energy	Chemical potential that is minimized when a system reaches equilibrium at constant pressure and temperature
Heterotrophic	Organism that cannot synthesize its own food and is dependent on complex organic substances for nutrition

Hydrophobicity	Repelling, tending not to combine with, or incapable of dispersing or dissolving in water
Isoelectric point	Point where the pH at a particular surface carries no net charge
Lipids	A fatty or waxy organic compound that is readily soluble in a non-polar solvent but not in a polar solvent. Its major biological functions involve energy storage, structural component of cell membrane, and cell signalling
Lyse	Breaking open cell to compromise its integrity
Motility	The ability to move spontaneously and actively
Newtonian fluid	Fluid in which the viscosity is independent of the shear rate
Phyla	Group of organisms: primary division of a kingdom
Planktonic	Suspended in a body of water
Precipitation	Dissolved particles formation of a solid in a solution or inside another solid during a chemical reaction or by diffusion in a solid
Protozoan	Eukaryotic organism belonging to a group characterized for being single-celled, mostly motile and heterotrophic
Steric effects	The influence of the spatial configuration of reacting substances upon the rate, nature, and extent of reaction
Vacuoles	Space or vesicle within the cytoplasm of a cell, enclosed by a membrane and typically containing fluid
Van der Waals forces	Weak, short-range electrostatic attractive forces between uncharged molecules, arising from the interaction of permanent or transient electric dipole moments
Yield stress	Stress at which a material begins to deform plastically
Zeta potential	Electrokinetic potential in colloidal systems

1 INTRODUCTION

The mass culture of algae is a growing industry, with algal products being used as a source of food, pharmaceuticals and, increasingly, as energy. Microalgae may provide many different types of biofuels such as methane produced by anaerobic digestion (Spolaore *et al.*, 2006); biodiesel derived from microalgal lipid, oils produced by hydrogenation (Chisti, 2007) and photobiologically produced biohydrogen (Akkerman *et al.*, 2002). The idea of using microalgae for the production of bioenergy is not new (Mohn, 1980; Levin *et al.*, 1962). Limited supply of crude oil leading to volatility of fuel prices and demand for alternative, environmentally friendly and renewable fuels, has caused renewed interest. The potential of algae in a biorefinery system to provide energy and a range of other products, as illustrated in Figure 1, is well recognised (Chisti, 2007). Crops have been considered for production of biofuels due to the natural fatty acid contents, but much debate has been raised around the land usage required for such projects. On the other hand, Chisti (2007) claimed algae have been estimated to require only 1 - 2% of current cropping areas to replace 50% of transport fuels required. Microalgae can also fix carbon dioxide and nitrogen (Harun *et al.*, 2010) and in some cases take up heavy metals (Matis *et al.*, 1996) thus reducing the environmental burden.

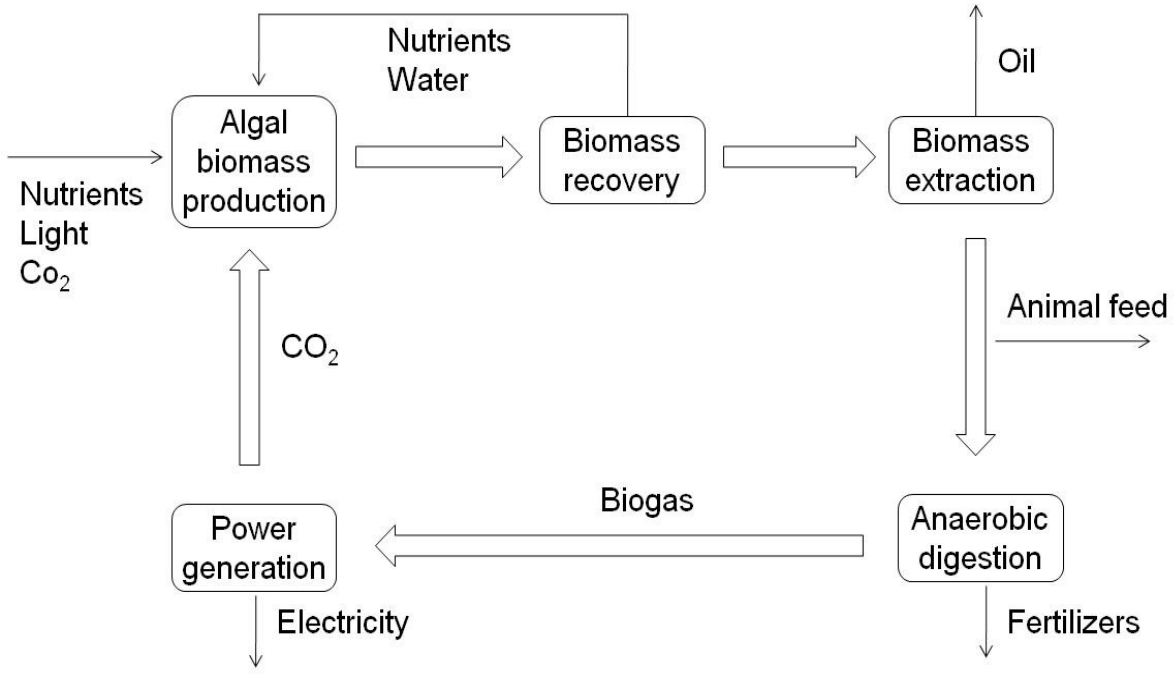

Figure 1: Conceptual overview of the microalgae process options

In order to be economically feasible, microalgal biodiesel must be cost competitive with petroleum-based fuels. At a crude oil price of $100 per barrel, microalgal biomass with an oil content of 55% must be produced at less than ~$340 per ton to be competitive (Brennan and Owende, 2010). Chisti (2007) estimated this cost at ~$3000 per ton of algal biomass. Griffiths *et al.* (2011a) investigated the economically feasibility of algal biodiesel and

concluded that algal biodiesel will not be economically feasible either in ponds or photobioreactors, at current costs below a biomass productivity of 1 $g.L^{-1}.day^{-1}$. At a lipid content of 50% DW, algal biodiesel becomes economically feasible at biomass productivities of 1.5 $g.L^{-1}.day^{-1}$ (US$ 130 per barrel crude oil), close to 2 $g.L^{-1}.day^{-1}$ (US$ 90), and 2.5 $g.L^{-1}.day^{-1}$ (US$ 50) in raceway ponds. At lower lipid contents, higher biomass productivity is required, e.g. at a lipid content of 25% DW, algal biodiesel only becomes cost effective at 2 $g.L^{-1}.day^{-1}$ for US$ 130 per barrel (Griffiths *et al.*, 2011a). Currently reported biomass productivities in outdoor raceway ponds average around 0.17 $g.L^{-1}.day^{-1}$, with a lipid content of 26% DW (Griffiths and Harrison, 2009), which is far from being economically feasible.

The harvesting and recovery of microalgae is identified as a major bottleneck in the process (de la Noue and de Pauw, 1988; Henderson *et al.*, 2008b; Uduman *et al.*, 2010; Danquah *et al.*, 2009b), contributing 20 to 40% to the total cost of producing the biomass (Gudin and Therpenier, 1986; Grima *et al.*, 2003). The challenge of separating algae can be attributed to the small cell size, hydrophilicity, dilute suspensions (1 - 10 $g.L^{-1}$) and in some cases, high salinity. Algae also have a specific gravity similar to water and this also limits the gravity settling driving force. Algae are often suspended in large volumes of water with some species being motile. For example, a concentration of 15% (w/v) is the minimum microalgal solid concentration required by Bio-Fuels, Pty Ltd. (Laverton, Victoria, Australia) for effective lipid extraction. Harvesting of biomass requires one or more solid-liquid separation techniques (Grima *et al.*, 2003), selected to exploit the natural properties of microalgal cells. The optimisation of biomass recovery is dependent on the algal species chosen, culturing technique and operating conditions. Furthermore, species present variable surface properties and sensitivities to the environment. A suitable low-cost, species-specific technique is therefore required for effective water and nutrient recycle, high recovery efficiency and concentration, whilst ensuring low energy and chemical usage and negligible cell damage.

Proposed techniques for the biomass recovery step in Figure 1 include filtration, centrifugation, sedimentation, flotation and flocculation. Microalgal properties such as surface charge, size, shape, hydrophobicity, adhesion and cohesion properties, and settling or floating velocities all underpin physical and chemical mechanisms for solid-liquid separations. In addressing their applicability in this study, each technology is introduced, its principle of operation explained, literature performance data reviewed and preliminary conclusions drawn on their usefulness at an industrial scale. Characteristics of algae morphology and suspensions are presented to allow effects on the recovery methods to be highlighted and to form a basis for method selection.

This dissertation aims to identify and measure the physico-chemical properties of commonly studied algal cell surfaces and culture suspensions. These parameters are exploited to identify potential biomass recovery techniques using an approach based on first principles drawn from current literature. The results generated are primarily empirical due to the novel nature of the problem. Two microalgal strains are used as model examples throughout the thesis. A similar approach for other species may be adopted. *Chlorella vulgaris* and *Scenedesmus sp*. are well studied microalgal strains. They have high lipid content and boast reasonable growth rates, resulting in higher lipid productivities than many species essential for biodiesel production (Griffiths *et al.*, 2011; Griffiths and Harrison, 2009). Both

species are grown with relative ease and may be cultivated in a range of reactor configurations. *Scenedesmus sp.* and *Chlorella vulgaris* may be cultivated in freshwater at neutral pH and room temperature. They have a low nutrient requirement and a moderate tendency to undergo contamination or predation.

This thesis is divided into eight chapters. Chapter 2 provides background information on (i) algal biology, (ii) factors affecting biomass separation, (iii) rheology, (iv) current algal recovery techniques and (v) preliminary literature conclusions. Chapter 3 outlines the key questions, problem statement and objectives addressed in this thesis whilst Chapter 4 presents details of the experimental procedures and approaches used. Chapter 5 and 6 presents the results obtained in this research. Chapter 5 presents the algal growth and bacterial growth as well as investigating the relationship between absorbance and dry weight. The suspension characteristics, carbon mass balance and surface properties are characterised across the growth phase. Chapter 6 presents the separation results, investigating natural settling, chemical induced, auto- and bioflocculation, followed by a study on the ability to grow microalgae on the separation recycled effluent. Chapter 7 provides the main discussion around these results. First are discussed the results of the growth parameters of the investigated organisms followed by an investigation into each physico-chemical property. The effects of CO_2 and growth phase are presented in conjunction with the surface properties to show the interdependencies. Rheological characteristics and a carbon balance over the growth systems are presented. Due to the relationships between surface properties, growth, rheology, carbon balance and other suspension properties, each results section will provide a brief discussion to interrelate each of these parameters and make preliminary conclusions. These are used to design recovery targets and identify possible properties and suspension conditions to exploit. The results are then discussed in terms of all parameters and possible mechanisms suggested. An overall recovery design is proposed in Chapter 7. The thesis ends with the presentation of the overall conclusions and recommendations in Chapter 8. Supplementary material is provided through a set of appendices.

2 LITERATURE REVIEW

The research literature provides a relatively large and diverse body of research on microalgae. Much of this literature is devoted to areas of taxonomy, evolution, growth, algal blooms and wastewater treatment. Only recently has there been renewed interest in using microalgal biomass as a renewable energy source. The processes involved in producing commercial biofuels are presently ill defined and there is room for much improvement in all areas of the process. Research groups and companies report use of different algal strains, cultivation techniques, harvesting techniques and downstream processes. They highlight varying regions as bottlenecks to the overall process. One such region centres on biomass harvesting and recovery which is the focus of this thesis. Here, in particular, few rigorous studies are reported in the literature and it is a challenge to discern accurate and useful information from the literature within this research area. Most research on microalgae recovery is offered from wastewater treatment research where the focus is on water purification rather than biomass recovery. While some research groups have investigated microalgae harvesting and recovery techniques and their mechanisms, large variances in results between reports devalue this literature (Appendix 1A). As there are many unknowns in most areas of this research field, there is a need to re-analyse this process from first principles.

In this literature review, the biology behind microalgal cells is investigated first to inform decision on which species are best suited for commercial processing. Factors affecting separation are then discussed followed by evaluation of current harvesting technologies and results. Challenges and gaps are subsequently identified, followed by a proposed approach to answer these questions in Section 3.2.

2.1 Algal biology

Algae are one of the oldest life forms, found in many different shapes and forms and widely distributed in the sea, freshwater and wastewater. Most are microscopic, but some are quite large, with some marine seaweeds exceeding 50 m in length (Clixoo, 2010). Microalgae generally lack roots, stems, leaves, conducting vessels, and complex sex organs (Brennan and Owende, 2010) and commonly range between 3 and 300 µm. Photosynthetic algae may either be obligatory autotrophic or facultative heterotrophic; the former use only inorganic compounds such as CO_2, salts and a light energy source; whilst the latter can grow on either organic carbon or CO_2, salts and light (Brennan and Owende, 2010). Photoautotrophic microalgae fix carbon and release oxygen as a by-product. Excess energy may be stored within the algal cell in the form of lipids and fatty acids. Some algal types may accumulate these fatty acids and lipids to greater than 40% of their overall mass (Table 1). This lipid content may be increased to 60% in some cases by nitrogen limitation (Griffiths *et al.*, 2011a; Griffiths *et al.*, 2011) and contributes to the calorific value of the biomass. The fatty acid component can be converted into biodiesel or this and other fractions of the cell used to provide a variety of forms of bioenergy.

Table 1: Lipid content of various algal species under nutrient sufficient conditions

Species	Phyla	% Lipid	Species	Phyla	% Lipid
Scenedesmus	Chlorophyta	12 – 40[a]	*Porphyridium*	Rodophyta	9 - 14[a]
Prymnesium	Haptophyta	22 - 30[a]	*Dunaliella*	Crysophycean	6 - 8[a]
Chlorella	Chlorophyta	14 - 22[a]	*Tetraselmis*	Chlorophyta	3[b]
Spirogyra	Chlorophyta	11 - 21[a]	*Spirulina*	Cyanophyta	6-9[b]
Chlamydomonas	Chlorophyta	21[a]	*Synechoccus*	Cyanophyta	11[b]
Euglena	Euglenophyta	14 - 20[a]	*Anabaena*	Cyanophyta	4-7[b]

[a] (Satin, 2006), [b] (Becker, 1994)

The diversity within alga phyla aggravates definition of a set of generalised algal characteristics due to variances in cell wall, storage products and photosynthetic pigments (Peretti *et al.*, 2007). Therefore every species of microalgae may respond differently to suspension conditions and require a different separation technique based on its particular physico-chemical properties. The simple structure of unicellular algae allows the cell to adapt readily to culture conditions (Brennan and Owende, 2010). This acclimation ability implies the cell characteristics may vary with culture conditions and the algae may adjust to under non-optimal growth conditions e.g. on recycled water and nutrients.

2.1.1 Strain selection

Microalgae are a promising alternative source of lipid for biodiesel production. One of the most important decisions is the choice of species to use. There are about 80000 different species of microalgae identified; each with specific growth preferences and physical properties. To be considered for commercial-scale production, algae should boast a high growth rate and biomass concentration to maximise growth productivity (Griffiths and Harrison, 2009) and allow the population to replenish itself quickly after harvesting (Barsanti and Gualtieri, 2006). For many applications, lipid productivity, the product of lipid content (Table 1) and growth rate, is an important selection criterion, as is the ability to harvest, minimal nutrient requirements and the resistance to contamination and predation (Brennan and Owende, 2010; Griffiths and Harrison, 2009). Much of the data defining these criteria are deficient; hence a best case selection approach is required. Each microalgae species has differing characteristics which may be exploited in solid-liquid separation e.g. density, surface charge, shape, size, hydrophobicity, salinity, buoyancy and cohesiveness. Table 2 highlights the variation of some of these characteristics.

Table 2: Typical microalgae characteristics

Algae strain	Density ($kg.m^{-3}$)	Zeta potential (mV)	Culturing pH	Morphology	Diameter, length (µm)
Microcystis	1200	-7.5 to -26	5.6 - 9.5	Globular sphere	3 - 7
Chlorella vulgaris	1070	-17.4	6 - 9	Single cell spherical	3.5
Cyclotella sp.	1140	-19.8 to -22.3	4 - 10	Chains of spheres	6.1
Syendra acus	1100	-30 to -40	7.6	Needles	4.5 - 6, 100 - 300

*(Henderson *et al.*, 2008b)

2.1.2 Growth conditions

Microalgae have five well defined batch growth phases; namely, lag, exponential, declining growth rate, stationary and death phase (Fogg and Thake, 1987). During each of these phases the culture has specific growing requirements such as temperature, sterility, pH, lighting, agitation and nutrients and undergoes a range of physico-chemical changes. In the initial lag phase, cells acclimatise to the growth environment and low cell concentration. Exponential growth follows where growth is not compromised by nutrient or energy limitation. The duration of exponential phase depends upon the size of the inoculum, the growth rate and the capacity of the medium and culturing conditions to support algal growth. In algal cultures, exponential growth is typically followed by linear growth rates where growth is controlled by availability of light or dissolved CO_2. Declining growth occurs where a specific requirement for cell division is limiting or reproduction is inhibited. Most typically a nutrient salt, limiting carbon dioxide or light limitation becomes the primary cause of declining growth. Variation in pH can change the distribution of carbon dioxide species and carbon availability, alter the availability of trace metals and essential nutrients, and, at extreme pH levels, potentially cause direct physiological effects (Chen and Durbin, 1994).

Light limitation occurs on attenuation of light on passage through fluid or when cells absorb most of the incoming irradiation and individual cells shade each other. Cultures enter stationary phase when net growth is zero, and undergo associated biochemical changes, depending on the growth limiting factor (Petrusevski *et al.*, 1995). Light limitation results in increasing pigment content of most species and shifts in fatty acid composition. Lipid content may vary with environmental conditions (Griffiths *et al.*, 2011a; Griffiths *et al.*, 2011; Peretti *et al.*, 2007) and increases with nutrient limitation under carbon excess, typically nitrogen limitation (Brennan and Owende, 2010). This influences the density of the algal slurry and the buoyancy of the cells.

Danquah *et al.* (2009a) investigated the effect of the growth phase and surface characteristics of a mixed culture *Tetraselmis suecica* and *Chlorococum sp.* on the settling rates and found a strong dependence of growth phase on the settling rate. Fattom and Shilo (1994) observed cyanobacteria to become more hydrophobic and adhere to solids under optimal growth conditions whilst van Loosdrecht *et al.* (1987) showed bacteria to become increasingly hydrophobic during exponential growth. Filtration, sedimentation and flocculation efficiencies have all been reported to improve whilst harvesting during the stationary phase (Danquah *et al.*, 2009b; Lee *et al.*, 1998). This is postulated to result from changes in the surface charge, and in some cases the chemical structure of the cell wall varies with growth phase (Bernhardt and Clasen, 1994). Due to elevated kinetics of cell growth during the exponential growth phase, there is minimal intercellular interaction between individual cells in the culture owing to a net electronegative zeta boundary around the cells, creating cell repulsions. It has been postulated that this phenomenon is due to variations in quantity and composition of extracellular organic material (EOM) attached to the cell surface (Bernhardt *et al.*, 1985). Reported EOM concentrations range from 1.8 $mg.L^{-1}$ for the cyanobacteria *Synechocystis* to 81 $mg.L^{-1}$ from the green genus *Chlorella* (Hoyer *et al.*, 1985).

Both EOM and NOM (non-organic materials) may influence the surface chemistry of particles and promote or inhibit flocculation (Henderson *et al.*, 2008b). The EOM

concentration increases and uronic acid decreases with the age of the algae whilst environmental conditions affect the quality of the polysaccharides produced. Tenney *et al.* (1969) reported a steep increase in extracellular metabolites to occur during the stationary and death phases of microalgal growth. The exopolysaccharides produced by microalgae are indistinguishable from those produced by bacteria (Shipin *et al*., 1999). Bacteria are typically co-cultured during the culturing of microalgae. Bacterial counts ranging from 10^2 to 10^8 cells.ml^{-1} culture of algae have been reported during outdoor cultivation *Scenedesmus* and *Chlorella (Binova et al., 1998)*.

It is therefore important to analyse the literature and compare relative separation success at similar growth conditions as this may influence efficiencies.

2.2 Factors influencing separation

2.2.1 Cell morphology and motility

Eukaryotic algal cells contain three types of double-membrane-bound organelles: the nucleus, the chloroplast, and the mitochondrion. The plasma membrane is the outermost cell surface, which separates the cell from the external environment. The plasma membrane is composed primarily of proteins and lipids, especially phospholipids. The structure outside the cell membrane is comprised of cellulose and called the cell wall. Cell walls provide structural strength to the cell and resist mechanical pressures. They are porous allowing solutes to pass through easily. The cell membrane forms the biological boundary, controlling passage of solutes into and out of the cell. Some species of algae have flagella, external appendages responsible for cell repulsion. Most species have a unique cell structure.

Morphological characteristics that influence algal behaviour in harvesting include size, shape, cell locomotion of eukaryotic flagellates or the gliding motility of certain diatoms, cell wall elongations, cell unification and the presence of a mucilage layer or capsule attached to the cell wall (Petrusevski *et al*., 1995; Jarvis *et al*., 2009). Smaller particles have a larger surface area and surface energy (Hiemenz and Rajagopalan, 1997) allowing increased potential for adsorption and agglomeration. Depending on the strain, this motility could be detrimental to algal separation as the algae may mobilise out from the concentrated suspension, especially under gravimetric sedimentation. Each phylum also presents a unique natural ability to gain competitive advantages over other microalgae. Microalgal cells range from 3 to 300 µm in size (Henderson *et al*., 2008b) (Table 2). Larger particles allow for easier separation due to the increased surface area per cell and mass (Stoke's law). Microalgae have developed many techniques to reduce their sinking rate to gain a natural competitive advantage. These methods include: motility, reduction of cell dimensions, increment of the drag forces (Conway and Trainor, 1972), reduction in cell densities via gas vacoules as seen in the Cyanobacteria for adjusting intracellular water (Anderson, 2005) and lipid accumulation to increase buoyancy (Brennan and Owende, 2010).

Algal cell densities vary from 1070 to 1140 kg.m^{-3} for green algae and diatoms respectively (Edzwald and Wingler, 1990). Diatoms have a silica-rich hard outer wall, increasing density. Increasing density and cell size result in increasing settling velocity, hence sedimentation or centrifugal separation. Single spherical cells are frequent for both green alga and cyanobacteria (e.g. *Chlorella sp.* and *Synechocystis minuscula*). These single cells may

colonise and produce complex structures such as filaments (Henderson *et al.*, 2008b). Species with filamentous morphology, attached appendages or large diameters allow for easier filtration as the individual cells are unable to pass through the filter pores.

2.2.2 Rheology

Morphology of the cells, growth conditions, presence of extracellular polysaccharide and surface charge all impact the fluid rheology of culture suspensions (Chen *et al.*, 1997). Algal fluid rheology needs to be understood prior to the choice and design of any separation- or process-based application to determine engineering limitations to downstream processing. In contrast to the vast literature available on rheological properties of microbial cultures, there are few reports on the rheology of microalgae.

Figure 2 depicts possible rheological behaviours typically observed for most fluids. Each rheological behaviour may be modelled using a variety of functions. Table 3 describes the most common of these models where τ is the shear stress (Pa), τ_0 is the yield shear stress (Pa), γ is the shear rate (s^{-1}), K is the plastic viscosity constant, μ is the dynamic viscosity (Pa.s) and μ_a is the apparent viscosity (Pa.s).

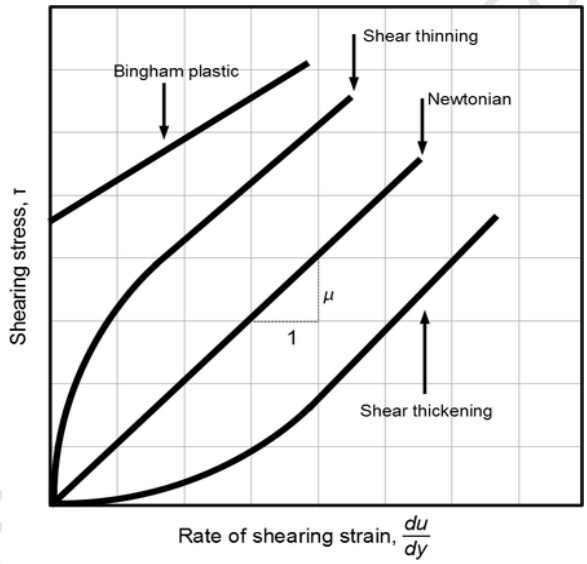

Figure 2: Types of fluid viscosities

Table 3: Rheological models used to describe fluid flow of microalgae

Fluid	Equation	Apparent viscosity	Equation*
Newtonian	$\tau = \mu\gamma$	$\mu_a = \mu$	1
Pseudoplastic	$\tau = K\gamma^n$, n<1	$\mu_a = K\gamma^{n-1}$	2
Dilatant	$\tau = K\gamma^n$, n>1	$\mu_a = K\gamma^{n-1}$	3
Bingham plastic	$\tau = \tau_0 + K_p\gamma^n$	$\mu_a = \frac{\tau_0}{\gamma} + K_p$	4
Casson plastic	$\tau^{\frac{1}{2}} = \tau_0^{\frac{1}{2}} + K_p\gamma^{\frac{1}{2}}$	$\mu_a = \left[\left(\frac{\tau_0}{\gamma}\right)^{\frac{1}{2}} + K_p\right]^2$	5
Herschel-Bulkley	$\tau = \tau_0 + K_p\gamma^n$	$\mu_a = \frac{\tau_0}{\gamma} + K_p\gamma^{n-1}$	6

*(Atkinson and Mavituna, 1991)

The yield strength or yield point of a material is defined in engineering and materials science as the stress at which a material begins to deform plastically. The yield stress and fluid flow behaviour of microalgal suspensions as a function of biomass concentration must be defined to determine maximum cell concentrations that allow for optimum fluid flow. This knowledge can be used to set upper limits for concentration factors and maximum allowable mass concentrations. Wu and Shi (2008) investigated *Chlorella pyrenoidosa* fluid characteristics and demonstrated the fluid followed Newtonian characteristics for cell concentrations under 175 $g.L^{-1}$, whilst Chen *et al.* (1997) tested *Haematococcus lacustris* and reported the suspension to become non-Newtonian at cell concentrations over 10 $g.L^{-1}$. Reported apparent viscosities for Newtonian algal cultures range between 10 – 50 mPa.s (Wu and Shi, 2008). Literature on viscosity profiles as a function of algal biomass concentrations is scarce.

Filamentous and irregular shaped species follow very specific rheology, typically determined empirically. Where spherical particles may be assumed, the theoretical viscosity of a suspension may be estimated by the Einstein equation for low cell concentrations (Coulson *et al.*, 1983):

$$\frac{\eta}{\eta_0} = 1 + 2.5\emptyset \tag{7}$$

where η is the viscosity of the suspension (mPa.s), η_0 is the viscosity of the solvent (mPa.s) and ∅ is the volume fraction of the particles.

The Vand equation for a suspension of spheres (volume fraction,ϕ) in a Newtonian liquid of viscosity μ_L is another, more accurate estimation:

$$\mu = \mu_L(1 + 2.5\emptyset + 7.25\emptyset^2) \tag{8}$$

2.2.3 Colloid stability and surface charge

The stability of all colloids always tends in the direction of decreasing Gibbs free energy (Stumm, 1992). Therefore the separation of a two-phase dispersed system is a change in the direction of decreasing Gibbs free energy (Hiemenz and Rajagopalan, 1997). When particles within a colloid aggregate together, their individual kinetic stability is lost and this may be described by colloidal instability. Size, shape, pH, conductivity and concentration determine the properties of this dispersion (Petrusevski *et al.*, 1995). Diffusion of ions is responsible for the diffuse electrical double layer, present around all solid particles in a solution, whilst diffusion of particles is responsible for the collision and transport of particles. These particles acquire charge in a number of ways; the most common of these is the adsorption of an ion from solution onto an initially uncharged surface and the ionisation or dissociation of a surface group on the solid particle surface (Hiemenz and Rajagopalan, 1997).

Where no mechanisms of biological recognition are present (e.g. ligand-receptor interactions), the overall colloidal stability of the algal culture is dependent on the electric repulsion between algal cells. Colloids with high absolute zeta potential (negative or positive) are electrically more stable than colloids with low zeta potentials due to van der Waals and steric repulsion forces. Most algae have negatively charged surfaces under

culture conditions. This charge is a function of the algal species, ionic strength of medium, pH and EOM (Bernhardt *et al.*, 1985). In aquatic environments, these surface charges are counterbalanced by oppositely charged ions, some of which are bound to the surface whereas the rest are distributed in a diffuse layer. The thickness of this diffuse electrical double layer depends on the ionic strength of the solution and the valencies of the counter ions. The electrical interactions between particles (including bacteria and microalgae) in suspension are governed by the extension of the diffuse layer: increasing salt concentration results in a decrease in electrical interactions between two particles charged alike (van Loosdrecht *et al.*, 1987). This theory has been extensively studied and named the DLVO theory (Rutter and Vincent, 1984). Zeta potential, an abbreviation for electro-kinetic potential in colloidal systems, is typically used in characterising surface charge. Electrostatic interactions between the cells and between cells and surfaces, directly influences adhesion, adsorption and flocculation properties of the alga. The zeta potential (Z_p) of a particle measured in mV is defined following Smoluchowski's formula:

$$Z_p = E_m.4\pi\eta/D \quad (9)$$

where E_m is the electrophoretic mobility ($cm^2.V^{-1}s^{-1}$), η is the viscosity ($g.cm^{-1}s^{-1}$) and D is the dielectric constant ($C.V^{-1}cm^{-1}$).

Figure 3 (adapted from Malvern instruments Technical Manual, 2000) describes the zeta potential of a solid particle in a solution. Colloidal particles dispersed in a solution are electrically charged due to their ionic characteristics and dipolar attributes. The development of a net charge at the particle surface effects the distribution of ions in the neighbouring interfacial region, resulting in an increased concentration of counter ions called the stern layer. Outside this fixed layer, there are varying compositions of ions of opposite polarities, forming a diffuse area called the Gauy-Chapman layer. An electrical double layer is therefore formed in the region of the particle-liquid interface. The difference in charge between the bulk fluid and surface of the particle is defined as the zeta potential (mV). Zeta potential is a reflective underestimation of the surface potential.

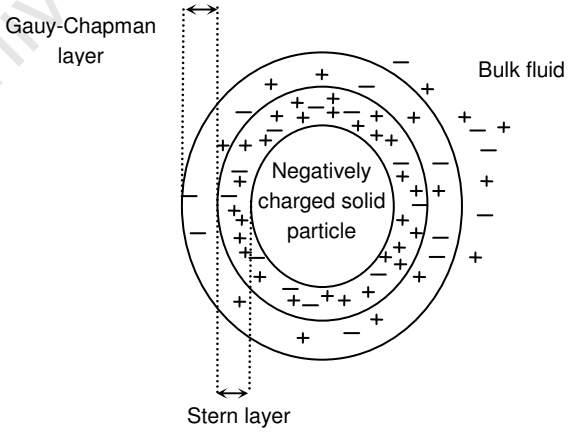

Figure 3: Zeta potential schematic

The magnitude of the zeta potential depends on the surface potential, the concentration and charge of the counter ions (Wills, 1985). Zeta potential is an indication of the degree of repulsion between adjacent, similarly charged particles in a dispersion. A high zeta potential

confers stability to the solution as the dispersion resists aggregation. When the potential is low, inter-particle attraction exceeds repulsion and results in flocculation. Particles with zeta potentials more positive than +30 mV or more negative than -30 mV are considered stable (Hiemenz and Rajagopalan, 1997; Lyklema, 2000). At very negative zeta potentials, a positive particle attracts and adheres to the microalgal cells inducing autoflocculation.

A point where the pH at a particular surface carries no net charge is defined as an isoelectric point or point of zero charge (PZC). At this point, the particles become unstable and the rate of auto-flocculation is rapid, allowing for easier flotation or sedimentation. The isoelectric point of most algae is around pH 3 – 4 (Liu *et al*., 1999). Henderson *et al.* (2008b) reported the life cycle of microalgae to influence its zeta potential due to acclimation and reproduction activities. Zeta potential is extremely dependent on the pH of the solution as this changes the ionic strength and hence the charge activity surrounding the particle. Greater surface charges are developed at higher ionic strengths and greater surface potentials at lower ionic strengths (Stumm, 1992). This is attributed to the decrease in the double layer thickness as ionic strength increases. The addition of flocculants has also been reported to shift the isoelectric point (Chen *et al*., 1998). These factors allow for control over microalgal flocculation via manipulation of the zeta potential. Surface charge is dependent on the suspension conditions and may affect other particle parameters such as particle floc size. van Loosdrecht *et al*. (1987) found the effect of the electrokinetic potential to increase with decreasing hydrophobicity. Zeta potential is therefore an important physical property to examine when designing a separation technique for any colloid system.

2.2.4 Hydrophobicity

Hydrophobicity is a non-electrostatic interaction and is a crucial property in understanding and controlling the cohesion of algal particles to each other and adhesion to other external surfaces. The hydrophobic effect is the entropy-dominated association of molecules (Hiemenz and Rajagopalan, 1997) and is a driving factor in cell flocculation. Microalgae are mostly hydrophilic particles (Fattom and Shilo, 1984; Pott, 2009; Ayoub and Koopman, 1986). With increasing hydrophobicity, the particles tend to adhere onto bubbles, filters or other separative catalysts. Flocculation increases with increasing hydrophobicity where salinity, pH and surfactant dosing may alter the hydrophobicity of algal particles (Jameson, 1999). Cell-surface hydrophobicity and charge of bacteria and algal cells are postulated to govern this flocculation via the primary adsorption of cells to other surfaces in suspension (Castellanos *et al*., 1997). The composition and properties of EPS, particularly proteins, also contribute to hydrophobic properties of cells. Protonation of cell surfaces neutralise part of the cells' natural negative charge and this may result in an increased effective hydrophobicity of the cell surface, which has been shown to result in increased adhesion strength (van Loosdrecht *et al*., 1987). It seems reasonable to assume that proton translocation activity plays a role in the initiation of microbial aggregation.

Hydrophobicity may be measured in a number of ways. Carbon adhesion techniques are based on free energy of transfer of particles from water to a purely hydrocarbon solvent (Tanford, 1921). One such method is the use of two-phase partitioning via carbon adhesion (Pedersen *et al*., 1998; Fisher *et al*., 1998). The most common of these methods is the measurement of the contact angle between the liquid and solid surfaces; however the latter is complicated for very small particles. Hydrophobicity is often quantified using a

hydrophobicity index to quantify relative partitioning of particles between the hydrophilic and hydrophobic phases:

$$\text{Hydrophobicity index (\%)} = \left[1 - \frac{OD_{t=0}}{OD_{t=t}}\right] \text{x } 100 \quad (10)$$

2.3 Criteria for assessing algal harvesting

In order to assess the performance of different separation techniques effectively, a number of quantitative separation factors have been developed. These are drawn primarily from the wastewater treatment industry where water clarification is the primary objective. Most of the literature encountered on microalgal solid-liquid separations is focussed on the clarification of solution and report removal efficiencies and percentage removal of total suspended solids (TSS). The focal point of this research is the efficient recovery of the solids, requiring different assessment criteria. In a batch system configuration, the volumetric reduction factor (VRF) and concentration factor (CF) of microorganisms are defined as:

$$VRF = V_0 / V_f \quad (11)$$

$$CF = C_f / C_0 \quad (12)$$

where V_0 and C_0 are, respectively the initial volume of the entire suspension system and cell concentration, V_f and C_f are the final volume and cell concentration (Rossignol *et al.*, 1999). Equation 11 assumes that all the cells are concentrated into the final volume and Equation 12 assumes C_f to be the concentrated segment/pellet of the suspension after time t. These factors are respectively independent of concentration and volume which causes discrepancies in literature reports. Therefore as concentration and volume reduction factors are dependent on the throughput and size of vessel used, a more general factor also reported in the literature is algal settling/recovery efficiency:

$$\text{Recovery efficiency (\%)} = \frac{C_0 - C_f}{C_0} \text{ x } 100 \quad (13)$$

where C_0 is the initial average concentration of the algal system and C_f is the final decreased concentration of the upper level of the separation system (see Section 4.4.9 jar tests).

For algae-algae bioflocculation:

$$\text{Recovery efficiency (\%)} = \left[1 - \frac{\frac{OD_{A750}(t)}{OD_{A750}(t_0)}}{\frac{OD_{B750}(t)}{OD_{B750}(t_0)}}\right] \text{x } 100 \quad (14)$$

where A is microalgal species 1 and B is microalgal species 2 at initial time, t_0 and final time, t_f.

Flocculation efficiency is also defined as recovery efficiency as in Equation 13, (Buelna *et al.*, 1990):

$$\text{Flocculation efficiency (\%)} = (1 - A/B) \text{ x } 100 \quad (15)$$

where A is the optical density (OD) of the coagulated sample and B is the control OD.

The major variables measured to determine algal recovery include absorbance, turbidity and concentration measurements of the resulting microalgae-water slurry. For algal recovery, the best quantification measure of success is the measure of the amount of algal cells in the suspension before and after the experiment. However there is also a need for rate data pertaining to this suspension quantification. The concentration, quantification approach is most appropriate for algal settling efficiency measurements as concentration is a function of volume and mass. Comparison of concentration factors and recovery efficiencies across different settling conditions is dependent on mixing and settling time and measurements must be taken at the same height within the settling vessel (see Section 4.4.9 jar tests). To determine which algal concentrating method is suitable for which species, a number of factors should be considered to determine the overall efficiency of the dewatering technique. The following list serves as a guideline:

- General reliability
- Capital and operational costs
- Continuous/ discontinuous process
- Cleaning and maintenance requirements
- Ability to handle fluctuations in conditions
- Concentration procedure and possible coupling of techniques
- Environmental impact
- Recycle streams
- Volume throughput
- Suitable strains
- Concentration limits
- Time taken for effective concentrating
- Concentration factor
- Removal efficiency
- Chemical dosages
- Cell viability

2.4 Flocculation

The small size of microalgal cells contributes significantly to the difficulty of dewatering. This can be partly overcome by inducing cell collision and clumping into larger effective particle size through flocculation. Through flocculation, an engineer attempts to increase size to facilitate easier and quicker separation via Stoke's law (Equation 17). Flocculation is often suggested as an operation preceding filtration, sedimentation, centrifugation or flotation to enhance efficiency and cost of operations (Schenk *et al.*, 2008). Much literature is available on the advantages of flocculation of microalgae for filtration, flotation and sedimentation efficiencies (Appendix 1A). Flocculation is therefore an attractive initial step in algal harvesting provided the process is reversible. A potential problem with flocculation techniques is the possible unfavourable alterations to the biochemical nature of the end product (Csordas and Wang, 2004) and the unpredictable behaviour in larger systems.

Fine particles can become larger particles through flocculation, aggregation, coagulation and precipitation. It is important that we have a stable larger particle. Agglomeration, aggregation, coagulation and flocculation are generally loosely interchanged within the literature (Svarovsky, 1985; Mullin, 2001). For this work, these particles will be regarded as flocs (see Glossary). Flocculation is mediated by destabilising the colloidal suspension by reducing repulsion forces; thereby lowering the energy barrier and enabling the particles to aggregate (Bernhardt and Clasen, 1994; Holt *et al.*, 2002). Hence the resultant floc sizes and floc stability are largely dependent on shear stress (Bache and Rasool, 2001). The extent of flocculation is also dependent on a number of variables such as pH, temperature,

density differences, hydrophobicity, surface charge (Shelef *et al.*, 1984; Zita and Hermansson, 1997) and growth phase (Lee *et al.*, 1998). Light inhibition and salinity may also affect flocculation efficiency (Danquah *et al.*, 2009b; Shelef *et al.*, 1984; Bilanovic and Shelef, 1988; Danquah *et al.*, 2009a). Hydrophobicity index is a determinant factor in interfacial interactions, considering that higher surface hydrophobicity is associated with lower surface charge and higher flocculance. As pH has been widely reported to affect both flocculation and zeta potential (Bernhardt *et al.*, 1985; Education committee of American Waterworks Association and U. S. Public health service, 1968), flocculation efficiencies may be expected to depend on zeta potentials.

Solution properties have a direct influence on microalgal surface properties. By changing these properties it is possible to manipulate cell interactions. This may be done by adjusting the culture operating conditions or by the addition of chemicals or other biological elements. Much of the literature and knowledge on microalgal flocculation is derived from wastewater treatment and flocculation efficiencies and techniques derived around flocculation have been focused on water purification and not biomass recovery. Floc strength, size and stability are also important factors to consider when screening results as in any process flocs are subject to shear or compressive stresses or both.

2.4.1 Flocculation mechanisms

Flocculation is defined as the process by which small micro-organisms destabilise and asexually aggregate within a colloid by approach to the point of zero charge, electrical double layer compression, charge patch neutralisation (Salim *et al.*, 2010), polymer bridging, hydrophobic interaction, and enmeshment within sweeping floc (Rattanakawin, 2005). Cell flocculation has been divided into specific (molecular recognition) and nonspecific (double-layer interactions, van der Waals forces, hydrophobic interactions, salt bridges, and steric repulsion) interactions (Dengis *et al.*, 1995).

Bridging flocculation occurs when segments of the same ion, molecule or particle are attached to more than one particle, thereby linking the particles together. The strength of the floc thus depends on the number of bridges formed. An important factor during bridging is the availability of adsorption sites on particles, thus making the concentration of the bridging particles crucial. Correct mixing is important for bridging flocculation to be successful; as mixing increases contacting through cell collision but extreme mixing may break the bridges formed. Charge neutralisation is induced by the reduction in the electric double layer repulsion between particles due to adsorption of highly charged polyelectrolytes on oppositely charged particles. Where non-ionic and anionic polyelectrolytes are applied to a negatively charged colloidal dispersion, a destabilisation mechanism may be accounted for by the bridging technique. However when a charged dispersion carries oppositely charged particles, the bridging model becomes irrelevant (Bratby, 2006). Rather than adsorption at discrete sites, a mosaic of bridges within alternating regions of positive and negative charges gives way to virtually complete adsorption of the particles. The electrostatic patch flocculation is thought to be operative for very high charge density particles interacting with oppositely charged particles of low charge density. In the absence of steric contributions due to polymers or polyelectrolytes, the total long-range interaction between two surfaces charged alike is composed of two additive terms: electrostatic repulsion and van der Waals attraction (van Loosdrecht *et al.*, 1987).

Many different techniques have been proposed to induce flocculation. These are discussed hereafter. As the current literature is not consistent in its description of the many forms of flocculation, the following sections provide the definition of the flocculation techniques used in this dissertation with reference to algal flocculation.

2.4.2 Chemical flocculation

Bernhardt and Clasen (1994) suggested that adsorption coagulation with charge neutralisation forms the basis of destabilisation and aggregation of algal suspensions. These processes can be promoted by adding specific positively charged chemicals which interact with the negatively charged algal surface. Chemicals often used in the flocculation of algae and other zooplankton include mineral additives (lime, calcium, salts), hydrolysing metal salts (aluminium sulphate, ferric chloride), pre-hydrolysed metals (polyaluminium chloride), inorganic polyelectrolytes, organic cationic and anionic polyelectrolytes, non-ionic polymers, natural occurring flocculants (starch derivatives, tannins) and amphoretic and hydrophobically modified polymers. In some cases a combination of these may be used (Bernhardt and Clasen, 1994; Bilanovic and Shelef, 1988; Knuckey *et al.*, 2006; Renault *et al.*, 2009).

Flocculation according to charge neutralisation can be induced by addition of stochiometrically determined doses of cationic polyelectrolytes in relation to the charge density (Bernhardt and Clasen, 1994). Cell surface area can be used to predict an approximate coagulant dose (Henderson *et al.*, 2008b). However, differences in EOM composition, ionic strength, pH, viscosity and concentration affect the complexing of metal coagulants or sterically interfere with flocculation (Bernhardt and Clasen, 1994; Bernhardt *et al.*, 1985; Bilanovic and Shelef, 1988). Polymer flocculants physically link cells together (Harun *et al.*, 2010). They exhibit high flocculation rates due to their high molecular weights but high doses are required, making the process expensive (Pushparaj *et al.*, 1993) and renders the effluent water contaminated and typically unsuitable for recycle without pre-treatment. Increased ionic strength has been reported to improve flocculation efficiency by: reducing the double layer repulsion, enhancing adsorption of polyelectrolytes on surfaces of like sign, and reducing the polymer chains by screening charges and reducing the repulsions between them (Ives, 1978).

Inorganic flocculants are able to form polyhydroxy complexes at certain pH (Uduman *et al.*, 2010). Shelef *et al.* (1984) conducted a review on inorganic flocculants investigating optimal chemical flocculant dose and pH (Table 4). Metal complex flocculants are often used in wastewater treatment where the objective is to clarify and recover the water. Much of the algal separation literature is focused on this goal. Alum has been found to display improved flocculation compared to ferric sulphate in terms of optimal dose of flocculant and pH (Moraine *et al.*, 1980), whilst lime was found to exhibit good flocculation, it required suspension magnesium concentrations above 10 $mg.L^{-1}$ (Folkman and Wachs, 1973).

Table 4: Chemical flocculants, optimal doses and pH for microalgal flocculation

Type	Flocculant	Optimal Dose ($mg.L^{-1}$)	Optimal pH
Inorganic	Alum	80 – 250	5.3 – 5.6
	Ferric sulphate	50 – 90	3.0 – 9.0
	Lime	500 – 700	10.5 – 11.5
Polymeric	Purifloc	35	3.5
	Zetag 51	10	>9
	Dow 21M	10	4.0 – 7.0
	Dow C-31	1 – 5	2.0 – 4.0
	Chitosan	100	8.4

*(Shelef *et al.*, 1984)

Bilanovic *et al.* (1988) investigated the differences between marine and fresh species and the effect of different inorganic flocculants on these species and were able to remove above 90% of the fresh species by flocculation but negligible amounts of the marine species (Table 21, Appendix 1A). The addition of seawater into fresh samples has been shown to significantly increase microalgal cell recovery during pH induced flocculation as calcium carbonate flocs have a negative charge, while the magnesium hydroxide flocs have a positive charge. $CaCl_2$ was reported by Oh *et al.* (2001) to increase flocculation efficiency as a co-flocculant. As microalgal cells are negatively charged, the magnesium hydroxide flocs induce charge destabilisation (Ayoub and Koopman, 1986). Knuckey *et al.* (2006) tested 10 marine species and obtained >80% removal efficiencies using ferric chloride (Table 21, Appendix 1A). Moreover Knuckey and co-workers (2006) successfully deflocculated the suspensions to single cells showing that this system is potentially reversible.

Major drawbacks of chemical flocculants are the high dosages required, the need for pH correction (Pushparaj *et al.*, 1993), and the residual accumulation and contamination of the harvested biomass and spent media. Some flocculation mechanisms may also cause cell lysis resulting in a higher contamination of the effluent media (Lee *et al.*, 2009a). A summary of the literature on chemical flocculation of microalgae is presented in Table 21 of Appendix 1A.

2.4.3 Auto-flocculation

In autoflocculation, attraction of cells to one another is induced by surface charge neutralisation (Csordas and Wang, 2004), mediated by altering the pH through CO_2 supply or direct addition of alkali or acid. Nitrogen, light and carbon limitation has also been reported to induce autoflocculation (Schenk *et al.*, 2008; Sheehan *et al.*, 1998). This may be due to physical cell changes with regards to buoyancy and hydrophobicity. During autoflocculation positively charged precipitate (supersaturated calcium and phosphate ions (Uduman *et al.*, 2010)) or particles, causes initial nucleation that is promoted by the microalgal cells acting as the solid surface (Shelef *et al.*, 1984). The calcium phosphate precipitate is positively charged in the presence of excess calcium ions and this is adsorbed and reacts with the negatively charged microalgal cells resulting in agglomeration (Uduman *et al.*, 2010).

It has been proposed that aside from the precipitation of inorganics, autoflocculation may be assigned to excretion of organic macromolecules (Benemann *et al.*, 1980), inhibited release of microalgal daughter cells (Arad *et al.*, 1981) and aggregation between microalgae and bacteria (Lee *et al.*, 2009a). Calcium, magnesium, phosphate and carbonate salts are often suggested to be the driving reagent for flocculation. Natural pH fluctuations also affect autoflocculation. Photosynthesis, nitrate and phosphate assimilation increase pH, while respiration and ammonia assimilation decrease pH. Autoflocculation may however cause cell composition changes and is considered to be too unreliable (Benemann *et al.*, 1980). Shelef *et al.* (1983) hypothesized the cell point of zero charge to directly increase autoflocculation. Autoflocculation is not a well understood phenomenon for microalgae with a number of researchers proposing different mechanisms and causes of flocculation.

Knuckey *et al.* (2006) investigated the autoflocculation of a range of microalgal cells by adjusting the pH with NaOH and reported recovery efficiencies of greater than 95% in some cases (Table 21, Appendix 1A).

2.4.4 Bio- flocculation

Bioflocculation is the formation of cellular aggregates mediated by aggregation with associated microorganisms and extracellular biopolymers with species-specific characteristics (de la Noue and de Pauw, 1988). Bacteria (Oh *et al.*, 2001), starch (Vandamme *et al.*, 2010), chitosan and other species of microalgae (Salim *et al.*, 2010) have been shown to induce bioflocculation whilst addition of polyelectrolytes and inorganics, carbon limitation, EPS formation and pH shifts may also assist spontaneous flocculation (Schenk *et al.*, 2008). The mechanisms behind bioflocculation at present are not well understood and much research is required in this field. Since the structure and properties of bacterial surfaces largely vary between species, their flocculation patterns and mechanisms may also vary (Strand *et al.*, 2002). There are therefore two main systems of bioflocculation mechanisms. One instance is in the presence of EPS and the other is induced from interactions with biopolymers or other biomolecules. However in some cases these mechanisms may overlap.

All known microalgae produce exopolysaccharides such as uronic and glycolic acid which are responsible for cell adhesion. The biopolymer flocculants cause aggregation of particles and cells, by bridging and charge neutralization in the presence of the EPS (Lian *et al.*, 2008b). Bacterial adhesion to surfaces can be seen as a two-step event: reversible adhesion due to long-range forces and subsequent interactions mediating a direct contact between surfaces, such as hydrophobic interactions due to bacterial surface structures (Zita and Hermansson, 1997). Although some authors have indicated an influence of the electrical charges of bacteria and solid surfaces on adhesion (Gordon and Millero, 1984; Hermansson *et al.*, 1982; Larsson and Glantz, 1981), the influence of electrostatic interactions is generally ignored. Bioflocculation has been proposed to occur initially via particle attraction through oppositely charged ionic attraction (Spolaore *et al.*, 2006) and then by adsorption via bridging (Lian *et al.*, 2008b). The effectiveness of the bridging mechanism depends on the molecular weight of the extracellular biopolymeric flocculants (EBFs), the charge on the polymer and the particle, the ionic strength of suspension, and the nature of mixing (Salehizadeh and Shojaosadati, 2001). Bioflocculation in this sense might be attributed to zeta potential differences and chemical composition of the medium

and cell walls. However Strand *et al.* (2002) investigated flocculation of 8 bacteria with chitosan and found no direct relationship between zeta potential, hydrophobicity and flocculation efficiency. A complex combination of these factors is hence a probable explanation for the flocculation mechanisms observed.

The algal-bacterial suspensions tend to form commensal or symbiotic flocs of 0.1 mm or more in diameter (Lembi and Waaland, 1988). Most bacterial and microalgal surfaces are negatively charged with similar polysaccharides comprising the surfaces (Becker, 1994), hence the same flocculants may be used to aggregate microalgae. This process may be done by isolating and culturing bacteria, extracting the bio-flocculant and applying it in a pure form (Oh *et al.*, 2001). Soil and activated sludge have been identified as the best sources of organisms producing EPS. EPS production may also be improved by optimising culture conditions and carbon sources (Prasertsan *et al.*, 2008). Co-culturing of bacteria and microalgae has also been suggested by Lee *et al.* (2009). This will eliminate the possibility of harmful contamination of recycle effluent compared to introducing different isolated bacteria as the co-cultured bacteria is naturally present in the microalgal inoculation. The use of bacteria could reduce the chemical load required for flocculation, making the effluent media more suitable for recycle. However the use of bacteria will require additional bioreactors and nutrients to produce the quantities of bacteria required.

Some microalgae naturally flocculate more easily than others and this may be exploited to concentrate traditionally non-flocculating microalgae (Salim *et al.*, 2010). Not much literature is available on this topic. Salim *et al.* (2010) bioflocculated *C. vulgaris* with *S. obliquus* and *A. falcatus* and demonstrated increased recovery rates by way of bridging and patching mechanisms respectively, however the data was not presented rigorously enough for performance predictions. An advantage of this technique is that both microalgae may contribute biomass to the final desired product. Examples of bioflocculation and the experimental conditions are presented in Table 21 of Appendix 1A.

Major advantages of bioflocculation are the maintenance of cell integrity, opportunities to reuse media and use of low-cost and readily available substrates (Lee *et al.*, 2009a; Lian *et al.*, 2008b). Microbial flocculants are biodegradable and their degradation products are typically harmless to the environment. EBFs may be produced at high rates from microorganisms including bacteria, fungi, yeast, and algae are easily recovered from the culture (Salehizadeh and Shojaosadati, 2001). The use of small amounts of high molecular weight polymers to improve the flocculation, settling characteristics and harvesting efficiency of the basic bioflocculation process has been suggested (Sheehan *et al.*, 1998). This may improve floc stability and optimise sedimentation whilst pH and bioflocculant loading are the largest contributors to recovery efficiency (Oh *et al.*, 2001; Lian *et al.*, 2008b; Harith *et al.*, 2009). However this addition increases chemical loads within the recovery system.

Literature reports very little information on bioflocculation mechanisms and control thereof. As sources report up to 95% removal efficiencies (Oh *et al.*, 2001) (Table 21), further research into the general applicability and optimisation of this technique is recommended to address its possible industrial application.

2.4.5 *Electrolytic coagulation/flocculation*

Electro-coagulation involves the use of sacrificial, reactive electrodes to produce metal ions to induce coagulation. The amount of metal dissolved in solution (w) is proportional to the current (i) passed through the system described as follows:

$$w = \frac{itM}{nF} \tag{16}$$

with M being the molar mass, n the number of electrons in the oxidation/reduction reaction, and F is Faraday's constant.

The process proceeds via (Mollah *et al.*, 2004): the formation of coagulants, destabilisation of the colloidal suspension and the aggregation of this suspension to form flocs. Electro-coagulation is a form of chemical dosing correlated to dosing equivalence (Holt *et al.*, 2002; Alfafara *et al.*, 2002). Alternatively electrolytic flocculation may proceed by the migration of negatively charged algal particles towards the anode at which it loses the surface charge, allowing aggregation. This mechanism is coupled with the electrolysis of water, producing bubbles at the cathode. These bubbles provide flotation of the flocs. Some literature findings and experimental conditions regarding electrolytic coagulation/flocculation are presented in Table 22 in Appendix 1A.

2.4.6 *Pre-oxidation*

Oxidation of algae prior to concentration may improve recovery efficiencies (Shelef *et al.*, 1984). Oxidants such as ozone, chlorine, potassium permanganate and potassium ferrate have been suggested to improve algal recovery by inactivation (Henderson *et al.*, 2008b; Plummer and Edzwald, 2002; Chen *et al.*, 2009). In a review by Henderson *et al.* (2008b), improvements from pre-oxidation were attributed to four mechanisms: a significant change in external cell architecture occurs on oxidation (Chen *et al.*, 2009; Ma and Liu, 2002); the motion of flagellated species and gliding action of other species is impeded (Petrusevski *et al.*, 1996); diatoms excrete increased chitin which behaves as a coagulant aid (Petrusevski *et al.*, 1996); EOM may be degraded to remove its interference with flocculation (Hoyer *et al.* 1985).

Pre-oxidation has some drawbacks. Disinfection by-products form when using chlorine (Henderson *et al.*, 2008b). Pre-ozonation increases the dissolved organic carbon (DOC), decreases the algal viability and reduces algal cell size (Plummer and Edzwald, 2002; Hung and Liu, 2006). Chen *et al.* (2009) demonstrated an optimal dose of pre-oxidant for a specific microalgal strain. The type and amount of oxidant used is highly dependent on the system. Pre-oxidation is an attractive technique to improve the capability of dewatering techniques but is highly dependent on the system (Table 23, Appendix 1A).

2.5 Separation techniques

Solid-solid and solid-liquid separation technologies commonly used have been designed to enable separation on a broad range of physico-chemical properties. These properties of microalgae are typically strain-specific and may be modified or enhanced to increase recovery efficiencies. The magnitude of the driving force for each technique is determined by the design of the separation equipment to exploit the natural or induced suspension and

cell characteristics. Table 5 introduces these techniques and defines the algal suspension characteristics relevant to each technique in an initial attempt to construct a framework for separation based on first principle characteristics. Flocculation and sedimentation are dependent on the most physical properties.

Table 5: Suspension characteristics exploited by separative techniques

	Centrifugation	Electrolysis	Filtration	Flocculation	Flotation	Pre-oxidation	Unaided settling
Suspension concentration		X	X	X	X	X	X
EOM		X		X			
Cell density	X						X
Hydrophobicity	X			X	X		X
Cell motility	X		X		X		X
pH		X		X	X		
Ionic strength		X		X	X	X	
Settling velocity	X				X		X
Cell shape	X		X	X	X		X
Cell size	X		X	X	X		X
Surface charge		X		X	X	X	

2.5.1 Sedimentation

Sedimentation is the process by which solid particles suspended in a fluid settle under the influence of gravity or some other force. Sedimentation is the most traditional method of dewatering and is generally coupled with coagulation and flocculation to produce flocs which improves settling (Vlaski *et al.*, 1997). The counter force is defined as drag force, and the equilibrium between these forces define the settling characteristics of the particle. The speed of settling of non-flocculated particles is given by Stokes Law:

$$u_s = \frac{K'' d^2 (\rho_p - \rho_f) g}{\mu_f} \quad (17)$$

where u_s is the settling velocity, K'' is a shape factor, d is the particle diameter, ρ_p is the density of the particle, ρ_f is the density of the fluid, g is the gravitational constant and μ_f is the viscosity of the fluid. Equation 17 assumes creeping flow so that Re << 1 and that particles are axis-symmetric.

Sedimentation is typically used in wastewater treatment due to the large volumes and low cost of operation. On these systems, it is considered efficient for separation of particles bigger than ca. 70 µm (Munoz and Guieysse, 2006). Thus the speed of settling is strongly dependent on the particle size and density, with larger, more dense particles settling most rapidly (Coulson and Richardson, 2002). Based on Equation 17, the theoretical settling velocity of a spherical cell, with diameter 5 µm and density of 1070 kg.m^{-3}, is 0.0001 mm.s^{-1}.

Therefore there is a need to induce clumping to increase this rate. Methods have been developed to both increase the size of the settling particles and the difference in density between the floc and the medium (Vlaski *et al*., 1997). By agglomerating many algal cells and using a suitable flocculant, the settling time can be much reduced (Liu *et al*., 1999; Chen *et al*., 1998; Ayoub and Koopman, 1986; Tenney *et al*., 1969). Furthermore if a dense precipitate, such as calcium carbonate, is flocculated with the algae the settling time is further reduced (Ayoub and Koopman, 1986; Han and Kim, 2001).

No significant observations have been made on the basis of algal morphology as Henderson *et al*. (2008b) demonstrated with *Microcystis* and *Chlorella,* not being removed to any greater extent than cells with more complex structures of *Asterionella* or *Pediastrum*. Danquah *et al.* (2009b) investigated the settling rates of a mixture of *Tetraselmis suecica* and *Chlorococum sp.* and found the microalgae to settle at a faster rate when stored in the dark. This may be due to a degree of autoflocculation as microalgae are photosynthetic viz. when light is limited, their metabolism decreases. This reduces the net electronegative zeta shielding effect, causing the cells to agglomerate and settle faster (Danquah *et al*., 2009b). However cell motility and natural autoflotation may reduce settling rates (Jodlowski, 2002). Minimum settling rates for sedimentation to be considered a feasible recovery process have been estimated at 10 $cm.hr^{-1}$ (0.028 $mm.s^{-1}$) for batch operation. Settling rates faster than 100 $cm.hr^{-1}$ (0.28 $mm.s^{-1}$) could be considered for continuous processes such as clarifiers (Benemann *et al*., 1980). A summary table of flocculant effects on sedimentation is presented in Table 27, Appendix 1A. Sedimentation has much potential for commercial biomass recovery if suitable flocculation techniques are able to increase particle sizes and hence sedimentation rates without deteriorating the cell or media effluent.

2.5.2 Centrifugation

Centrifugation is essentially similar to sedimentation except that the acceleration is increased under a rotational field rather than gravity (Coulson and Richardson, 2002). The separation is based on Stoke's law (Equation 17) where gravity acceleration is replaced by centrifugal acceleration. The maximum through-flow (Q) for which all particles larger than d are captured, in a tubular centrifuge, is given by:

$$Q = \frac{d^2(\rho_s - \rho_c)R\omega^2 V'}{18\mu h} \quad (18)$$

with Q being the flowrate through the centrifuge, d the diameter of the particles, ρ_s the density of the particle, ρ_c the density of the fluid, R the radius of the centrifuge, ω the angular speed, V' the volume of liquid within the centrifuge, μ the viscosity of the liquid and h the depth of liquid in the centrifuge (Coulson and Richardson, 2002).

Equation 18 illustrates the dependence of the separation on particle size and density. Biomass recovery depends on the slurry residence time and settling depth and hence many different types of centrifuges have been developed to handle different suspensions, leading to different methods of solid discharge (Bailey and Ollis, 1986).

Centrifuges can be sub-divided into two major categories, stationary devices and rotating devices. There are many different kinds of centrifuges, including those for much specialised purposes ranging from preparative continuous tubular centrifuges in solid bowl or conical plate designs. Centrifugation has been reported as the most efficient, reliable and preferred

method of separation except for the high operational costs required (Chisti, 2007; Mohn, 1980; Grima *et al.*, 2003; Haesman *et al.*, 2000). Many microalgae can be harvested by centrifugation. A notable exception is filamentous organisms with gas vacuoles e.g. *Spirulina.* Due to the high operational costs, centrifugation is only used for producing extended shelf-life concentrates and high-value metabolites (Haesman *et al.*, 2000). Mohn (1980) investigated four different types of industrial centrifuges and reported concentration factors between 5 and 150 (Table 24, Appendix 1A). Haesman *et al.* (2000) tested three centrifuges for a range of species with removal efficiencies between 5 and 100% (Table 28, Appendix 1A).

Many algal slurries require speeds up to 13000g to achieve satisfactory separation which results in high shear forces (Harun *et al.*, 2010; Knuckey *et al.*, 2006). Centrifugation can thus damage cells, especially delicate organisms with ejectile organelles (Anderson, 2005; Haesman *et al.*, 2000). Centrifugation is extremely energy intensive but might be necessary as a final dewatering step after a preliminary concentrating technique to increase product reactor efficiencies.

2.5.3 Filtration

Coulson and Richardson (2002) define filtration as the collection and retention of solids by means of a porous medium or screen while allowing the liquid to pass. This dewatering technique therefore exploits the cell size and morphology predominantly. Several methods of filtration have been investigated in the literature; each method pertaining to a different application with specific advantages and disadvantages. Filtration methods have higher energy and maintenance requirements compared to sedimentation; however simple filters may be used as pre-concentration steps. These methods of filtration include: microstraining, rotating drum filters, pressure and vacuum filters (Shelef *et al.*, 1984), magnetic filtration (Bitton *et al.*, 1975) and membrane filtration (Petrusevski *et al.*, 1995).

The conventional dead-end filtration process using a filter bed of diatomaceous earth or a filter cloth under pressure or suction is most appropriate for harvesting of relatively large (>70 µm) microalgae such as *Coelastrum* (Brennan and Owende, 2010) and filamentous algae such as *Spirulina* or colony forming microalgae such as *Micractinium sp.* (Grima *et al.*, 2003; Lee *et al.*, 2009a). For the recovery of smaller, fragile algal cells (<30 µm), membrane microfiltration and ultra-filtration are feasible options (Brennan and Owende, 2010; Petrusevski *et al.*, 1995). In the harvesting of filamentous algae, such as S*pirulina,* screen filtration is used with much larger pore diameters than the cellulosic or polycarbonate membranes used for bacterial harvesting (Spolaore *et al.*, 2006). This technique ensures the removal of unwanted protozoans and viruses depending on the filter size, allowing the filtrate to be recycled as media (Zhang *et al.*, 2010). Membrane filtration is therefore suitable for very shear sensitive suspensions (Rossignol *et al.*, 1999).

Middlebrooks *et al.* (1974) report on a number of research groups' results with microalgae and total suspended solids (TSS) removal efficiency of 85% or more on average for basic microstariners. Mohn (1980) tested five different pressure filtration systems, reporting final TSS concentrations between 5 and 27% starting from an initial concentration of 0.1% and five different vacuum filtration systems, reporting concentrating factors between 2 to 180. Petrusevski and co-workers (1995) found that recovery efficiencies were relatively insensitive to concentration factors and small cylindrical diatoms and *Rhodomonas* were

shown not to be suitable candidates for this method due to the low recoveries achieved, whilst *Stephanodiscus hantzschii* was removed by 97% given their larger size. This confirms that filtration is the dewatering process most susceptible to variations in algal functionality.

Filtration is an effective method of separation for several species of algae, but its effectiveness is strongly determined by the morphology of the species, cell size, extracellular organic material and density of the cultivated culture. The literature presents filtration to seem an attractive dewatering process option, but these techniques are associated with high operating costs and hidden pre-concentration requirements. Pre-concentration techniques as well as the use of other concentrating techniques in conjunction with filtration should therefore be investigated. A summary of the results presented in literature using filtration techniques to recover microalgae is presented in Table 25 in Appendix 1A.

2.5.4 Flotation

Flotation is a physico-chemical type of gravity separation and may be seen as the exploitation of the natural floating behaviour of microalgae. Growth and suspension conditions may impact on cell buoyancy, but in order for this physico-chemical property to be exploited, it must be coupled with mechanical flotation. Flotation is a selective process that operates by passing bubbles through the solid-liquid mixture allowing the desired solid particle to become attached to the bubble surface. The particles are carried to the surface of the liquid and accumulate. This accumulated material can then be skimmed off (Uduman *et al.*, 2010). Traditional methods of flotation include: dissolved air flotation, electrolytic flotation and dispersed air flotation. The predominant driving forces for this process are cell hydrophobicity, air-cell contacting mechanisms (Shelef *et al.*, 1984), bubble-cell transport and mechanical froth collection.

Flotation dewatering seeks to exploit the hydrophobic surface properties of the algal cell by addition of chemicals. As discussed in Section 2.2.3, algal cells have negatively charged surfaces. This may be adjusted by the addition of suitable chemicals and induce flocculation. Without coagulation, both air bubbles and particles carry negative zeta potentials. This causes a natural repulsion force between bubbles and algae. It is possible to produce particles and bubbles of opposite charge, which could produce electrostatic attraction (Edzwald, 2010). Hydrophobic forces also form van der Waals force attraction between bubbles and particles. Therefore the optimal operation would occur for hydrophobic particles that are neutrally or positively charged. The surface characteristics of algal cells seem to be fairly constant over a range of species, with collectors working on species with vastly different morphologies. This suggests that a common collector could be used for any algal flotation (Chen *et al.*, 1998; Yan and Jameson, 2004; Roh *et al.*, 2008).

Flotation can only occur if sufficient collision between the bubbles and particles, and the adhesion of the particles on the bubbles is obtained. The contacting mechanism has been proposed by way of bubble nucleation at a solid interface, bubble entrapment within flocs, and the collision and adhesion of preformed bubbles with particles (Henderson *et al.*, 2008a). Chen *et al.* (1998) and Liu *et al.* (1999) reported the electrostatic interactions between collector and cell surfaces to be critical in flotation efficiency. Therefore the choice in chemical addition is crucial to the success of the process. Further investigation of pH and

ionic strength yielded significant dependence of efficiency on these factors; whilst air flow rate and alkalinity fluctuations were shown to be less significant.

Algae produce oxygen during photosynthesis which diffuses into the surrounding medium. Depending on the oxygen saturation of the medium, it may leave the liquid phase and form bubbles. When these bubbles are included in the formation of algal flocs, the overall density of the flocs allow for separation via natural flotation (Lee *et al.*, 1992). Autoflotation works optimally when flocculation occurs undisturbed and mixing is at a minimum, thus the best operating conditions occur in a still tank, just after the period of strongest light.

Much work has been done on flotation as a method of waste algal removal. Results have been promising in terms of possible application to algal harvesting from concentrated cultures (Pott, 2009; Féris and Rubio, 1999; van Puffelen *et al.*, 1995). The efficiency of the separation is dependent on the bubble size, contacting and forces between the bubble and algal flocs (Yan and Jameson, 2004; Roh *et al.*, 2008; van Puffelen *et al.*, 1995). Without the use of coagulants (natural flotation), a low percentage (<40%) *Scenedesmus* recovery was observed in batch and pilot plant test results (Bare *et al.*, 1975). The addition of ferric sulphate and alum recovered greater than 90% of *Scenedesmus* in batch and pilot plant test units. Algal separation via autoflotation of up to 90% was achieved by Lee *et al.* (1992). A summary of the literature data is presented in Table 29 and Table 30 in Appendix 1A.

Flotation is considered to be quicker and more efficient than sedimentation (Henderson *et al.*, 2008b; Chen *et al.*, 1998; Shelef *et al.*, 1984) as it possesses the advantage of rapid operation (Liu *et al.*, 1999), low space requirements, flexibility of application and moderate cost (Lin and Huang, 1994); however compression costs to supply air for bubbles may be too energy intensive. Flotation, in whatever form, is a suitable method for algal concentration and, depending on the species being cultivated, may be the most effective method available. The addition of chemicals needs to be further investigated to determine if it is possible to have an efficient flotation separation without any contaminating chemicals. The energy requirements of compression must also be investigated.

2.5.5 Series of methods

In many cases, due to machinery limits it is typical to use one technique to maximise recovery of algae to a reduced volume (concentrate) and a different technique to dewater to maximise the concentration. In this instance, more than one harvesting technique may be used in series or in parallel to obtain the desired separation. Pre-oxidation has been proposed by a number of research groups to improve removal efficiencies (Table 23). If an effective method of flocculation is possible, this could ultimately precede all other methods. Coagulating microalgae to form larger flocs benefits almost all of the mechanical dewatering techniques (Table 30, Appendix 1A). Flocculation followed by sedimentation has the greatest potential if flocculation techniques are developed to reduce chemical requirements. Centrifugation may be required to further reduce the water content prior to product reactions.

2.6 Dehydration of biomass

Theoretically it requires approximately 3.5 MJ to remove 1 kg of water via thermal drying, thus any other dewatering technique is beneficial from an energy perspective. The before mentioned methods are used to concentrate algal suspensions of ca. 0.02 to 0.06% TSS into a slurry or paste containing ~5 to 25% TSS (Shelef *et al.*, 1984). This process may happen in one step or combination of many steps (Figure 4, adapted from Shelef *et al.* (1984).

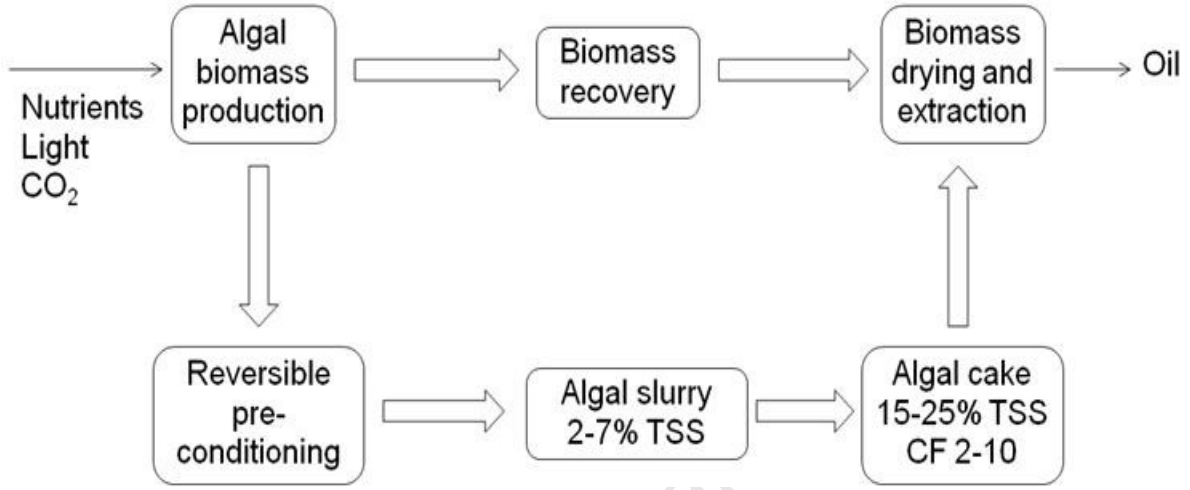

Figure 4: Schematic of microalgal biomass recovery and dewatering

The resultant concentration from the dewatering techniques has a great influence on the subsequent process steps such as drying and product extraction. The dehydration step in the process is one of the most expensive steps with literature values ranging from 20 to 75% of the total processing costs (Uduman *et al.*, 2010; Grima *et al.*, 2003; Shelef *et al.*, 1984). Shelef *et al.* (1984) highlighted a number of possible techniques for drying biomass, namely: flash drying, rotary driers, toroidal driers, spray drying and sun drying. The selection of drying technique is highly dependent on the scale of operation, desired product and requirements of the downstream extraction processes (Mohn, 1980). Biomass drying is therefore a crucial process of microalgae dewatering and requires much research prior to industrialisation.

2.7 Conclusions

The algal dewatering literature makes reference to many different species of microalgae. *Chlorella vulgaris* and *Scenedesmus* are most often reported and it has been demonstrated that these strains offer possible application for oil for biodiesel production due to their relative ease of cultivation and lipid contents (Griffiths *et al.*, 2011; Griffiths and Harrison, 2009).

Among the techniques investigated, flotation and sedimentation provide the most promising results with respect to the outlined criteria. These two techniques exploit the natural tendency of microalgae to float or sink. Table 6 provides a summary of the various techniques investigated.

Table 6: Summary table of techniques investigated and averaged literature removal efficiencies, concentration factors and energy requirements

Method	%TSS concentrate, (CF), [removal efficiency]*	Energy consumed ($kWh.m^{-3}$)*
Electrolysis	[85.97]	18.51
Unaided sedimentation	1.55, (15.5)	0.10
Ultrasound chamber	(20.8), [54.4]	300.
Flocculation/sedimentation	[78.82]	-
Centrifugation	10.7, (55.00), [72.3]	12.25
Filtration	11.46, (150.99), [77.7]	1.17
Flotation	[88.75]	7.65
Flotation/flocculation	[85.51]	-

*Averages from several sources of literature presented in Appendix 1A

The preceding table should only provide a general overview of each technique as every research group quoted has investigated many different algal strains with differing conditions. Filtration is also an attractive option, but due to the mechanical operation, could have many disadvantages. The literature reports dewatering success in many differing ways and this may cause confusion. For completeness, concentrating factor, removal efficiency and energy consumed should be reported. Due to the large difference in surface and suspension characteristics between strains, a first principles approach is required for each technique.

Cell and suspension density, EOM, hydrophobicity, pH, light and nutrients limitation, ionic strength, growth stage, surface charge, cell morphology, cell motility and temperature affect the choice and efficiency of dewatering techniques. These parameters are also intrinsically dependent on each other. If a time, concentration, chemical and energy efficient microalgal technique is to be developed, these physico-chemical properties need to be fully characterised. High costs and energy requirements eliminate the dewatering technique choice of centrifugation, ultrasound, filtration and flotation. Chemical flocculation and electrolysis require high concentrations of chemical dosing which increases downstream energy and cost requirements. Sedimentation is therefore the best choice provided that sedimentation rates and recovery efficiencies may be increased. To induce stable, larger particles, a form of flocculation must be induced in such a way to minimise downstream processing requirements of effluent water and nutrients, maximise particle size and stability and ensure negligible cell damage.

Flocculation has been identified as a fundamentally critical process to ensure effective dewatering. This technique has been reported to occur in many ways. Auto- and bioflocculation are poorly understood techniques with promising potential. Much research has been done on various flocculation techniques using many types of flocculants; however very little literature is presented on the flocculation dependency on EOM and the mechanisms governing these flocculation techniques. Flocculation without the use of toxic chemicals followed by sedimentation is therefore seemingly the optimal process. However not much literature is reported on process efficiencies and feasibilities with regard to a series of techniques. Current research papers scarcely mention the recycle of water.

Separation in the absence of toxic chemicals is a priority due to the large volumes of water within the system. Cross-flow membrane filtration may be a possible technique to purify the effluent water by removing cell debris, bacteria and any other contaminants. The dehydration of this concentrated biomass also needs to be investigated.

Many different dewatering techniques have been proposed and investigated. The literature on each of these techniques is diverse and widespread over a range of different fields of interest. It was observed through the literature, the effects of surface and suspension properties on separation. While the principle of operation of solid-liquid separation techniques has been discussed previously, a summary of the performance of each approach with respect to algal dewatering is presented in Table 21 to Table 30 in Appendix 1A. These tables allow for the reader to assess the usefulness, conditions under which these techniques were used and the success of each technique. This leads to the need for a first principles approach to characterize and modify these techniques for optimisation.

3 PROPOSED WORK

3.1 Problem statement

In addition to their potential role in high-value products, market trends and fuel demands have initiated renewed interest in microalgae for bioenergy. However the recovery of the biomass from the algal suspension has been claimed to contribute 20 to 40% to the total cost of production (Gudin and Therpenier, 1986; Grima *et al.*, 2003). Algae are often low value products suspended in large volumes of water. Therefore there is much need for efficient algal dewatering techniques with concomitant water recovery. These unit operations are typically dependent on the algal species chosen, culturing technique and operating conditions. Each species presents an array of intrinsic challenges such as small cell sizes, low densities, dilute suspensions, variable surface properties and sensitivities to the environment. A suitable low-cost, species-specific technique is therefore required that allows for effective water and nutrient recycle, high algal removal efficiency and concentration, whilst ensuring negligible cell damage and minimal energy use. The problem is therefore to associate a specific or series of dewatering methods, at certain optimised conditions, to a specific strain at fixed optimised conditions. This operation should exploit the physico-chemical properties of the chosen strain. A general understanding of the effects of algal morphology and suspension characteristics on the dewatering methods may then be concluded.

3.2 Objectives and scope of study

The primary objective of this research project is to assign and optimise a low-cost and low-energy algal biomass recovery technique by investigating the effects of the species-specific properties of microalgae on biomass dewatering techniques. Within this objective, key suspension variables affecting recovery efficiencies are identified and quantified. The interdependencies of these properties are also studied. Suspension rheology is also characterised to obtain upper limits of cell concentrations allowed for transportation. This understanding may reveal possible improvements and optimisations on current techniques and methodology for concentrating microalgae. An approach from first principles is required. An efficient biomass recovery technique will contribute to the eventual design of an optimised biorefinery. These findings also contribute to cell colloid science with respect to suspension effects on cells.

The microalgal surface properties such as hydrophobicity and zeta potential, as well as cell morphology of the algae are examined. Microalgal characteristics are evaluated in terms of each technique's separative mechanism to decide which method suits which species best and why. Suspension properties such as pH and conductivity affect the chemical interactions between cells and other between other particles and therefore these will also be investigated. To enable this investigation suitable strains which have market potential are required. These species must meet commercial production criterion and therefore studies on optimal growth of the organisms is carried out to enhance recovery efficiency. This

dissertation initially describes the growth parameters and investigates a number of physico-chemical properties during the different growth phases. Broad understanding of the particle and suspension properties is needed to choose a suitable and optimal design and operating conditions of each separative technique. Some innovative improvements and procedures are needed to achieve these objectives and this thesis attempts to suggest a possible way forward. Downstream processes and effluent recycle are also investigated.

Separation results are compared to current recovery efficiencies found in literature, taking into account the time of separation, approximate energy requirements and chemical dosages required. Changes in suspension conditions are assessed by changes in cell surface properties achieved to improve colloidal instability. As many of these physico-chemical properties affect each other physically in a system, these properties are exploited to determine the inter-relationships between each parameter. The results sections discus each of these findings in relation to all other preceding results within in the report to draw preliminary conclusions and highlight particular operating conditions which show increased potential for separation. The discussion takes all findings into consideration to generate an overall mechanistic approach and understanding of the microalgal separation process as a whole. The discussion draws on each physico-chemical property investigated and comments on the interdependencies of these properties.

3.3 Hypotheses and key questions

1. The understanding of species-specific surface properties and cell morphology provides understanding to define how to manipulate and target suspension conditions.
   - What is the controlling principle of separation/mechanism in each of the chosen separation techniques and which factors may be best exploited to maximise recovery and concentration?

2. Microalgal suspensions display Newtonian rheological behaviour. Further, in the operating concentration regimes of both growth and biomass recovery, the resultant viscosities do not constrain process unit operations. Their prediction is required for design purposes.
   - What is the yield point?
   - What is the upper limit for suspension concentration to remain within a Newtonian flow regime?
   - Does flocculation affect rheology?

3. Auto-flocculation may be induced, in the absence of chemical flocculants, by understanding changes in cell surface properties through the growth cycle. Microalgae will tend to auto-flocculate reversibly around the isoelectric point due to neutralisation of the surface charge and/or hydrophobic interactions.
   - What variance in pH, surface charge, hydrophobicity, cell size and EOM is present during growth of the algae? Are these inter-related?
   - Does the manipulation of pH allow for autoflocculation and what role does surface charge have?

4. Bio-flocculation may be induced by the introduction of a bacterium at a specific pH, causing bridging adhesion and floc formation between algae and bacteria. The bacteria cells form a bridge network between microalgal cells.
    - Which bacterium, typically co-cultured with algae, will produce bioflocculants, and is it possible to induce bioflocculation?
    - What effect does surface charge have on the degree of bioflocculation?
    - Can other biomolecules be used instead of bacteria?

5. Flocculation followed by sedimentation may be initiated in series without having to significantly alter suspension conditions for the separation of algae and recovery of effluent water.
    - What detrimental effects does the recycled effluent water have on growth and why?
    - How does this method compare to traditional chemical flocculation and what is the best technique to minimise chemical usage?

The following general questions relate to all of the preceding hypotheses:

- What effect does the growth phase have on the specific parameters and efficiencies and hence during which growth phase will separation be maximised?
- What is the optimal separation technique and what properties and suspension conditions are responsible?
- Which flocculation mechanism is the most efficient for each species with regards to flocculating agent and water contamination?

3.4 Experimental plan

The experimental approach in this work entails the selection and growth of suitable strains in airlift reactors to determine growth phases, assays, cell acclimations and biomass productivities. Isolated and co-cultured bacteria are also analysed. Investigation of naturally occurring surface properties of the algal suspension during growth is followed by changes in suspension properties to examine physico-chemical property changes of the cells. The effects of natural and induced flocculation as well as bioflocculation are then investigated in terms of suspension characteristics and flocculation efficiencies. Parameters such as pH, particle size, surface charge and hydrophobicity are related to the recovery mechanism. The separative mechanisms are then identified and characterised from the aforementioned results combined with microscopic images, followed by an investigation of non-floc sedimentation. An evaluation of the removal efficiency, mechanisms and performance of the process is then carried out. Effluent water and culture medium is then recycled to assess the quality of the effluent. Reactor starting pH, conductivity as well as CO_2 feed concentration are varied to examine the effects and to classify any growth inhibitions. Results are compared to literature findings and discussed with recommendations.

The following diagram represents a summary overview of the proposed experimental studies.

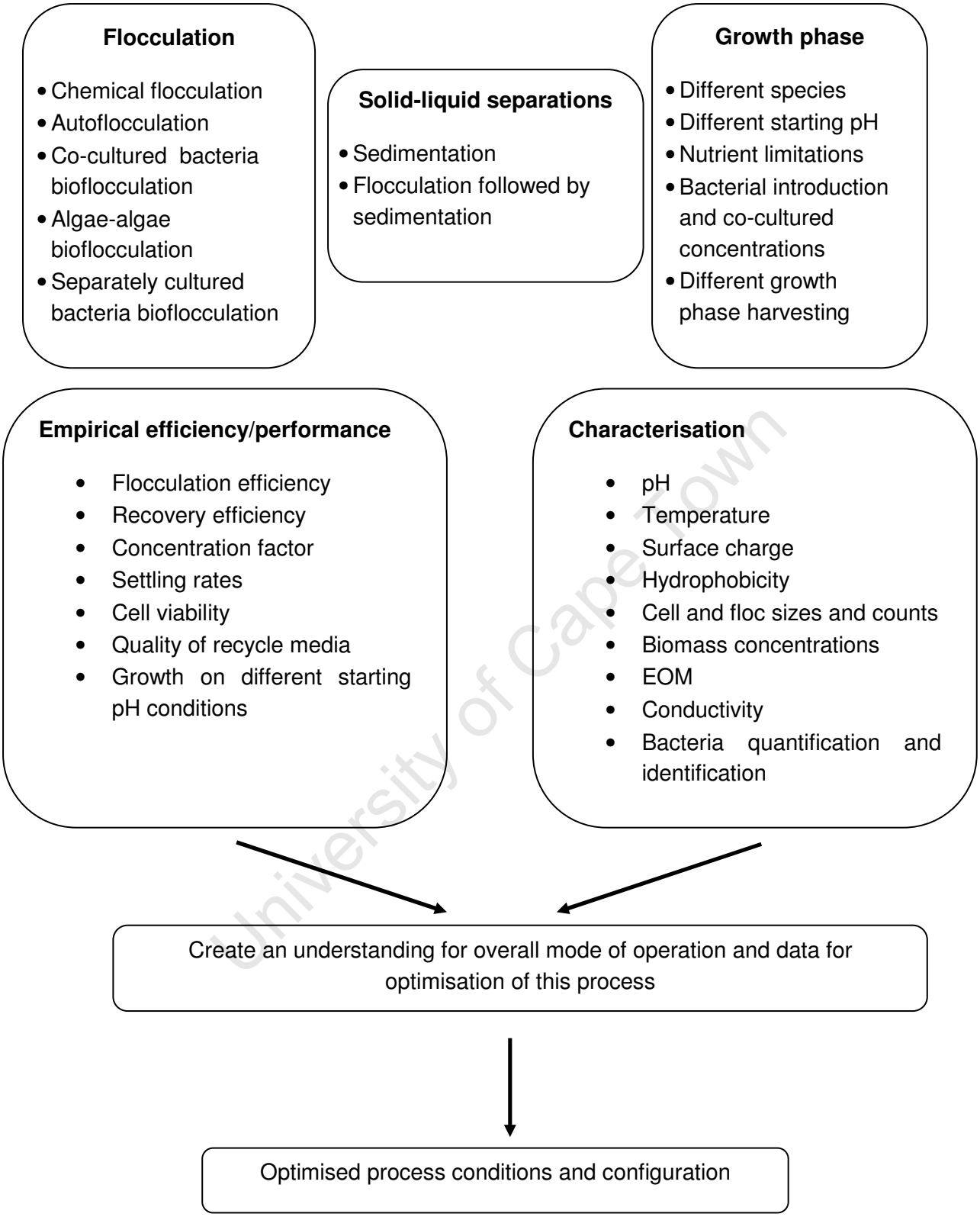

Figure 5: Conceptual overview of proposed experimental plan

4 MATERIALS AND METHODS

4.1 Microbes

4.1.1 Microalgae

Two freshwater, green microalgae were investigated. *Chlorella vulgaris* (UTEX 395) was obtained from the University of Texas, Austin, USA (UTEX), and *Scenedesmus sp.* was isolated from Upington, South Africa. The microalgae were cultivated in 3.2 L airlift photobioreactors using sterile, modified Bristol (UTEX) media containing ($mg.L^{-1}$): 750. $NaNO_3$, 25.0 $CaCl_2.2H_2O$, 75.0 $MgSO_4.7H_2O$, 75.0 $K_2HPO_4.3H_2O$, 175. KH_2PO_4, 25.0 NaCl, 750. Na_2EDTA, 97.0 $FeCl_3.6H_2O$, 41.0 $MnCl_2.4H_2O$, 5.00 $ZnCl_2$, 2.00 $CoCl_2.6H_2O$ and 4.00 $Na_2MoO_4.2H_2O$.

Stock cultures of both species were grown in 1 L Schott bottles under constant illumination with two 18 W cool white lights with photon irradiance of 300 $\mu mol.m^{-2}.s^{-1}$ and sparged with 1% CO_2 at 1 $L.min^{-1}$. The gas line was filtered through a hydrophilic PVDF 0.45 µm Millipore filter prior to entering the stock cultures. Stock cultures were grown on sterile modified Bristol (UTEX) media at neutral pH and the cultures were replenished with media after inoculating the airlift photobioreactors to a suitable level. Aliquots for inocula were aseptically transferred in a laminar flow hood to avoid contamination. Figure 6 depicts the stock cultures of *Scenedesmus sp*. and *Chlorella vulgaris*.

Figure 6: *Scenedesmus sp.* and *Chlorella vulgaris* stock cultures

4.1.2 Bacteria

Escherichia coli, BL21 (DE3) was obtained from the Biocatalysis Laboratory of Professor Martie Smit, University of the Free State, South Africa. *Bacillus sp.* was locally isolated and donated by Dr. Caryn Fenner.

Bacteria co-cultured with *Scenedesmus* sp. and *Chlorella vulgaris* in the airlift photobioreactors were isolated by plating out 100 µL culture on Luria broth agar (LBA) plates to isolate axenic colonies. Colonies were analysed both by eye and under a light

microscope (100x) to identify distinct morphologies which would indicate individual species. Each distinct parent colony was then used to inoculate 5 ml of Luria broth and grown at room temperature with gentle agitation until a turbid culture was obtained. Samples were pelleted through centrifugation and DNA was extracted by kit (High Pure PCR template extraction kit, Roche).

A ~1.4 kb 16S rRNA fragment was amplified by PCR (Hybaid thermal cycler, Thermo-Fisher) with universal 16S primers (Sequences not published) and Universal Pro Fast Mastermix (KAPA Biosystems) as per manufacturer's instructions. Cycling conditions of 1x (95℃, 5 minutes), 35x (95℃, 10 seconds; 60℃, 15 seconds; 72℃, 20 seconds) were used. The PCR product was subjected to electrophoresis on a 1% agarose gel at 75mV until separation was achieved. The 1.4 kb fragment was isolated and purified using the QIAquick gel extraction kit (Qiagen). The purified fragments were then ligated into pGEM-T Easy (Promega) as per manufacturer's instructions. *E. coli* BL 21 heat-shock competent cells were transformed with the constructed plasmids and plated onto Xgal/IPTG/Ampicillin Luria broth plates, as per manufacturer's instructions.

The transformed colonies (white) were used to inoculate 5 ml Luria broth containing ampicillin and grown overnight at 37℃, with shaking. Plasmid was harvested from the culture using the GenElute kit (Sigma-Aldrich). The purified plasmids were quantified on a Nanodrop ND-2000 (Thermo) and sequenced (Central Analytical Facility, University of Stellenbosch). Sequences were then analysed by BLAST via NCBI (National Library of Medicine, 2011) to identify species by species homology.

4.2 Chemicals

Chemical name	Chemical formula	Manufacturer	Art/CAS #
Agar bacteriological	-	Merck	HG000BX1.500
Antifoam 204	-	Sigma	A6426-500G
Calcium chloride	$CaCl_2.2H_2O$	Ass. Chem. Ent.	10043-52-4
Carbon dioxide	CO_2	Air Liquide	UN1013
Chitosan	(from crab)	Sigma-aldrich	417963-25G
Cobalt chloride	$CoCl_2.6H_2O$	Merck	1.02539.0250
Hydrochloric acid	HCl	Merck	SAAR306302LP
Ferric chloride	$FeCl_3.6H_2O$	Unilab	2340520
Sodium nitrate	$NaNO_3$	Merck	SAAR5824000E
Magnesium sulphate	$MgSO_4.7H_2O$	Merck	SAAR4124000E
Magnesium chloride	$MgCl_2$	Merck	SAAR4123000E
Manganese chloride	$MnCl_2.4H_2O$	Merck	SAAR412000EM

Dipotassium hydrogen phosphate	$K_2HPO_4.3H_2O$	Merck	A0074404009
Potassium dihydrogen orthophosphate	KH_2PO_4	Merck	SAAR50436600E
Pancreatic digest of casein	(tryptone powder)	Merck	HG000BX4.250
Potassium chloride	KCl	Merck	SAAR5042020E
Sodium di-hydrogen orthophosphate	Na_2HPO_4	Merck	5822680EM
Perchloric acid	$HClO_4$	Holpro	76544Q
Sodium chloride	NaCl	Merck	SAAR5224000E
EDTA disodium	$C_{10}H_{14}N_2Na_2O_8.2H_2O$	Merck	SAAR2236020E
Sodium molybate	$Na_2MoO_4.2H_2O$	Univar	5823900
Sodium hydroxide	NaOH	Merck	SAAR191396LL
Yeast extract	-	Merck	HG00013X6.500
Zinc chloride	$ZnCl_2$	Merck	SAAR7581220

4.3 Reactor design and operation

Scenedesmus sp. and *Chlorella vulgaris* were cultivated in glass and stainless steel airlift internal loop reactors which were specifically designed for the purposes of microalgal cultivation. The reactors (Figure 7) were equipped with a thermocouple to monitor temperature and had multiple sampling points at the top of the reactor. The reactors were equipped with cooling coils near the gas inlet. The glass and stainless steel reactors were 0.6 m high with an external diameter of 0.1 m, a draft tube of 0.05 m diameter and a working volume of 3.2 L. The vertical reactors were arranged next to each other and the surrounding areas of the reactor were covered in aluminium foil to reflect maximum light. The sparger at the bottom of the draught tube was a 0.22 µm stainless steel HPLC inlet filter. The gas line was filtered through a hydrophilic PVDF 0.45 µm Millipore filter prior to entering the reactor. Figure 7 depicts the airlift photobioreactor used with size dimensions.

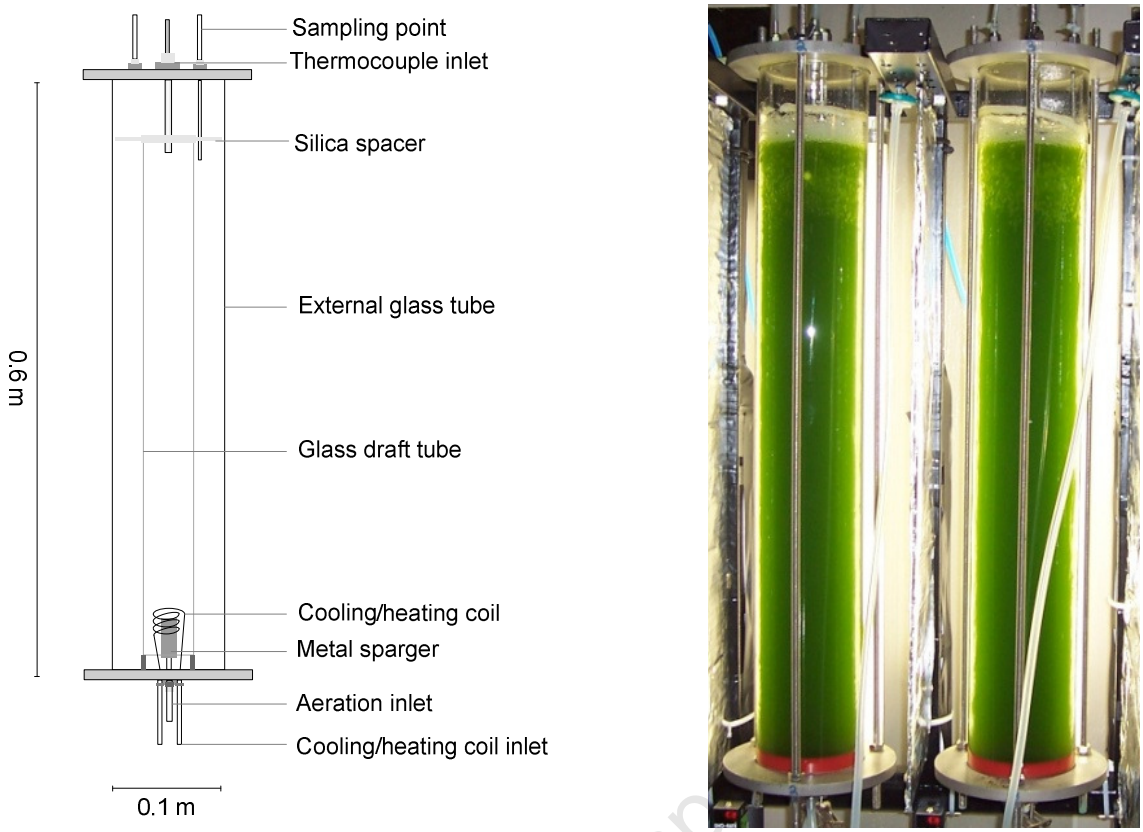

Figure 7: Closed airlift photobioreactor with working volume of 3.2 L

The cultures were grown at 25 ± 2℃ with an initial pH of 6.9 ± 0.1 and constantly illuminated with three 18 W cool white lights with photon irradiance of 300 µmol.m^{-2}.s^{-1} at a distance of 3 cm from the column surface. A 30 µL aliquot of Antifoam 204 was added to each reactor to increase mass transfer and reduce foaming. The airlift photobioreactors were filled with growth media prior to autoclaving for sterilisation (Everlight Vertical Type Autoclave, Laboratory Supplies, RSA). Cultures were then inoculated to approximately 0.03 g.L^{-1} from stock shakeflask cultures. Reactors were sparged at 2 L.min^{-1} on either air or 2900 ppm CO_2 controlled by Brooks smart II mass flow controllers (KDG Flowmeters, England; Sho-rate rotameters, Control Valve Technology, SA) throughout the growth cycle and blended in an inline mixer. This allowed for 1.5 and 5.5 seconds residence time in the draft tube and downcomer respectively. Due to daily evaporation, the reactors were topped up with approximately 100 ml sterile distilled water.

4.4 Assay procedures

4.4.1 Dry weight

To determine biomass concentrations for the construction of growth curves, a dry weight assay of the microalgal suspensions was needed. As the cultures are dilute and the cells are microscopic, a suitable filtration technique was needed. Depending on cell density, 10 to 40 ml of algal culture was vacuum filtered using 0.45 µm cellulose nitrate (Sartorius stedium) filter papers. Filter papers were then dried overnight in a 60°C oven to remove any remaining water. Dried filters were weighed on an analytical scale with a detection limit of 1x 10^{-4} g. For cell concentrations above 200 $g.L^{-1}$, 2 ml Eppendorf tubes were used and dried overnight in an 80°C oven. Bacterial concentration was measured using serial dilution plates to determine viable counts, optical density readings at 600 nm to measure concentration through turbidity and dry biomass. Dry mass was determined by centrifuging 2 ml of culture in microfuge tubes at 13000 rpm for 5 minutes in a Heraeus Pico Biofuge. After decanting the supernatant, the pellet was washed once, re-centrifuged and decanted. The pellet was dried overnight to obtain a cell dry weight. Triplicate measurements were done for error analysis and standard calibration curves were constructed. Standard deviations are presented in Section 5.1.

4.4.2 Cell concentrations

Cell sizes, shapes and counts change according to biomass concentrations and growth phase. Microscopy was used for floc identification and evaluation of floc sizes, cell sizes, cell counts, cell viability and variances in data. Flocculant-algae interactions were also observed under microscopy. A Hawksley Thoma cell counting chamber was used for cell counting (Appendix 8.6.2). An aliquot of 1.2 µL of well-mixed cell culture was analysed under 40x phase contrast objective for algal cells and 100x for bacteria cells using an Olympus BX40 microscope with a built in Colourview digital camera. An example of the counting is presented in Appendix 1A. As this technique only focuses on small samples of culture at a time, 6 samples were counted to render standard deviations presented in Section 5.1 with concentration calculated as:

$$Cells.ml^{-1} = 3.125*10^{5} \text{ x total cells counted in 4 big squares} \quad (20)$$

where the coefficient is derived from the cell dimensions (Figure 65).

4.4.3 Cell pigment measurements

Absorbance or optical density can be used to approximate biomass concentration on the basis that denser cultures absorb more light. For algal cultures, a wavelength of 750 or 680 nm was used, with 750 nm being outside the range of absorbance by the pigments present. Light at a wavelength of 680 nm is absorbed by chlorophyll; hence the absorbance per unit biomass changes with pigment content. The concentration of well mixed aliquots of 2 ml cell cultures was analysed using a Unicam, Helios α spectrophotometer with rotating carousel. Algal spectrometry readings were taken at 680 and 750 nm whilst bacteria samples were analysed at 600 nm. All the samples were diluted so that the OD measurements lay within the suitable range (<0.8). Above this, the Beer-Lambert relationship is no longer linear. Sterile distilled water was used as the zero value. Standard calibration curves were

constructed using appropriate dilutions. Cells lysis or bleaching due to acidic or alkaline conditions was determined by measuring the chlorophyll *a* content via spectrometry at 680 nm. This measurement was compared to a dry weight value from a standard calibration curve (Figure 67) at 750 nm. Standard deviations are presented in Section 5.1.

4.4.4 Conductivity and pH

Culture media contains dissolved salts which contribute to ionic strength together with EOM and pH. Ionic strength may be approximated by conductivity at low concentrations. Conductivity is the ability of a material to conduct electric current. Since the charge on ions in solution facilities the conductance of electrical current, the conductivity of a solution is proportional to its ion concentration. In some situations, however, conductivity may not correlate directly to ion concentration at high ionic strengths (Griffin and Jurinak, 1973). Cell surface chemistry is predominantly affected by pH and conductivity (Bernhardt *et al.*, 1985) and hence these variables need to be characterised to understand microalgal colloid science.

Conductivity and pH were measured during microalgal growth and all dewatering experiments. A Cyberscan 2500 meter and Cyberscan micro electrode EC620-133 from Wirsam were used for pH measurements. Conductivity was measured using an AZ 86555 conductivity meter. Conductivity was adjusted using $MgCl_2$. NaOH and HCl were used for pH adjustments. As pH affects ionic strength, phosphate buffered saline (PBS) was prepared using ($g.L^{-1}$): 8.0 NaCl, 0.20 KCl, 1.44 Na_2HPO_4 and 0.24 KH_2PO_4 to buffer the suspensions. The effects of growth of microalgae in photobioreactors on pH and conductivity of the suspending medium were also investigated. Conductivity and pH detection limits were 1 $mS.cm^{-1}$ and 1 x 10^{-2} pH units respectively. Standard deviations are presented in Section 5.1.

4.4.5 Suspension rheology and apparent viscosity

Concentration and suspension conditions affect the rheology of a culture (Chen *et al.*, 1997). Algal fluid rheology needs to be understood prior to the choice and design of any separation- or process-based application to determine any engineering limitations to downstream processing. Shear stress, shear rates and viscosities were measured across a range of concentrations for *Scenedesmus sp.*, *Chlorella vulgaris* and the co-cultured bacteria at 25°C using a Physica Rheolab MC1 instrument with remote control. For viscosities up to 0.2 cP, a Z1 DIN double gap spindle was used. For viscosities above 0.2 cP, a Z2 DIN 45 mm spindle was used. Changes in viscosity due to flocculation were also investigated by the addition of $MgSO_4$ or a suitable bioflocculant with pH adjustment. Matlab 2009a (cftool) was used to fit models to data and describe apparent viscosity and shear thickening trends. The rheometer detection limit was 1 x 10^{-6} cP. Standard deviations are presented in Section 5.1.

4.4.6 Size distribution

Floc and cell sizes vary with changes in suspension conditions during growth. Due to the high number of cells in a sample, a quick, efficient technique for estimating particle size was required. Laser diffraction is a common technique employed to obtain these results. Laser diffraction units do not measure particle size distributions but carry out light scattering

experiments. The relationship between the light scattered by the particles and the final particle size distribution reported depends upon assumptions made about the optical properties of the material under study (Wedd, 2003), such as: complex refractive index, the dispersion procedure, the dispersion medium, the theory used to calculate the PSD from the diffraction angles, and the shape of the particles.This technique was therefore complemented by microscopy sizing techniques, described in Section 4.4.2 and shown in Section 6.6.

A Malvern Hydro 2000G Mastersizer was used to determine microalgal size distributions during growth and flocculation. Obscurations of between 11 and 18% were used depending on the size of the particles measured. A standard operating procedure was created for green microalgae having a refractive index of 1.013 (Aas, 1996; Bricaud *et al.*, 1988) and absorbance of 0.35 (Malvern Hydro 2000G mastersizer user manual). Ultrasound was employed only during growth size distribution studies to break up particles; however no ultrasonic mixing was used during flocculation tests. Flocs were induced *in situ* via autoflocculation and bioflocculation and the floc sizes were measured over a range of pump speeds (75 – 2500 rpm) with a constant agitation speed of 30 rpm (n = 4). Pump speeds were correlated to shear rates by the following correlation:

$$\text{Shear rate} = \frac{Q}{R^3} * 1.124 \qquad (19)$$

where shear rate is measured in s^{-1}, Q is flowrate ($L.min^{-1}$) and R is internal diameter (cm). The correlation between pump speed and flowrate is present in Figure 85.

Mean values for daily recordings were utilised to account for natural flocs formed during cell reproduction. The instruments detection limit was between 1 x 10^{-3} µm and 100 µm. Standard deviations are presented in Section 5.1.

4.4.7 Zeta potential

Diffusion of ions is responsible for the diffuse electrical double layer, present around all solid particles in a solution (Hiemenz and Rajagopalan, 1997). The overall colloidal stability of the algal culture is dependent on the electric repulsion between algal cells and this can be estimated by the zeta potential. This is measured by the difference in charge between the bulk fluid and surface of the particle.

Bacteria and algal culture suspensions were centrifuged at 7000 and 4000 rpm respectively for 5 minutes in a Heraeus Pico Biofuge. Samples were washed with sterile dH_2O and vortexed for 2 minutes. Centrifugation was repeated for 5 minutes, the supernatant disposed of and samples diluted to an optical density of 0.1 (optical density tests shown in Appendix 8.6.4). The pH of the suspension was adjusted using HCl or NaOH. The zeta potential of each algal and bacterial sample was determined using a Malvern Zetasizer nano ZS with DTS 1060C clear disposable cuvettes at 25°C. The cuvettes were washed with the solution and 5 ml of sample was injected whilst avoiding any air bubbles in the cuvette. The standard operating procedures (SOP) used were developed for aqueous suspensions of *Scenedesmus sp.*, *Chlorella vulgaris* and co-cultured bacteria with respective refractive indices and absorbance factor. Green microalgae has a refractive index of 1.013 (Aas, 1996; Bricaud *et al.*, 1988) and absorbance of 0.35 (Malvern Hydro 2000G mastersizer user manual), whilst bacteria have a refractive index of 1.00 and

absorbance of 0.1 (Malvern Hydro 2000G mastersizer user manual). A Smoluchowski's constant of 1.5 was used throughout. Each measurement was repeated three times, each of which took 30 measurements. Standard deviations are presented in Section 5.1.

4.4.8 Hydrophobicity

Hydrophobicity experiments were carried out using a traditional carbon adhesion technique to induce two-phase partitioning. Carbon adhesion techniques are based on free energy of transfer of hydrocarbon molecules from water to a purely hydrocarbon solvent (Tanford, 1921). The microbial adherence to hydrocarbon (MATH) method (Rosenberg, 1984) was modified for accuracy. Samples were centrifuged using a Beckman Avanti J-25 centrifuge at 7000 rpm or BOECO U-320 centrifuge at 4000 rpm. Samples were washed with sterile distilled water and resuspended by vortexing. Samples were then centrifuged again and resuspended in distilled water, media or PBS solution to an optical density of ca. 0.6. A 5 ml aliquot of the sample was transferred to a test tube and 0.5 ml of hexadecane added. The resultant suspension was vortexed for 1 minute. The suspension was left for 10 minutes to allow phases to equilibrate and avoid settling. The optical density of the bottom aqueous phase was taken and the following formula applied to obtain an index:

$$\text{Hydrophobicity index (\%)} = \left[1 - \frac{OD_{t=t}}{OD_{t=0}}\right] \text{x } 100$$

Experiments were conducted in triplicate over a range of conductivities, growth phases and pH. Standard deviations are presented in Section 5.1.

4.4.9 Settling rates

The speed of settling of non-flocculated, spherical particles is described by Stoke's Law (Equation 17). Many different techniques of defining and measuring the parameters in this equation have been suggested in the literature, especially with regards to the settling vessel. If the ratio of the diameter of the vessel to the diameter of the particle is greater than ~100, the walls of the container have no effect on the rate of sedimentation. For smaller values, the sedimentation rate may be reduced because of the retarding influence of the walls (Coulson and Richardson, 2002). Glass or perspex graduated cylinders and small jars are predominantly used in research. For ease of cleaning and to eliminate geometrical problems sedimentations were done in jar tests using 25 ml McCartney bottles.

For samples with settling times of over 1 hour, a series of 25 ml McCartney bottles were used. Samples were spun down at 6000 rpm for 5 minutes in a Heraeus Pico Biofuge, resuspended in sterile dH_2O and centrifuged again. Samples were then resuspended in dH_2O to the desired concentration to ensure no extracellular material affected the results. Spectrometry was used to analyse the settling rates every 10 minutes by taking 2 ml samples at fixed points within consecutive McCartney bottles to ensure sampling did not affect the results. These values were compared to a standard initial concentration reading and analysed using the follow equation:

$$\text{Recovery efficiency (\%)} = \frac{C_0 - C_f}{C_0} \text{ x } 100$$

where C_0 and C_f are the optical density initially and after sedimentation time respectively. Standard deviations are presented in Section 5.1.

4.4.10 Flocculation rates

Flocculation tests were analysed using a similar method to sedimentation to enable direct comparison of results. A series of 25 ml McCartney bottles were used for samples. Preliminary tests were done on all flocculating samples to determine the approximate speed of complete flocculation and flocculant induced settling rates. Suspensions were doused with relevant flocculants and conductivity and pH buffers and mixed for 1 minute at maximum stirrer speed. Flocculated samples were then left stationary on the benchtop for 20 minutes and left to settle; thereafter 2 ml was carefully removed using a pipette 2 cm from the top liquid level. Samples were analyzed with a spectrophotometer (750 and 600 nm for microalgae and bacteria respectively) before and after induced flocculation to obtain flocculation efficiency:

$$\text{Flocculation efficiency (\%)} = \frac{C_0 - C_f}{C_0} \text{ x } 100$$

where C_0 and C_f are the optical density initially and after flocculation time respectively.

Quicker flocculating and settling flocculant samples (95% biomass flocculate and settle in less than 7 minutes) needed to be analysed in real time to observe the settling profiles accurately. Spectrometry was used to analyse settling rates of flocculated microalgae over 10 minutes by continuously recording the optical density at a fixed point within a standard cuvette.

Preliminary settling speed tests were also performed. *Scenedesmus sp.* and *Chlorella vulgaris* were autoflocculated at pH 12 to induce floc sizes of around 2 – 3 mm. These tests were done in a burette where particles and bulk settling speeds were recording using a stop watch. Standard deviations are presented in Section 5.1.

4.5 Growth studies

4.5.1 Microalgal growth

Scenedesmus sp. and *Chlorella vulgaris* were grown in the airlift photobioreactors, after stock culture inoculation, until death phase was reached or after 18 days. Cells were harvested and used for dewatering experiments detailed in Section 4.6 and were stored for short periods of time in a coldroom at ± 5℃ to avoid cell degradation. Experiments were conducted to investigate the effects of CO_2 concentrations on growth. Air and 2900 ppm CO_2 concentrations were used and time dependent growth calibration standard curves were constructed for each growth condition for both species. These curves are presented in Appendix 8.6.2. During growth, pH, conductivity, carbon uptake and accumulation, temperature, biomass concentration, cell flocculation and size, zeta potential and hydrophobicity were measured to gain an understanding of how the cells respond to and acclimatise to the different natural growth phases. Samples were taken two or three times daily initially during the exponential phase and once daily thereafter. These samples were taken from the top sampling point on the reactor (Figure 7) and a constant liquid level was maintained by addition of sterile distilled water before sampling. Optical density and dry weight measurements (Section 4.4.2) were taken to obtain instantaneous specific growth

rates (μ) calculated as the slope of a graph of the natural logarithm of biomass concentration against time:

$$\mu = \frac{\ln X_2 - lnX_1}{t_2 - t_1} \quad (21)$$

4.5.2 Bacterial growth

Co-cultured and isolated bacterial samples were grown initially on Luria broth plates at 30°C. *Nocardioides aromaticivorans* SB10005 was the predominant bacteria present in the *Scenedesmus sp.* culture and *Microbacterium chocolatum* RW56 in the *Chlorella vulgaris* culture as shown in Section 5.1. These bacteria were isolated from plates and cultured in 2 L shake-flasks at 30°C and neutral pH using Luria broth containing ($g.L^{-1}$): 2.50 pancreatic digest of casein (tryptone powder), 2.50 NaCl, 1.25 yeast extract and 3.75 bacterial agar for plate applications. Stock cultures of these bacteria were maintained by inoculating autoclaved 2 L shake flasks containing 750 ml Luria broth and closed with a cotton wool bung to prevent contamination and allow for gas transfer. New stock cultures were made every two weeks. Long term stocks were kept on plates and refrigerated. Working stocks were maintained by inoculating from long term stocks each time.

Samples were taken two or three times daily initially during the exponential phase and once daily thereafter. Growth calibration standard curves were constructed for both species. These curves are presented in Section 5.2. Bacteria cultures were harvested during the stationary growth phase to a constant mass at 25°C for subsequent experiments. Cells were harvested and used for dewatering experiments detailed in Section 4.6 and were stored for short periods of time in a coldroom at ± 5°C to avoid cell degradation. Excess culture was disposed of using a traditional biocide. Biomass concentration, zeta potential and hydrophobicity were measured throughout growth and the growth rates and biomass productivity were determined similarly to algae as described in Section 4.5.1. These measurements were all conducted in a laminar flow hood to avoid contamination.

4.5.3 Carbon loop analysis

A carbon mass balance was performed over the airlift photobioreactors to improve current knowledge on the airlift system and to quantify carbon distribution with focus on flocculation and EOM within the system. A known carbon flowrate into the reactor was defined. The offgas carbon concentration and flowrate may be measured using simple gas capturing bags. The accumulation of carbon with the reactor may be quantified by analysing the reactor suspension. This was done by measuring the concentration coupled with the carbon fraction of each element in the reaction culture.

Offgas readings were taken using a Hartmann and Braun, Advance Optima (Magnos 16) offgas reader. CHN elemental analysis of microalgae and bacteria growing within the photobioreactors were investigated. Samples were isolated and freeze dried to ensure accuracy and analysed by the University of Cape Town, Chemistry Department. These results are presented in Table 11. Total inorganic carbon and total organic carbon (TICTOC) analysis was done by filtering the algal supernatant with 0.22 μm cellulose nitrate filters to remove any biomass and particulate matter. Samples were then acidified to pH 3.5 using dilute perchloric acid (0.1 M) to remove any inorganic carbon and purged with nitrogen gas for at least 15 minutes. An ANATOC Series 2 TOC analyzer was used to quantify the

organic and inorganic carbon. Dry weights of bacteria and microalgae within the reactor were also recorded to complete the carbon balance with the difference being attributed to EOM or clumping cells. Standard deviations are presented in Section 5.1.

4.6 Solid-liquid separations

This dissertation aims to investigate sedimentation and flocculation as methods to recover microalgal biomass. The flocculation mechanisms, ease of flocculation, recovery efficiencies, chemical and flocculant dosages, time for effective separations, settling profiles and optimisation concerns for *Scenedesmus sp*. and *Chlorella vulgaris* were all factors considered. Sedimentation rates, efficiency and speeds were investigated (Section 4.4.9) to determine the unaided capabilities of *Scenedesmus sp*. and *Chlorella vulgaris*. The microalgal and bacterial species (Sections 4.5.1 and 4.5.2) were then flocculated and the settling speeds and flocculation efficiencies measured to analyse improved settling and hence separation performance. *Scenedesmus sp., Chlorella vulgaris* and all other bacteria were harvested at stationary phase to negate any effects of growth phase on the results. Chemical-, auto- and bio-flocculation were investigated using a range of bioflocculants, autoflocculants, co-flocculants and chemicals.

Bioflocculation was investigated using increasing concentrations of co-cultured bacteria, *Bacillus sp*., *E. coli* BL2 (DE3) and green microalgal cells. Induced autoflocculation was investigated by adjusting only the conductivity and pH of the suspensions. *In situ* autoflocculation was investigated by analysing the carbon balance (Section 4.5.3) and biomass growth (Section 4.5.1) data. Chemical flocculation tests were done as a baseline exercise to compare chemical loading and efficiencies to other techniques of flocculation examined in this thesis. Chitosan, alum and algal growth media components were used in flocculation experiments (Section 4.4.10). Conductivity, pH, media salt loading and bacteria concentrations were all investigated at varying concentrations to obtain effects, optimised conditions and interrelationships to determine each properties independent influence on separation. Reasons for observed maxima in flocculation efficiencies were then investigated by studying the surface chemistry relationships at the relevant concentrations, conductivities and pH by making reference to zeta potentials and hydrophobicity. This approach allowed for the proposal of possible flocculation mechanisms.

4.7 Water recycle

An objective of this research was to identify a technique or series of techniques to recover algal biomass without contamination of the effluent water. Flocculation followed by sedimentation was the chosen method for dewatering as described in Section 4.6. The use of the chosen chemicals (Section 4.6) to induce flocculation of biomass therefore needed to be investigated with respect to the effect of these chemicals on the growth of *Scenedesmus sp.* and *Chlorella vulgaris*. To investigate these effects, starting algal growth media pH, and hence conductivity, was varied across a range of values that were highlighted as increased flocculation activity regions in previous results. These tests were done in the airlift photobioreactors to compare the results with standard growth data previously investigated. The reactor conditions were identical to those described in Section 4.1.1 and growth parameters measured and methods were similar to those described in Section 4.5.1.

5 RESULTS: ALGAL GROWTH, SUSPENSION AND CELL SURFACE

In the presentation of results, the following are considered:

- Reproducibility of experiments
- Biomass growth and its analysis
- Properties of the algal suspension, in terms of algal surface properties, solution properties and suspension rheology
- Algal flocculation and sedimentation (Chapter 6)
- Water recycle (Chapter 6)

Growth of *Scenedesmus sp.* and *Chlorella vulgaris* in airlift photobioreactors was investigated under standard conditions defined in Section 4.5.1 to determine growth rates, growth phases, standard curve assays (to convert between OD, cell numbers and biomass dry weight) and biomass productivities. The relationship between suspension absorbance and dry weight measurements was investigated and related to algal cell changes during growth. Different techniques of analysing the growth data were compared to obtain the best estimation of the specific growth rates, biomass productivity and maximum biomass concentrations. The effect of CO_2 concentration on these parameters was explored. Isolated and co-cultured bacteria growth parameters were also analysed.

Investigation of naturally occurring surface properties of the algal suspension during growth were investigated to determine significant physico-chemical properties of the algal cultures and to obtain cell acclimation data to the reactors in terms of cell size, reproduction phases and surface charge. The rheological behaviour of the bacterial and microalgal suspensions was characterised to obtain an upper concentration limit beyond which transport is impeded and to investigate regions of Newtonian flow rheology. The change in physico-chemical properties of the cells in response to changing suspension pH and conductivity was examined. These parameters were explored in terms of the significant characteristics to determine any interrelationships and regions that may be exploited to induce flocculation and increase sedimentation recovery efficiency.

The effects of natural and induced flocculation as well as bioflocculation were investigated in terms of suspension characteristics and flocculation efficiencies. Induced flocculation results were compared to unaided sedimentation rates. Brief optimisation and efficiency studies were carried out. Factors affecting flocculation and its underlying mechanisms were investigated with the aid of light microscopy. Parameters such as pH, particle size, surface charge and hydrophobicity were compared to suggest or identify the mechanisms of separation.

After biomass recovery, it is desirable to recycle the effluent water and culture medium. The potential for growth on these liquid streams was analysed, incorporating all the properties identified to determine the toxicity limits for recyclable water.

5.1 Reproducibility

No data has value unless it has been demonstrated that it was both accurate and reproducible. For all measured parameters a reproducibility experiment was performed (Table 7). This was performed by taking 1 sample and measuring the required parameter 5 times to obtain a standard deviation and mean error value. For hydrophobicity, CO_2, settling efficiencies and viscosity readings, the error analysis was done using 5 different samples to ensure accuracy, as these tests' method of measurement altered the suspensions during quantification. In the case of hydrophobicity and settling tests, the error in the optical density measured was incorporated into the error results. As shown in Table 7, all measured parameters had a mean error of less than 9.0% other than hydrophobicity. The hydrophobicity tests resulted in a mean error of 24.0%. This value is high in comparison to other parameter errors; however hydrophobicity tests were used only to gain understanding to which suspension conditions regions were optimal and not for absolute values.

Table 7: Reproducibility summary for experimental measurements

Reproducibility	Zeta potential	Electrophoretic mobility	Conductivity	pH	Hydrophobicity	Optical density	CO_2	Settling tests	Size distribution	Viscosity
Units	**(mV)**	**(µm.cm.V^{-1}s^{-1})**	**(mS.cm^{-1})**		**(%)**	**(A.U)**	**(ppm)**	**Recovery efficiency (%)**	**(µm)**	**(cP)**
1	-22.50	-1.765	14.10	8.00	8.47	0.707	3013	50.40	5.257	0.000814
2	-21.50	-1.687	14.50	8.00	5.45	0.705	3002	54.40	5.271	0.000808
3	-22.40	-1.758	14.90	8.01	4.62	0.705	2995	53.60	5.270	0.000811
4	-26.70	-2.089	15.10	8.00	7.75	0.706	3056	52.20	5.271	0.000810
5	-23.30	-1.824	14.60	8.01	6.76	0.705	3071	48.90	5.272	0.000809
Average	-23.28	-1.825	14.64	8.00	6.61	0.706	3027	51.90	5.268	0.000810
Stdeva	2.02	0.156	0.38	0.01	1.59	0.001	33.99	2.26	0.006	0.000002
Mean error	0.09	0.085	0.03	0.001	0.24	0.001	0.01	0.04	0.001	0.002794

5.2 Algal growth and characterisation

By describing the physical properties of the cells accurately as a function of the growth phase, a better understanding of the ability to manipulate and control these cellular parameters may be attained. The relative characteristics may then be exploited to achieve increased recoveries and product yields. Further approaches to refine separation techniques through this understanding can be sought. In this section the surface and solution properties throughout the growth phase of *Scenedesmus sp.* and *Chlorella vulgaris* are investigated as a function of growth rate.

5.2.1 Standard growth curves

Standard growth conditions were selected for this study from the work of Griffiths *et al.* (2011). Under these conditions, the algae were grown in the airlift photobioreactors (Figure 7) at an aeration rate of 2 $L.min^{-1}$ with CO_2 enrichment of the sparged gas to 2900 ppm CO_2. The reactor temperature was 25 ± 2℃ with an initial pH of 6.9 ± 0.1 and constant illumination at 300 $\mu mol.m^{-2}.s^{-1}$. The characteristic growth curves of *Chlorella vulgaris* and *Scenedesmus sp*. are presented in Figure 8. After an initial, insignificant lag period, exponential phase growth was seen between point A and B, followed by linear growth from point B to C, declining growth during C and D and finally the cells entered death phase after point D (Figure 8). *Chlorella vulgaris* and *Scenedesmus sp*. reached maximum biomass concentrations of 2.26 ± 0.01 and 3.22 ± 0.01 $g.L^{-1}$ respectively, shown at point D (Figure 8). Both species were seen to grow with similar biomass productivities until day 6; however, *Chlorella vulgaris* growth became inhibited at this point. *Scenedesmus sp*. reached a higher biomass concentration compared to *Chlorella vulgaris* as *Scenedesmus sp*. only entered stationary growth phase after day 9 of growth. *Chlorella vulgaris* and *Scenedesmus sp*. were therefore harvested on day 8 and 10 at their respective stationary growth phases for subsequent experiments to ensure cell and suspension consistency.

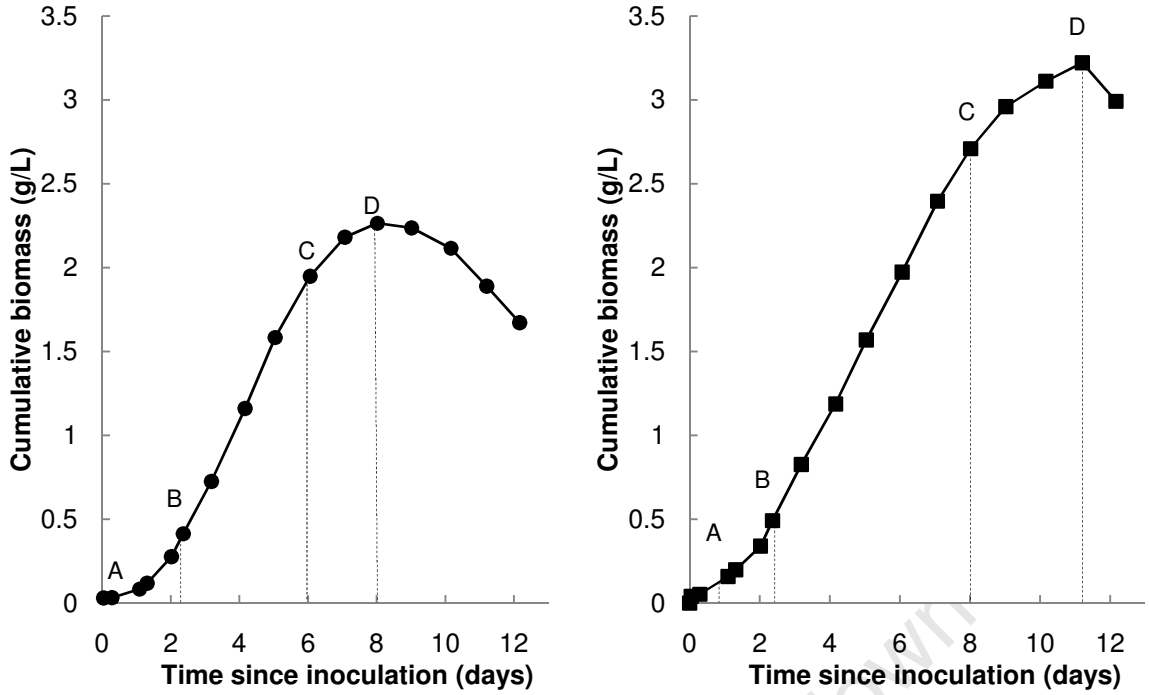

Figure 8: Standard growth curves of *Chlorella vulgaris* (—●—) and *Scenedesmus sp.* (—■—) in the airlift photobioreactors grown on 2 L.min^{-1} 2900 ppm CO_2 at 25 ± 2°C with an initial pH of 6.9 ± 0.1 and constantly illuminated at 300 µmol.m^{-2}.s^{-1}

5.2.2 Absorbance and dry weight relationship

Algae are complex optical systems which consist of single or multi layers with different light absorption and scattering properties (Mercado *et al.*, 1996). Chlorophyll absorbs all wavelengths of visible light except green, which it reflects, producing the green colour of microalgae. The amount of light absorbed by a suspension of cells can be related directly to cell mass or cell number (Griffiths *et al.*, 2011b). The correlation is a complex function of particle size, shape and refractive index (Clesceri *et al.*, 1998). Optical density is used frequently as a rapid and non-destructive measurement of biomass (Shuler and Kargi, 2005), where the absorbance or turbidity is a measure of the decrease in the amount of light transmitted through a suspension of particulate matter such as a cell culture, relative to a blank containing the suspending liquid and no particles. Absorbance of light at a particular wavelength can be related to cell concentration using a suitable standard curve (Griffiths *et al.*, 2011b). The shape, size and basic morphology of *Scenedesmus sp.* and *Chlorella vulgaris* undergo minor changes during the different stages of growth. Intracellular vacuoles have also been reported to change in size and composition. These changes in microalgal cells all affect light adsorption.

The presence of pigment within the cells can affect this absorbance measurement, as the colour absorbs in a particular region of the light spectrum (Clesceri *et al.*, 1998) and therefore pigmented cells can affect the measurement of cell concentration. Microalgae have relatively high pigment contents, between 0.1 and 9.7% of wet biomass, consisting of mainly chlorophylls and carotenoids (Becker, 1994; Nicholls and Dillon, 1978). If the pigment content of the cells were a constant, the increase in absorbance could be taken into account by an appropriate standard curve; however the pigment content of microalgae is

known to vary with culture and environmental conditions (Healey, 1975). This relationship is, however, species-specific and dependent on the reactor conditions.

Figure 9 provides an example of the correlation of dry weight and optical density measured at 680 and 750 nm wavelengths. These relationships were measured throughout the growth phase for *Scenedesmus sp*. and *Chlorella vulgaris* grown on air and 2900 ppm CO_2 and are presented in Appendix 8.6.2. The gradient or x-coefficient for each assay, termed the "dry weight coefficient" represents the average conversion factor from optical density to dry weight at a specific condition measured at either 750 or 680 nm. The dry weight coefficient was determined for each species and set of growth conditions as a function of time since inoculation. These are provided in Figure 10 to obtain a function to describe the change in the average conversion factor as a function of time across the growth phase. The data obtained was fitted to a quadratic equation. This assay was modelled to ensure improved biomass concentration quantification whilst only physically measuring algal suspensions optical density.

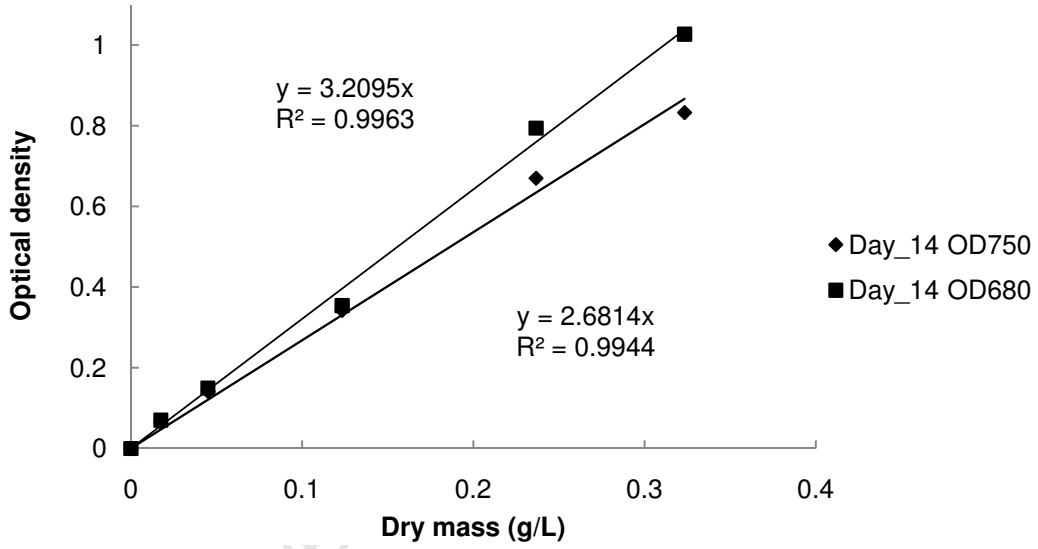

Figure 9: Day 14 growth phase assays for *Scenedesmus sp.* grown on air in the airlift photobioreactors comparing optical density measurements at different wavelengths

Griffiths *et al.* (2011b) showed that pigment content of *Chlorella vulgaris* cells decreased with culture age from 5.5 to 2.5% DW and that absorbance at 680 nm was strongly related with the pigment content of the cells. This is because spectrophotometry of green alga at 680 nm is a measure of chlorophyll *a*, which has been reported to vary up to 30-fold with changes in species composition, temperature and nutrient and light availability (Healey, 1975) . Griffiths *et al.* (2011b) further stated that even outside of the range of pigment absorption (750 nm), the change in the correlation between OD and dry weight is not eliminated. Figure 10 shows readings taken at 680 nm, compared to 750 nm, follow a similar trend but the function is shifted up hence underestimating the dry weight of the cultures. This trend is however not a default constant. Absorbance readings at 750 nm therefore predict dry weight concentrations more accurately but still contain intrinsic error. The models for cultures grown on air followed similar trends but are broadened curves, compared to the CO_2 sufficient (2900 ppm CO_2) cultures, as the rate of cell growth was lower. Comparing Figure 10b and d to Figure 10a and c showed *Chlorella vulgaris* had a

greater variance over *Scenedesmus sp.* in chlorophyll *a* content during growth. This assay allows for a more accurate dry weight recording compared to the linear relationships estimated between optical density and dry weight typically used in literature (Appendix 8.6.2). Therefore for each species and growth condition examined in this thesis, a specific dry weight- absorbance assay was constructed (Figure 10). A more accurate dry weight measurement was therefore obtained by using the dry weight coefficient from the appropriate quadratic equation found in either Figure 10a, b, c or d. This coefficient was then used to calculate the dry weight, as a function of time, following the equation:

$$\text{Algal dry weight } (g.L^{-1}) = \text{“dry weight coefficient (t)” x OD} \quad (22)$$

The increasing functions showed that concentration of chlorophyll *a* varies over time. As the cell culture became more concentrated in the reactor, the cells became increasingly light inhibited. The cells therefore increased the amount of chlorophyll to increase available light sensitive surface area. Towards the end of the stationary phase, cells became less metabolically active and some cells died and lysed, decreasing the chlorophyll content. This assay is therefore an improvement on current techniques and has been shown to reduce error by up to 10%, providing a greatly improved description of the growth phase (Figure 11 and Figure 12).

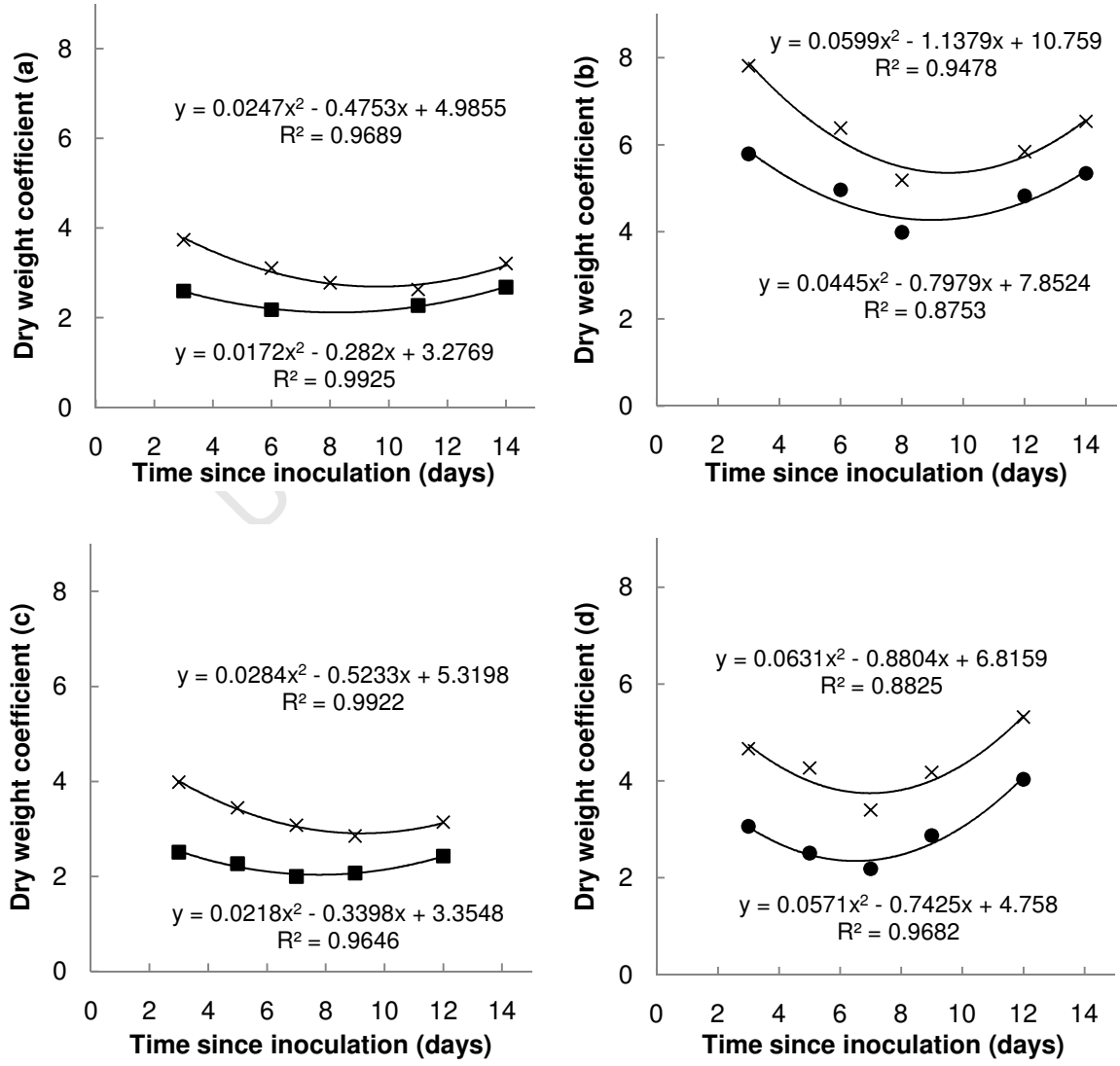

Figure 10: (a) *Scenedesmus sp.* on air, (b) *Chlorella vulgaris* on air, (c) *Scenedesmus sp.* on 2900 ppm CO_2, (d) *Chlorella vulgaris* on 2900 ppm CO_2 dry weight assays during growth curve in an airlift photobioreactor (■ 750 nm, × 680 nm)

To obtain accurate dry weight of cell biomass during growth through measuring absorbance, four models were developed to correlate optical densities for *Scenedesmus sp.* on air, *Chlorella vulgaris* on air, *Scenedesmus sp.* on 2900 ppm CO_2 and *Chlorella vulgaris* on 2900 ppm CO_2 (Figure 10). Dry weights calculated using the 680 and 750 nm models presented in Figure 10a, b, c and d were compared to traditional assays (similar to Figure 9, which are best described as averaged models as they assume a constant pigment content and strictly linear relationship between dry weight and optical density). There was a coefficient of variance between the averaged and polynomial models using spectrophotometry at 680 and 750 nm of 0.044, 0.44, 0.33 and 0.14 $g.L^{-1}$ for *Chlorella vulgaris* and *Scenedesmus sp.* cultured on air and 2900 ppm CO_2 respectively (Figure 11 and Figure 12). The dry weights correlated via the polynomials in Figure 10 were found to be the most accurate readings when compared with actual dry weight measurements (Figure 11 and Figure 12). This was expected from the findings in Figure 10. These results are however only valid for one algal species, at a specific CO_2 feed concentration, grown in the specified airlift photobioreactors and measured at a suitable wavelength. Even though the model approach is the most accurate, these limitations in biomass concentration measurements make this technique only valid for when many similar growth studies are conducted.

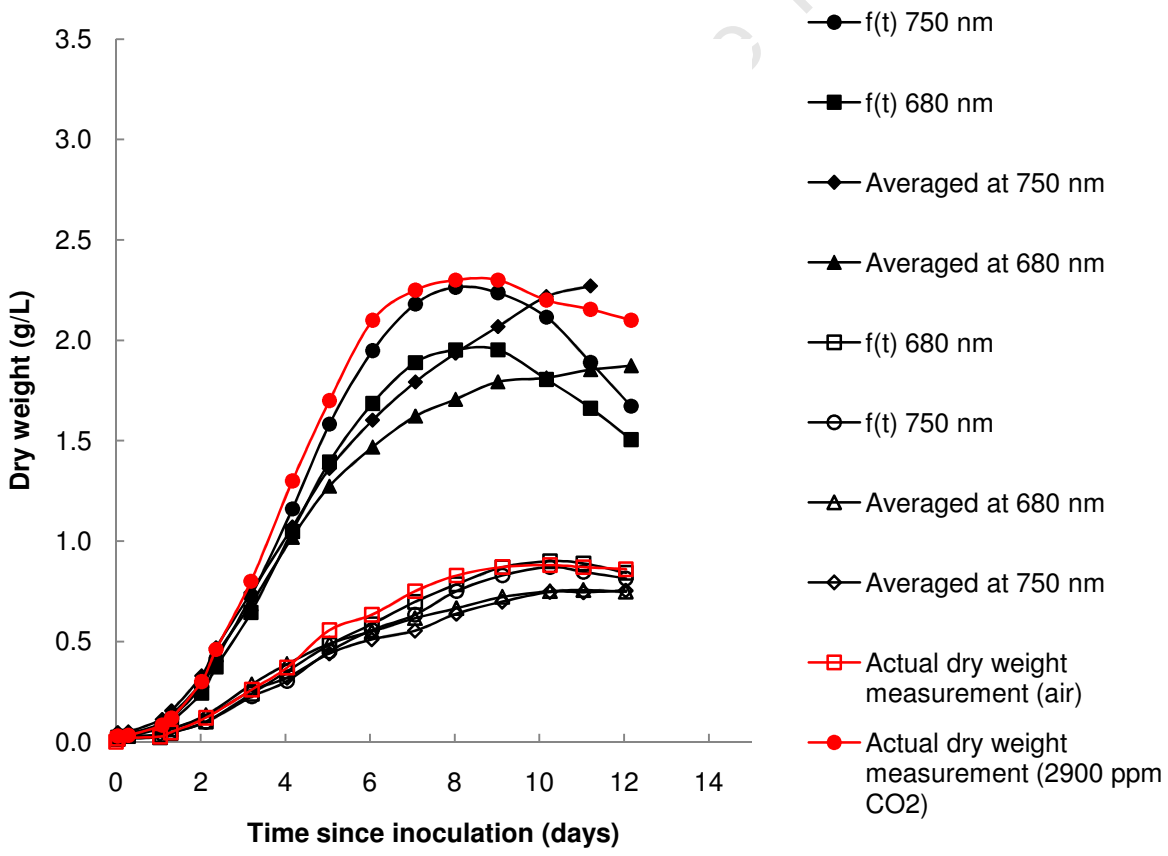

Figure 11: Growth curves of *Chlorella vulgaris* on air and 2900 ppm CO_2 at 2 $L.min^{-1}$ using different assay models in an airlift photobioreactor (●, ◆, ▲, ■ 2900 ppm CO_2; ◇, □, △, ○ air) and actual dry weight measurements

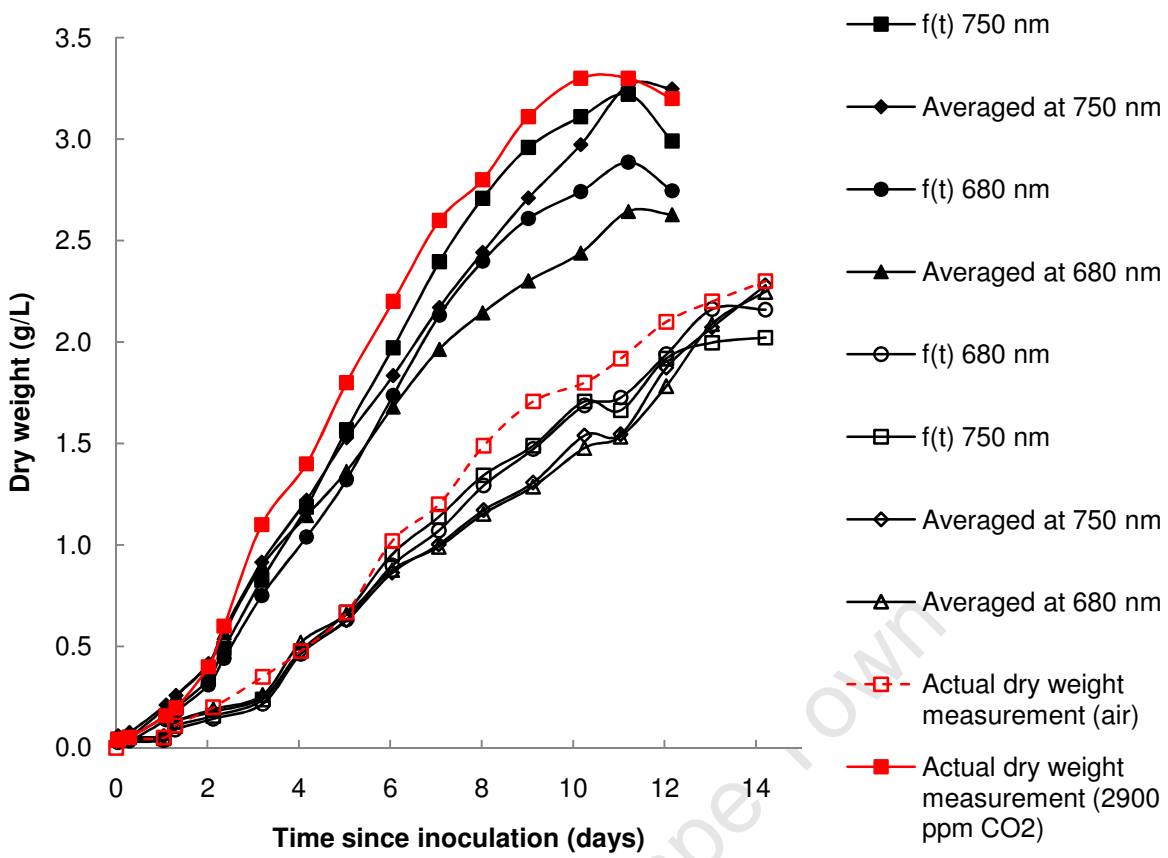

Figure 12: Growth curves of *Scenedesmus sp.* on air and 2900 ppm CO_2 at 2 L.min^{-1} using different assay models in an airlift photobioreactor (●, ◆, ▲, ■ 2900 ppm CO_2; ○, △, ◇, □air) and actual dry weight measurements

5.2.3 *Growth rates and productivities*

This investigation was important to identify the different growth phases of the species accurately as this is postulated to affect settling and recovery efficiencies (Danquah *et al.*, 2009b). The 'best fit' model to dry weight was used to calculate the dry weights of each algal culture, Figure 13 shows the natural log of *Chlorella vulgaris* and *Scenedesmus sp.* cell concentrations as a function of time in the airlift photobioreactors. *Chlorella vulgaris* and *Scenedesmus sp.* were in exponential growth from day 0.5 to 2.5 respectively with both species following similar growth trends. These cultures had maximum growth rates of 1.20 ± 0.03 and 1.38 ± 0.04 day^{-1} (n = 8) and were in stationary growth phase between days 8 – 9.5 and 10.5 - 12 for *Chlorella vulgaris* and *Scenedesmus sp.* respectively. Linear growth rates of 0.37 ± 0.04 day^{-1} and 0.36 ± 0.02 day^{-1} for *Chlorella vulgaris* and *Scenedesmus sp.* were observed with respective maximum linear growth biomass concentrations of 1.95 ± 0.09 and 2.81 ± 0.11 g.L^{-1}.

Chlorella vulgaris and *Scenedesmus sp.* cultured on air portrayed a lower maximum specific growth rate than when cultured on 2900 ppm CO_2 of 1.11 ± 0.06 and 1.20 ± 0.07 day^{-1} respectively (n = 2). The respective linear growth rates over day 3 to14 were also lower in accordance with the reduced rate of CO_2 mass transfer at 0.21 ± 0.08 and 0.24 ± 0.07 day^{-1} for *Chlorella vulgaris* and *Scenedesmus sp.* respectively. The cultures reached a maximum biomass concentration of 0.87 ± 0.05 and 2.16 ± 0.11 g.L^{-1} on day 10 and 14 of growth respectively (Figure 13). The *Scenedesmus sp.* culture was still in linear growth when the

airlift photobioreactors were harvested suggesting that the cells were not light limited as yet. A summary of the growth parameters for *Scenedesmus sp*. and *Chlorella vulgaris* grown either 2900 ppm CO_2 or air are presented hereafter in Table 8.

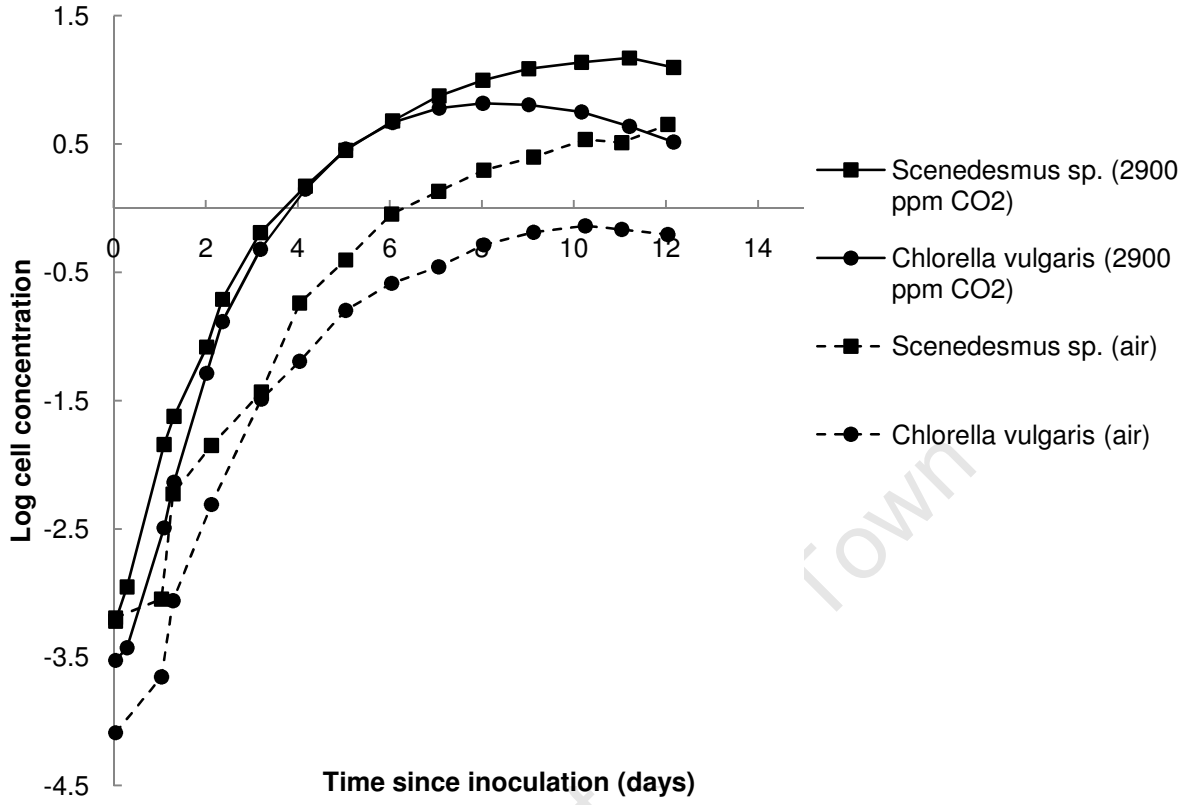

Figure 13: Growth curves for *Chlorella vulgaris* and *Scenedesmus sp.* grown on 2 $L.min^{-1}$ 2900 ppm CO_2 or air at 25 ± 2℃ with an initial pH of 6.9 ± 0.1 and constantly illuminated in the airlift photobioreactors

Table 8: Summary of growth parameters for *Scenedesmus sp.* and *Chlorella vulgaris* grown on 2900 ppm CO_2 or air in the airlift photobioreactors

Species (ppm CO_2)	**Units**	***Scenedesmus sp.* (air)**	***Scenedesmus sp.* (2900)**	***Chlorella vulgaris* (air)**	***Chlorella vulgaris* (2900)**
μ_{max}	(day^{-1})	1.20 ± 0.07	1.38 ± 0.04	1.11 ± 0.06	1.20 ± 0.03
Duration of exponential phase	(days)	1 - 3	0.5 – 2.5	1 - 3	0.5 – 2.5
Linear growth rate	(day^{-1})	0.24 ± 0.07	0.36 ± 0.02	0.21 ± 0.08	0.37 ± 0.04
Duration of linear growth phase	(days)	3 - 13	2.5 – 10.5	3 – 8.5	2.5 – 8.5
Maximum linear growth biomass concentration	($g.L^{-1}$)	2.08 ± 0.10	2.81 ± 0.11	0.72 ± 0.05	1.95 ± 0.09
Maximum biomass concentration	($g.L^{-1}$)	2.16 ± 0.11	3.22 ± 0.14	0.87 ± 0.05	2.26 ± 0.12
Duration of maximum productivity	(days)	3 - 10	2.5 - 7	3 - 7	2.5 - 5

Figure 14 and Figure 15 respectively describe the specific growth rates and average biomass productivities compared to the cumulative biomass concentration for *Scenedesmus sp.* and *Chlorella vulgaris* grown on 2900 ppm CO_2 at 2 L.min^{-1}. As the airlift bioreactor increased in biomass concentration, the growth rate decreased until death phase occurred or until cells began to agglomerate onto each other or onto the reactor surfaces. This demonstrates the effects of light limitations on the batch system. As the cell density increased, less light was available to cells that are not near the reactor wall, depicted in Figure 7, due to cell shadowing and absorbance, thus causing the light deficient cells to die or agglomerate. During cell death, the contents of the microalgal cell were expelled into the suspension, increasing EOM and hence promoting autoflocculation of the remaining viable cells. The maximum biomass productivity was observed during between day 2 and 7 (Figure 15) when the biomass concentration was increasing and cell growth was limited only by CO_2 or light provision. Both species displayed similar growth rates and average biomass productivities. The main difference was observed after day 6 of growth when the specific growth rate of *Chlorella vulgaris* decreased below that of *Scenedesmus sp*. owing to a lower ability to scavenge light. Concomitantly the biomass productivity decreased and was followed by the measured specific growth rate becoming negative indicating that the culture biomass was lysing or agglomerating. If downstream processing was simple without any problems, the reactors would be operated at the points of maximum productivities. However the selection of microalgae harvesting point requires a compromise between higher biomass concentrations, biomass productivities and ease of harvesting.

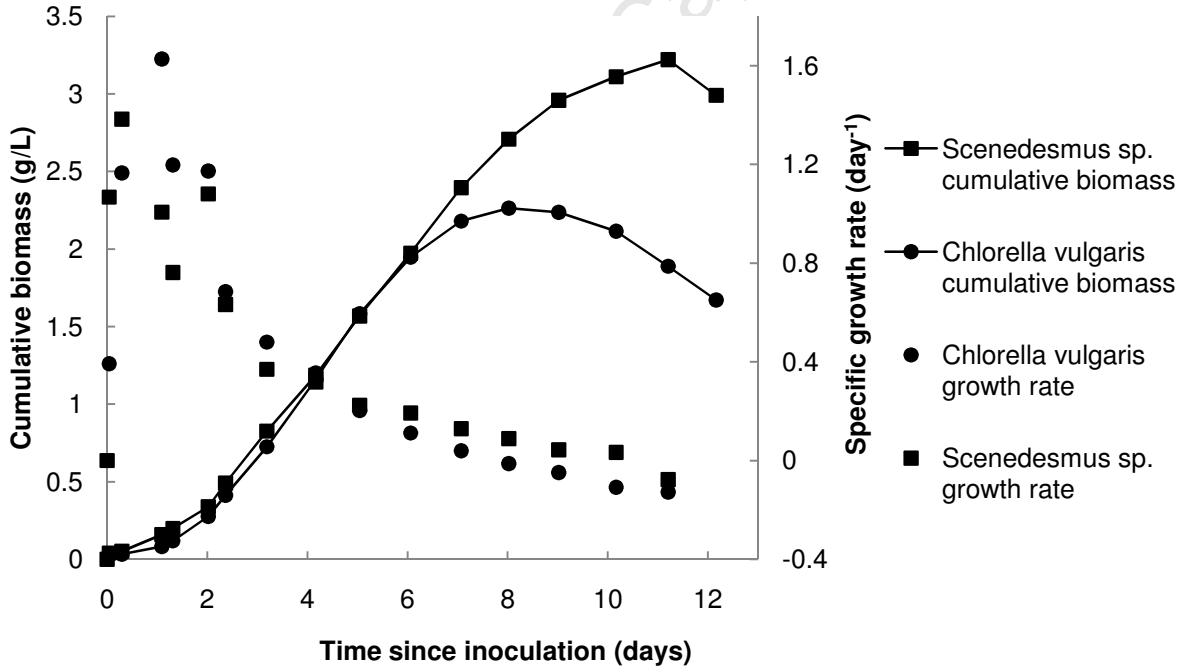

Figure 14: Cumulative biomass concentration and specific growth rates for *Scenedesmus sp.* and *Chlorella vulgaris* in the airlift photobioreactors cultured on 2900 ppm CO_2 at 2 L.min^{-1}

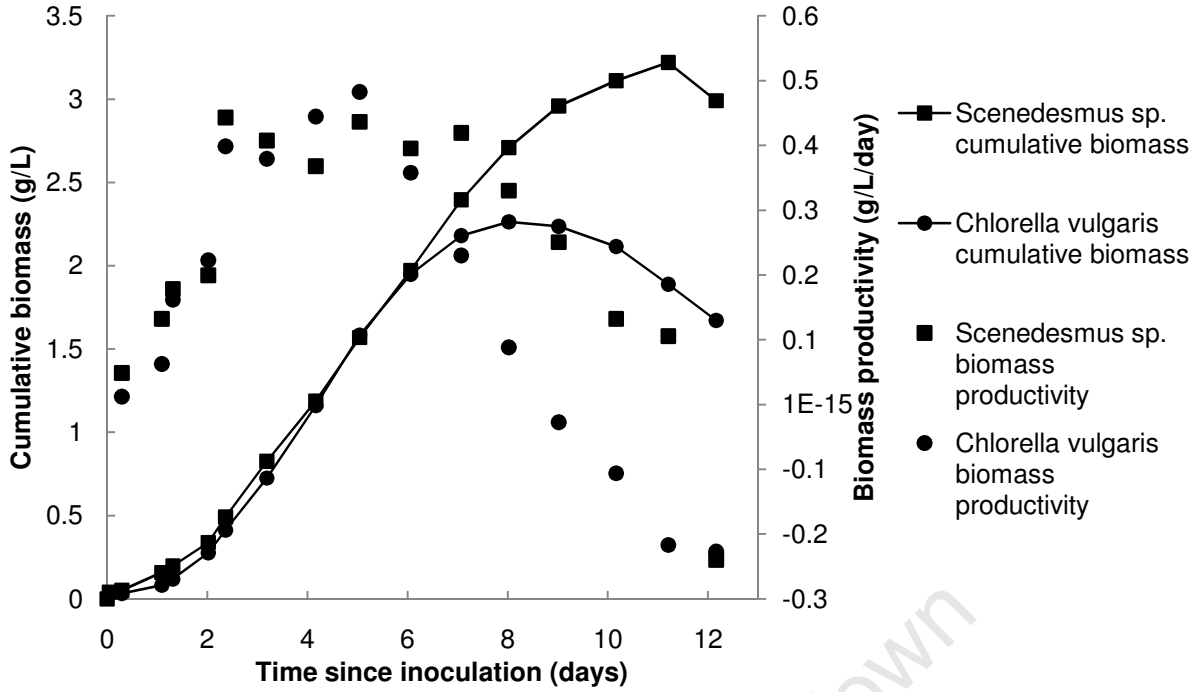

Figure 15: Cumulative biomass concentration and average biomass productivities for *Scenedesmus sp.* and *Chlorella vulgaris* in the airlift photobioreactors cultured on 2900 ppm CO_2 at 2 L.min^{-1}

5.2.4 Effect of CO_2 availability

Both *Scenedesmus sp.* and *Chlorella vulgaris* showed increased biomass productivity with increasing feed CO_2 concentrations (Figure 11 and Figure 12). Above 2900 ppm CO_2, no significant increase in productivity was observed for *Chlorella vulgaris*. Hence at 2900 ppm CO_2 at 2 L.min^{-1}, there was CO_2 sufficiency whilst a feed gas supply of air resulted in carbon limitations. *Scenedesmus sp*. exhibited CO_2 sufficiency at 5000 ppm. Both species demonstrated exponential growth over days 0.5 – 2.5. The decline in the exponential growth suggests a limitation in reactor conditions prohibiting further growth. This was predominantly due to light inhibition within the airlift photobioreactor for *Chlorella vulgaris* and both light and CO_2 limitation for *Scenedesmus sp*. After day 10, *Chlorella vulgaris* was seen to agglomerate within the airlift photobioreactors causing an erroneous decrease in measured biomass. This phenomenon is investigated subsequently in Section 5.5. Figure 12 shows *Scenedesmus sp.* leaves exponential growth phase and hence showed biomass productivity limitations after day 10 when cultured on 2900 ppm CO_2. However, when air was used as a feed, the cultures continued to accumulate biomass with linear productivity for extended periods until nutrient or light limited. This further supports the explanation of a declining growth curve due to light deficiencies. *Scenedesmus sp.* grown on 2900 ppm CO_2 reached a maximum biomass concentration on day 11 of growth whilst *Scenedesmus sp.* cultured on air was still in the linear growth phase but at a much lower biomass concentration due to the sustained lower carbon fixation and therefore biomass productivity. Figure 13 illustrated the effect of CO_2 inlet concentrations on the growth phases of *Chlorella vulgaris* and *Scenedesmus sp*. in the airlift photobioreactors. The maximum biomass concentration of *Scenedesmus sp*. culture grown on 2900 ppm CO_2 was 1.06 g.L^{-1} (approximately 50%) higher than that cultured on air (Table 8).

In Figure 16, the efficiency of CO_2 assimilation into biomass is considered. The ratio of cumulative CO_2 entering per unit biomass formed during growth of *Chlorella vulgaris* and *Scenedesmus sp*. cultured on constant 2900 ppm CO_2 and air at 2 L.min^{-1} in the airlift photobioreactors was determined. Initially there was a significant increase in the carbon supply: biomass ratio as cell concentration in early exponential phase was extremely low and hence not all the carbon entering the reactor was assimilated into biomass. The cultures grown on 2900 ppm CO_2 increased at a quicker rate and the ratio remained higher throughout the growth phase.

The ratio for the cultures grown on air remained under 1 throughout the growth curve until day 12 when cell growth declines. This indicates that throughout the growth phase the cells are carbon inhibited when grown on air. The cultures grown on 2900 ppm CO_2 surpassed a carbon supply: biomass ratio of 1 at the beginning of exponential phase. After this, cell biomass rapidly increased and hence a decrease in the ratio was observed in Figure 16. However this ratio remained above 1 indicating that the cells were not carbon inhibited. When cells entered stationary growth phase, the ratio began to exponentially increase. If this were true stationary and death phase, the ratio should tend to infinity, however initially during these phases, some CO_2 was still being dissolved into the system. The CO_2 supply remained constant whilst biomass productivity decreased and became negative (Figure 15) thus providing evidence that carbon was not the primary growth limiting factor inducing stationary phase in these systems at 2900 ppm CO_2. This trend was echoed by the cultures grown on air even though the cultures were already carbon inhibited. The cultures grown on air therefore became light and carbon inhibited towards the end of their growth phases.

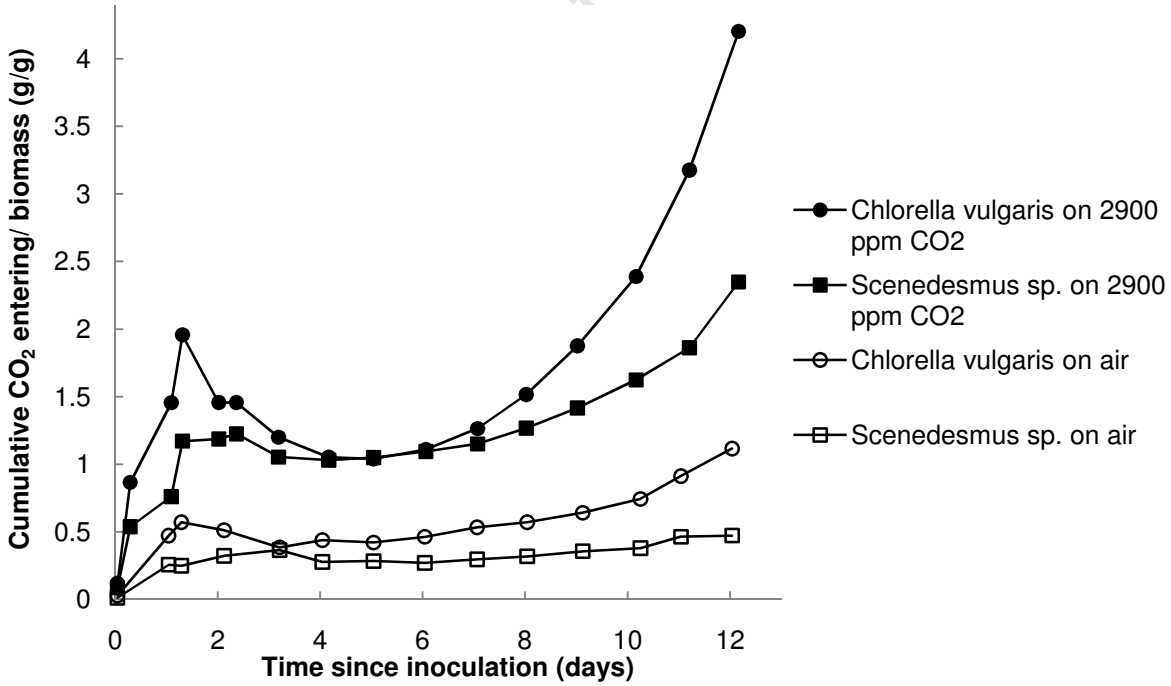

Figure 16: Cumulative CO_2 supplied per unit biomass during growth of *Chlorella vulgaris* and *Scenedesmus sp*. cultured on 2900 ppm CO_2 at 2 L.min^{-1} and air in the airlift photobioreactors

5.2.5 *Isolated and co-cultured bacteria growth*

Although the bioreactor and media were sterilised prior to experiments and the process operated hygienically, it is well recognised that bacteria are naturally co-cultured with algae hence bacteria-free inocula are not common (Ueda *et al*., 2009). The co-culturing of bacteria with *Scenedesmus sp*. and *Chlorella vulgaris* was observed in the airlift photobioreactor system. These bacteria were each isolated and identified using PCR with 16S primers, sequencing and BLAST analysis, as described in Section 4.1.2. The sequence data are provided in Appendix 8.6.1. In order of dominance, the bacteria isolated were *Nocardioides aromaticivorans* SB10005, *Microbacterium chocolatum* RW56, *Stenotrophomonas maltophilia, Acinetobacter, Azospirillum, Chryseobacterium and Rhizobium gallicum*. The relative abundance of contaminant co-cultured bacteria was measured qualitatively using plates. *Nocardioides aromaticivorans* and *Microbacterium chocolatum* were the predominant strains observed in *Scenedesmus sp.* and *Chlorella vulgaris* cultures respectively. *Bacillus sp*. and *E. coli* BL2 (DE3) were also used in autoflocculation studies, but not co-cultured with the algal species. All bacteria isolated during or used in the study are described in Table 9.

Table 9: Brief description of the bacteria isolated or used in this thesis

Bacteria	Description*
Nocardioides aromaticivorans	Actinobacteria phylum. Gram-positive, asporogenous, nonmotile rods. Colonies are smooth, round and milky-white on complex agar media. Strictly aerobic, heterotrophic and chemoorganotrophic.
Microbacterium chocolatum	Actinobacteria phylum. Gram-positive, heterotrophic non-motile rods. Colonies are circular, low convex with entire margins, opaque and moist. Orange or dull orange pigment is produced. Chemoorganotrophic.
Stenotrophomonas maltophilia	Proteobacteria phylum. Aerobic, autotrophic, motile, gram-negative non-fermentative bacillus previously known as *Pseudomonas maltophilia* and *Xanthomonas maltophilia*. The bacterium is an obligate aerobe that is common throughout the environment, particularly in water. Chemoorganotrophic.
Acinetobacter	Proteobacteria phylum. Gram-negative, heterotrophic bacteria belonging to the *Gammaproteobacteria*. Non-motile, oxidase-negative, and occur in pairs under magnification. Coccobacillary morphology on nonselective agar. Rods predominate in fluid media.
Azospirillum	Proteobacteria phylum. Curved plump rods. Cells are typically heterotrophic, gram negative. Cells are motile in semisolid or liquid media, typically moving by corkscrewbording or vibratory motion.
Chryseobacterium	Bacteroidetes phylum. Gram negative rod shaped bacteria. Obligate aerobic, non-fastidious, non-spore

	forming, nonfermentative; nonmotile; slender; slightly curved rod; and catalase positive, oxidase positive, and indole-positive
Rhizobium gallicum	Proteobacteria phylum. Gram-negative, aerobic, motile, nonspore-forming rods.
Bacillus	Firmicutes phylum. Gram-positive, heterotrophic cells rod-shaped, straight or slightly curved, occurring singly and in pairs, some in chains, and occasionally as long filaments.
E. coli	Proteobacteria phylum. Gram-negative, rod-shaped, heterotrophic, facultative anaerobic and non-sporulating.

*(Boone *et al.*, 2001)

The concentrations of the co-cultured bacteria, measured throughout the growth of *Scenedesmus sp.* and *Chlorella vulgaris* in the photobioreactors under standard conditions using plate counts, are presented in Figure 17. Although the cell concentrations of the bacteria were relatively high, no significant biomass was accumulated due to the small cell sizes. *Microbacterium chocolatum* and *Nocardioides aromaticivorans* biomass (~ 99% dominant bacterial strains) was approximately 1.2 and 4.0 wt% of *Chlorella vulgaris* and *Scenedesmus sp.* biomass concentrations respectively. This bacterial fraction may have however affected the nature of the colloid system due to the different surface properties of the bacteria cells. Binova *et al.* (1998) reported outdoor *Scenedesmus* and *Chlorella* to contain uncharacterized bacteria of 10^2 to 10^8 cells.g^{-1} of algal culture. In the current study, concentrations were measured using plate counts and correlated using a standard dry weight-OD-cell count assay (Appendix 8.6.2). *Chlorella* grown *Microbacterium chocolatum* increased to a maximum of 5.45 x 10^{10} cells.L^{-1} and 0.0276 g.L^{-1} (1.97 x 10^{12} cells.g^{-1}) on day 13 whilst the *Scenedesmus* grown *Nocardioides aromaticivorans* reached a maximum on day 5 at 2.67 x 10^9 cells.L^{-1} and 0.128 g.L^{-1} (2.09 x10^{10} cells.g^{-1}). The *Nocardioides aromaticivorans* cells have a larger mass per cell compared to *Microbacterium chocolatum* cells. The average sized bacterium (Section 6.6) is about 2 µm long and 0.5 µm in diameter, with a cell volume of 0.6 - 0.7 µm^3 which corresponds to a mass of ca. 0.8 pg (Kubitschek, 1990). The *Microbacterium chocolatum* and *Nocardioides aromaticivorans* cell were calculated to weigh ca. 0.51 and 41 pg respectively from cell number/ weight ratios.

Chlorella vulgaris and the co-cultured *Microbacterium chocolatum* reached the death phase at day 8 and 12 respectively whilst *Scenedesmus sp.* and co-cultured *Nocardioides aromaticivorans* reached the death phase at day 11 and 5 respectively (Figure 17). Growth of the bacteria was therefore dependent on the reactor conditions and the growth of the respective co-cultured microalgae. In Figure 18, the growth curves of the isolated bacterial species in pure culture on Luria broth are presented. The culture pH increased form pH 6.6 to 8.8. Pure cultured *Nocardioides aromaticivorans* and *Microbacterium chocolatum* reached maximum biomass concentrations of 3.36 and 3.82 g.L^{-1} (6.99 x 10^{10} and 7.55 x 10^{12} cells.L^{-1}) after 1.3 and 2.3 days of cultivation respectively. *Microbacterium chocolatum* and *Nocardioides aromaticivorans* showed maximum specific growth rates of 2.80 and 1.79 day^{-1} respectively during algal co-culturing in the airlift photobioreactors (Figure 17) and 9.58 and 13.17 day^{-1} (0.40 and 0.55 h^{-1}) respectively during pure culture growth on

heterotrophic medium in shake flasks (Figure 18), suggesting that growth in algal suspensions is limited by the provision of organic carbon in solution to support growth.

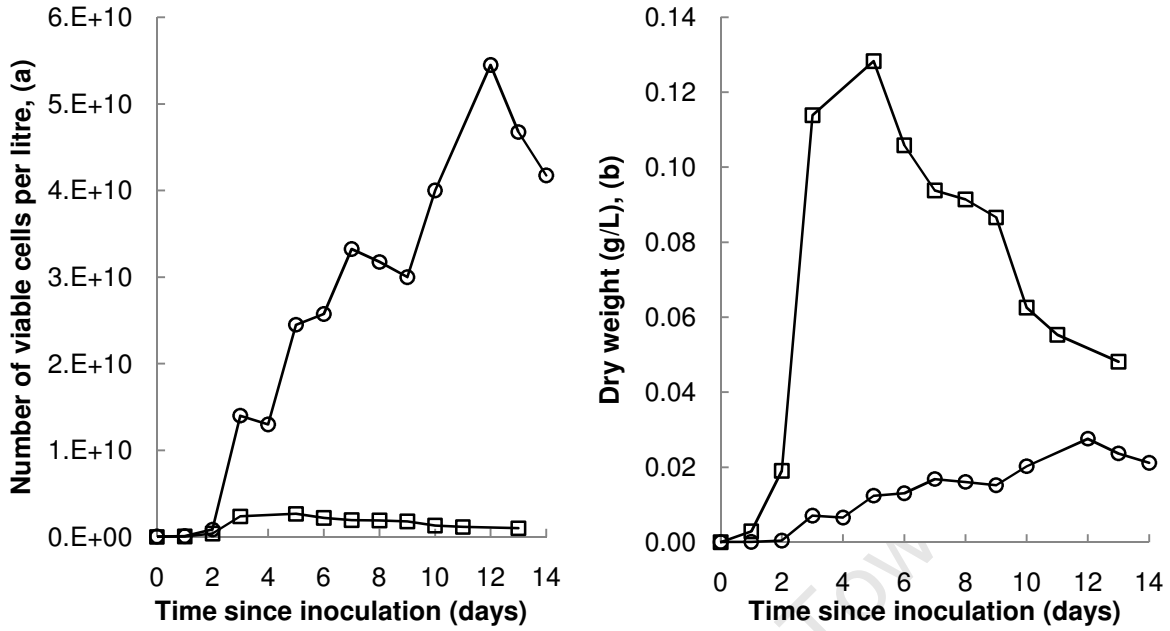

Figure 17: Cell concentrations (a) and dry weight, calculated using dry weight correlation assay (b) of *Nocardioides aromaticivorans* SB10005 (—□—) co-cultured with *Scenedesmus sp.* and *Microbacterium chocolatum* RW56 (—○—) co-cultured with *Chlorella vulgaris* during microalgal culture in the airlift photobioreactors and standard conditions and 2900 ppm CO_2

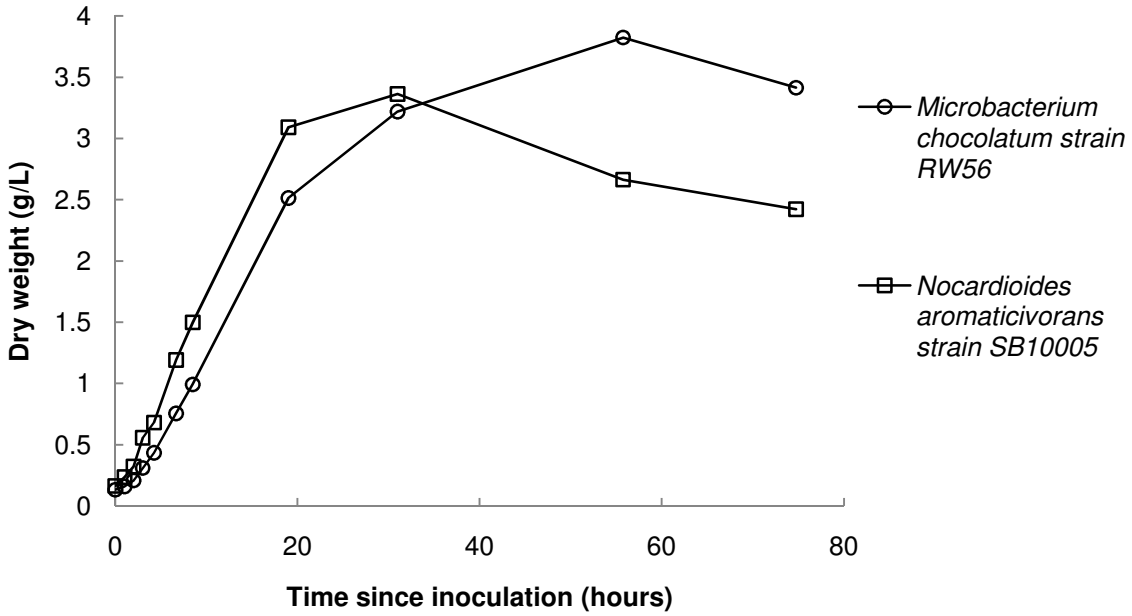

Figure 18: Isolated *Microbacterium chocolatum* RW56 and *Nocardioides aromaticivorans* SB10005 growth curves in 2 L shake-flasks at 30℃ and neutral pH

5.3 Characterising algal suspensions across growth phases

For the purpose of this dissertation, the exponential and stationary phases are of significant interest. The cell properties are a function of the growth phase and may be expected to influence how the cells respond to suspension conditions. These differences may provide insight into which physico-chemical properties are susceptible to exploitation. Figure 19 represents the natural logarithmic of cell concentrations as a function of time to determine the maximum specific growth rate and identify the exponential and stationary growth phases. A summary of these results are presented in Table 10.

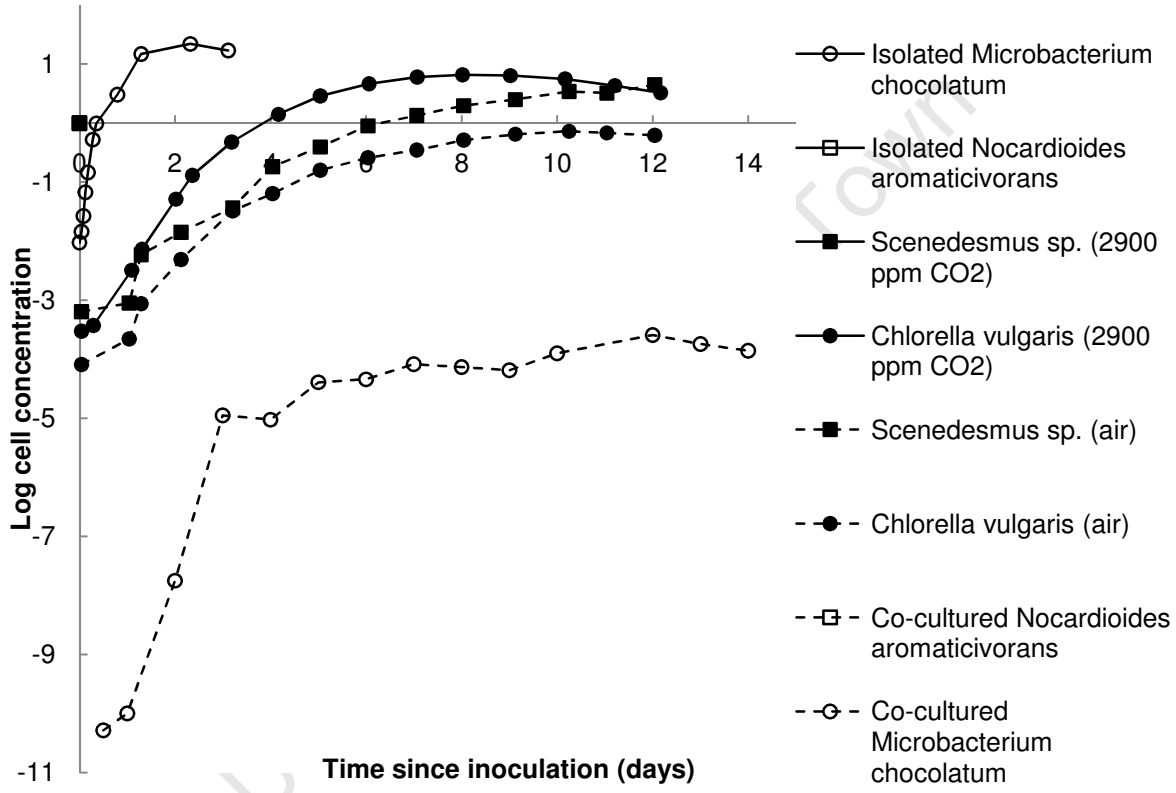

Figure 19: Growth curves for *Chlorella vulgaris* and *Scenedesmus sp.* grown on 2 L.min^{-1} 2900 ppm CO_2 or air at 25 ± 2°C with an initial pH of 6.9 ± 0.1 and constantly illuminated in the airlift photobioreactors; and isolated or co-cultured *Microbacterium chocolatum* RW56 from *Chlorella vulgaris* culture and *Nocardioides aromaticivorans* SB10005 from *Scenedesmus sp.* culture, in shake flasks at 30°C

Table 10: Summary of growth parameters for *Scenedesmus sp., Chlorella vulgaris, Microbacterium chocolatum* and *Nocardioides aromaticivorans*

Species	Maximum cell concentration ($g.L^{-1}$), [day]	μ_{max} (day^{-1})	Exponential growth phase (day)	Stationary growth phase (day)
Chlorella vulgaris (2900 ppm CO_2)	2.26, [8]	1.20	0.5 – 2.5	8 – 9.5
Scenedesmus sp. (2900 ppm CO_2)	3.22, [11]	1.38	0.5 – 2.5	10 - 12
Chlorella vulgaris (Air)	0.87, [10]	0.90	1 – 3	8.5 – 11
Scenedesmus sp. (Air)	2.16, [14]	0.83	1 – 3	13 –
Microbacterium chocolatum (*Chlorella vulgaris* Co-cultured)	0.028, [12]	2.80	1 – 3	-
Nocardioides aromaticivorans (*Scenedesmus sp.* Co-cultured)	0.13, [5]	1.79	1 – 3	-
Microbacterium chocolatum (Isolated)	3.82, [2.3]	9.58	0 - 0.35	1.3 – 1.7
Nocardioides aromaticivorans (Isolated)	3.36, [1.3]	13.17	0 – 0.27	2 – 2.5

Scenedesmus sp. showed very similar maximum specific growth rates to *Chlorella vulgaris.* Isolated *Nocardioides aromaticivorans* had a higher maximum specific growth rate than isolated *Microbacterium chocolatum* but the opposite was evident for the co-cultured bacteria growth rates. This suggests that the airlift photobioreactor conditions were slightly more favourable for the growth of *Microbacterium chocolatum*. Co-cultured bacteria had a lower growth rate and maximum concentration, compared with bacteria cultured in pure culture on complex media, even though it was cultivated for much longer periods. This was due to the limiting supply organic of nutrient by the autotrophic algal system and reactor conditions optimised for algal growth. The co-cultured bacteria are postulated to have become inhibited. Possible reasons for this are investigated later in this thesis with regards to suspension and surface conditions. The microalgae and co-cultured bacteria were in the exponential growth at the same time confirming a mutualistic or commensal relationship between the species.

Figure 20 represents the pH profiles for *Scenedesmus sp.* and *Chlorella vulgaris* cultured on air and 2900 ppm CO_2. The inocula were at a high pH due to the nature of their stock culturing which was immediately adjusted once inoculated into the airlift reactors. The biggest change in pH in all experiments was observed from day 0 – 2 where the microalgae acclimatise to the bioreactor. The cultures grown on 2900 ppm CO_2 became less alkaline, compared to cultures grown on air, due to the formation of carbonic acid through dissociating CO_2. *Scenedesmus sp.* and *Chlorella vulgaris* follow similar pH trends throughout and the suspension pH is a notable function of growth. Inocula pH was found to be at pH 12.1 and 9.8 for *Scenedesmus sp.* and *Chlorella vulgaris* respectively. These inocula were taken from culture sources grown on air over a period of ca. 2 weeks. However

the airlift photobioreactors were initially at neutral pH conditions. This change in pH might contribute to the length of the acclimatisation period for cells.

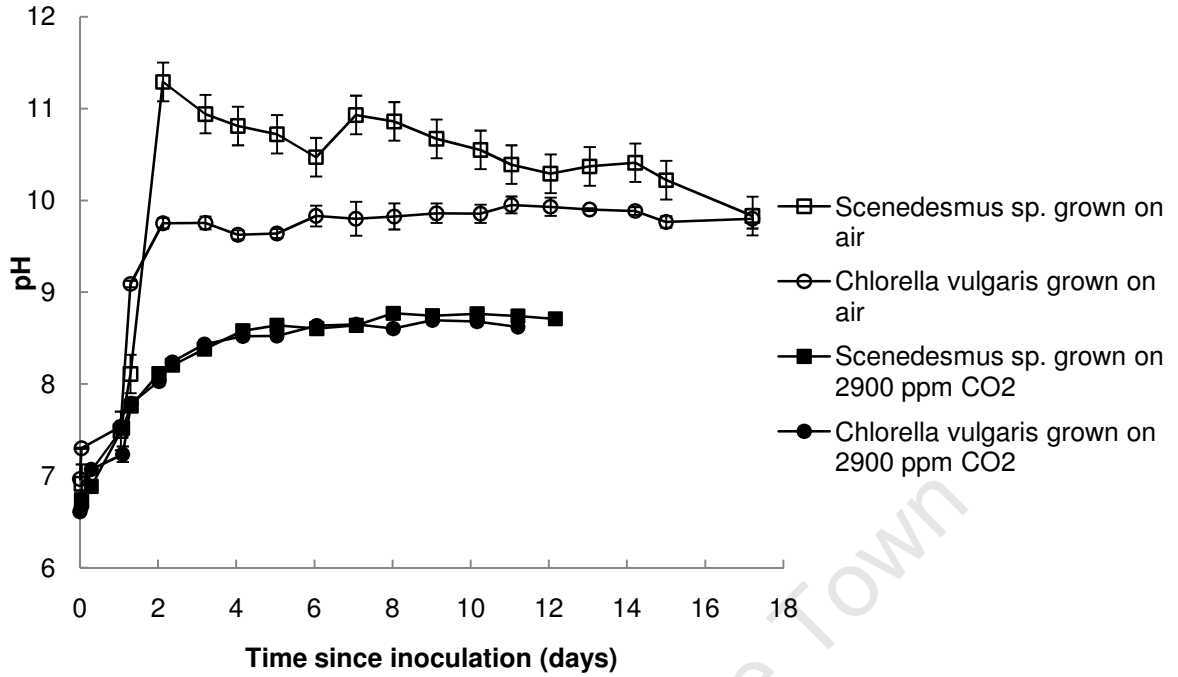

Figure 20: pH profiles during growth of *Chlorella vulgaris* and *Scenedesmus sp.* cultured on air and 2900 ppm CO_2 at 2 L.min^{-1}

Ionic strength was also a function of cell growth due to the uptake of ions from the media matrix of salts with growth (Figure 21a). This suggests that uptake of ionic species was greater than the rate of formation of extracellular products. The cultures grown on air remained at a slightly higher conductivity than those supplemented with CO_2 due to the lower growth rates and hence slower nutrient depletion. Dissolved carbon dioxide occurs mainly in three inorganic forms: free aqueous carbon dioxide [CO_2 (aq.)], bicarbonate (HCO_3^-), and carbonate ions (CO_3^{2-}). A minor form is true carbonic acid (H_2CO_3) whose concentration is less than 0.3% of [CO_2 (aq.)]. As the cultures were above pH 8 for most of the growth curve, CO_3^{2-} was the predominant form of CO_2 present in solution. Even though the increased CO_2 concentration in the reactor for cells grown on 2900 ppm CO_2 increased carbon ion loading, the excess carbon ions did not affect the ionic strength as the conductivity of the cultures grown on air were consistently higher.

Similarly to pH, the greatest decrease in conductivity occurred during the initial growth phases, followed by a decreasing rate of change in conductivity. However, cell concentrations did not increase consistently during stationary and death phases. Therefore conductivity did not correlate consistently with cell biomass concentration over the extended growth cycle (Figure 21b). This is postulated to be due to cell-ion chelation. This phenomenon was observed regardless of species and carbon supply and suggests that lysis was not the dominant effect. Dry mass remained constant whilst conductivity measurements decreased. Changes in suspension proton concentration and conductivity, as a function of biomass productivity, was investigated to determine if there was any relationship between these parameters that may explain the chelation phenomenon observed in Figure 21. However no relationship was observed (Appendix 8.6.3).

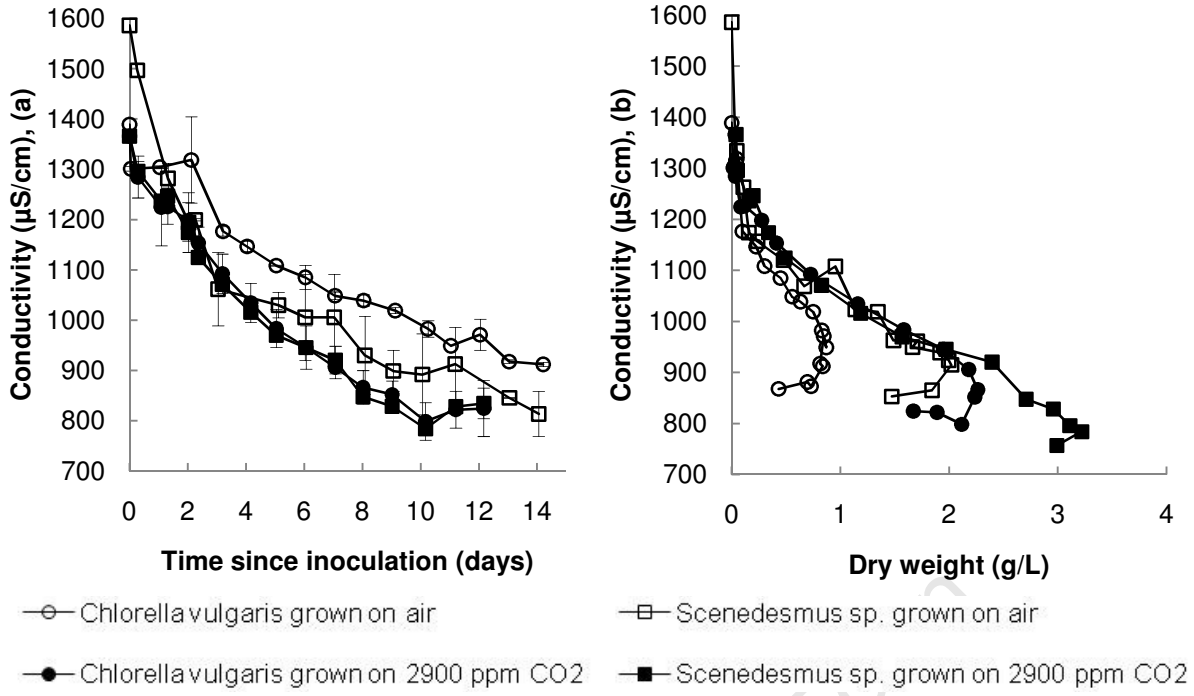

Figure 21: Conductivity profile during growth of *Chlorella vulgaris* and *Scenedesmus sp.* cultured on air and 2900 ppm CO_2

5.4 Characterising algal cell properties across the growth phases

Due to cell acclimation and reproduction mechanisms, the size of the cells change as a function of their growth phase. From microscope analyses, *Chlorella vulgaris* cells are spherical particles 2.50 ± 0.76 µm in diameter whilst *Scenedesmus sp*. are prolate, ellipsoidal cells with an average, major axis diameter of 6.90 ± 1.27 µm and an average, minor axis diameter of 2.78 ± 0.70 µm (Section 6.6).

Figure 22 shows the average effective particle size profile for *Scenedesmus sp.* and *Chlorella vulgaris* during growth, measured by laser light scattering. This size is not necessarily the size of single cells, but encompasses clump sizes. This particle size is most important for harvesting microalgae using sedimentation techniques. *Scenedesmus sp.* and *Chlorella vulgaris* reached a mean maximum effective particle diameter of 5.84 ± 0.11 and 4.67 ± 0.10 µm respectively after 1 day of cultivation. Particle sizes were at a maximum during the exponential phase and a minimum during stationary growth phase for both species. During exponential growth, the investigated microalgae formed small clusters of cells whilst multiplying (See Appendix 8.6.3 for size distributions). Lee *et al*. (1994) found a similar average cell size profile for *Chlorella vulgaris.* During the exponential phase, cells accumulated nutrients at the highest rate (Figure 21b). After this acclimation phase, cells divided and this was seen in the decrease in effective particle diameter. Cell sizes increased slightly after day 9 as cell growth rate decreased, hence decreasing division of cells.

Figure 22 gives some evidence that cells increased in size. Danquah *et al.* (2009a) found similar results with *Tetraselmis suecica / Chlorococum sp*. and showed this increase in cell size to be due to improved intercellular cohesion and agglomerations. *Chlorella vulgaris* in particular showed increased signs of autoflocculation (sticking to the wall and settling out of the reactor in clumps) towards the end of the growth curve. Figure 10 demonstrated maximum cell chlorophyll content between days 6 and 9 where Figure 22 shows a minimum in effective particle size diameter during this region. The chlorophyll content was the highest when cells were small and dividing rapidly.

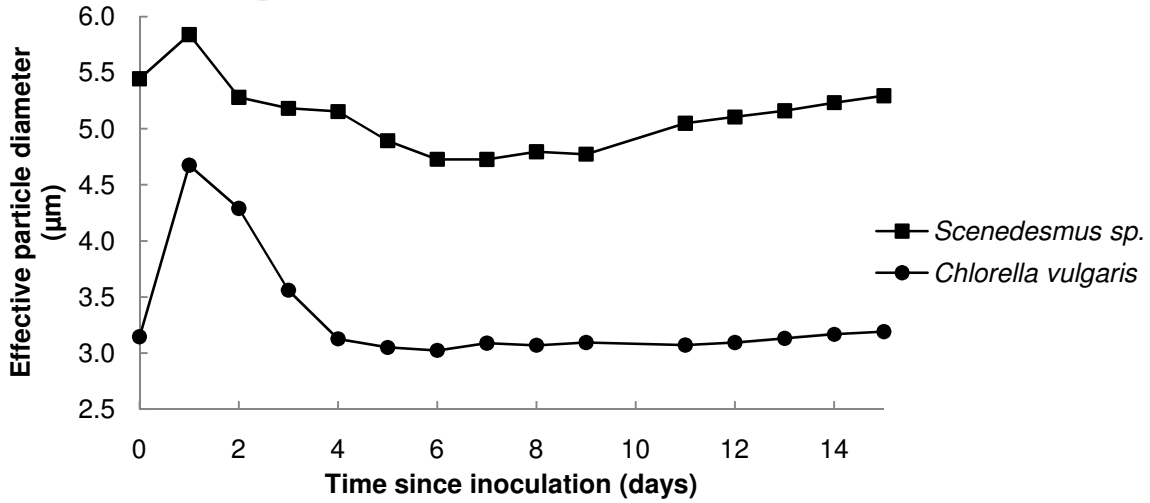

Figure 22: Mean effective size distribution of cell sizes for *Scenedesmus sp.* and *Chlorella vulgaris* during growth

The zeta potential profile of the microalgal culture was determined during the cultivation process in order to understand the physical intercellular interactions between the microalgal cells. By characterising the physical forces of attraction and repulsion between cells, an improved understanding of cell response to suspension conditions may lead to optimised harvesting conditions and explain autoflocculation phenomenon. All previous growth characteristics between species have been similar thus far. Figure 23 shows the zeta potential profiles of *Scenedesmus sp.* and *Chlorella vulgaris* cultured on air and 2900 ppm CO_2. Zeta potential was decoupled from any other influential factor, particularly that of suspending medium, by measuring the samples in a standard buffer solution of PBS (Section 4.4.4).

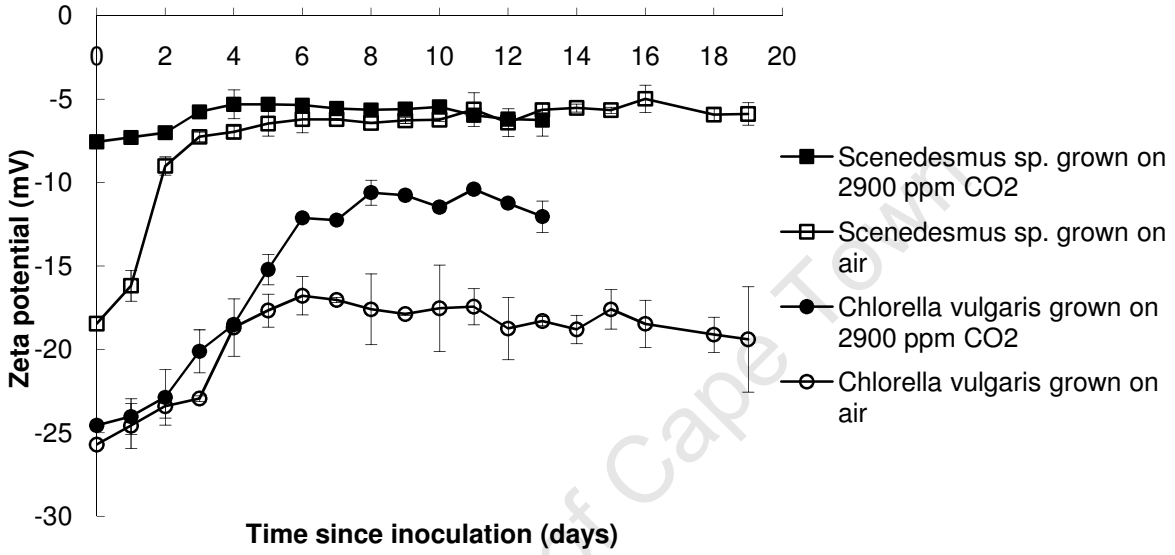

Figure 23: Zeta potential for *Scenedesmus sp.* and *Chlorella vulgaris* grown on air and 2900 ppm CO_2 at constant buffered pH 6.5 ± 0.1 in the airlift photobioreactor

Similar to most organisms, both species exhibited negatively charged surfaces throughout their life cycles. This is partly because the dispersion solution consists of dissociated cations making up the the growth media. *Scenedesmus sp.* exhibited the same electrokinetic behaviour when grown on air or 2900 ppm CO_2 with the biggest changes in electronegativity seen during the exponential growth phase. Although the inocula were at different conditions, *Scenedesmus sp.* acclimated to an average steady charge of -5.75 ± 0.36 mV whether grown on air or 2900 ppm CO_2. *Chlorella vulgaris* took until day 6 to reach a steady surface charge. Figure 23 shows the dependence of *Chlorella vulgaris* surface charge on CO_2 concentration reaching steady state at -11.08 ± 0.61 and -18.63 ± 0.53 mV for 2900 ppm CO_2 and air respectively.

During the exponential growth phase of the microalgal cells, there was a maximum growth rate and hence the metabolic rate, mobility and growth kinetics of the cells were optimal. Due to the increase in the kinetics of cell growth, there was minimal intercellular interaction between individual cells in the culture and this induced a net electronegative zeta shield around the cells (Danquah *et al.*, 2009b), thus creating repulsion between the cells. As this phenomenon decreased, so the zeta potential and pH increased. Comparing zeta potential (Figure 23) and pH (Figure 20) profiles, a significant relationship is observed even whilst zeta potential measurements were taken at a fixed pH. As the cultures entered exponential

growth, pH and zeta potential increased, eventually reaching a steady state during stationary growth. On approaching and during the stationary phase, the metabolic rate of the microalgal cells was low and this reduced the electronegative zeta shield around the individual cells; resulting in improved intercellular interactions and hence increased cell agglomeration. To exploit the natural zeta potential trends observed in Figure 23, cells should be harvested after the exponential phase where cells have a minimum surface charge indicating a maximum in colloidal instability.

Similarly to the microalgae, the zeta potential of the co-cultured bacteria is governed by different growth phases and follows a similar profile. The *Chlorella* grown *Microbacterium chocolatum* had a similar zeta potential to *Scenedesmus sp*. ranging between -6.5 and -11.0 mV, whilst the *Scenedesmus* grown *Nocardioides aromaticivorans* had a similar zeta potential to *Chlorella vulgaris* of between -18.0 and -22.5 mV. This shows that the dominant bacteria and microalgae in each system follow different electrokinetic profiles and this may be manipulated to increase or decrease bacteria-microalgae interactions. Van Loosdrecht *et al.* (1987) found results for a range of bacteria tested and identified the exponential phase to be the optimal growth region for cell adhesion due to lower electrophoretic mobilities.

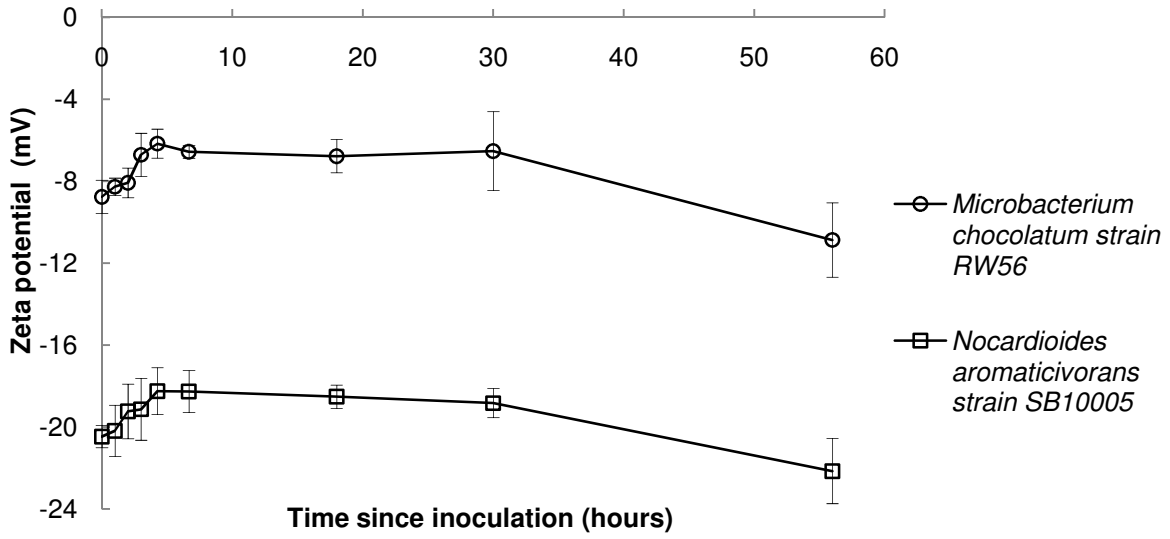

Figure 24: Zeta potential for *Nocardioides aromaticivorans* SB10005 and *Microbacterium chocolatum* RW56 during growth at constant buffered pH 6.5 ± 0.1

Figure 25 shows the hydrophobicity indices of *Scenedesmus sp*. and *Chlorella vulgaris* during exponential and stationary growth phases. Both microalgal species revealed similar hydrophobic behaviour throughout the growth phase. Repeated experiments revealed large variances in the data (Table 7) due to slightly different growth conditions in each experiment. Hydrophobicity was therefore more dependent on suspension conditions as a result of growth phase and not on the cell growth metabolisms and reproduction phases. In the exponential phase, *Chlorella vulgaris* was slightly more hydrophobic compared to *Scenedesmus sp*. At pH 10 and in the absence of any EOM, the microalgal cells were relatively hydrophilic with a relative index less than 8%. Conductivity, pH and EOM must therefore be manipulated to increase the hydrophobic activity to induce flocculation and hence improve recovery efficiencies.

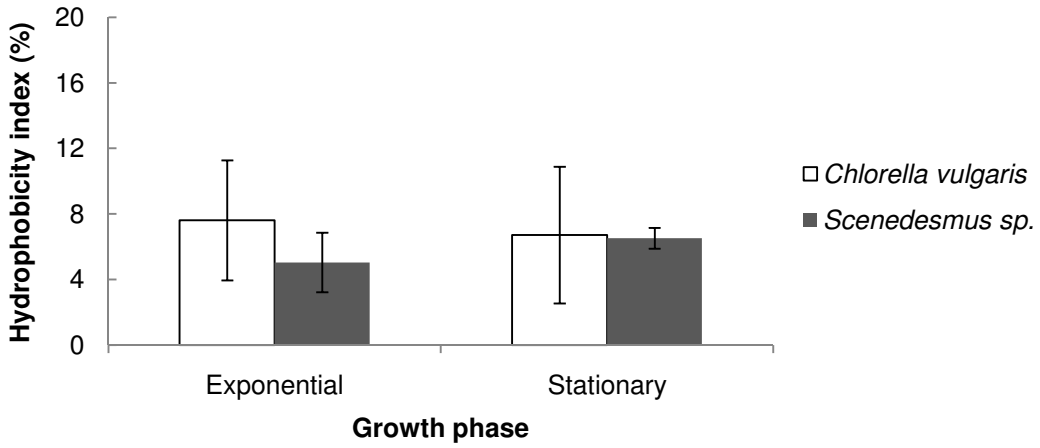

Figure 25: Hydrophobicity of *Scenedesmus sp*. and *Chlorella vulgaris* during exponential and stationary growth phases grown on 2900 ppm CO_2, at constant buffered pH 10

5.5 Carbon loop

During the microalgae cultivation in the airlift photobioreactors, autoflocculation (predominately *Chlorella vulgaris*) was observed during the stationary and death phases. This was observed as cells sticking to the reactor walls and sparger and forming larger clumps and settling to the bottom of the reactor. Literature suggests a range of explanations for this phenomenon including nitrogen, light and carbon limitations (Schenk *et al.*, 2008; Sheehan *et al.*, 1998), excretion of organic macromolecules (Benemann *et al.*, 1980), inhibited release of microalgal daughter cells (Arad *et al.*, 1981) and aggregation between microalgae and bacteria (Lee *et al.*, 2009a). EOM concentrations may also influence the surface chemistry of particles and promote flocculation (Henderson *et al.*, 2008b). Figure 26 shows the total extracellular carbon concentration during the growth of *Scenedesmus sp.* and *Chlorella vulgaris*. This phenomenon was initially shown by Tenney *et al.* (1969) where a steep increase in extracellular metabolites during the stationary and death phases of microalgal growth was described. Throughout the experiment, *Chlorella vulgaris* had a higher EOM and lower biomass concentration compared to *Scenedesmus sp.* The EOM for both species increased during growth until reaching a maximum of 36.5 and 25.0 $mg.L^{-1}$ on day 7 for *Chlorella vulgaris* and *Scenedesmus sp.* respectively. Thereafter the EOM remained at a relatively constant level similar to that of the inocula. The inocula were found to have extracellular concentrations of 35 and 20 $mg.L^{-1}$ for *Chlorella vulgaris* and *Scenedesmus sp.* respectively. These EOM concentrations correspond with literature findings ranging from 1.8 to 81 $mg.L^{-1}$ (Hoyer *et al.*, 1985). This increased EOM coupled with minima in zeta potential offers a possible explanation for increased autoflocculation towards the end of the growth phase of microalgae in the airlift photobioreactors.

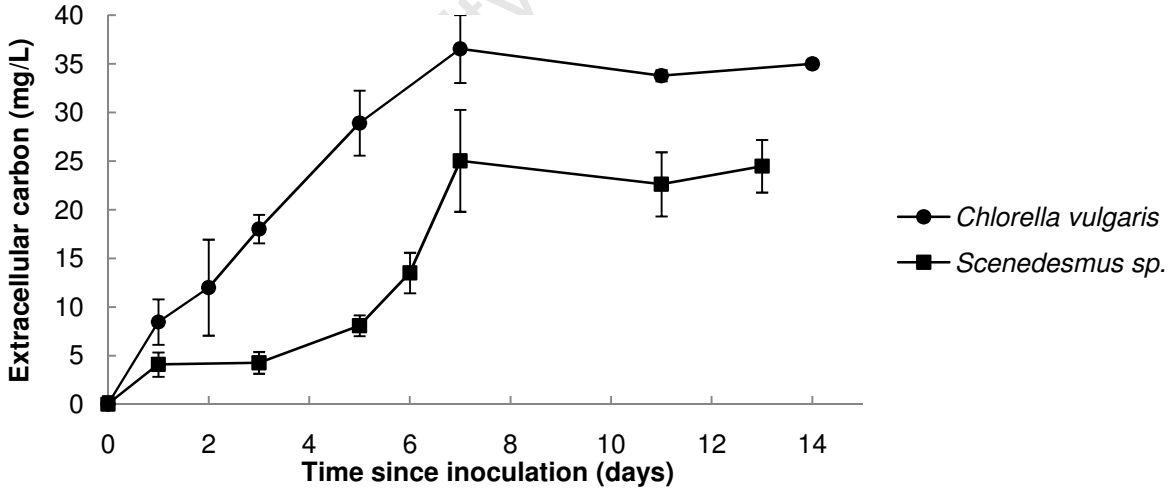

Figure 26: Total organic and inorganic carbon (TICTOC) as extracellular product in *Scenedesmus sp.* and *Chlorella vulgaris* cultures during growth in airlift photobioreactors at 2 $L.min^{-1}$ 2900 ppm CO_2 and 25 ± 2℃ following the pH profiles in Figure 20

Understanding carbon utilisation in microalgae is an important factor not only for CO_2 sequestration but also to understand the fundamentals of how the overall batch reactor operates in terms of products, by-products and the accumulation thereof. Knowledge of these factors may lead to an improved understanding of microalgae cell behaviour, factors that affect autoflocculation and other physical suspension properties. Figure 27 and Figure

28 represent the full carbon balance over the airlift photobioreactors for *Chlorella vulgaris* and *Scenedesmus sp*. respectively. Extracellular carbon was calculated theoretically based on a mass (m) balance around the reactor as follows:

$$mCO_{2\ in} - mCO_{2\ out} = mCO_{2\ accumulation} \quad (23)$$

$$mC_{\ accumulation} - mC_{\ algal\ biomass} - mC_{\ bacteria\ biomass} = mC_{\ extracellular} \quad (24)$$

To determine the amount of carbon in the bacterial and algal cells, an elemental analysis was performed of *Chlorella vulgaris, Scenedesmus sp., Microbacterium chocolatum RW56* and *Nocardioides aromaticivorans SB10005* and is presented in Table 11. The algal species were found to have similar CHN compositions as were the two bacteria. The bacteria were found to have lower carbon compositions compared to the bacteria.

Table 11: CHN analyses of microalgae and co-cultured bacteria in the airlift photobioreactors, cultured on 2 L.min^{-1} 2900 ppm CO_2

Dry weight (%)	*Microbacterium chocolatum*	*Nocardioides aromaticivorans*	*Chlorella vulgaris*	*Scenedesmus sp.*
C	34.65	33.89	48.21	46.11
H	6.06	7.78	7.08	7.44
N	8.55	9.24	9.41	4.07
Other	50.74	49.09	35.3	42.38

In both reactors, bacterial biomass contributed less than 5% to the total carbon accumulation. The CO_2 uptake was an instantaneous measurement and represents an average CO_2 uptake rate by the bioreactor over daily measurements. This measurement represents the $mCO_{2\ accumulation}$ term in Equation 23. The cumulative carbon uptake graph represents the amount of carbon the bioreactor was accumulating in terms of carbon mass. The cumulative fixed carbon in biomass represents the actual dry weight biomass measurements without bacteria. The theoretical cumulative extracellular carbon was then calculated using Equation 24. The extracellular carbon in the reactors for both *Chlorella vulgaris* and *Scenedesmus sp*. initially increased until day 7, following the trend shown in Figure 26. After day 7, comparing Figure 26 with Figure 27 and Figure 28 it can be concluded that the theoretical carbon in the extracellular material follows a similar trend to that of the measured carbon but is an overestimation. This is due to the measurement of the biomass excluding wall growth and sedimented biomass. After day 7 of growth, the cultures became dense and light limited. The microalgae began to autoflocculate and adhere to the reactor walls over-emphasizing the decline in biomass. The increase in extracellular carbon coincided with an increase in autoflocculation. This theoretical measurement is thus a combination of extracellular carbon and carbon in microalgal flocs. A direct relationship is therefore observed between EOC increases and autoflocculation induction.

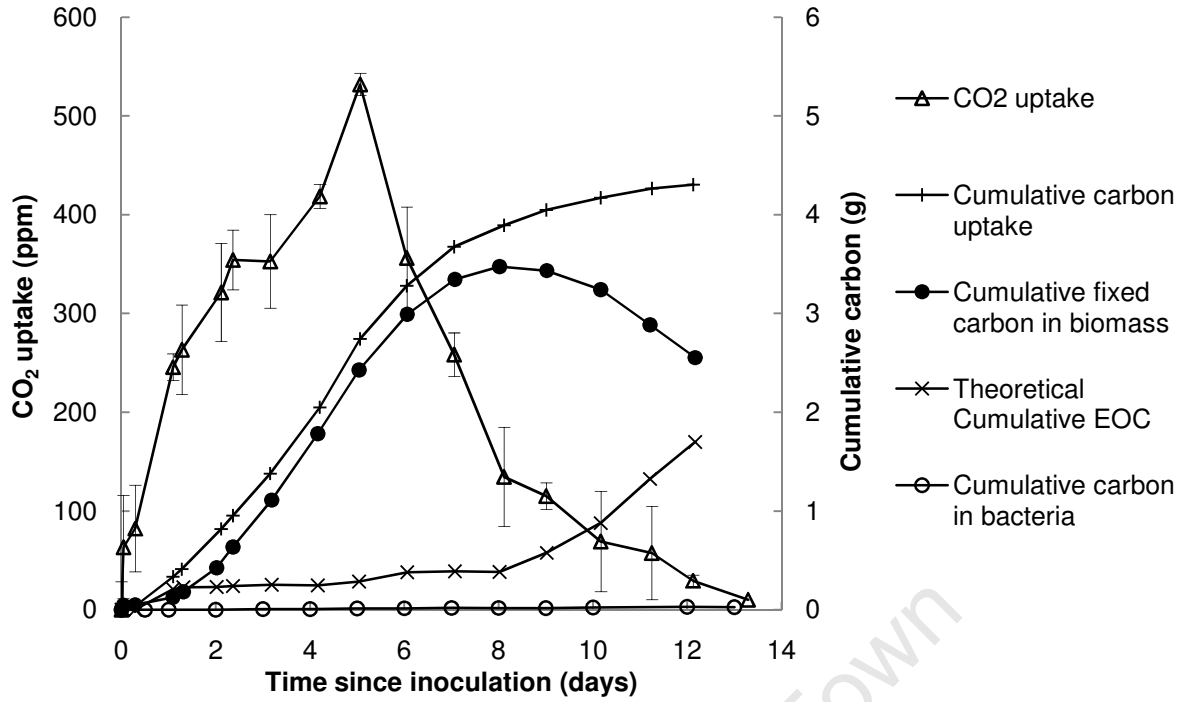

Figure 27: *Chlorella vulgaris* carbon balance during growth in an airlift photobioreactor at 2 L.min^{-1} 2900 ppm CO_2 and 25 ± 2℃ following the pH profiles in Figure 20

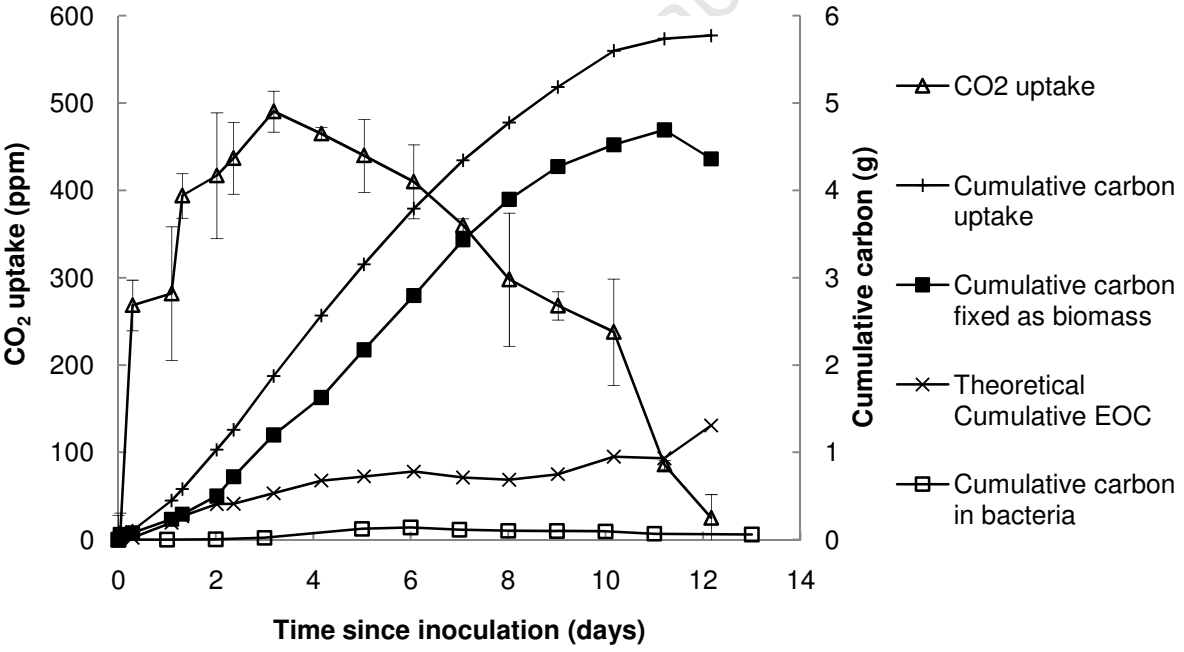

Figure 28: *Scenedesmus sp.* carbon balance during growth in an airlift photobioreactor at 2 L.min^{-1} 2900 ppm CO_2 and 25 ± 2℃ following the pH profiles in Figure 20

Bilanovic and Shelef (1988) reported autoflocculation to be induced by increased ionic strength. This ionic strength is predominately attributed to increase in pH from cationic acids or anionic bases. However organic material may also induce bio-autoflocculation (Lian *et al.*, 2008). From qualitative analysis, both microalgal species, especially *Chlorella vulgaris*, began to autoflocculate starting from day 8 of the growth cycle. During this phase the cell zeta potential and hydrophobicity remained constant. This coincided with an increase in

extracellular carbon and a minimum in conductivity (Figure 29). It is therefore postulated that an increase in extracellular organic loading increases autoflocculation.

Figure 29 shows the theoretical extracellular carbon and measured extracellular TICTOC. As mentioned before, the theoretical quantification is an overestimation but suggests a qualitative trend with regards to increasing extracellular carbon (similar to TICTOC analysis). An increase in EOM and cell-ion chelation (Figure 21b) decreases the electric double layer repulsion between particles due to adsorption of the highly charged polyelectrolytes on oppositely charged cells. This promotes an increase in charge neutralisation and hence autoflocculation.

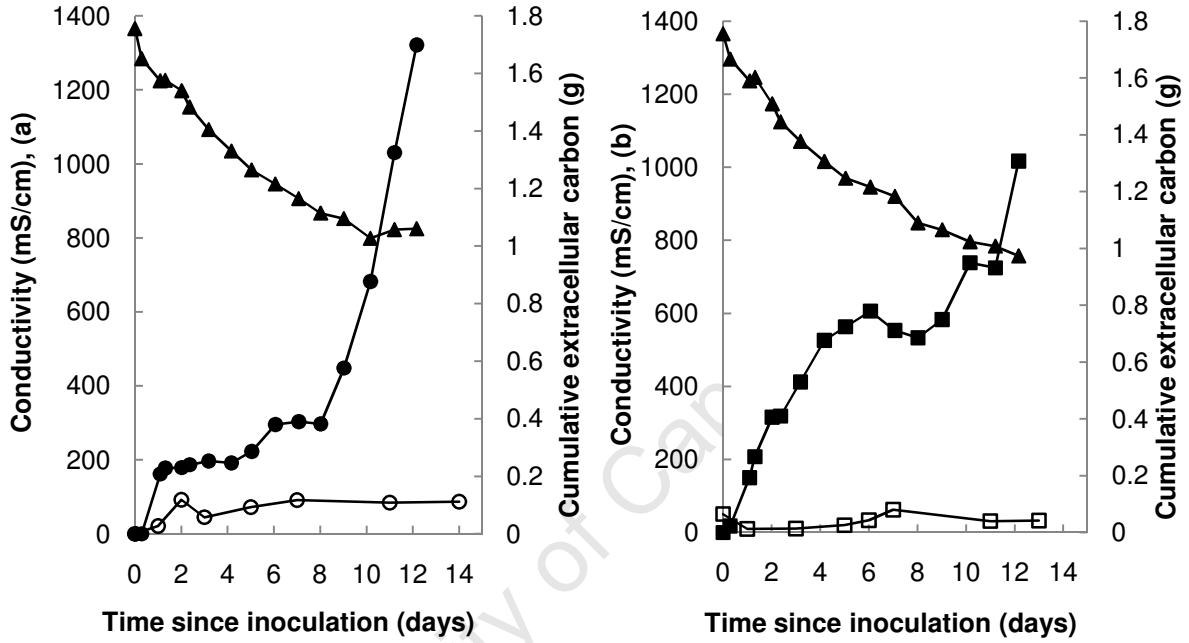

Figure 29: *Chlorella vulgaris* (a) and *Scenedesmus sp.* (b) conductivity (—▲—), theoretical extracellular carbon (—●—) and measured extracellular carbon (TICTOC) (—○—, —□—) during growth in an airlift photobioreactor at 2 L.min^{-1} 2900 ppm CO_2 and 25 ± 2°C following the pH profiles in Figure 20

5.6 Characterising algal surface properties across suspension conditions

Microalgae characteristics such as hydrophobicity, surface charge, morphology, motility, cell density and the EOM composition and concentration change to some degree during or at different suspension conditions. These algal characteristics have been identified as key factors to be manipulated to ensure successful algal recovery. From the growth profiles described in Section 5.4, pH and conductivity were found to vary the most naturally through the growth phases. The measurement of zeta potential and hydrophobicity were sensitive to the change in ionic strength (conductivity) and since ionic strength and pH are affected by each other (Figure 78, Appendix 8.6.4), zeta potential, hydrophobicity and other surface properties were also dependent on pH.

Conductivity was used as a measure of ionic strength and was varied in solution through addition of $MgCl_2$. The concentration of $MgCl_2$ was assumed to be the only contributing factor towards ionic strength in suspensions of re-suspended algae as EOM and growth media salts were removed through washing. Electrophoretic mobility was measured as a function of ionic strength and presented in Figure 77, Appendix 8.6.4. Electrophoretic mobility normally increases with decreasing salt concentration (van Loosdrecht *et al.*, 1987). However, micro-organisms may conduct part of the current, which leads to a reduction of mobility, particularly when the conductivity of the solution is low.

Figure 30 shows the relationship between zeta potential and ionic strength for *Scenedesmus sp.*, *Chlorella vulgaris* and the respective co-cultured bacteria. Throughout the range of ionic strengths studied (generated by $MgCl_2$), all species remained electronegative. An increase in conductivity to 1 $S.cm^{-1}$ significantly increased the zeta potential of all species from the range -27 to -56 mV to -5 to -15 V. Increasing salt concentration increased ionic strength which resulted in a decrease in electrical interactions between two particles charged alike because the difference between the ionic concentration in the bulk fluid and the stern layer surrounding the solid particle was minimised. An increase in ionic strength compresses the solid surface double layer and thus reduces the stability of the colloid (Stumm, 1992). Therefore at increased ionic strength above 1 $S.cm^{-1}$, cell colloids were notably less stable and repulsion between particles was at a minimum. This led to increased autoflocculation behaviour. While *Chlorella vulgaris* and *Scenedesmus sp.* had similar low zeta potentials at low ionic strength (-28 and -32 mV respectively), at conductivities great than 2 $S.cm^{-1}$, these increased to -12 and -4 mV respectively, suggesting that *Scenedesmus* flocculates more readily.

Figure 30 also describes the dependence of cell hydrophobicity on conductivity for *Scenedesmus sp*. and *Chlorella vulgaris*. These exhibited respective maximum and minimum hydrophobic behaviour in de-ionised water. Figure 25 showed a slight increase in hydrophobicity for *Scenedesmus sp*. on progression from exponential to stationary phase, with an associated decrease in culture media conductivity (Figure 21). This agrees with Figure 30 demonstrating a decrease in hydrophobicity as conductivity increases. *Scenedesmus sp*. was therefore most hydrophobic towards the end of the growth phase when conductivity was at a minimum. *Chlorella vulgaris* was most hydrophobic at 1 $S.cm^{-1}$.

Not much change was observed in surface charge and hydrophobicity above 8 $S.cm^{-1}$. The system was therefore saturated with respect to cell-ion interactions.

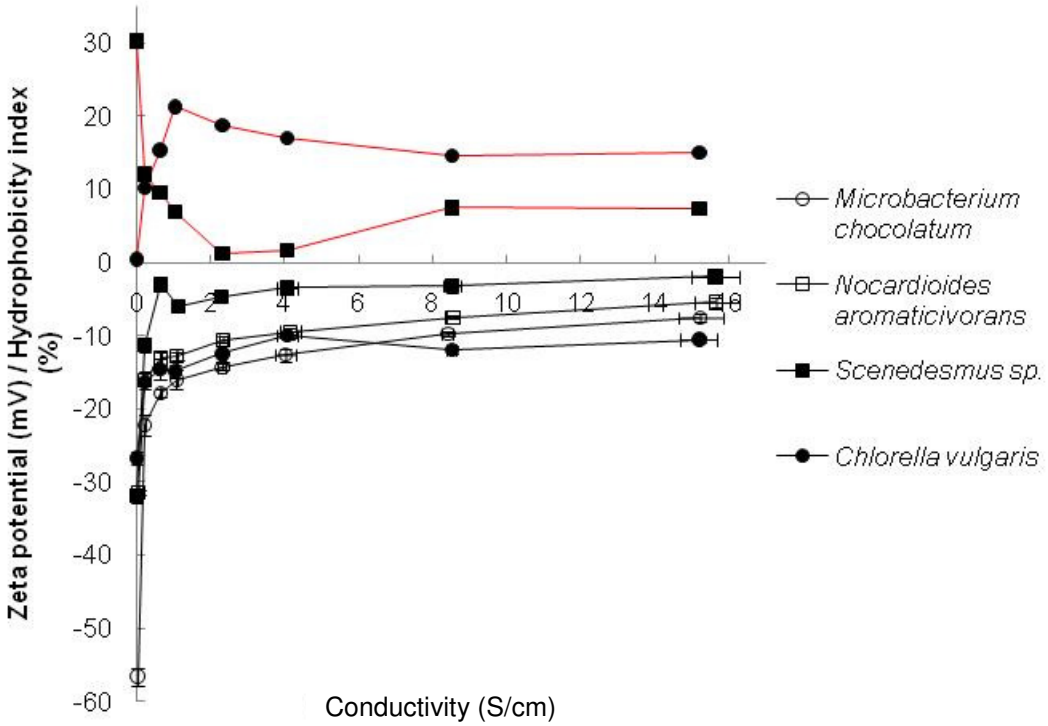

Figure 30: Ionic strength (adjusted with $MgCl_2$) effects on surface charge (——) and hydrophobicity (——) of *Chlorella vulgaris*, *Scenedesmus sp.*, *Microbacterium chocolatum* and *Nocardioides aromaticivorans* (pH~7.8)

To investigate the effect of pH on inter-cellular activity, the isoelectric point for *Scenedesmus sp*. and *Chlorella vulgaris* was examined (Figure 31 and Figure 32 respectively). The point of zero charge (PZC), also known as isoelectric point, constitutes a point at which negligible inter-cellular repulsion is experienced and autoflocculation is characteristic in an ionic solution. The zeta potentials were investigated to determine significant differences in potential charge between species. The effect of growth phase, feed CO_2 concentration and resuspension media was investigated to determine the dominant influences on the isoelectric point. From Figure 31, the isoelectric point of *Scenedesmus sp*. is shown at pH 4.34 ± 0.17. This isoelectric point was found to be independent of harvesting time, suspension conductivity and culturing CO_2 concentration. The cells were the most electronegative at very alkaline conditions above pH 12. When suspended in the growth media, the zeta potential profile was dampened due to increased ionic strength within the suspension. At a pH of 8 to 10, typical of culture conditions, the zeta potential varied from -4 to -12 mV in media to -24 to -40 mV in distilled water. This suggests that *Scenedesmus sp*. suspensions are more stable in de-ionised water and confers with zeta potential data in Figure 30. The growth phase and CO_2 feed concentration had smaller effects on the zeta potential profile of *Scenedesmus sp*. However across a range of ionic strength and during exponential and stationary phase, cultures grown on air displayed a slightly dampened surface charge profile compared to cultures grown on 2900 ppm CO_2. Similarly at different ionic strengths and CO_2 concentrations, exponential phase cultures exhibited slightly dampened surface charge profiles compared to stationary phase harvested cells. These differences are best shown in the differences between the *Scenedesmus sp.* sample grown

on air, measured in media and harvested during the exponential phase compared to the samples grown on 2900 ppm CO_2, measured in dH_20 and harvested during the stationary growth phase with the biggest difference in surface potential of 35.6 mV at pH 9.59. Therefore depending on the surface charge region required a specific culture condition (i.e. harvest growth phase, re-suspension conductivity and concentration of CO_2) could be targeted.

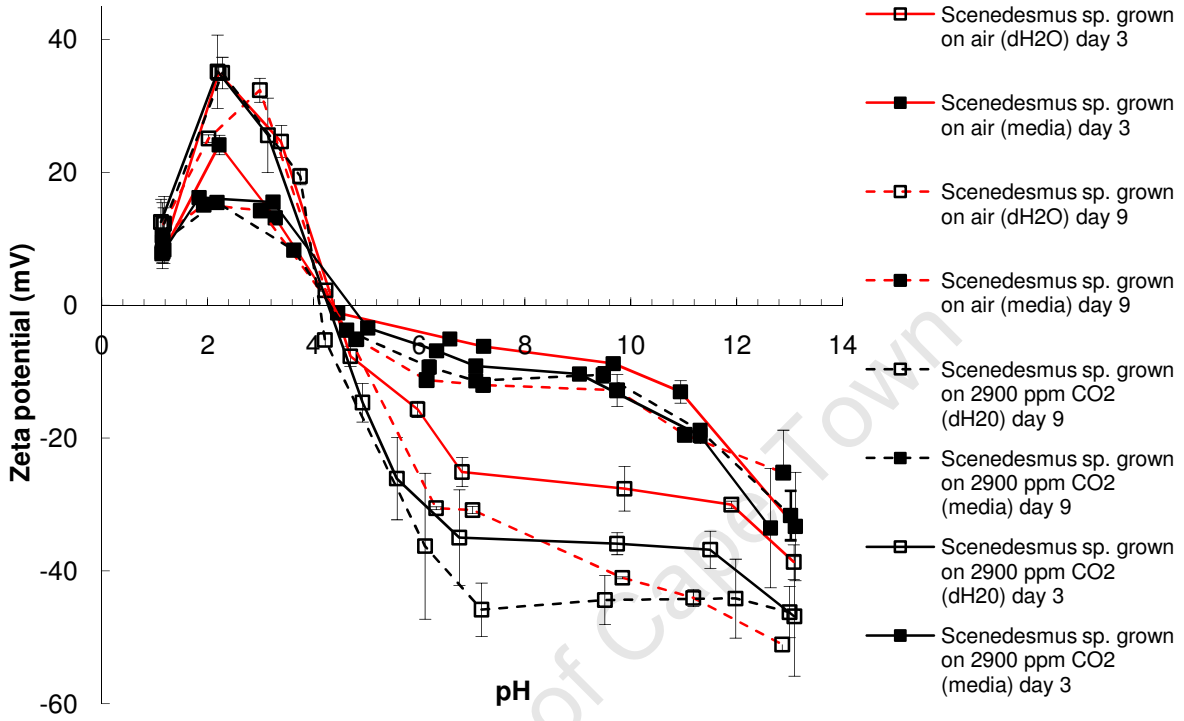

Figure 31: *Scenedesmus sp.* zeta potential profile and point of zero charge on air (—) and 2900 ppm CO_2 (—) during exponential (—) and stationary (--) growth phases and resuspended in dH_2O (-□-) or media (-■-)

In Figure 32 the zeta potential of *Chlorella vulgaris* as a function of pH is presented, showing the isoelectric point at pH 1.03 ± 0.15. Similarly to *Scenedesmus sp.,* this isoelectric point was found to be largely independent of harvesting time, suspension conductivity and culturing CO_2 concentration. The ionic strength of the suspension matrix had little effect on the *Chlorella vulgaris.* An increased CO_2 feed concentration resulted in a more electronegative zeta potential profile regardless of the growth phase of the cells. *Chlorella vulgaris* had a strictly decreasing surface charge profile with the largest variance in zeta potential between samples conditions of 21.7 mV found at pH 5. Certain growth, suspension and harvesting conditions presented no PZC for *Chlorella vulgaris* under the conditions investigated. Autoflocculation via charge neutralisation would not be possible under these circumstances. Unlike the zeta potential sinusoidal profile followed by *Scenedesmus sp., Chlorella vulgaris* was a strictly decreasing function of pH.

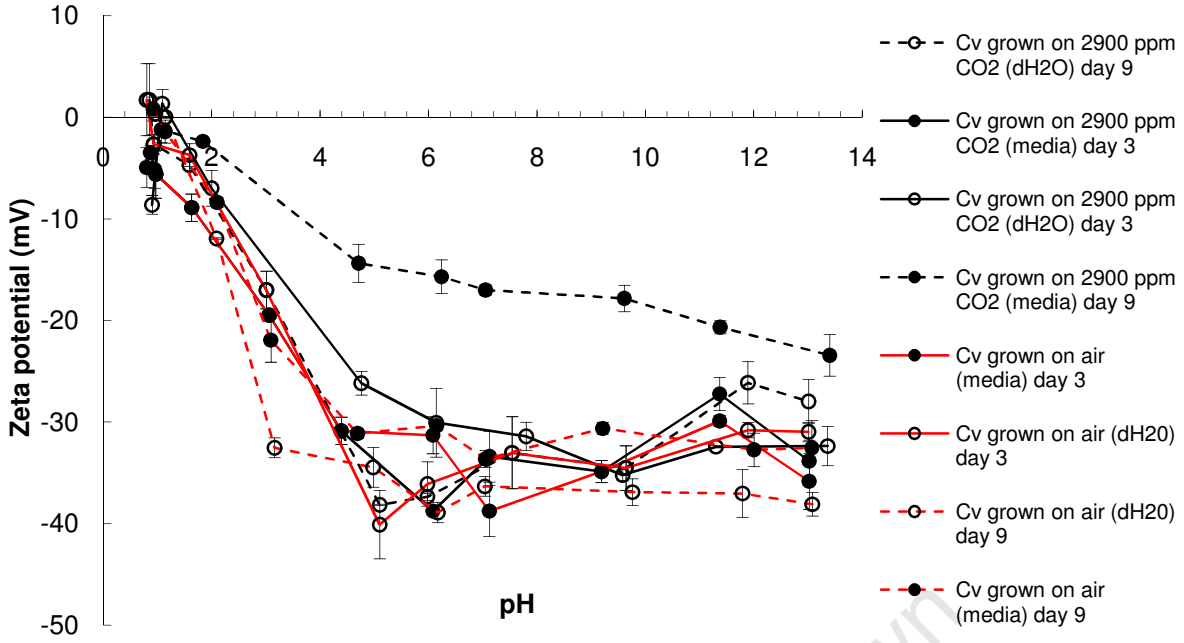

Figure 32: *Chlorella vulgaris* zeta potential profile and point of zero charge on air (—) and 2900 ppm CO_2 (—) during exponential (—) and stationary (--) growth phases and resuspended in dH_2O (-▫-) or media (-■-)

Both microalgal species exhibited predominant electronegative surface charges, especially in an alkaline environment. The largest zeta potential difference between species was between pH 2.5 and 3.5. However at pH 2.8 the attractive interactions between the cells of the different species were at a maximum as the cells were oppositely charged with equal magnitude. Opposite charges on the cell surface will cause attraction whilst like charges will promote repulsion. As *Chlorella vulgaris* was predominantly electronegative, this species would best be autoflocculated in a high ionic solution via a bridging mechanism as the cations in solution could easily be saturated to form a bridge network between cells.

Zeta potential of the bacterial species of interest is presented as a function of pH in Figure 34. *E. coli* BL2 (DE3), *Bacillus sp.* and *Nocardioides aromaticivorans* had a PZC at pH 3.00 ± 0.03, 2.75 ± 0.02 and 1.60 ± 0.07 respectively. *Microbacterium chocolatum* did not display a PZC under the conditions investigated as it remained electronegative throughout the tested pH range under testing conditions (Figure 33). The isoelectric point may lie between the tested pH values of 1.91 and 3.33, but this measurement has little value as the trend was relatively smooth. This trend may be amplified by changing culturing and harvesting conditions following findings from Figure 31. *Scenedesmus sp., Bacillus sp.* and *E. coli* BL2 (DE3) all exhibited sinusoidal zeta potential trends, whilst *Chlorella vulgaris* and *Nocardioides aromaticivorans* are better described by a decreasing logarithmic function. At pH 13 all the species had a noticeable change in zeta potential. This phenomenon was due to the increased conductivity of the sample solution and followed the trend observed in Figure 30. At increased alkalinity, cells were at a minimum zeta potential whilst ionic strength was at a maximum. The positive charged ions thus adsorbed onto the negatively charged cells forming a bridge network of cells and cations. As salt loading had an effect on the zeta potential, it also impacts on the other physical solution properties and must be considered as another variable in estimating flocculation activities.

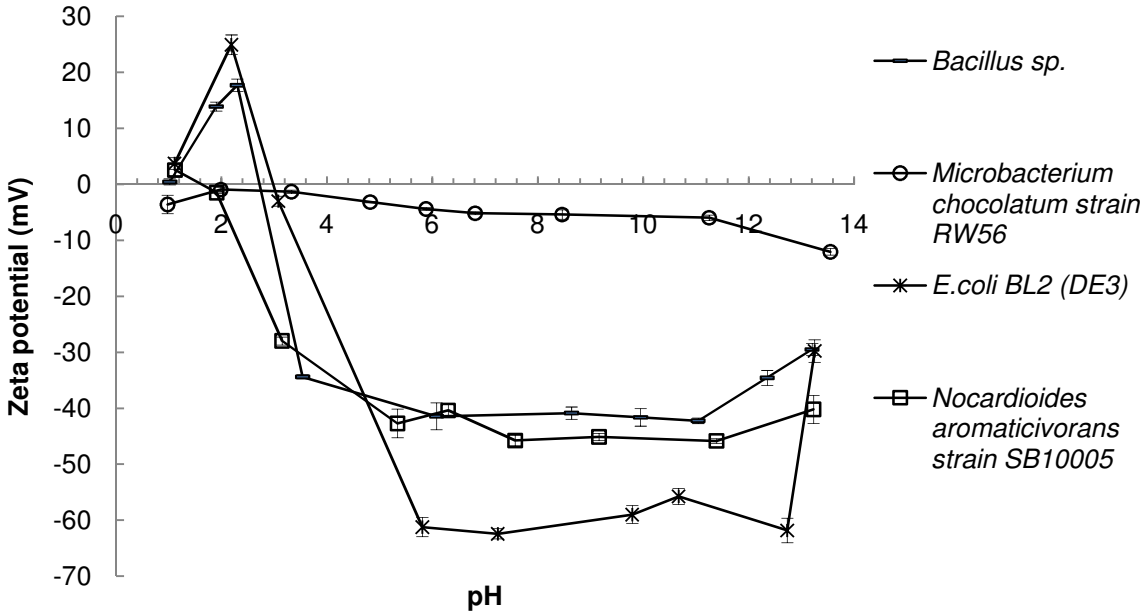

Figure 33: *Bacillus sp.*, *E. coli* BL2 (DE3), *Microbacterium chocolatum* RW56 and *Nocardioides aromaticivorans* SB10005 points of zero charge

In Figure 34a, it is seen that *Chlorella vulgaris* and *Nocardioides aromaticivorans* followed similar trends in zeta potential with no substantial difference in electronegativity. *Bacillus sp.* and *E. coli* showed positive zeta potentials at pH 2.6, showing a significant difference in the zeta potential compared to *Chlorella vulgaris,* including the opposite charge. *Chlorella vulgaris* would therefore tend to bioflocculate between pH 1 and 3 with these bacteria due to van der Waals attractions. The co-cultured, *Microbacterium chocolatum* approached a PZC near pH 3 and maintained a low electronegativity throughout the pH range (-1 to -10 mV). Hence the greatest attraction between *Chlorella vulgaris* and a bacterium is expected for this pair at pH 3.

In Figure 34b, it is seen that *Scenedesmus sp.*, *Bacillus sp.* and *E. coli* BL2 (DE3) exhibited similar trends of zeta potential dependence on pH. However as the zeta potential profile of *Scenedesmus sp*. between pH 1 and 6 was higher than the bacteria and had a higher PZC at pH 4, there are regions where there are large differences in zeta potential between bacteria and *Scenedesmus sp*., particularly between pH 3 and 4. As the *Microbacterium chocolatum* zeta potential profile remained negative, attractive forces between *Scenedesmus sp.* and this species are expected between pH 1 and 4 with the optimal being at pH 3.75. The co-cultured bacteria, *Nocardioides aromaticivorans*, yielded the biggest range and greatest magnitude of difference in zeta potential in comparison to *Scenedesmus sp.* between pH 1 and 4.1. Figure 34 therefore depicts the regions where cell bioflocculation is expected via patching mechanisms solely based on van der Waals attractions. This was further investigated in Section 6.3 and micrographs are presented in Section 6.6. Table 12 summarises the surface charge findings of all the bacteria and microalgae investigated in this dissertation.

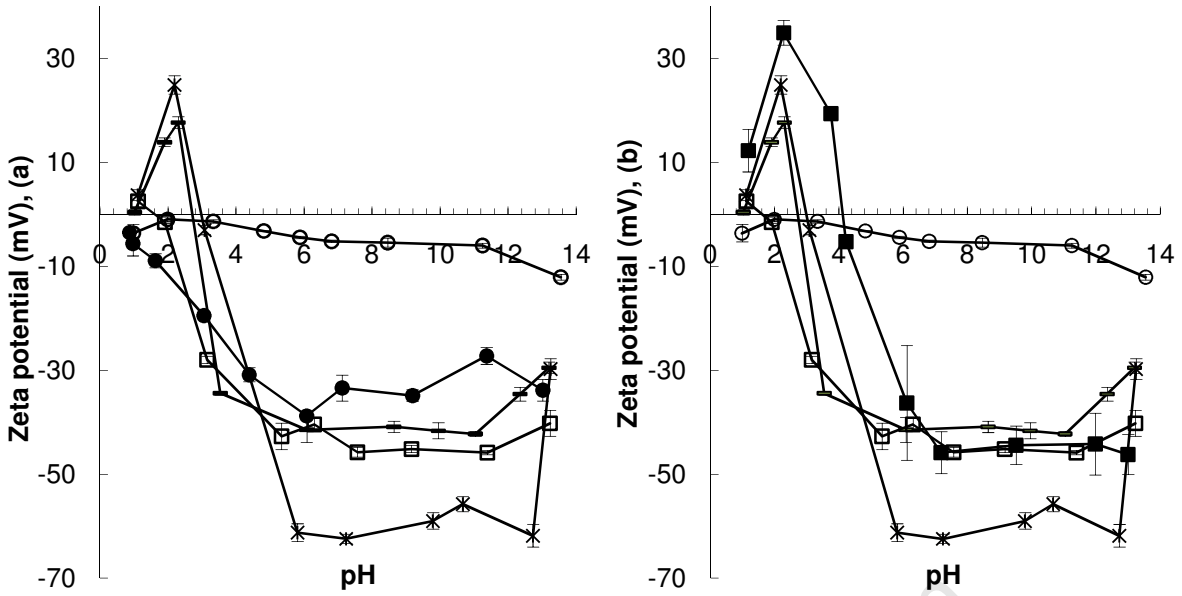

Figure 34: *Bacillus sp.* ( ), *E. coli* BL2 (DE3) ( ), *Microbacterium chocolatum* RW56 ( ), *Nocardioides aromaticivorans* SB10005 ( ) and *Chlorella vulgaris* ( ) / *Scenedesmus sp.* ( ) points of zero charge

Table 12: Summary of zeta potential findings for microalgae and bacteria

	PZC (pH)	Minimum surface potential (mV), [pH]	Maximum surface potential (mV), [pH]
Scenedesmus sp.	4.34 ± 0.17	-46.2 [13.0]	+35.0 [2.28]
Chlorella vulgaris	1.03 ± 0.15	-38.8 [6.08]	+1.72 [0.80]
Nocardioides aromaticivorans SB10005	1.65	-45.8 [11.39]	+2.55 [1.12]
Microbacterium chocolatum RW56	-	-12.1 [13.55]	-1.32 [3.33]
Bacillus sp.	2.70	-42.2 [11.04]	+17.7 [2.30]
E. coli BL2 (DE3)	2.95	-61.8 [12.73]	+24.9 [2.19]

Hydrophobicity is widely reported to vary over a pH range (Jameson, 1999). Figure 35 shows the relationship between the hydrophobicity index and pH for a range of bacterial and microalgal species. Every species exhibited a global maximum between pH 0.80 and 3.33 and a local maximum at ca. pH 13. The *Microbacterium chocolatum*, *Chlorella vulgaris* and *Nocardioides aromaticivorans* were highly hydrophobic between pH 2 and 4. *Bacillus sp.* and *E. coli* BL2 (DE3) had relatively low hydrophobic indices below pH 3 and above pH 4. *Scenedesmus sp.* showed very low hydrophobicity throughout the pH range investigated (also described in Figure 30). Most species revealed a small increase in hydrophobicity at pH 12 and above. This was due to the increased salt loading increasing the solution ionic strength and charge density which compresses the electric double layer around the solid particles (Stumm, 1992). All species, except *Scenedesmus sp.*, showed a maximum hydrophobicity between pH 2 and 4. This represents an unstable area for the suspensions investigated both in terms of hydrophobicity and surface charge, and should therefore be exploited as a possible flocculation region. The differences in surface charges and hydrophobicity profiles across microbial cells of similar structure have been reported in

literature. For example *Bacillus* has been found to have increased hydrophobic behaviour compared to *E. coli* as shown in this dissertation. The hydrophobicities of mixtures of hydrophilic and hydrophobic cells are also reported to be linearly correlated with the cell mixing ratio *(Daffonchio et al., 1995).* Therefore the use of hydrophobic bacteria such as the co-cultured bacteria will affect the suspension properties, improving bioflocculation efficiencies.

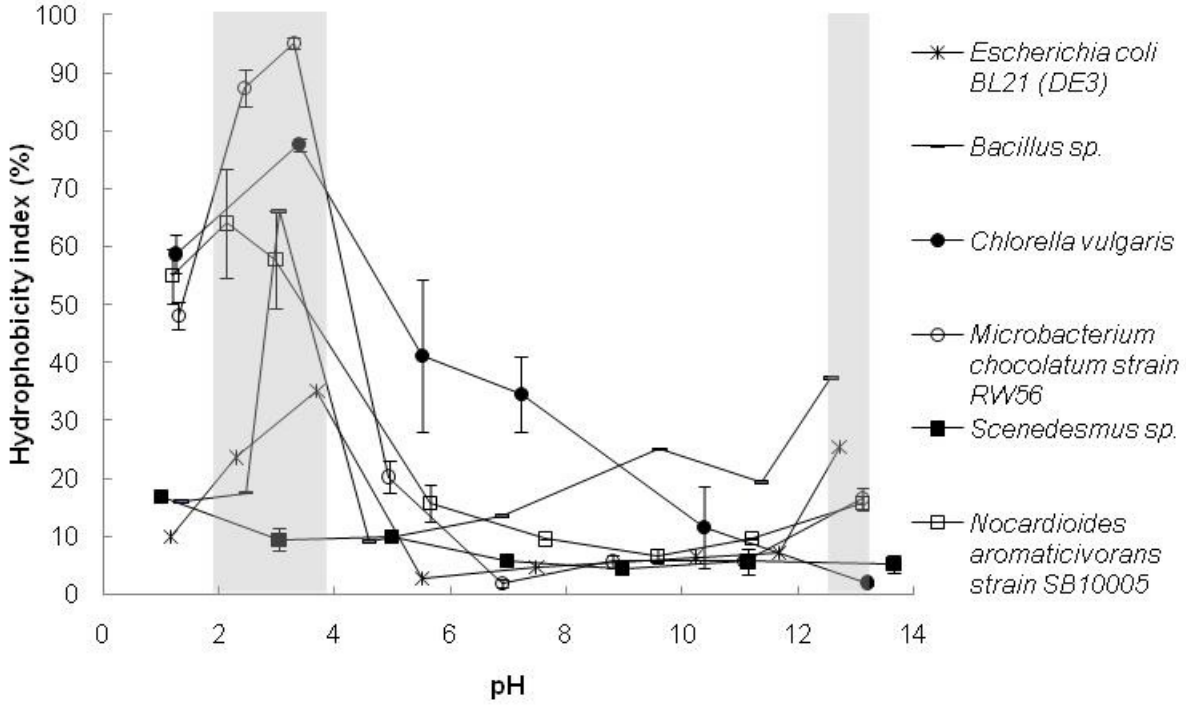

Figure 35: Hydrophobicity index profiles of microalgae and bacteria resuspended in dH_2O over a range of pH, measured via the carbon adhesion technique

5.7 Rheology

To consider the concentration of microalgae for commercial use, the fluid flow characteristics of the suspensions need to be characterised as a function of algal concentration and morphology. The rheology results provide shear stress response approximations for the relative species and hence an upper limit for recovery efficiencies and concentration factors. The flow characteristics also provide useful information on species specific interactions when concentrated and flocculated. This information is useful for floc stability and mechanism explanations.

In Figure 36 the Newtonian shear profiles for *Chlorella vulgaris* (a) and *Scenedesmus sp.* (b) respectively are presented. The linear goodness of fit and gradient data are presented in Table 13 thereafter. The *Chlorella vulgaris* shear profile was examined up to a dry biomass concentration of 275 g.L^{-1} and remained linear throughout. *Scenedesmus sp.* suspensions were found to follow a linear shear profile up to 205 g.L^{-1}. Extrapolating the data to a zero shear stress confirmed a yield stress of approximately zero. A zero yield stress and a linear shear profile verified Newtonian fluid flow behaviour (Figure 2) for both species up to 200 g.L^{-1}. The initial variance in values observed between shear rates of 300 and 500 s^{-1} was due to mechanical inaccuracies and was consistent across all samples including a blank run. The readings were restricted between 100 and 1000 s^{-1} due to equipment restrictions; however blank runs showed this range of measurement to be accurate and gave conclusive characterisation of standards.

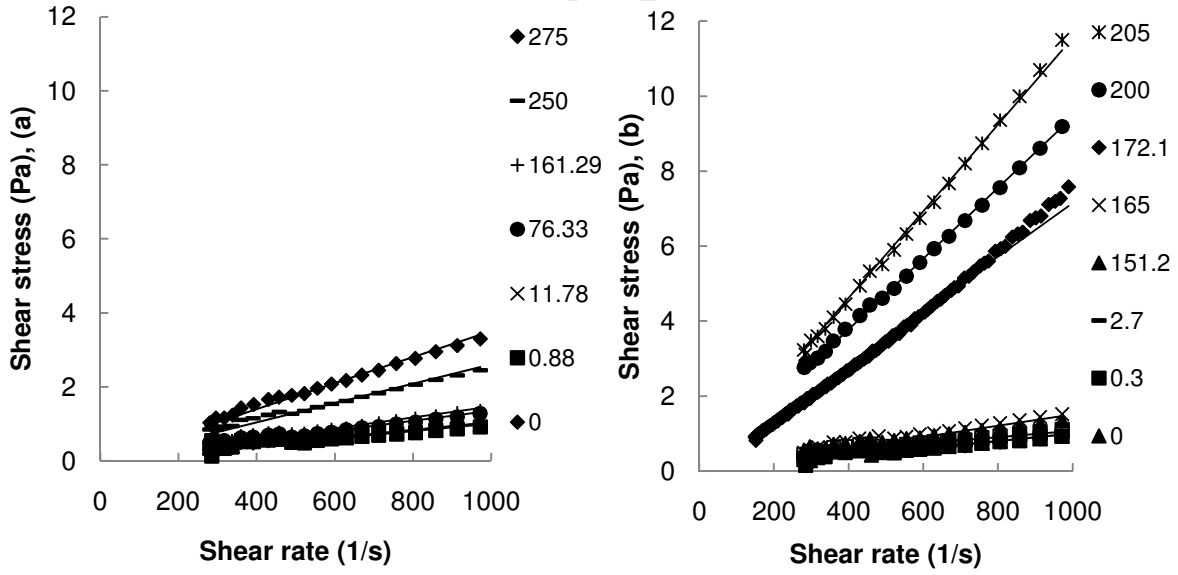

Figure 36: Newtonian shear for *Chlorella vulgaris* (a) and *Scenedesmus sp.* (b) at different mass concentrations (g.L^{-1}) at 25℃

Table 13: Linear goodness of fit for *Scenedesmus sp.* and *Chlorella vulgaris*

Species	Concentration (g.L^{-1})	Slope (Pa.s)	R^2
Chlorella vulgaris	275	0.0036	0.9856
	250	0.0027	0.9756
	161	0.0014	0.9407
	76	0.0012	0.9058
	0 - 40	0.0011	0.8252
Scenedesmus sp.	205	0.0116	0.9982
	200	0.0094	0.9988
	172	0.0071	0.9914
	0 - 165	0.0010 - 0.0015	0.8123

As described in Table 3, Section 2.2.1, apparent viscosity is described as the rate of change of shear stress with respect to the shear rate. Figure 37 illustrates the Newtonian rheology of *Chlorella vulgaris* and *Scenedesmus sp.* up to 275 and 205 g.L^{-1} respectively. *Chlorella vulgaris* demonstrated a consistently lower apparent viscosity compared to that of *Scenedesmus sp*. The relatively low viscosity exhibited by both species was evidence that very little or no extracellular polysaccharides were produced (Chen *et al*., 1997). The measurement system used predicted a dynamic viscosity of 0.0010 Pa.s for de-ionised water which is slightly higher than 0.00089 Pa.s reported in literature. The presented results at low viscosities (0.0008 to 0.0040 Pa.s) are therefore slight overestimations of the respective apparent viscosities. At higher viscosities above 0.0040 Pa.s, the results were accurate with tested standards.

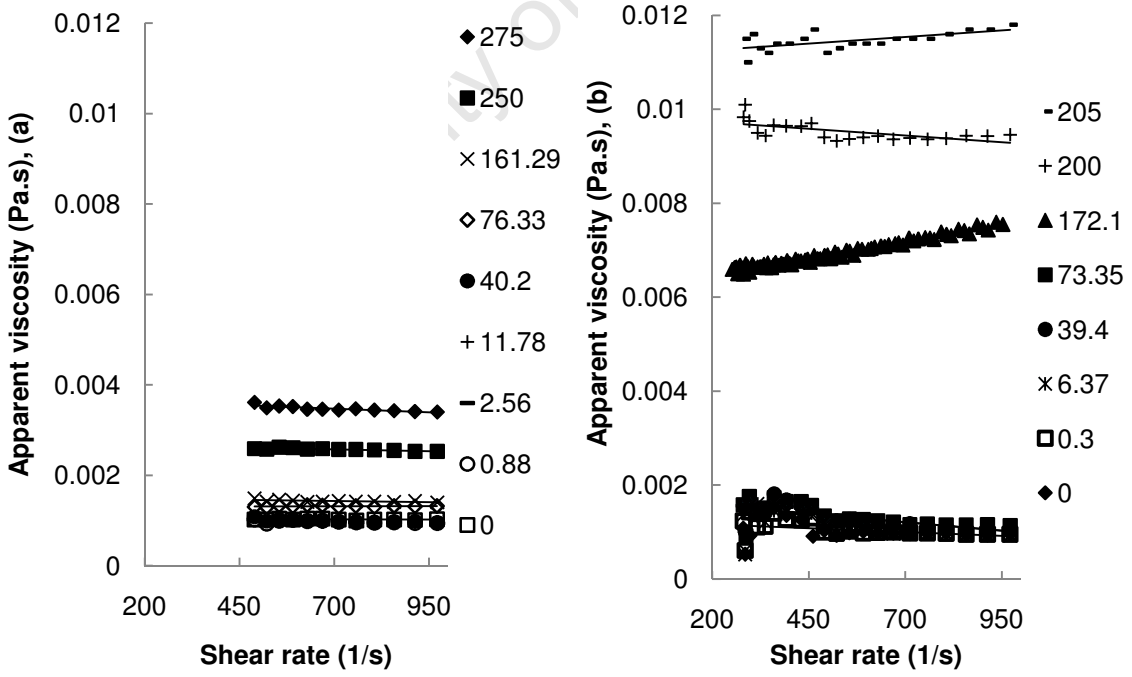

Figure 37: Newtonian viscosity for *Chlorella vulgaris* (a) and *Scenedesmus sp.* (b) at different mass concentrations (g.L^{-1}) at 25℃

Scenedesmus sp. and *Chlorella vulgaris* displayed similar, linear apparent viscosities up to a dry biomass concentration of 165 g.L^{-1} as shown in Figure 38. *Scenedesmus sp.* exhibited a higher apparent viscosity which increased exponentially between 165 and 205 g.L^{-1}. A

notable increase in viscosity with biomass concentration was noted for *Chlorella vulgaris* above 233 g.L^{-1} with a viscosity of 0.0036 Pa.s reported at 275 g.L^{-1}. Wu and Shi (2008) demonstrated a similar rheological profile for *Chlorella spp.* An increase in viscosity with concentration due to the dispersed particle concentration may be described in terms of a power series in concentration c (Coulson *et al.*, 1983):

$$\eta = A + Bc + Cc^2 + ... \quad (25)$$

where A, B, C, ... are constants.

The marked difference in apparent viscosity between *Scenedesmus sp.* and *Chlorella vulgaris* is postulated to be due to differences in cell size and surface charge (Chen *et al.*, 1997; Sherman, 1970) as well as inter-particle forces. For commercial harvesting of microalgae, both investigated species show Newtonian fluid rheology at concentrations typically attained with the achievable concentration factors of typical unit operations. The data provided are useful for the design of flow systems used for harvesting and conventional transport of *Scenedesmus sp.* and *Chlorella vulgaris* biomass. Further dewatering of algal suspensions, prior to drying and processing as dense suspensions, can be expected to yield highly viscous and non-Newtonian suspensions.

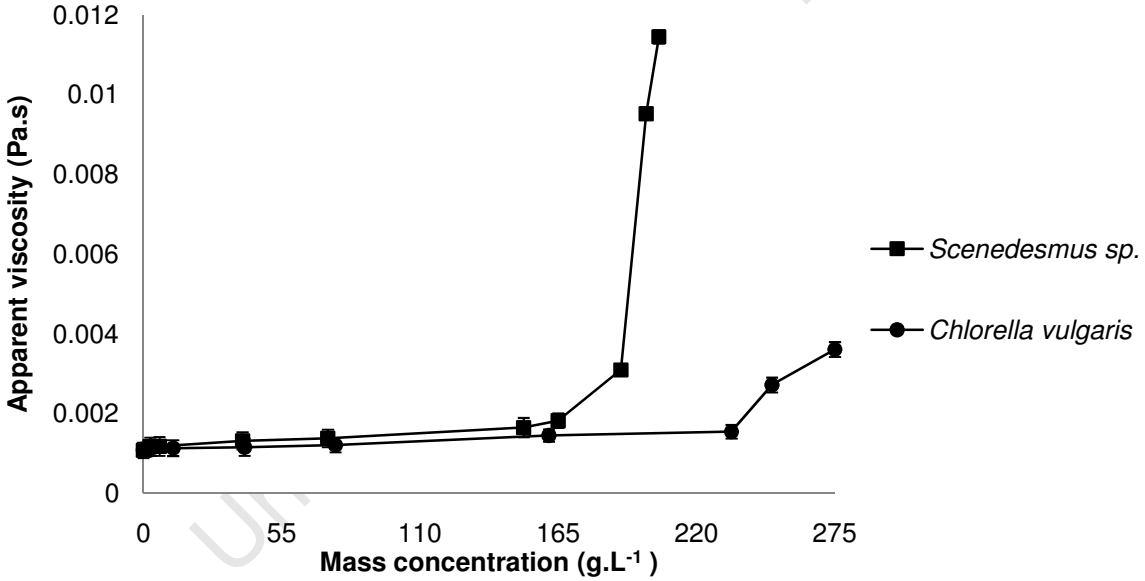

Figure 38: Newtonian rheology for different mass concentrations (g.L^{-1}) for *Scenedesmus sp.* and *Chlorella vulgaris* at 25°C

Scenedesmus sp. was found to behave as a dilatant (shear thickening) fluid when concentrated above 205 g.L^{-1} (Figure 39). Examples of Matlab curve-fit data supporting this are presented in Appendix 8.6.5. A dilatant material is one in which viscosity increases with the rate of shear. Such a shear thickening fluid is an example of a non-Newtonian fluid. The dilatant effect occurs when closely packed particles are combined with enough liquid to fill the spaces between them. The liquid acts as a lubricant at low velocities, and the dilatant fluid flows easily. However at higher velocities, the liquid is unable to fill the gaps created between particles, and friction greatly increases, causing an increase in viscosity (Cheremisihoff and Nicholas, 1988). Figure 39 shows that even at high concentrations with shear thickening behaviour, *Scenedesmus sp.* had a zero yield stress and hence portrayed

no elasticity. The dilatant fit parameters for the *Scenedesmus sp*. cultures are presented thereafter in Table 14.

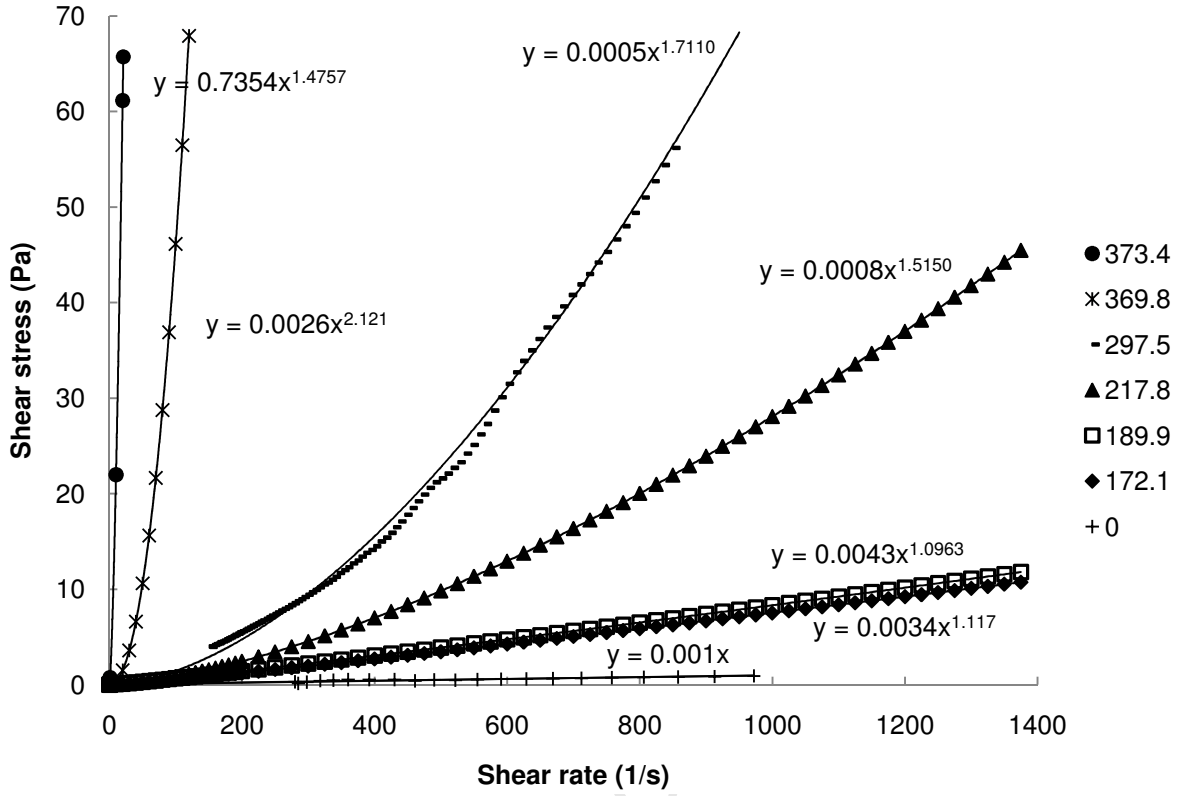

Figure 39: Dilatant rheological behaviour of *Scenedesmus sp.* at different mass concentrations ($g.L^{-1}$) at 25℃

Table 14: *Scenedesmus sp*. dilatant fit parameters as a function of dry biomass concentrations

Biomass concentration ($g.L^{-1}$)	K	n	R^2
172.1	0.0034	1.117	0.999
189.9	0.0043	1.096	0.997
217.8	0.0008	1.515	0.987
297.5	0.0005	1.711	0.997
369.8	0.0026	2.121	0.999
373.4	0.7354	1.476	0.998

If bioflocculation were to be a viable recovery option for *Scenedesmus sp*. or *Chlorella vulgaris*, the fluid rheology of the bioflocculants would have to be understood. This is because concentrated microalgae would be transported after flocculation and would consist of microalgae, bacteria and various salts. The flocculated microalgal biomass therefore exhibit different surface, particle size and suspension properties compared to pure isolated samples which have been reported to affect apparent viscosities (Sherman, 1970). Figure 40 and Figure 41 shows the apparent viscosity and shear profiles for the microalgal co-cultured bacteria: *Nocardioides aromaticivorans* SB10005 and *Microbacterium chocolatum* RW56. At low concentrations both bacteria species exhibited Newtonian rheological

behaviour. As concentration increased above 35 g.L^{-1} the bacterial suspensions became increasingly shear thinned. This slight pseudoplastic behaviour may be attributed to the extracellular polymeric substances excreted by the bacteria or the specific surfaces properties (Chen *et al.*, 1997).

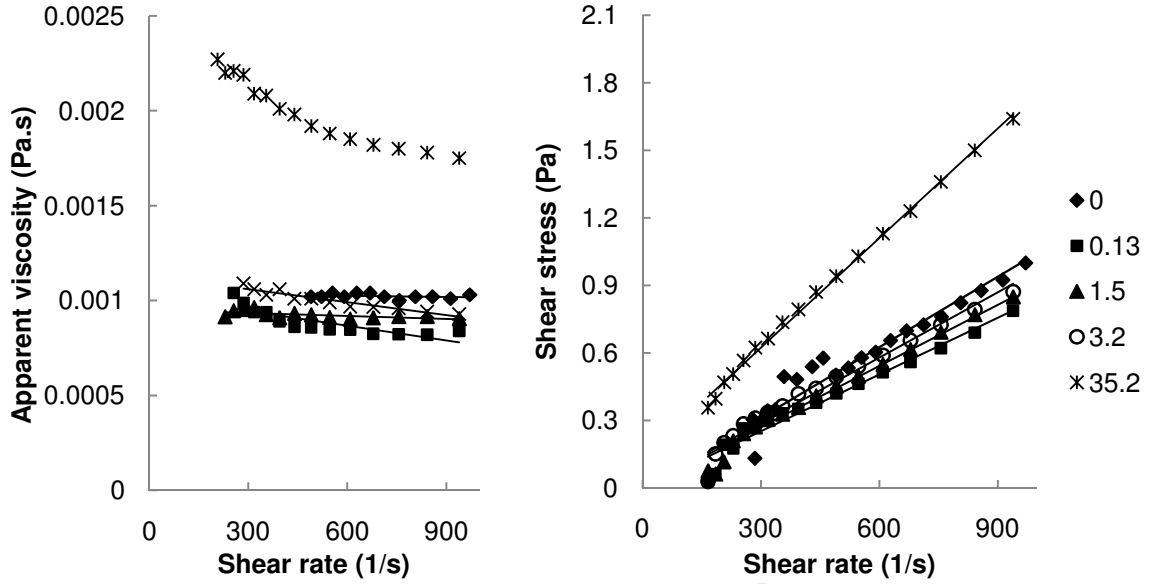

Figure 40: *Nocardioides aromaticivorans* SB10005 viscosity and shear profile against shear rate at different mass concentrations (g.L^{-1}) at 25°C

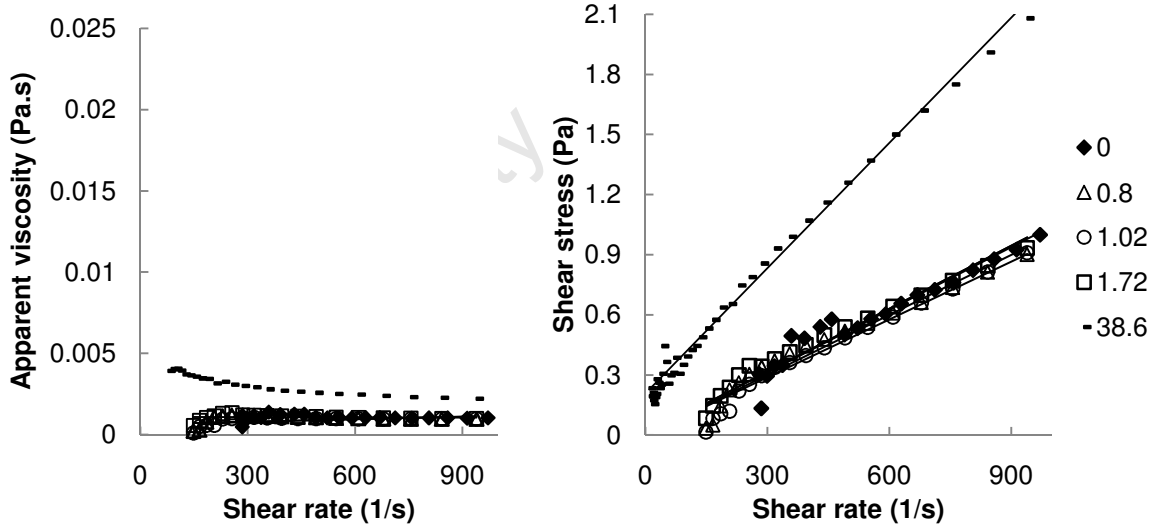

Figure 41: *Microbacterium chocolatum* RW56 viscosity and shear profile against shear rate at different mass concentrations (g.L^{-1}) at 25°C

The presence of fine particles in a liquid increases the viscosity because of the effect it has on the flow pattern. Bigger particles should induce a slower fluid flow due to the increased energy required to move the particles (Hiemenz and Rajagopalan, 1997). When a floc is formed, the shearing forces associated with viscosity which operate across the floc disrupt and rearrange the aggregate. This corresponds to a dissipation of the translational energy (Hiemenz and Rajagopalan, 1997) and hence contributes to the viscosity.

Figure 42 and Figure 43 demonstrate an increased apparent viscosity for flocs for *Chlorella vulgaris* and *Scenedesmus sp*. respectively. This increase in apparent viscosity is relatively small but offers insight into the nature of these flocs.

Figure 42 shows the apparent viscosity of *Chlorella vulgaris,* when flocculated at 14 $g.L^{-1}$, to increase above the non-flocculated concentrate of 161 $g.L^{-1}$. Figure 43 shows the apparent viscosity of *Scenedesmus sp.,* when flocculated at 10.6 $g.L^{-1}$, to increase above the non-flocculated concentrate of 151 $g.L^{-1}$. This shows that when microalgal cells flocculate, there was a greater than 10-fold increase in apparent viscosity and hence surface interactions.

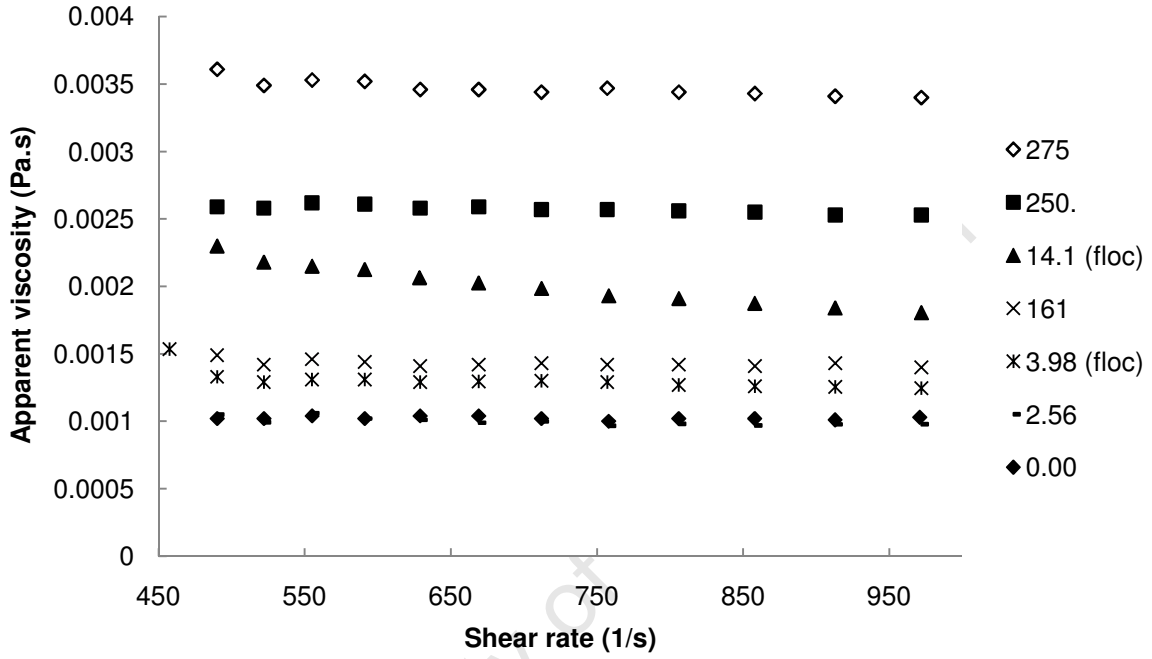

Figure 42: Chemical flocculated *Chlorella vulgaris* increased viscosity at 25℃

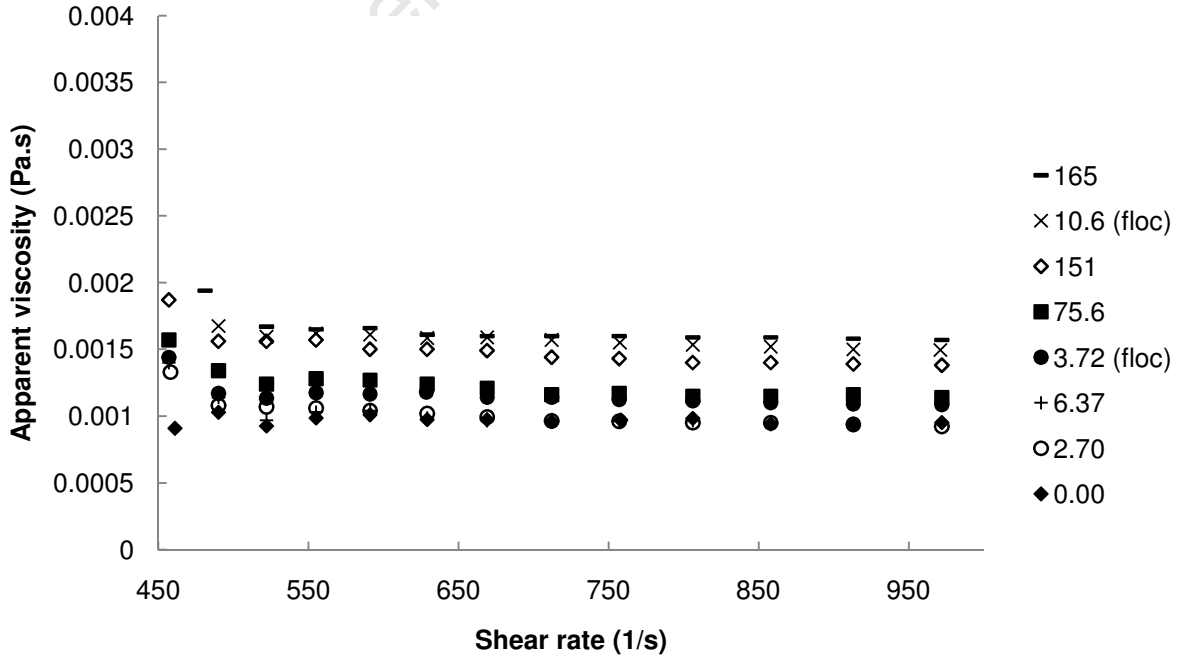

Figure 43: Chemical flocculated *Scenedesmus sp.* increased viscosity at 25℃

5.8 Summary of key findings

- *Chlorella vulgaris* and *Scenedesmus sp*. (grown on 2900 ppm CO_2) reached maximum biomass concentrations of 2.26 ± 0.01 and 3.22 ± 0.01 $g.L^{-1}$ with maximum growth rates of 1.20 ± 0.03 and 1.38 ± 0.04 day^{-1} (n = 8) respectively.
- *Chlorella vulgaris* and *Scenedesmus sp*. were CO_2 sufficient at 2 $L.min^{-1}$ at 2900 and 5000 ppm CO_2 but became light inhibited at day 8 and 10 respectively.
- *Microbacterium chocolatum* and *Nocardioides aromaticivorans* biomass was approximately 1.2 and 4.0 wt% of *Chlorella vulgaris* and *Scenedesmus sp.* biomass concentrations respectively.
- *Scenedesmus sp.* and *Chlorella vulgaris* follow similar pH and ionic strength trends throughout and the suspension pH and ionic strength are notable functions of growth.
- *Chlorella vulgaris* cells are spherical particles 2.50 ± 0.76 µm in diameter whilst *Scenedesmus sp*. are prolate, ellipsoidal cells with an average, major axis diameter of 6.90 ± 1.27 µm and an average, minor axis diameter of 2.78 ± 0.70 µm.
- Both species of microalgae and bacteria exhibited negatively charged surfaces throughout their life cycles.
- Hydrophobicity remained relatively constant during the growth phase of the microalgae.
- After day 7 of growth, theoretical carbon in the extracellular material follows a similar trend to that of the measured carbon but is an overestimation for both algal species. This is due to the measurement of the biomass excluding wall growth and sedimented biomass.
- A direct relationship is observed between EOC increases and autoflocculation induction.
- Cell hydrophobicity and surface charge is dependent on ionic strength and pH.
- *Chlorella vulgaris* and *Scenedesmus sp.* had an isoelectric point at pH 1.03 ± 0.15 and pH 4.34 ± 0.17 respectively, both of which were found to be largely independent of harvesting time, suspension conductivity and culturing CO_2 concentration.
- *Scenedesmus sp.* was found to behave as a dilatant (shear thickening) fluid when concentrated above 205 $g.L^{-1}$ dry weight ($\tau = 0.0008\gamma^{1.52}$ for 218 $g.L^{-1}$) whilst *Chlorella vulgaris* remained Newtonian up to 275 $g.L^{-1}$ dry weight ($\tau = 0.0035\gamma$ for 275 $g.L^{-1}$).
- Flocculation was found to increase the apparent viscosity of *Chlorella vulgaris* and *Scenedesmus sp*.

6 RESULTS: SEPARATION OF ALGAL BIOMASS

6.1 Introduction

In Section 5.2, the variation in the characteristics of the microalgae cells, co-cultured bacteria and suspension during the cultivation in the airlift photobioreactors was studied as a function of culture conditions. Particle size, pH, zeta potential, biomass concentration and productivity, conductivity, hydrophobicity, carbon accumulation and bacteria concentration were found to vary during the growth phase to differing extents. Section 5.6 demonstrated the inter-dependence of these physico-chemical properties on each other. Preliminary regions within the surface properties have been determined for possible exploitation. Flocculation and hence sedimentation relies predominantly on colloid instability which is dependent on the solution physico-chemical properties (Stumm, 1992) and hence a change in any of these afore-mentioned surface properties either promotes instability or must be counteracted against by another property. The effect on separation via natural or chemical induced sedimentation may be characterised in a number of ways (Section 2.3). In this chapter, the effects of chemical and biochemical additions on the respective microalgal suspensions are quantified by measuring separation/flocculation efficiencies (Equations 13, 14 and 15) and separation/flocculation rates using jar tests and spectrophotometry (described in Section 4.4).

6.2 Natural sedimentation

The most energy efficient method for microalgal recovery is sedimentation, however this technique is quite time inefficient (Mohn, 1980) and much improvement needs to be made with regards to settling rates and recovery efficiencies. Fattom and Shilo (1984) and van Loosdrecht *et al.* (1987) reported the growth stage to affect a number of surface properties fundamental to increasing separation efficiencies. The change in cell density, predominately altered by change in lipid content, also influences sedimentation (Griffiths and Harrison, 2009). This parameter is not explored in this work, however as nitrogen decreases towards the end of the growth cycle, lipid accumulates (Griffiths *et al*., 2011; Lee *et al*., 1998; Shifrin and Chisholm, 1981) thus making the cell less dense.

Lee *et al.* (1998) and Danquah *et al.* (2009a) reported the optimal harvesting stage to be during the stationary growth phase. Figure 44 shows the natural settling rates of *Chlorella vulgaris* and *Scenedesmus sp*. during the exponential and stationary growth phases. Initially cells settled from the exponential phase cultures more quickly than stationary phase cells. After 5 hours of unaided settling, the microalgae settled at similar rates. Based solely on these settling profiles there was no advantage to harvesting cells at a specific growth phase in terms of separation. This was echoed in previous findings where hydrophobicity was shown to remain fairly constant across the growth phase (Figure 25). *Scenedesmus sp*.

settled noticeably more quickly than *Chlorella vulgaris,* due to the cell morphology. The larger cells translate into a greater mass concentration per particle and faster settling rate following Stoke's law (Equation 17). After 6 hours, 48 and 83% and after 10 hours, 78.9 and 91.4% of *Chlorella vulgaris* and *Scenedesmus sp*. had settled respectively. The percentage settled biomass at 50 hours only increased to 84.1 and 93.2% respectively. Typical unaided settling rates for freshwater green microalgae at STP range from 0.128 to 0.262 $m.day^{-1}$ (Stutz-McDonald and Williamson, 1979). *Scenedesmus sp*. and *Chlorella vulgaris* were found to naturally settle at an average of 0.187 ± 0.006 and 0.160 ± 0.004 $m.day^{-1}$ respectively.

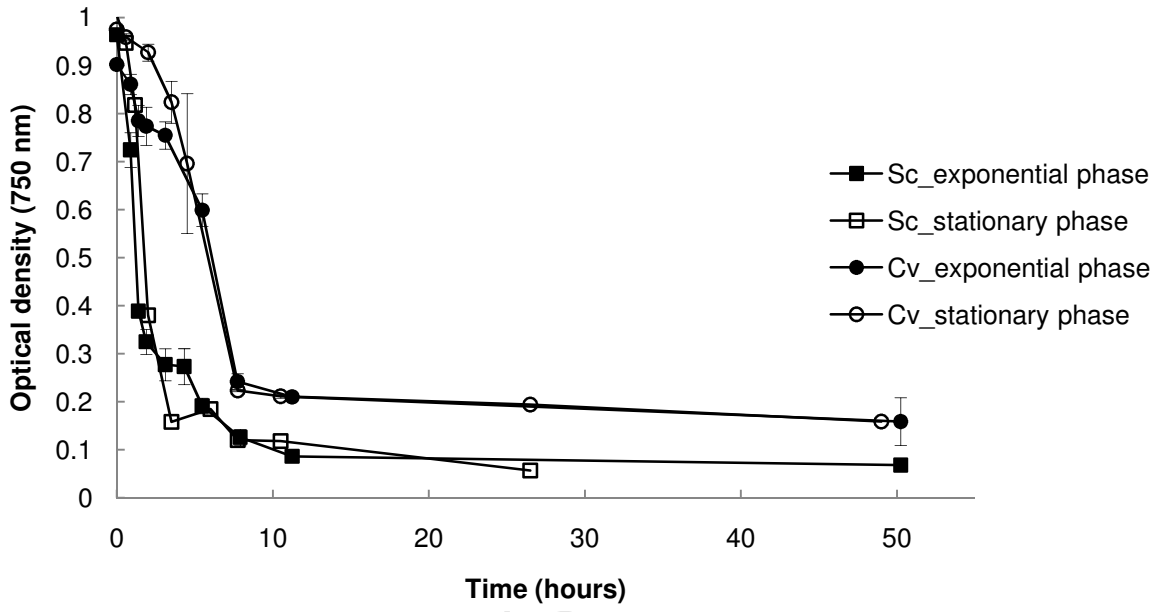

Figure 44: *Scenedesmus sp.* and *Chlorella vulgaris* unaided settling rates at exponential and stationary growth phases via 20 minute jar tests at 25℃, at pH 7

Figure 45 shows the effect of conductivity (adjusted using $MgCl_2$) on the settling efficiency of *Scenedesmus sp*. and *Chlorella vulgaris*. The lowest unaided settling efficiency was seen at de-ionised water conditions. Culture growth media has a conductivity of 1366 ± 37 $mS.cm^{-1}$ initially which decreased to 790 ± 47 $mS.cm^{-1}$ (Figure 21). Settling efficiency increased up to a solution conductivity of 630 and 4000 $mS.cm^{-1}$ for *Chlorella vulgaris* and *Scenedesmus sp*. respectively. A similar trend was seen when electrophoretic mobility (only supporting data presented in Figure 77, Appendix 8.6.4) and zeta potential (Figure 30) were observed with an increase in conductivity. This provides explanation to the phenomenon observed hereafter. As ionic strength increases, the electric double layer surrounding the suspended solid particles decreases (Hiemenz and Rajagopalan, 1997) which leads to colloidal instability and hence an increase in settling efficiency. Similarly to the effects of ionic strength on zeta potential, at conductivity above 4 $S.cm^{-1}$ the system became saturated and no significant increase in settling efficiency was observed. *Scenedesmus sp.* settling efficiency was shown to increase more than *Chlorella vulgaris* with increasing conductivity even though *Chlorella vulgaris* displayed a greater hydrophobic dependence on conductivity (Figure 30). However *Scenedesmus sp*. displayed a greater increase in zeta potential with increasing conductivity (Figure 30) and therefore it can be concluded that surface charge had a greater effect on colloidal stability in microalgal cultures.

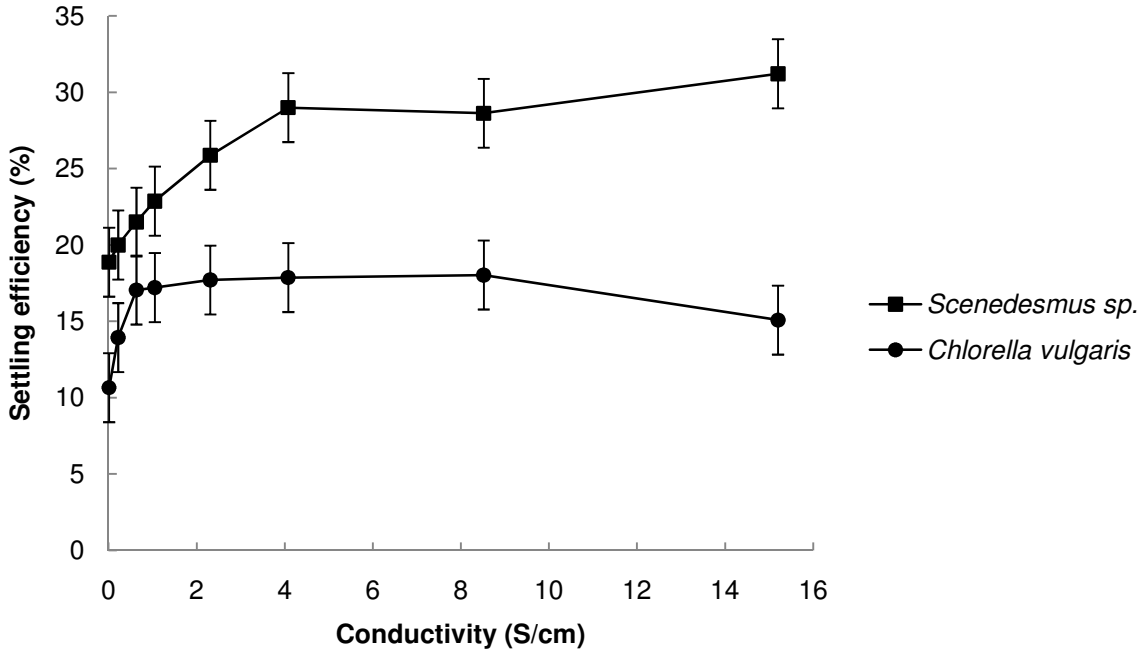

Figure 45: Conductivity effects on *Scenedesmus sp.* and *Chlorella vulgaris* settling efficiency at constant pH 5.5 at 25℃

Figure 46 shows the effect of pH on the settling profile of *Chlorella vulgaris* and *Scenedesmus sp*. after resuspension in a constant conductivity buffer. The approximate relationship between pH and conductivity is presented in Figure 78, Appendix 8.6.4 (only support data). For both species, the acidic conditions promoted sedimentation more than alkaline conditions. This was predominantly due to the maximum hydrophobicity experienced by the cells (Figure 35) and zeta potentials approaching the point of zero charge (Figure 31 and Figure 32) at acidic conditions. These experimental results demonstrated that the settling rate may be improved by exploiting the surface properties. Both surface charge and hydrophobicity contributed to the settling efficiencies of microalgae. Under these conditions, *Scenedesmus sp*. again showed a higher settling rate than *Chlorella vulgaris*. Comparing Figure 46 to Figure 44 it was evident that the *Scenedesmus sp*. settling rate doubled at both alkaline and acidic conditions. This could be attributed to increased ionic strength and charge neutralisation. The *Chlorella vulgaris* settling rate increased at acidic conditions but decreased at alkaline conditions compared to Figure 44. While hydrophobicity and surface charge increased with respect to increasing ionic strength, the surface charge of *Chlorella vulgaris* at pH 13 was at a minimum (-28 mV) which conferred to maximum colloid stability.

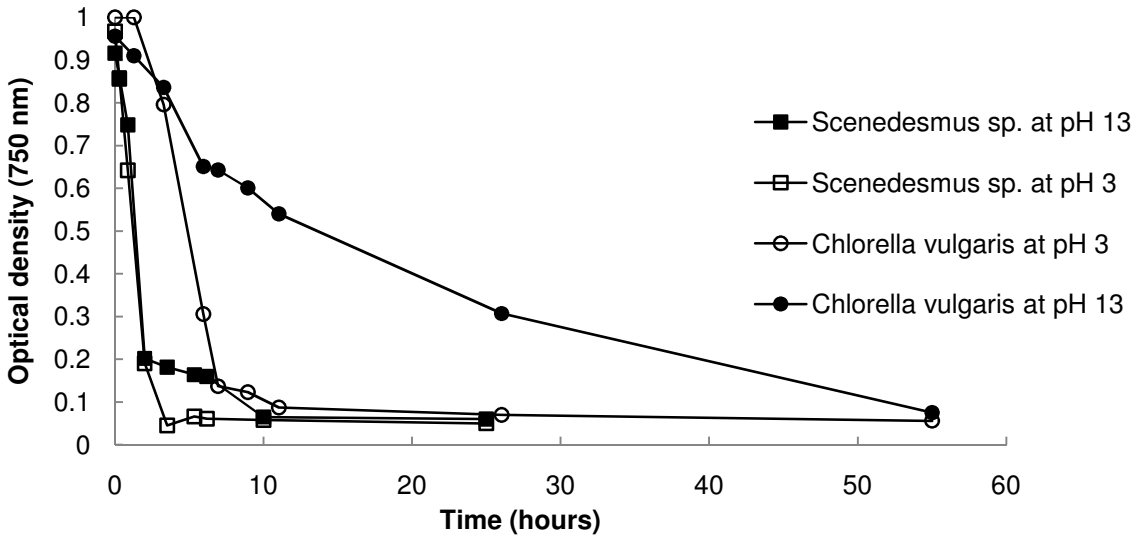

Figure 46: pH effects on *Scenedesmus sp.* and *Chlorella vulgaris* resuspended in dH_2O settling rate at constant conductivity at 25℃

6.3 Chemical flocculants to enhance flocculation and settling

In studying natural flocculation and settling, the effects of pH and ionic strength on improving recovery efficiency of the microalgae were shown. If these parameters can be controlled and the effects and mechanisms understood, the microalgal physico-chemical properties may be exploited to achieve the desired biomass recoveries. For the purpose of this thesis, all stable, clusters of particles formed are termed 'flocs' regardless of whether the formation of these particles is due to precipitation, aggregation, coagulation or flocculation. Many different types of flocs may be formed to increase sedimentation rates. Each of these floc types follows a different flocculation mechanism and associated bonding, hence behaving in different ways. Because of this, some forms of flocculation may be more suitable for microalgae than others, depending on criteria set for each specific system. This section investigates chemical flocculation using pH adjustment (NaOH or HCl), algal media components, chitosan and alum to determine the respective mechanistic reasons why these occur.

For sedimentation to be a viable microalgal recovery technique, settling efficiency and settling rates need to be optimised. Benemann *et al*. (1982) defined acceptable settling rates for microalgae to be a minimum of 0.17 $cm.hr^{-1}$ but preferably several fold higher. If these conditions are optimised through exploiting surface properties, and settling rates are high enough, continuous processes could be implemented. Settling velocity has been well defined to follow Stoke's law (Equation 17). Methods have been developed to both increase the size of these settling particles and the difference in density between the floc and the medium (Vlaski *et al*., 1997) thus improving the rate of particle settling. This agglomeration of algal cells may be induced using a suitable flocculant (Liu *et al*., 1999; Chen *et al*., 1998; Ayoub and Koopman, 1986; Tenney *et al*., 1969) or by inducing adsorption between particles.

6.3.1 Use of pH to enhance flocculation and settling

Chlorella vulgaris, *Scenedesmus sp.*, *Microbacterium chocolatum* and *Nocardioides aromaticivorans* were autoflocculated by pH adjustment (Figure 47). Species were initially autoflocculated over a range of pH to determine the maximum bulk and particle settling rates. Autoflocculated *Chlorella vulgaris* had a maximum bulk and floc particle settling speed of 2.77 ± 0.13 and 8.40 ± 1.65 $cm.min^{-1}$ respectively whilst autoflocculated *Scenedesmus sp.* bulk and floc particle settling speeds were found to be 3.71 ± 0.21 and 8.45 ± 1.36 $cm.min^{-1}$ respectively. The autofloc particles for both species settled at similar velocities. Bulk *Scenedesmus sp.* settled quicker due to the larger particles and this was observed previously with the effects from ionic strength and pH (Figure 45 and Figure 46). This higher bulk settling velocity was also due to the increased flocculation efficiency of *Scenedesmus sp*. over *Chlorella vulgaris*. The bulk settling velocity of *Scenedesmus sp.* was almost a centimetre per minute quicker than *Chlorella vulgaris* and this was not due to individual particle settling velocities. The *Scenedesmus sp.* flocs portrayed a greater bulk settling velocity due to interlinking of the flocs which formed a chain of flocs. This has been described in literature as sweep flocculation (Rattanakawin, 2005).

All species showed peaks in autoflocculation in two regions. *Nocardioides aromaticivorans* and *Microbacterium chocolatum* flocculated at pH 2 and pH 2.3 - 3.7 respectively (Figure 47). These values were slightly higher than the PZC value of *Nocardioides aromaticivorans* of pH 1.6 and the lowest electronegativity of *Microbacterium chocolatum* found at pH 2.5 (Figure 33). *Chlorella vulga*ris demonstrated peaks in flocculation at pH 1 and 13.5 whilst *Scenedesmus sp.* autoflocculated at pH 4.7 and 14. Similar to the bacteria, *Scenedesmus sp.* and *Chlorella vulgaris* demonstrated a peak in autoflocculation at marginally more acidic conditions than their PZC values of pH 4.2 and above pH 1.03 respectively. *Scenedesmus sp.* and *Chlorella vulgaris* both autoflocculated at pH 13 and above. These data therefore suggest the autoflocculation of cells via two different mechanisms of flocculation. This is discussed in Section 7.3.

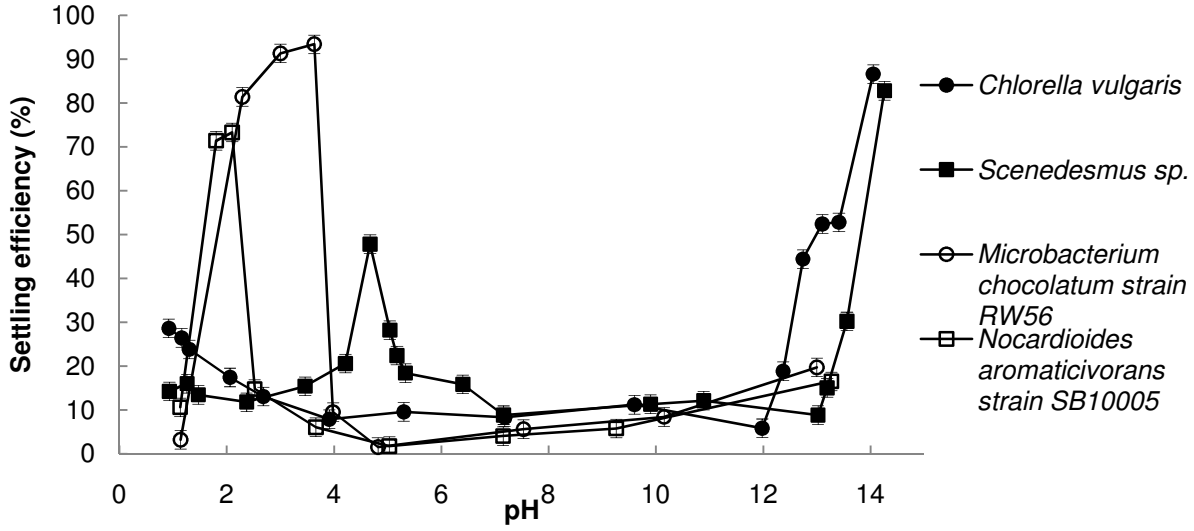

Figure 47: Settling efficiencies as a function of pH of *Nocardioides aromaticivorans* SB10005, *Microbacterium chocolatum* RW56, *Scenedesmus sp.* and *Chlorella vulgaris* after 20 minutes settling, via jar tests, directly from reactor effluent at stationary growth phase

6.3.2 *Effect of presence of salts on flocculation and settling*

The flocculation results presented in Figure 47 were collected using cultures directly from the bioreactors at stationary growth phase such that the algae were suspended within the growth media. The resultant ionic strength of the cultures was found to be significant even during the stationary and death phases (Figure 21). This ionic strength affected the cell surface properties (Figure 30) and hence the sedimentation rates (Figure 45). Therefore the different ions within this media matrix were investigated to determine which of the salts have the greatest effects on flocculation efficiency (Figure 48). These experiments were all carried out at pH 13 where the algal cells had minimum surface charges and hence these results would represent the maximum efficiencies achievable under these conditions. Distilled water was used as a base line and the effect of media components was compared to a commercial wastewater flocculant ($Al_2(SO_4)_3$) at constant pH. All flocculation tests presented in Figure 48 were done in jar test experiments over 20 minute settling periods. Figure 48 illustrates that *Chlorella vulgaris* was found to have higher flocculation efficiency throughout the tests across all salts. This was because *Chlorella vulgaris* was a smaller particle and therefore there was a larger surface area and surface energy to induce flocculation (Hiemenz and Rajagopalan, 1997). One mechanism of flocculation of microalgae results from charge neutralisation due to the reduction in the electrostatic force of repulsion between charged microalgal cells in suspension and inter-particle bridging. Flocculants that have a higher charge density are therefore more effective (Thapa *et al.*, 2009) as these increased electrical interactions induce increased adsorption. The trivalent salt, $Al_2(SO_4)_3$ was found to be the most effective flocculant followed closely by $MgSO_4$. $CaCl_2$ was found to have minimal effect on flocculation of both *Scenedesmus sp*. and *Chlorella vulgaris*. However qualitative experiments showed $MgSO_4$ flocs to be unstable compared to a combination of $CaCl_2$ and $MgSO_4$ induced flocs. This supports the work of Oh *et al.* (2001) who showed that calcium ions serve as a co-flocculant to stabilise the floc.

Figure 49 displays the effects of calcium and magnesium salt concentration on flocculation. Flocculation efficiency of *Chlorella vulgaris* cells showed a constant increasing relationship to increasing Mg^{2+} and Ca^{2+} concentration, reaching an asymptote plateau of 51% at 0.2 $g.g^{-1}.L^{-1}$. This plateau could be due to initial sweep flocculation (Rattanakawin, 2005) of all the available $MgSO_4$ salts. Addition of low concentrations resulted in inefficient and highly variable flocculation with low efficiencies. At the higher concentrations of over 2.5 $g.g^{-1}.L^{-1}$, flocculation was efficient and predictable; however at these higher concentrations the formed flocs contained significantly higher amounts of salt as an increase in salt loading had a less efficient effect on flocculation efficiency. This phenomenon is illustrated following in Figure 56a and Figure 55j, Section 6.6. *Chlorella vulgaris* autoflocs were found to be between 50 and 100 µm, whilst *Chlorella vulgaris* flocculation via $MgSO_4$ at pH 13, were found to be between 20 and 50 µm. Similar results have been reported in the literature (Knuckey *et al.*, 2006; Tenney *et al.*, 1969; Divakaran and Pillai, 2002) where oversaturation of flocculating salts form larger bridged networks which entrap cells. This technique is not only inefficient but also renders effluent water higher contaminated.

Chitosan is reported to be an alternative, environmentally friendly flocculant (Renault *et al.*, 2009; Strand *et al.*, 2002; Divakaran and Pillai, 2002); however Figure 48 suggested that this expensive alternative was relatively inefficient compared to traditional salts. Microscopic

images of these flocs may be seen in Section 6.6. In Section 6.6, flocs induced via different mechanisms are shown to be different in size and character.

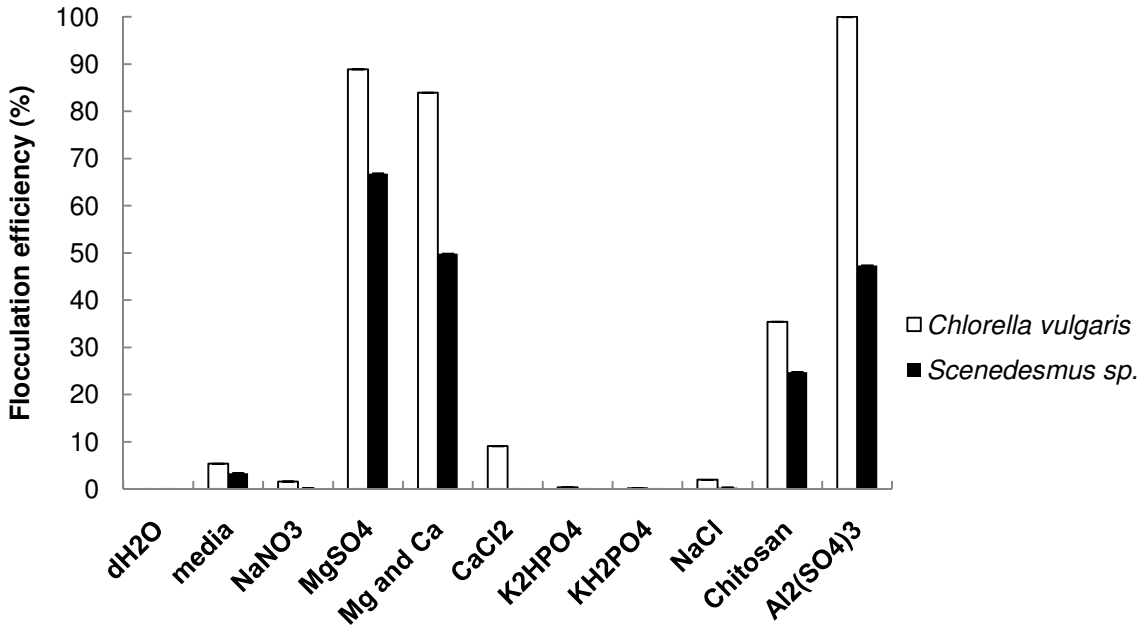

Figure 48: Flocculation efficiencies of stationary phase *Scenedesmus sp.* and *Chlorella vulgaris* after 20 minutes dosed with 1 $g.L^{-1}$ at pH 13 for media components comparison at 25℃

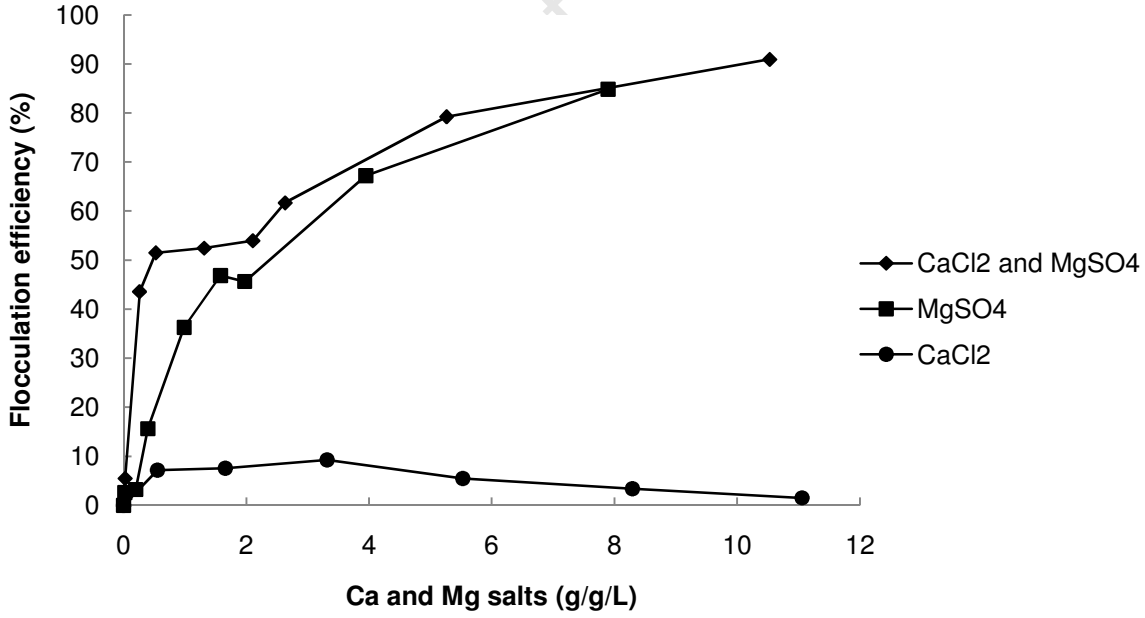

Figure 49: Magnesium and calcium salt concentration effects on *Chlorella vulgaris* flocculation efficiency at 25℃ and constant buffered conductivity

6.4 Bioflocculation

Bacteria were introduced over a pH range to investigate bioflocculation of *Scenedesmus sp.* and *Chlorella vulgaris* (Figure 50a, b and c). Each combination of cells produced a pH region of increased bioflocculation activity. *Bacillus sp.*, *E. coli* BL2 (DE3), *Nocardioides aromaticivorans* SB10005 and *Microbacterium chocolatum* RW56 successfully bioflocculated both microalgal species with varying results. The two microalgae were mixed and tested over a pH range to investigate the bioflocculation activity between the two types of cells (Figure 50d).

The bioflocculation peaks observed in Figure 50 were at low pH conditions either at the PZC of the respective species or in regions where opposing charges were present (Figure 33 and Figure 34). Limited bioflocculation was observed at neutral pH. This suggests potential limitation to bioflocculation prior to recycle. As shown in Figure 47, increases in flocculation were observed at extreme alkaline conditions.

Bacillus sp. was the most efficient bacterial bioflocculant for *Scenedesmus sp.*, allowing 54% recovery of algal cells in 20 minutes. This occurred at the least extreme conditions at pH 3.35. The co-cultured *Microbacterium* was the most efficient bioflocculant for *Chlorella vulgaris* allowing 97% recovery of cells. However this was achieved at pH 1 where cell lysis may occur. Further, the cost of acidification and neutralisation of the effluent media and its potential to increase salinity on recycle may negatively impact the process. This is investigated in Section 6.7. The algae-algae bioflocculation provided the most promising results with 81% cell recovery of both species at pH 2.55. Both these two microalgal species produce lipids and contribute to the end product for bioenergy production. A peak in bioflocculation efficiency was observed for most experiments at extreme alkaline conditions. This correlates notably with data shown previously in Figure 47 indicating that at these conditions both types of cells in the suspension are experiencing autoflocculation.

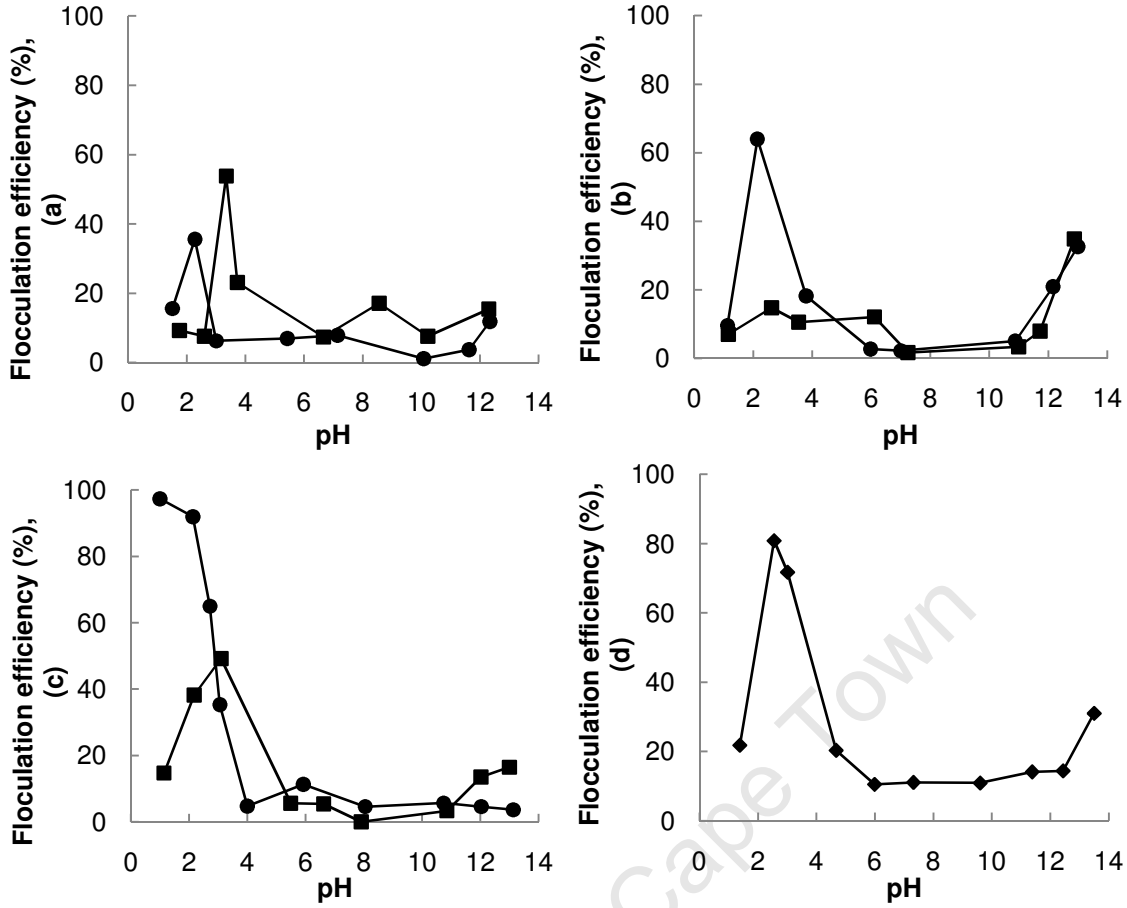

Figure 50: Bioflocculation efficiency of *Scenedesmus sp.* (—■—) and *Chlorella vulgaris* (—●—) bioflocculated via (a) *Bacillus sp.*, (b) *E. coli* BL2 (DE3), (c) co-cultured bacteria *Nocardioides aromaticivorans* SB10005, *Microbacterium chocolatum* RW56 respectively and (d) *Scenedesmus sp.* and *Chlorella vulgaris* algae-algae bioflocculation with 0.3 $g.L^{-1}$ each using jar tests with 20 minutes settling time at 25℃

The flocculation of algae observed in Figure 50 was dependent on flocculation time, pH and concentration ratio of the different cells. Bioflocculation of microalgae via addition of bacteria was found to be dependent on the bacterial dosage and pH of the combined solution. The flocculation efficiencies may therefore be increased by optimising the attraction mechanism conditions. In Figure 51, flocculation of algae with co-cultured bacteria shown in Figure 50c is extended to identify an optimal bacterial loading and pH. For both *Scenedesmus sp.* and *Chlorella vulgaris*, a bacterial loading of greater than 0.5 $g_{bacteria}/g_{algae}/L$ was sufficient, depending on recovery targets at the majority of pH conditions tested. *Chlorella vulgaris* showed a lower bacterial loading saturation point at more acidic conditions (pH 1.15 and 2.60) whereas at slightly less acidic conditions (pH 3.00 and 3.75), a greater bacteria-algae ratio was required. Conversely for *Scenedesmus sp.*, lower pH values (pH 1.65 and 2.55) required a higher bacteria-algae ratio. The optimum condition for flocculation efficiency of *Scenedesmus sp.* was pH 3.55 and 0.25 $g_{bacteria}/g_{algae}/L$. This optimum is species dependent due to the differences in surface charge profiles.

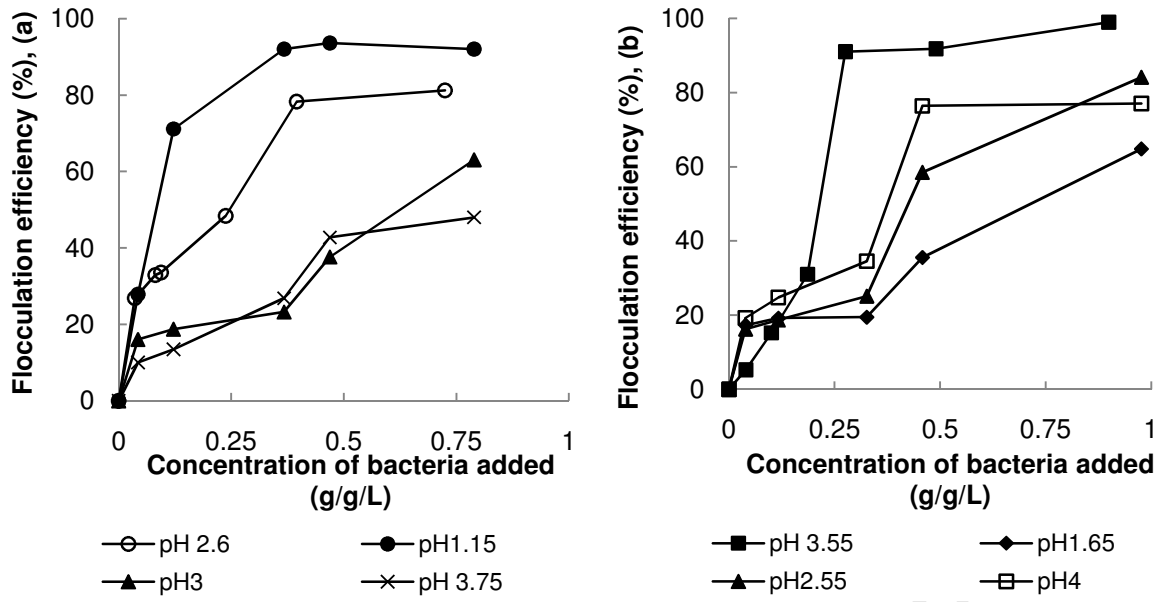

Figure 51: Optimum (a) *Chlorella vulgaris* bioflocculation via *Microbacterium chocolatum* RW56 and (b) *Scenedesmus sp.* bioflocculation via *Nocardioides aromaticivorans* SB10005 and pH using jar tests with 20 minutes settling time at 25℃

6.5 Flocculation mechanisms

Different types of flocs are postulated to form via different mechanisms which are reflected in floc sizes, floc stability and floc formation time. Floc stability can be investigated by time-based response to exposure to shear rate under conditions of pumping or agitation. Figure 52 shows the average effective floc size for *Scenedesmus sp.* and *Chlorella vulgaris* as a function of shear rate and mode of flocculation. Autoflocs for both species were found to be more stable than bioflocs. This difference in floc stability is postulated to result from flocculation mechanism and cell aggregation capacity within the chosen flocculation conditions. *Chlorella vulgaris* flocs were more stable at low shear rates, where typical commercial applications apply, than *Scenedesmus sp*. Figure 83 and Figure 84 in Appendix 8.6.6 show the decrease in floc size at different pump speeds for *Chlorella vulgaris* and *Scenedesmus sp*. respectively. Pump speed is correlated to shear stress in Figure 85 (supplementary material only).

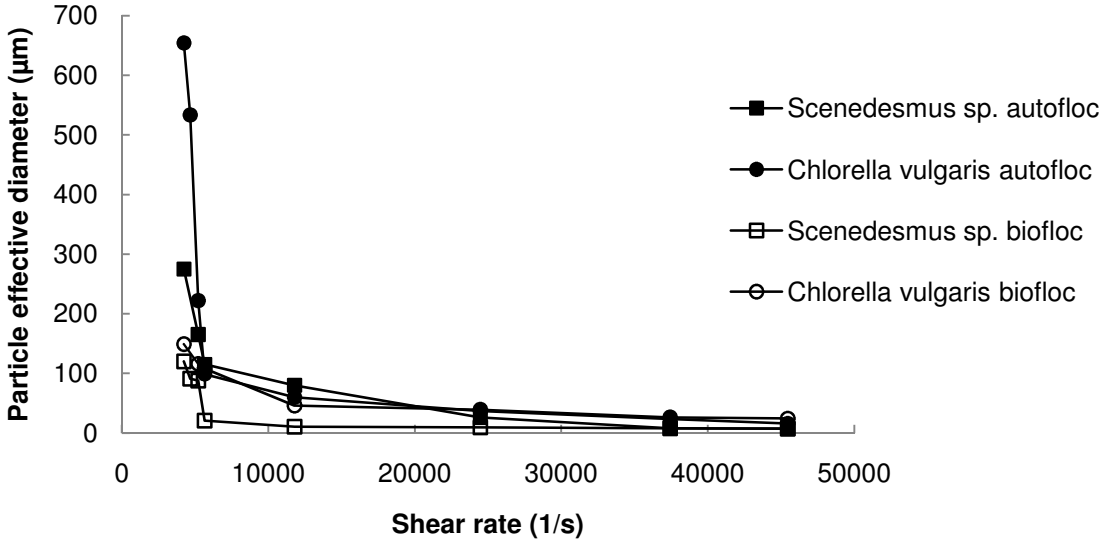

Figure 52: Floc stability of *Scenedesmus sp.* and *Chlorella vulgaris* during auto- and bioflocculation at respective optimum flocculation conditions

While the relationship between flocculation type and mechanism has been suggested by many researchers (Bernhardt and Clasen, 1994; Bernhardt *et al.*, 1985; Stumm, 1992; Salim *et al.*, 2010; Rattanakawin, 2005; Benemann *et al.*, 1980; Oh *et al.*, 2001; Strand *et al.*, 2002; Lembi and Waaland, 1988; Lian *et al.*, 2008a; Sukenik and Shelef, 1984), no conclusive link between macro- and microscopic interactions has been documented. Autoflocculation occurs between homogeneous cells at acidic and alkaline conditions for microalgae due to the relative opposing surface properties (Figure 47). At acidic autoflocculation conditions the cells are slightly electronegative but close to their respective isoelectric points (Figure 31 and Figure 32). At these conditions, the cells are immersed in an ionic solution. These positive ions form patching bonds onto microalgal cells via adsorption in order to induce autoflocculation. Microalgal cells were therefore bonded together via attractive van der Waals forces in a patching nature shown conceptually in Figure 53a and by microscopy in Figure 56. The bioflocculation between different types of cells (Figure 50) occurred when there was a large difference in surface charge between these cells (Figure 34). This may have occurred if the microalgae are negatively charged and the bacteria or bridging cells are positively charged or vice versa. No intermediate bonding of ions was required in this case which was postulated to be the rate limiting step for flocculation. Hence, bioflocculation occurred faster as described on Figure 53. Microscope images of these different types of flocculation are presented in Figure 56 and Figure 55.

Figure 54 shows the difference in settling profiles observed for autoflocs and bioflocs for *Scenedesmus sp.*, *Chlorella vulgaris*, *Microbacterium chocolatum*, *Nocardioides aromaticivorans* and *Scenedesmus sp.-Chlorella vulgaris* induced bioflocs. In all cases, the initial algal optical density was 1 and the experimentally determined optimal pH, shown in Figure 50 and Figure 47, was used. Due to the nature of spectrophotometric readings the results were smoothened. Reproducibility is shown in Figure 82 for *Scenedesmus sp.* autoflocculation. Each sample portrayed varying amounts of instability initially depicted by the fluctuations in optical density. *Chlorella vulgaris, Scenedesmus sp.* and *Nocardioides aromaticivorans* required a 200 second equilibration period before settling when

autoflocculated. *Chlorella vulgaris* and *Scenedesmus sp*. bioflocs and the *Microbacterium chocolatum* autofloc settled almost instantly as shown in Figure 54. Bioflocculation is postulated to occur via electrostatic van der Waals attractions which operate over several tens of nm (Ives, 1978). These factors would also influence the time required for flocculation as long-range forces are inherently stronger. These differences in settling rates are postulated to be because of different flocculation mechanisms resulting in different floc sizes and types (shown in Section 6.6).

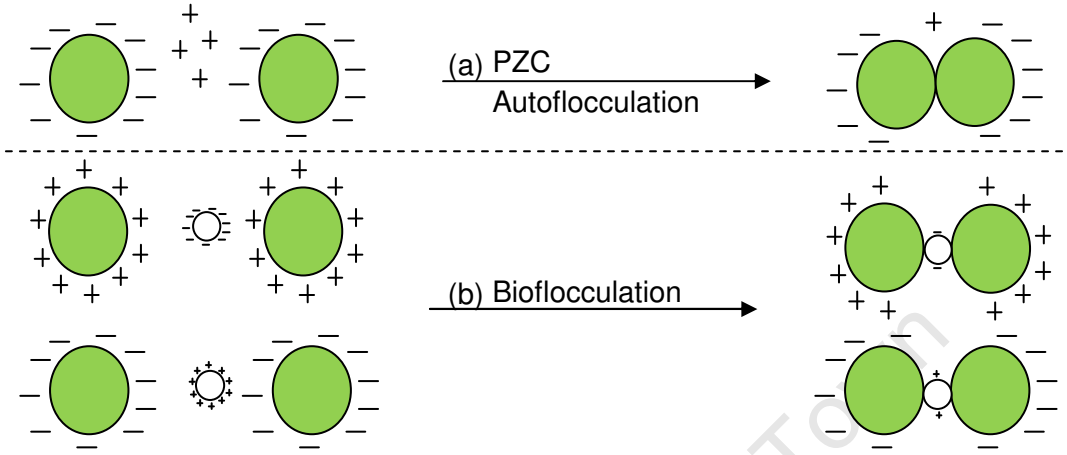

Figure 53: Proposed mechanisms of auto- and bioflocculation for *Scenedesmus sp.* and *Chlorella vulgaris*.

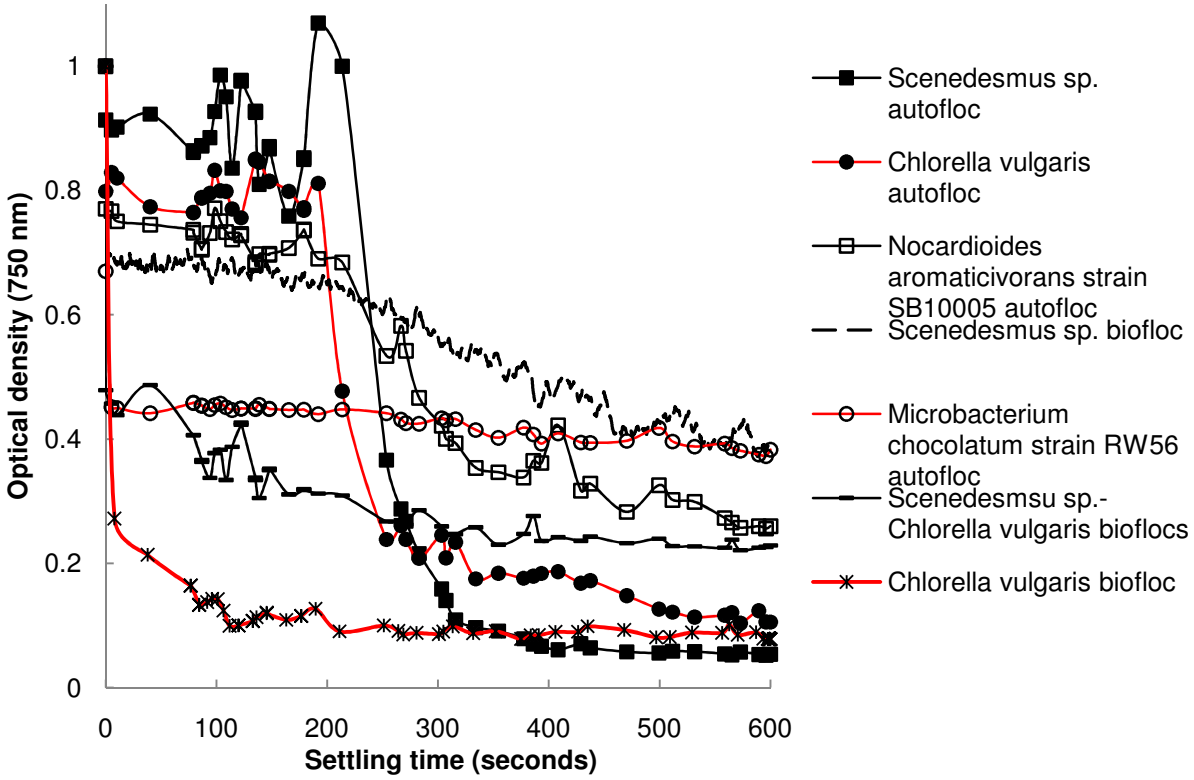

Figure 54: *Scenedesmus sp.* (pH 4.6, 3), *Chlorella vulgaris* (pH 2, 13), *Microbacterium chocolatum* RW56 (pH 3.5) and *Nocardioides aromaticivorans* SB10005 (pH 2.1) autoflocs, *Scenedesmus sp.-Chlorella vulgaris* induced bioflocs (pH 3, 0.3 $g.L^{-1}$), *Scenedesmus sp.* bioflocculated with *Nocardioides aromaticivorans* (pH 5.5), and *Chlorella vulgaris* bioflocculated with *Microbacterium chocolatum* (pH 2.2), real time settling from spectrometry at respective pH. All samples started at an optical density of 1.

6.6 Observing flocculation by microscopy

Microscopic analyses of *Scenedesmus sp., Chlorella vulgaris* and bacteria was undertaken to determine the cell physiology and to support or disprove postulated theories on flocculation mechanisms. Figure 55 shows images of non-flocculated *Chlorella vulgaris* (a) and *Scenedesmus sp*. (b) and isolated, co-cultured *Nocardioides aromaticivorans* SB10005 (c) at stationary growth phase. The microalgae are present as single cells and no floc formation is observed. *Chlorella vulgaris* cells are spherical particles 2.50 ± 0.76 µm in diameter whilst *Scenedesmus sp*. are prolate, ellipsoidal cells with an average, major axis diameter of 6.90 ± 1.27 µm and an average, minor axis diameter of 2.78 ± 0.70 µm. The bacteria shown in Figure 55c, (*Nocardioides aromaticivorans* SB10005) are present as single, rod-shaped cells ranging from 3 to 11 µm in length and approximately 1 µm in width. All the bacteria studied were of similar sizes as shown in Figure 55f and g.

Figure 55d depicts *Microbacterium chocolatum* RW56 autoflocculating at its PZC at pH 3.9. The comparison of Figure 55a, b and c, with Figure 55e, f, g, h and i confirms that the addition of bacteria at specific pH values improves the flocculation efficiencies and hence recoveries of *Scenedesmus sp*. and *Chlorella vulgaris*. Figure 55j depicts the bioflocculation of *Scenedesmus sp*. with *E. coli* BL2 (DE3) at pH 13. At pH 13 both species cells are electronegative and are attached via bridging through salts in the solution. Figure 55k shows the bioflocculation between *Scenedesmus sp*. and *Chlorella vulgaris* and further confirms a bridged bonding via charge neutralisation between cells compared to a patching interaction between *Scenedesmus sp*. and chitosan in Figure 55l. The proposed flocculation mechanisms for the autoflocs and bioflocs were discussed in Figure 53.

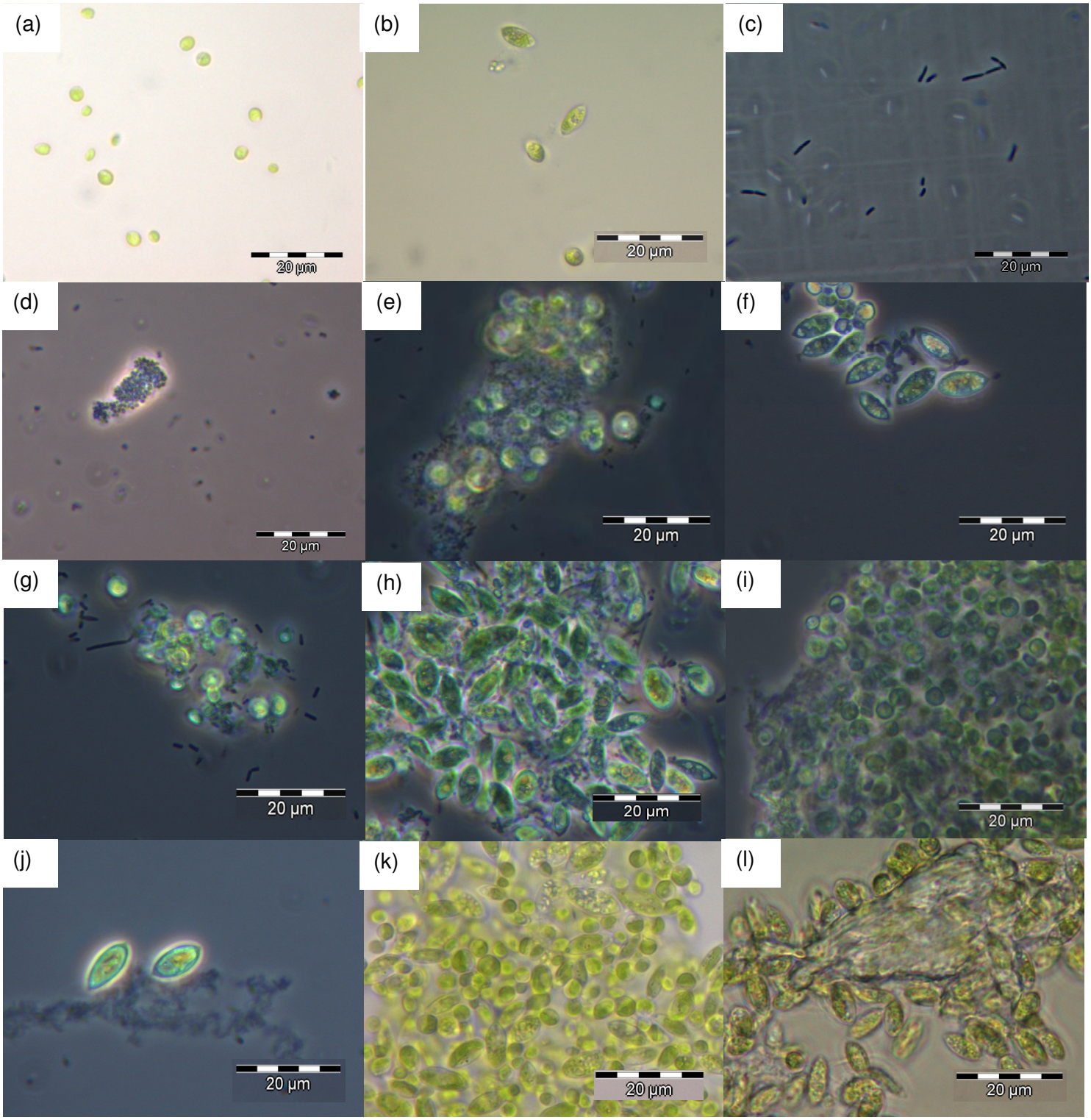

hase, (c) Isolated co-cultured
56 autoflocculation at pH 3.9
pH 3, (f) *Scenedesmus sp.*
lla vulgaris bioflocculated with
3.35, (i) *Chlorella vulgaris*
. coli BL2 (DE3) at pH 13, (k)
edesmus sp. flocculated with

Chlorella vulgaris was found to autoflocculate during the death phase of its growth curve and at pH 13 shown in Figure 56a and b respectively. The autoflocculation at pH 13 induced larger flocs, 50 µm to 2 mm (b) compared to the naturally occurring autoflocs of 10 to 40 µm (a). This is because the flocs present in Figure 56b were induced by van der Waals forces from attractive surface charges discussed in Section 5.6. The flocs present in Figure 56a are postulated to be caused from increased organic loading in the surrounding matrix and cell-ion chelation discussed in Section 5.5. Figure 56c represents *Chlorella vulgaris* flocculation via $MgSO_4$ addition. The individual cells were bonded together through Mg^{2+} providing a salt bridge for ionic bonding to form flocs as discussed in Figure 53. This type of chemical flocculation is prone to sweep floc and flocs were found to range from 50 µm to 3 mm due to the extensive bridge networks formed between salts and cells.

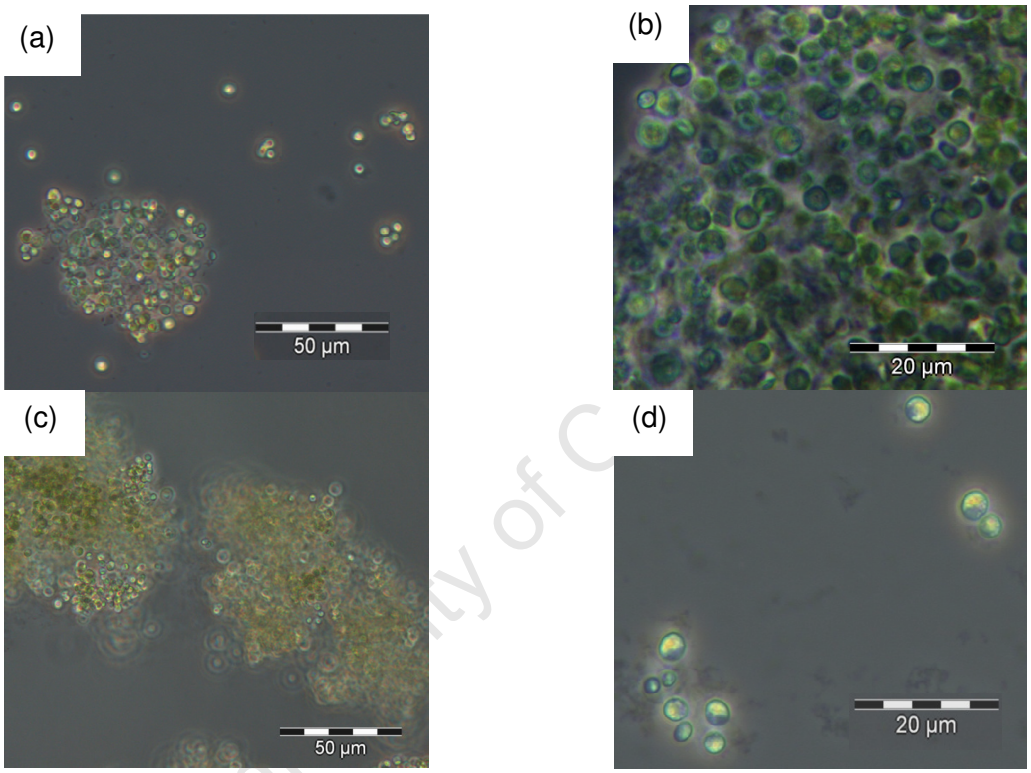

Figure 56: (a, b) *Chlorella vulgaris* autoflocculation in photobioreactor during death phase, (c) *Chlorella vulgaris* autoflocculation at pH 13, (d) *Chlorella vulgaris* flocculation via $MgSO_4$

6.7 Integrated separation system

Current separation recovery techniques are energy intensive (centrifugation, flotation) or make use of toxic chemicals (electrolysis, chemical flocculation).The preferred algal recovery unit operation is one that has low energy requirements, low chemical costs, uses no toxic components and allows recycle of water and media components. Hence, on evaluating low energy auto- and bioflocculation techniques, the potential to recycle the process effluents needs to be considered. As described in Section 6.3.1, optimum flocculation efficiencies occur in alkaline or acidic conditions with increased ionic strength. This may impact the cell integrity and downstream processing of the effluent nutrients and water. Acidic (HCl) and alkaline (NaOH) catalysts have been suggested to improve lipid transesterification, with acidic catalysts resulting in higher fatty acid production (Ehimen *et al.*, 2010). Therefore the concentrated product processing may benefit from acidic or alkaline concentrating, however for these methods to be considered, the effect of pH and conductivity on algal growth was investigated. In Figure 57, it is seen that *Chlorella vulgaris* was much more susceptible to cell bleaching at low pH with 16% bleaching at pH 0.98 compared to 4% bleaching of *Scenedesmus sp.* at pH 0.93. At pH 2, bleaching was reduced to 2 to 3% in both cases and at pH 6.5, bleaching was not evident. Cell wall porosity has been reported to increase with lower pH conditions, increasing cell lysis potential (Zemke-White *et al.*, 2000).

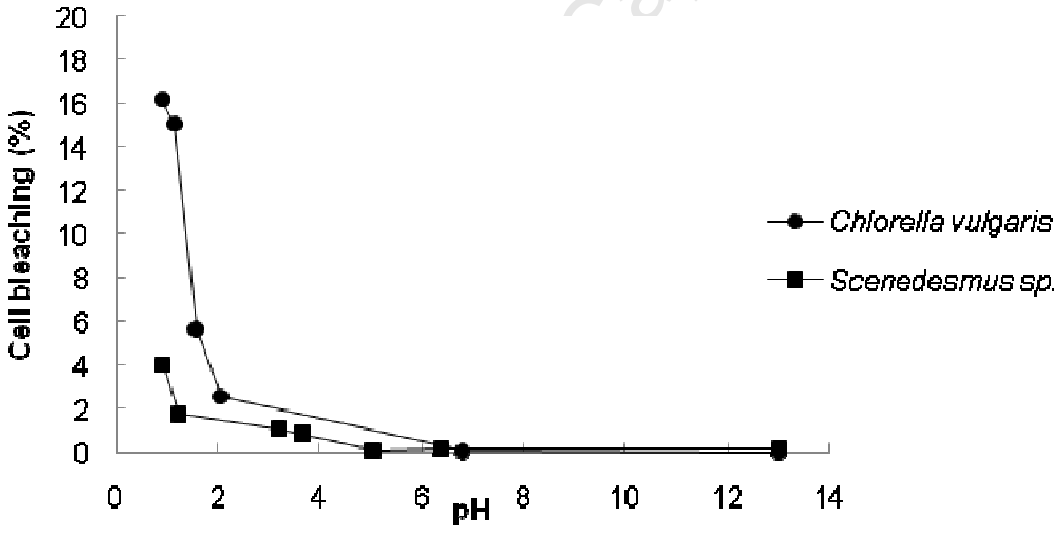

Figure 57: *Chlorella vulgaris* and *Scenedesmus sp.* cell viability from pH adjustment

In Section 6.3, the pH for optimal flocculation was identified for each species. To observe the effects of the increased ionic strength and extreme pH conditions, *Chlorella vulgaris* and *Scenedesmus sp.* were grown in the airlift photobioreactors at these starting conditions. Starting pH ranged from 2 to 13 and ionic strength between 1.5 and 9.5 $S.cm^{-1}$. Figure 58 depicts the effect of starting pH on the growth of *Chlorella vulgaris* and *Scenedesmus sp.* The growth curves were compared against the standard curve grown at starting pH 6.6. As seen in Figure 57, *Chlorella vulgaris* was prone to lyse at acidic conditions and no growth was seen for this species at pH values below 3 (Figure 58a). At extreme alkalinities, inhibited growth was also observed due to induced autoflocculation of the cells due to

reasons discussed in Section 6.7. At pH 4, *Chlorella vulgaris* grew at a similar rate to the control. Whenever growth of the microalgae was observed, the lag, exponential, stationary and death phases all occurred at similar times. *Scenedesmus sp.* grew much better under extreme pH conditions compared to *Chlorella vulgaris* (Figure 58b). Little growth (OD < 0.5) was observed at pH 13; however at alkalinities near pH 10 and 12, the microalgae exhibited satisfactory growth ($DW_{max,\ day\ 14}$ of 2.4 and 2.1 $g.L^{-1}$ compared to 3.22 $g.L^{-1}$ under standard conditions, μ_{linear} of 0.15 and 0.16 day^{-1} compared to 0.36 day^{-1}). Cultures grown at starting pH 5, 10 and 12 were still in the linear growth phase at the end of the 15 day experiment at ~2.40 $g.L^{-1}$ whilst the culture grown on starting pH 3 exhibited the highest concentration 2.47 $g.L^{-1}$ on day 11 but then entered death phase. In Table 15, the maximum biomass concentrations and linear growth rates for *Scenedesmus sp.* and *Chlorella vulgaris* at different starting pH conditions are compared.

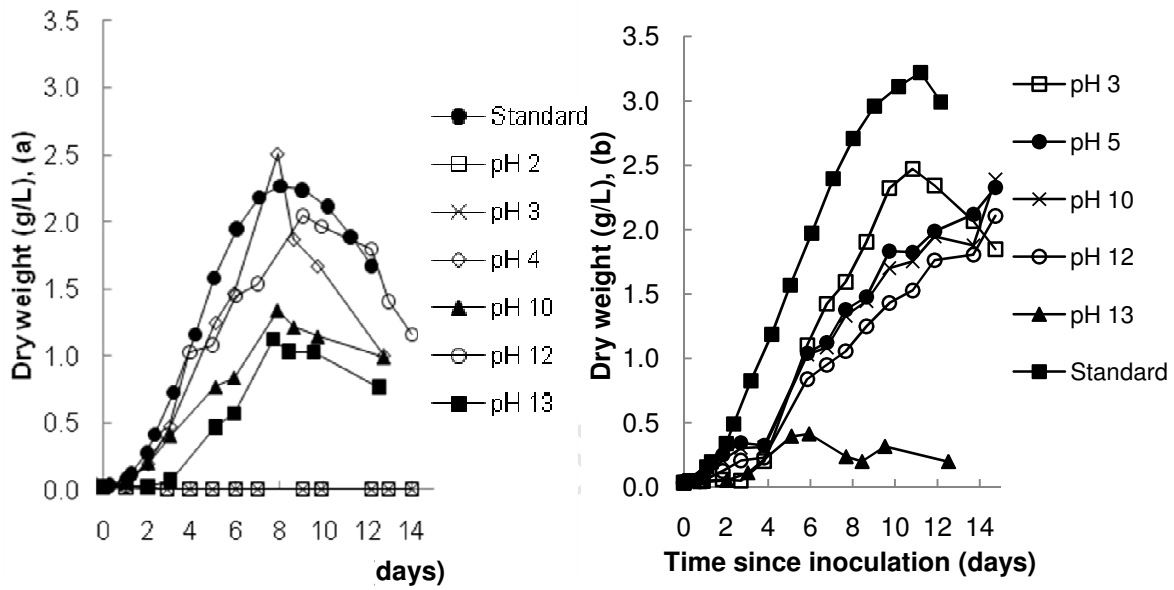

Figure 58: Growth curves for (a) *Chlorella vulgaris* and (b) *Scenedesmus sp.* with different starting pH in airlift photobioreactors

Table 15: Comparison of maximum biomass concentrations and linear growth rates for *Scenedesmus sp.* and *Chlorella vulgaris* at different starting pH conditions

Species	***Scenedesmus sp.***					
pH	3	5	10	12	13	
Maximum biomass concentration ($g.L^{-1}$) [day]	2.34 [11]	2.32 [14]	2.38 [14]	2.10 [14]	0.49 [6]	
μ_{linear} (day^{-1})	0.17	0.14	0.15	0.16	0.11	
Species	***Chlorella vulgaris***					
pH	2	3	4	10	12	13
Maximum biomass concentration ($g.L^{-1}$) [day]	0	0	2.51 [8]	1.35 [8]	2.01 [9]	1.21 [8]
μ_{linear} (day^{-1})	-	-	0.37	0.10	0.25	0.09

Figure 59 shows the change in pH for *Chlorella vulgaris* and *Scenedesmus sp*. cultures from different pH starting values. *Chlorella vulgaris* was seen to adjust and acclimate within 2 days of inoculation for pH 4, 10, 12 and 13 (Figure 59a). Using starting pH of 2 and 3, no change in acidity was observed; concomitantly, as shown in Figure 58a, no growth was observed. *Scenedesmus sp.* was able to adapt more efficiently at every starting pH from 3 to 13 (Figure 59b), but starting pH 2 was not tested as *Scenedesmus sp.* was not flocculated at this pH. Microalgae starting at pH 3 took the longest period of 4 days to acclimate, where other cultures took 2 days, and this was reflected in the growth curve in Figure 58b.

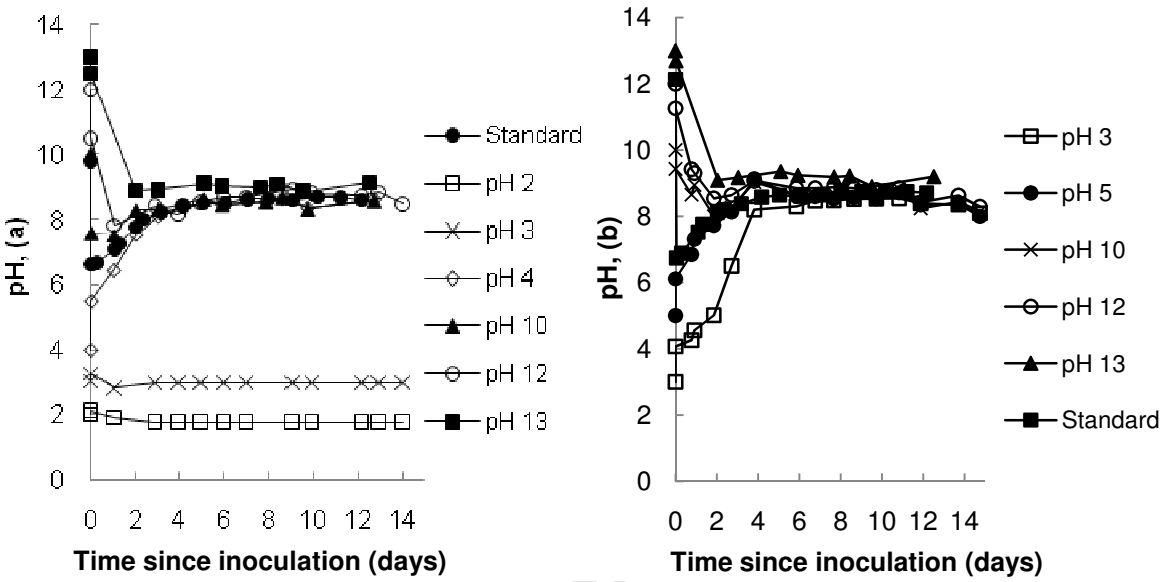

Figure 59: pH profiles during growth of (a) *Chlorella vulgaris* and (b) *Scenedesmus sp.* with different starting pH in airlift photobioreactors

The more acidic or alkaline a solution, the more dissociated ions required to achieve this pH and hence an increase in ionic strength results. This increase in ionic strength is proportional to the increase in conductivity which may inhibit cell growth if too high. This relationship is best described by the Henderson-Hasselbalch equation:

$$pH = pKa + log\frac{[salt]}{[acid]} \quad (22)$$

The ionic strength of the solution is a function of the salt concentration and therefore as the pH rises, the buffer ionic strength also rises. Ionic strength is also a function of the molarity of the acid added. Figure 60 shows the conductivity profiles for *Chlorella vulgaris* and *Scenedesmus sp*. at a range of starting pH. All conductivities decreased proportionally to growth in Figure 58. The higher conductivities are comparable to the cultures which exhibited minimal or negligible growth in both species. Comparing Figure 58 and Figure 60 it may be concluded that *Chlorella vulgaris* and *Scenedesmus sp*. growth was inhibited above 3 $S.cm^{-1}$ ionic strength. This was therefore the upper limit for flocculation induced conductivity.

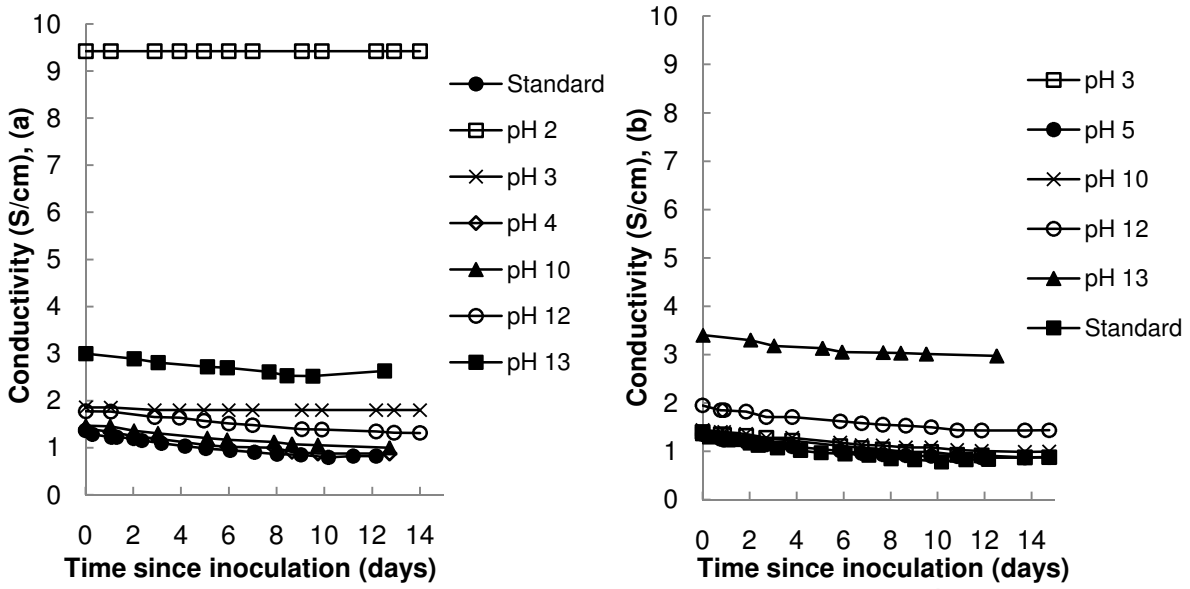

Figure 60: Conductivity profiles during growth of (a) *Chlorella vulgaris* and (b) *Scenedesmus sp.* with different starting pH in airlift photobioreactors

6.8 Summary of key findings

- *Scenedesmus sp*. and *Chlorella vulgaris* were found to settle naturally at an average of 0.187 ± 0.006 and 0.160 ± 0.004 m.day^{-1} respectively.
- Harvesting time did not affect settling efficiency.
- Increased settling efficiencies were observed near the bacterial and microalgal cells' PZC.
- The greatest bioflocculation efficiencies were observed in regions where the greatest differences in surface charge was evident. The bioflocculation of *Chlorella vulgaris* with *Microbacterium chocolatum* and *Scenedesmus sp*. with *Bacillus* sp. were the best combinations reaching 98 and 58% algal flocculation efficiency after 20 minutes.
- An 81% algal cell recovery was observed on the combined bioflocculation of *Chlorella vulgaris* and *Scenedesmus* sp.
- Alkali autoflocculation induced formation of flocs of 50 µm to 2 mm, whilst autoflocs formed in the death phase were 10 to 40 µm. Chemical flocs were found to range from 50 µm to 3 mm. Bioflocs sizes were approximately between 50 µm to 5 mm.
- Different mechanisms are responsible for different types of flocculation and the dominant mechanism is dependent on ions present, pH and other cell surface charges.
- *Chlorella vulgaris* and *Scenedesmus sp*. showed ability to acclimatise to a range of starting pH (2 - 13) and ionic strength (1 – 10 S.cm^{-1}) conditions in their growth cycle.
- At a starting pH of 10 and 12, *Scenedesmus sp.* reached a maximum biomass concentration after 14 days of 2.4 and 2.1 g.L^{-1} compared to 3.22 g.L^{-1} under standard conditions, and a μ_{linear} of 0.15 and 0.16 day^{-1} compared to 0.36 day^{-1} under standard conditions.
- At a starting pH of 4 and 10, *Chlorella vulgaris* reached a maximum biomass concentration after 8 days of 2.51 and 1.35 g.L^{-1} compared to 2.23 g.L^{-1} under standard conditions, and a μ_{linear} of 0.37 and 0.10 day^{-1} compared to 0.37 day^{-1}.

7 DISCUSSION OF RESULTS

7.1 Gaps in literature and fundamental understanding

The current understanding of microalgal recovery systems is limited owing to inconsistencies in the data presented in the literature and its interpretation. These empirical findings have been summarised in Appendix 1A and reviewed critically in Chapter 2. There is a need for critical review within this area of research to discern between possible and practicable methods and place more focus on the plausible methods. Large scale centrifugation, flotation, electrolysis and unaided filtration are restricted in their application to algal systems to high value products due to high energy and chemical requirements. This energy requirement stems directly from method inefficiencies due to the nature of the cells suspensions (dilute, hydrophilic, similar density to water, microscopic cell sizes). Current methods require large energy inputs due to the large volumes of water that must be removed from the biomass. This required energy may be reduced by allowing cells to settle out of the water; however this is time consuming due to the low settling rates. Flocculation serves as an inexpensive method to increase particle size and thereby settling velocity.

On achieving appropriate settling velocities, sedimentation may be used to increase biomass concentration within minutes. Similarly, the improved fundamental understanding of the colloid system and its flocculation provides insight into the optimisation of other techniques exploiting natural physico-chemical properties. Much of the flocculation literature has been developed for application in wastewater treatment with the primary focus on water clarification and not biomass recovery. A range of flocculation techniques have been investigated, exploiting different physical agglomeration mechanisms. The basis of these mechanisms needs to be further understood to optimise cell flocculation, particularly for the recovery of biomass of appropriate quality and activity, while maintaining the quality of the water or spent medium for recycle.

While the flocculation of microalgal systems aided by pH adjustment, temperature, extracellular material, light, growth phase, co-flocculants and salt loading is reported, mostly the relationships causing destabilisation of the algal suspension are described empirically with limited fundamental understanding. Nevertheless these findings contribute to the overall understanding of the algal system. By analysing the influence of these factors on a microalgal suspension independently of each other, and considering interactions, a holistic understanding may be developed to exploit these characteristics. A “first principles” approach can aid this.

To execute this approach, the inter-relationships between surface and suspension properties must be fully understood and characterised. The nature of the effluent media and concentrated biomass is dependent on the recovery technique applied. This affects downstream processes as well as the potential for recycle of water and residual media components. Biomass drying also needs to be investigated as very little research has been published on this problem. Table 16 summarises the complex interdependence between surfaces and culture suspension parameters. It serves as a map for relationships between

variables encountered in dewatering literature and highlights the complexity of experimental investigation of microalgal dewatering. The column (y-axis) of variables presented in Table 16 represents the independent variables of which the rows (x-axis) of variables are dependent on. For example, Ionic strength is a function of extracellular material, the growth phase and pH. A subset of these parameters were investigated in this thesis, future work within CeBER may investigate further interactions. Throughout the experimental approach undertaken for this dissertation, interdependent variables were investigated to achieve the relationship trends.

7.2 Understanding the importance of microalgal growth

In Section 5.2, physico-chemical properties of *Chlorella vulgaris* and *Scenedesmus sp*. during growth were investigated. For both species, the surface properties varied between the exponential and the stationary phase, apart from hydrophobicity which remained relativity constant. Zeta potential, pH and effective particle size increased during exponential growth from the minimums at inoculation. This was due to the acclimation of the cells to the new system and increased metabolic rates.

During this initial growth phase, zeta potential was at a minimum (Figure 23) and conductivity (Figure 21) was at a maximum. Ions not specifically adsorbed (i.e. higher ionic strength solutions), compressed the double layer and therefore reduced the stability of the system. Species that form surface complexes and adsorb onto the particle surfaces (eg. Ca^{2+}) affect the surface charge of the colloid and therefore the surface potentials, thereby affecting system stability (Stumm, 1992). This slight decrease in colloid stability is postulated to induce minor aggregation of cells. This explains the increased floc stability when $CaCl_2$ was added as a co-flocculant (Figure 49). This phenomenon, coupled with increased reproduction rates (Figure 11 and Figure 12), explains the increase in effective particle size during the exponential growth phase (Figure 22).

Section 5.2 was pivotal in exposing the differences between the two species studied and offers some insight into the different conditions needed to exploit the surface properties for recovery of biomass of these two species. The surface properties of *Chlorella vulgaris* and *Scenedesmus sp*. were a function of the suspension conditions, which varied with growth phase. In Section 5.6 this was demonstrated in terms of the effect of pH and conductivity on hydrophobicity and surface charge (Figure 21, Figure 22, Figure 23). For both species, conductivity decreased similarly (Figure 21). *Chlorella vulgaris* has a greater variance over *Scenedesmus sp.* in chlorophyll *a* content (Figure 10) and effective particle size (Figure 22). Zeta potential, pH, conductivity and effective particle size reached constant values during the stationary growth phase of the respective microalgae. This levelling off was further evidence that the cells' metabolic rate affected the external suspension conditions.

Table 16: Expected relationships between microalgal parameters

	Bacteria	Concentration	Ionic strength	Extracellular	Flocculation	Growth phase	Hydrophobicity	Particle size	Sedimentation	Zeta potential
Bacteria		X		X	X					X
Concentration	X			X	X	X		X		
Conductivity					X	X	X			X
Extracellular			X		X		X			X
Flocculation		X					X	X	X	
Growth phase	X	X	X	X	X		X	X		X
Hydrophobicity					X			X	X	
Light	X	X				X			X	
Particle size					X		X		X	
pH	X	X	X		X	X	X		X	X
Temperature	X	X		X	X	X			X	X
Zeta potential					X		X	X	X	

Despite all the variations in surface properties of both species, hydrophobicity and sedimentation rates were found not to be dependent on the time of harvesting under standard suspension conditions (Figure 44). While individual suspension conditions suggest varying colloidal instability at different growth phases, the culture system as a whole was stable under natural solution conditions with limited natural flocculation. *Chlorella vulgaris* cells are smaller than *Scenedesmus sp.* (Figure 55) and reached a lower, maximum mass concentration of 2.26 $g.L^{-1}$ compared to 3.22 $g.L^{-1}$ for *Scenedesmus sp.* (Figure 11 and Figure 12) and a reduced recovery (Figure 44). The larger cell size translated into a faster unaided settling rate for *Scenedesmus sp*. over *Chlorella vulgaris*. Similarly, the *Microbacterium chocolatum* cells are smaller than *Nocardioides aromaticivorans* and reached a lower mass concentration of 0.028 $g.L^{-1}$ and 0.13 $g.L^{-1}$ respectively (Figure 17). The *Chlorella-Microbacterium* system thus focused on cell number concentrations whilst the *Scenedesmus-Nocardioides* system focuses on cell size and mass concentrations.

Feed CO_2 concentrations were found to affect pH, conductivity and zeta potential of both species. Culturing pH was observed to be higher when cells were grown on air due to less dissociation of CO_2 into the culture medium. This could be advantageous in flocculation as less alkali is required to induce flocculation under alkaline conditions. No significant advantages were found in terms of conductivity and zeta potential effects using lower CO_2 concentrations (Figure 21, Figure 23) as profiles were very similar. However, cell growth limitation from CO_2 deficiency compels the choice of a higher CO_2 feed concentration system to maintain acceptable rates of growth. The cultures reached a maximum biomass concentration of 0.87 ± 0.05 and 2.16 ± 0.11 $g.L^{-1}$ on day 10 and 14 of growth respectively (Figure 13). The *Scenedesmus sp*. culture was still in linear growth when the airlift photobioreactors were harvested suggesting that the cells were not light limited as yet. *Scenedesmus sp*. grown on air continues to increase in biomass concentration after day 13, whereas the culture grown on sufficient CO_2 (2900 ppm) enters stationary growth phase on day 10 due to the higher biomass concentration inducing light limitations earlier. *Chlorella vulgaris* and *Scenedesmus sp.* maximum concentrations decreased by 62 and 33% respectively when cultured on air compared to 2900 ppm CO_2.

Salt loading, pH, zeta potential, hydrophobicity, particle size, EOM, cell age, light and nutrient deficiencies all influenced flocculation and sedimentation rates (Sections 2.4, 6.3.1 and 6.3.2); however the sedimentation rates observed during exponential and stationary phases were similar (Figure 44). The increased salt loading and extreme pH increased ionic strength, reducing the electric double layer surrounding the algal cells. A change in pH also allowed zeta potential PZC to be exploited to induce autoflocculation. Increases in particle sizes, via flocculation, increased the natural settling rates. EOM increased the potential for bridging between cells during flocculation. Each of the above mentioned parameters was dependent on the growth phase (Section 5.2). However these surface properties were also dependent on each other (Section 5.6) as tabulated in Table 16. It is this compromise of dependency that promotes colloid stability within the reactor and makes it intrinsically difficult to characterise each parameter independently and to predict an optimal operating point to maximise sedimentation and flocculation during a specific growth phase.

In Table 17, the zeta potential and hydrophobicity indices for *Chlorella vulgaris* and *Scenedesmus sp.* are predicted theoretically in terms of the respective measured conductivity and pH during growth. The theoretical values presented indicate the expected

hydrophobicity indices and surface charge where only pH and conductivity affect surface properties in the bioreactors, based on the relationships described in Figure 30, Figure 31 and Figure 32. These predicted *in situ,* physicochemical properties are compared with the actual measured properties.

Table 17: Predicted table of theoretical, *in situ* physicochemical properties of *Chlorella vulgaris* and *Scenedesmus sp*. during growth in airlift photobioreactors as a function of hydrophobicity or pH

Species	Conductivity ($mS.cm^{-1}$)	Predicted Hydrophobicity index (%)	Predicted Zeta potential (mV)
Chlorella vulgaris	1366 to 799	19 to 21	~ -32
Scenedesmus sp.	1366 to 757	9.2 to 5.5	~ -5
	pH		
Chlorella vulgaris	6.61 to 9.79	37 to 16	~ -15
Scenedesmus sp.	6.74 to 12.13	8.5 to 5.5	-8 to -32
		Actual Hydrophobicity index (%)	**Actual Zeta potential (mV)**
Chlorella vulgaris		7.2	-7.6 to -5.7
Scenedesmus sp.		5.8	-24.6 to -12.0

Hydrophobicity was found to remain constant across the growth phase (Figure 25) based on readings taken during exponential and stationary phases; this was not consistent with the predicted however changes in the hydrophobicity index of the cells based on changes in conductivity and pH (Table 17). Similarly the changes predicted for cell surface charge did not follow the measured trends during growth (Figure 23). This suggests that at different points during the growth curve, the inter-relationship between physico-chemical properties may vary or additional factors, not accounted for, may contribute. While the interactions between these and their impacts on sedimentation remain unexplained, with respect to the growth phase, the effect of pH, conductivity, biomass concentration, salt loading and particle size were found to be the dominant influential factor with regards to sedimentation and flocculation as described in Section 6.2 to 6.4.

Figure 17b described the differences in mass concentrations of the *in situ,* co-cultured bacteria. When the bacteria were cultivated in isolation under identical conditions (Figure 18), similar growth curves were observed for the two strains. The co-cultured bacteria were hence found to be highly dependent on the respective microalgal culture systems. This is postulated to be as a result of the rate of supply of organic carbon source by the algae. However, preliminary experiments showed no effect on microalgal growth with respect to initial co-cultured bacterial contamination concentrations. *Nocardioides aromaticivorans* and *Microbacterium chocolatum* were easily cultivated on Luria broth and reached a maximum concentration of 3.36 and 3.82 $g.L^{-1}$ respectively in less than 60 hours under non-optimised conditions. Therefore, these two bacterial strains may have potential for bioflocculation (Figure 55e and f) as they are easily grown independently, exhibited sufficient bioflocculation results and have negligible effect on microalgal growth as a contaminant. However some strains of bacteria produce large amounts of EPS that induces increased flocculation and therefore additional strains should be screened and EPS should be investigated further as this is expected to increase auto-bioflocculation.

Flocculation has also been described to occur from increased EOM concentrations which influence the surface chemistry of particles and promote flocculation (Henderson *et al.*, 2008b). Section 5.5 investigated the carbon balance over the airlift photobioreactors where autoflocculation (predominately *Chlorella vulgaris*) was observed during the stationary and death phases (Figure 56). Extracellular carbon was found to increase towards the end of the growth curves for both species (Figure 29). Bioflocculation has been proposed to occur initially via charge-based particle attraction (Spolaore *et al.*, 2006) and then by adsorption via bridging between cells which is augmented in the presence extracellular carbon (Lian *et al.*, 2008b). Towards the end of the growth phase of both species of microalgae, conductivity continued to decrease as a function of time in bioreactor (Figure 21a) whilst suspended biomass decreased (Figure 11 and Figure 12). The ion-chelation of cells (Figure 21b) in the presence of increased extracellular carbon was therefore postulated to increase the autoflocculation of cells in the airlift photobioreactor systems towards the end of the growth cycle. This was supported by the minima observed in zeta potential towards the end of the growth curve (Figure 23) and the slightly alkaline reactor conditions (Figure 20). At these conditions, the cells were at minimum electronegativity with chelated ions forming bridge networks between cells supported by microscopy (Figure 56).

The effect of growth on the algal system's physical parameters has now been well classified. Further, external factors influencing flocculation have been elucidated. However if these parameters are to be exploited to induce easier separation via colloid instabilities, their effect on growth must be investigated, particularly with respect to the recycle of effluent water and nutrients to culture new microalgae and the degree of neutralisation required. The use of light, temperature and nutrient deficiency to increase sedimentation rates will not affect the growth of a new culture grown on recycled effluent as these factors are normalised in the reactor. However, pH and conductivity of the recycled stream may affect the microalgal cultivation. This effect and the potential need to neutralise the recycled water was considered. A fluctuation in pH influences the availability of carbon to cells by altering the relative fraction of dissolved CO_3^{2-}, HCO_3^- and free CO_2 (Mayo, 1997). These have been found to affect the metabolic rates of *Scenedesmus* and *Chlorella* directly (Azov, 1982). The optimum growth pH of *Chlorella vulgaris* and *Scenedesmus* lies between pH 7 and 10 (Henderson *et al.*, 2008b). *Chlorella vulgaris* and *Scenedesmus sp.* survived and even grew under mild acidic and extreme alkaline conditions (Figure 58). The photosynthetic systems which are in the chloroplasts are surrounded by cytoplasm of neutral pH (Mayo, 1997). *Chlorella vulgaris* grew consistently better at alkaline starting conditions than at acidic starting conditions (maximum biomass concentration of 1.21 $g.L^{-1}$ on day 8 starting at pH 134 compared to no growth below pH 4) whilst *Scenedesmus sp.* grew consistently better at acidic starting conditions than at alkaline starting conditions (maximum biomass concentration of 2.34 $g.L^{-1}$ on day 11 starting at pH 3 compared to a maximum biomass concentration of 2.10 $g.L^{-1}$ on day 14 starting at pH 12) (Figure 58). However both species displayed a similar pH profile during regular growth.

Higher conductivity was also shown to improve settling efficiency (Figure 45). At ionic strengths above 3 $S.cm^{-1}$, minimal increases in settling rates were observed and microalgal growth inhibition was observed above this conductivity (Section 6.7). Thus 3 $S.cm^{-1}$ should be set as the upper limit for ionic strength. Comparing Figure 59 and Figure 60 it can be concluded that conductivity was affected directly by pH at extreme alkaline and acidic

conditions. Both *Chlorella vulgaris* and *Scenedesmus sp*. were able to auto-adjust the reactor suspension pH to standard conditions after 4 days when sufficient cell growth and acclimation had taken place (Figure 59); however system conductivity remained consistently higher throughout the growth of both species (Figure 60). Therefore it can be concluded that ionic strength had a more sustained effect on the microalgae than pH and thus if effluent water were to be recycled, the ionic strength must be controlled as a priority. This may be done by either a purge stream and introduction a freshwater to achieve the appropriate dilution or by adding an additional unit to decrease salt concentration. This is however an expensive technique achieved by ion exchange or reverse osmosis. The need to control ionic strength thus influences the choice of preferred flocculation technique.

Chlorella vulgaris and *Scenedesmus sp.* cultured on 2900 ppm CO_2 in the airlift photobioreactors reached a maximum concentration of 2.26 and 3.22 $g.L^{-1}$ after 8 and 11 days of growth respectively (Table 10). At these maximum concentrations the biomass productivity of the cells were at a minimum as the cultures were about to enter stationary growth phase (Figure 19). The maximum productivities were observed during linear growth phases, which partially highlight the limitations in cell growth (Figure 14). To exploit maximum productivity, the reactor must either be run continuously, harvesting of cells at this point in growth (Molina-Grima *et al*., 1999) or an optimum point of harvesting of the batch culture must be determines as a compromise between suspension cell density and biomass productivity.

7.3 Fundamentals from empirical data

The growth results of *Scenedesmus sp*. and *Chlorella vulgaris* highlighted the interdependence of the cells physico-chemical properties. Section 5.6 investigated these properties in relation to each other and their respective effect on flocculation and hence sedimentation. As previously mentioned, growth phase had little effect on flocculation and sedimentation efficiencies (Figure 44). Instead conductivity, pH and salt loading were used to alter zeta potential and hydrophobicity to a greater extent to influence the microalgae recovery (Figure 45, Figure 47 and Figure 49 respectively).

Generally it is known that some bacteria augment flocculation by excreted extracellular products. It is also known that increased salt loading and pH adjustment might increase all forms of flocculation. Current mechanisms are based on microscope images, limited theory and atomic force microscopy (Salim *et al.,* 2010). In this work, the surface charge and hydrophobicity was determined over a range of pH for the microalgae. Different strains of bacteria were also screened. Depending on the hydrophobicity and charge profile with respect to pH, a microalgal species may be bioflocculated with a strain of bacteria (or macromolecule with a surface charge) purely based on attraction via van der Waal forces (oppositely charged cells attract and bridge together forming an agglomerate of bacteria-microalgae-bacteria). Co-cultured bacteria may be used, especially if additional EPS is produced to aid flocculation, and will not contaminate the recycled water and nutrients after sedimentation (which is another key focus of this technique). Other types of microalgae with different surface charges across the pH profile may also be used and also contribute to lipid products.

To determine the optimum conditions for maximum flocculation and sedimentation whilst avoiding cell damage, and to gain a fundamental understanding of this flocculation, critical physico-chemical properties were analysed simultaneously and compared to regions of increased flocculation. The data are summarised in Figure 61 and Figure 62 hereafter as a function of pH. The grey regions indicate areas across the pH range where heightened colloidal instabilities were observed.

Figure 61 and Figure 62 show significant differences in hydrophobicity and zeta potential for all species at alkaline or acidic conditions, compared with neutral conditions. For *Chlorella vulgaris* and *Scenedesmus sp*. the regions between pH 1.5 to 4 and pH 12.5 to 14 represented maximum flocculation efficiencies and hydrophobicities and automatically had increased ionic strength. The interaction of cations with the negatively charged cell surfaces may result in large bridge networks. At acidic conditions, large peaks in hydrophobicity were observed. Increased ionic strength at higher acidities also contributed to the hydrophobicity in this region, through decreasing the double layer surrounding the solid particles causing colloid instability (Hiemenz and Rajagopalan, 1997). These phenomena increased floc sizes and hence increased the bulk particle density which induced higher rates of sedimentation. Figure 54 showed the time dependency of autoflocculation at these acidic conditions.

If hydrophobicity were to follow directly the trends of increased regions of flocculation efficiencies, there would be an increase in hydrophobicity as pH increased following the zeta potential negativity trends (Figure 31 and Figure 32). However hydrophobicity was at a maximum when the cell surfaces were most electropositive. This suggests that individual cells at lower pH values repel each other at the increased cationic loading when no other salts are present in the suspension matrix. At basic conditions, even though the cell surfaces are electronegative and immersed in a cationic solution, the absence of other metal salts such as magnesium results in a lower hydrophobic behaviour. The isoelectric point did have a small effect on hydrophobicity of cells demonstrated by the increase in hydrophobic index compared to when the cells are electronegative. This hydrophobicity was amplified by the increase in ionic strength at acidic conditions which also promotes colloidal instability (Stumm, 1992). This phenomenon also promotes increased bioflocculation and autoflocculation for all organic species at extreme acidic and alkaline conditions. Although pH was the main contributing affect on hydrophobicity, conductivity was also found to influence the hydrophobicity index (Figure 30) with *Chlorella vulgaris* and *Scenedesmus sp.* displaying respective maxima and minima hydrophobic indices in distilled water.

The effects attributed to hydrophobicity are not true hydrophobicity but rather allied effects driving the ability to partition cells into a polar phase which is often due to charge neutralisation as discussed throughout. This phenomenon is however frequently attributed to hydrophobicity as is the more robust measurement via contact angle measurement. The hydrophobicity measurement method used in this dissertation reflects the ability of the suspension (at adjusted conditions) to induce the microalgal cells to migrate out of the solution into a polar phase.

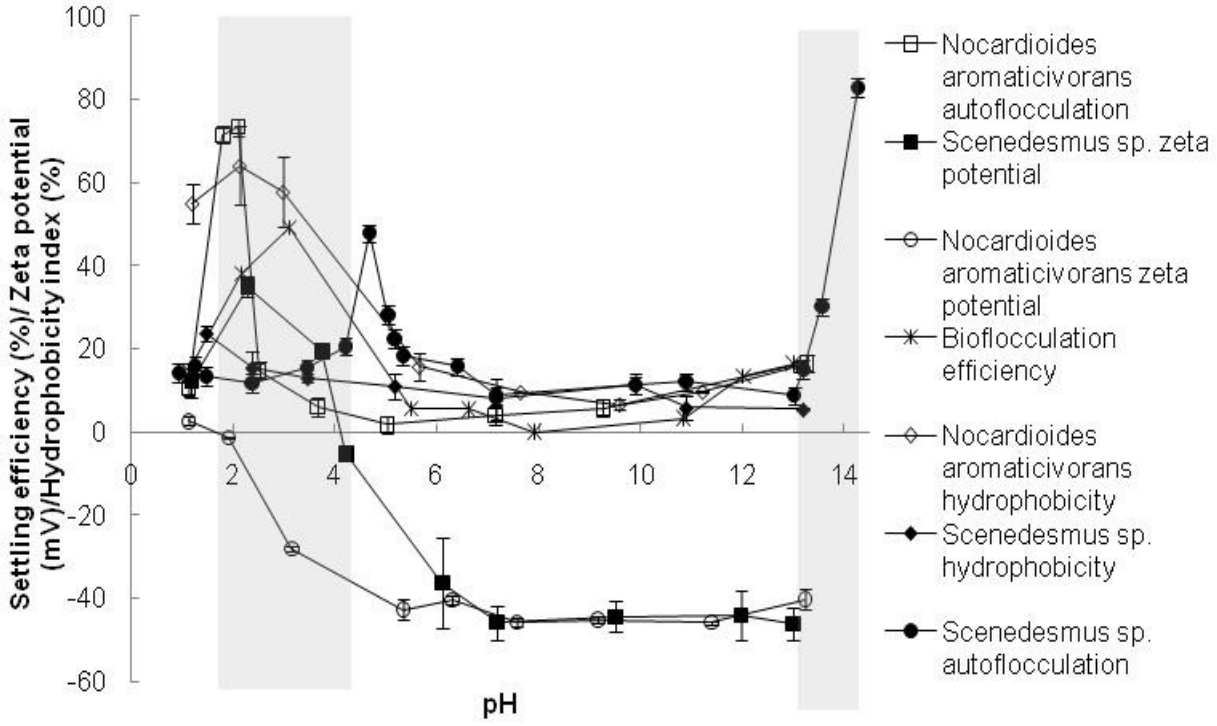

Figure 61: *Scenedesmus sp.* and *Nocardioides aromaticivorans* SB10005 zeta potentials, hydrophobicities, flocculation and co-cultured bioflocculation efficiencies as a function of pH

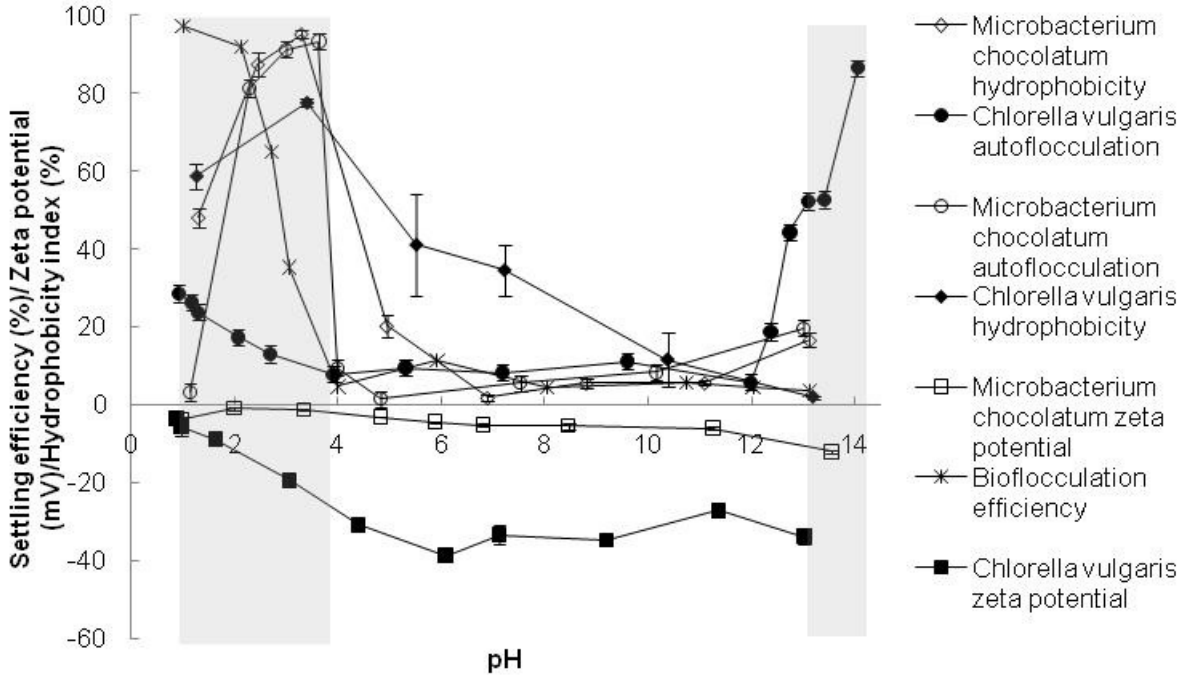

Figure 62: *Chlorella vulgaris* and *Microbacterium chocolatum* RW56 zeta potentials, hydrophobicities, flocculation and co-cultured bioflocculation efficiencies as a function of pH

Section 6.3 showed that the addition of bacteria or microalgae to other microalgae at specific pH values induced flocculation. This increased the rate of sedimentation and hence harvesting efficiency. Most species demonstrated increased flocculation activity at pH 13 and above (Figure 47, Figure 48a, b and c), and although hydrophobicity indices and zeta

potentials were shown to be local maxima (Figure 34 and Figure 35); these values were less noteworthy than at acidic conditions. Increased ionic strength has been widely reported to increase flocculation of microalgae (Bernhardt and Clasen, 1994). Positively charged polymers are commonly used to bind partly or completely to microalgal cells (Salim *et al.*, 2010). At increased dosages, dissociated NaOH, Na^+ ions physically link cells via cell surface adsorption (Lian *et al.*, 2008).

Salim *et al.* (2010) investigated *Scenedesmus sp.* used to bioflocculate *Chlorella vulgaris* and reported a maximum recovery of 37% in one hour at pH 7. In this investigation, with a decrease in pH to 2.55, an increase in recovery to 81% in 20 minutes was achieved (Table 18). This demonstrates the dependence of bioflocculation on cell surface charges. The bioflocculation between *Scenedesmus sp*. and *Chlorella vulgaris* at pH 2.55 also demonstrated the second best cell recovery with the advantage of requiring a less extreme pH 3.55. This technique was therefore the most attractive result for biofuel as both species will contribute to the final biomass product (Table 18).

Even though the zeta potential difference between *Chlorella vulgaris* and *Microbacterium chocolatum* was relatively insignificant at pH 3 and less, they both exhibited high hydrophobicities at acidic conditions. At these acidic conditions, both species had negligible surface charge. The cells therefore had diminished repulsion forces and as *Microbacterium chocolatum* cells remained slightly negatively charged, the acid induced positive ions within the solution may have acted as a bridging support between cells. This bridging was due to a lower Gibbs energy between the two surfaces (Stumm, 1992). The increased hydrophobicity also contributed to the high flocculation efficiencies (Strand *et al.*, 2002). The predominant co-culturing bacteria found in both the microalgae investigated displayed opposite surface charges in regions of good flocculation compared to the respective microalgal species. This advantage allows for the co-cultured strain to have a different zeta potential at certain optimised pH. This permits increased bioflocculation efficiencies and sedimentation rates.

Table 18: Optimal pH for sedimentation with maximum recovery efficiency (given in brackets as %) via auto- and bioflocculation performed in jar tests after 20 minutes settling

	Bacillus sp.	*E. coli BL2 (DE3)*	*Microbacterium chocolatum*	*Nocardioides aromaticivorans*	*Scenedesmus sp.*	*Chlorella vulgaris*
Scenedesmus sp.	3.35 (54)	13 (34)	(<10)	3.1 (49)	-	2.55 (81)
Chlorella vulgaris	2.28 (36)	2.14 (64), 13 (33)	1 (97)	(<10)	2.55 (81)	-
Autoflocculation	3	3.2	3.5 (93)	2 (73)	4.7 (48), 14 (83)	1 (29), 13.5 (87)

Table 18 shows the best scenarios for sedimentation at optimal pH via auto- and bioflocculation. *Scenedesmus sp*. autoflocculated at pH 4.7 and 14 and *Nocardioides aromaticivorans* autoflocculated at pH 2; however when the co-cultured bioflocculant was introduced at pH 2, 4.7 or 14, minimal flocculation (<15%) was observed. *Chlorella vulgaris* autoflocculated at pH 1 and 13.5 whilst *Microbacterium chocolatum* autoflocculated at pH 3.5; however bioflocculation between these two species occurred between pH 1 and 3.5. At pH 3.1, *Scenedesmus sp.* and *Nocardioides aromaticivorans* demonstrated a maximum bioflocculation efficiency of 49% and an average hydrophobicity index of 32.7% compared to a bioflocculation efficiency of 97% and average hydrophobicity index of 53.4% for

Chlorella vulgaris and *Microbacterium chocolatum* at pH 1. Throughout the bioflocculation experiments the optimum pH for bioflocculation existed between the PZC of the respective species, in a region where the cell types carry opposite charge. This suggests that the zeta potential defines the mechanism by which the cells adhere together throughout the pH profile. While hydrophobicity of cell surfaces affects the van der Waals interactions directly (Stumm, 1992), the hydrophobic interaction between the cells does not determine the success of the bioflocculation, rather the extent and magnitude of the flocculation.

Similar to the bacteria, *Scenedesmus sp.* and *Chlorella vulgaris* demonstrated a peak in autoflocculation at marginally more acidic conditions than its PZC at pH 4.2 and 1.1 respectively. *Scenedesmus sp.* and *Chlorella vulgaris* both autoflocculated at pH 13 and above. This phenomenon suggests the autoflocculation of cells via two different mechanisms. Ionic strengths at pH 13 and above are inherently higher than at pH values around the species' PZC. At extreme alkaline conditions all species had a minimum surface charge which would confer maximum suspension instability (Hiemenz and Rajagopalan, 1997). However the increased cation concentration in the solution coupled with the extremely negative surface charges induced a bridging network of saturated salts between the microalgal cells similar to chemically induced flocculation (Figure 55j). Autoflocculation observed near the PZC was postulated to occur via a patching mechanism where cells adsorb ions and patch together through charge neutralisation. The two flocculation mechanisms described earlier (Figure 53) were therefore revised to distinguish between PZC and alkaline saturation autoflocculation. The revised proposed flocculation mechanisms are presented in Figure 63. Bioflocculation was also postulated to occur through adsorption incorporating a bridge network of patching.

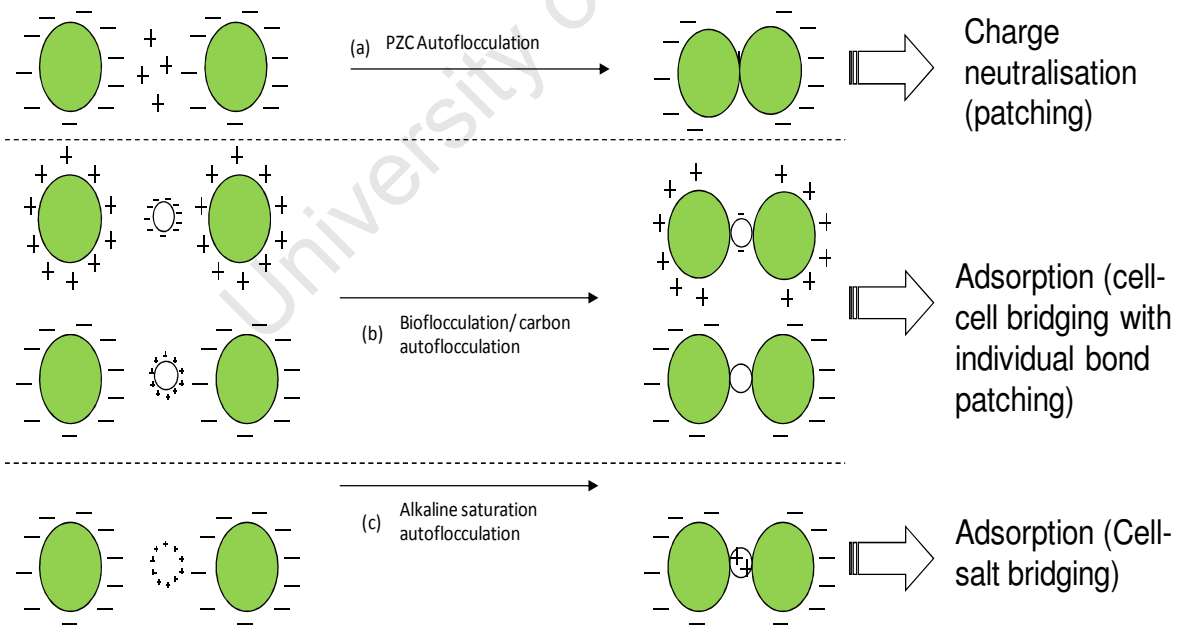

Figure 63: Proposed mechanisms of PZC and alkaline saturation auto- and bioflocculation for *Scenedesmus sp.* and *Chlorella vulgaris*

Depending on chemical and culturing costs and recovery targets, pH and bacterial loading could be optimised to achieve the desired separations for further downstream processing. As algae are highly adaptive organisms, pH correction of the recyclable water may be marginal thus making this technique an attractive alternative dewatering procedure.

7.4 Strategically designed separation mechanism

Figure 1 outlined the current microalgae to biofuel process. The work presented in this dissertation investigated the biomass recovery processing with particular focus on the feasibility of recycling nutrients and water whilst operating at low energy requirements. The chosen technique to achieve this was flocculation followed by sedimentation. Figure 64 explains a reviewed approach to the processing of microalgae based on Chisti's (2007) original work. The production of biomass would preferably need to be continuous with high biomass productivity. The exponential growth phase exhibited the highest growth rate, particle size and conductivity but has the lowest biomass concentration, EOM, zeta potential and pH. *Scenedesmus sp.* and *Chlorella vulgaris* at these conditions would favour acidic autoflocculation (Figure 47) or bioflocculation (Figure 50) to minimise chemical requirements. The *Chlorella vulgaris* inoculum failed to grow satisfactorily in acidic conditions (Figure 58), hence a control system for the recycle of the acidic stream is required. If the recycle is fed into a continuous process at an appropriate rate, the neutralisation associated with algal growth (Section 6.7) will assist to control pH into an acceptable range. Alternatively *Chlorella vulgaris* is well suited to bioflocculation at mildly acidic conditions or autoflocculation at alkaline pH. If cells were harvested during the stationary growth phase, growth rate and conductivity would be at a minimum with biomass concentration, zeta potential, pH and EOM a maximum. This would facilitate autoflocculation much more easily and would be the optimal method for reduced chemical usage. This is because increased EOM and pH increase ionic strength whilst a maximum in surface charge relates to a minimum in suspension stability. Bioflocculation was found to be less stable than autoflocculation (Figure 52); this could be due to the bridging nature of bonds between cells. Bioflocculation may require downstream "decontamination" whilst autoflocculation would require greater chemical use through acid and base addition. If the microalgae are to be bioflocculated using bacteria, the possible need for deflocculation may arise to enable separation of the bacteria and further concentration of the algae. Bioflocculation occurred much faster than autoflocculation (Figure 54). Chemical flocculation was found to be the most efficient method (Figure 49) with autoflocculation and bioflocculation largely dependent on the solution conditions for success (Figure 51). However chemical flocculation requires pH adjustment and chemical dosing which makes effluent recycling in this technique the most challenging.

Section 6.7 investigated the effects of flocculation effluents on the growth and acclimation of the microalgae. The most promising suspension operating regions with regards to microalgal flocculation lies in alkaline and acidic conditions. As previously mentioned, at these pH values, conductivity increases and subsequently inhibits growth (Figure 58). Autoflocculation is postulated to occur via a patching mechanism and requires an increased ionic strength and pH for success. At these conditions the surface charges must either be extremely electronegative or close to the PZC. Bioflocculation is postulated to occur via the bridging of different organic materials and requires a solution pH to produce oppositely

charged surfaces for success. This pH could range over the entire spectrum if suitable candidates were found. At pH neutral conditions, *Scenedesmus sp.* and *Chlorella vulgaris* were electronegative and hence if an electropositive material was used at these conditions no additional chemicals would be needed. However this addition may cause contamination and lead to increased downstream processing. The algae-algae bioflocculation of *Scenedesmus sp*. and *Chlorella vulgaris* (Figure 55k, Figure 50d) is another alternative approach to consider. The final choice of flocculation technique is expected to be dependent on both algal system of interest and expected use of product algae. However all techniques investigated thus far required addition of acid or base to exploit the cells surface properties. There is therefore a need to neutralise the pH and ionic strength to an acceptable level by assessing desired growth outputs described in Figure 58 whilst considering purge and freshwater make-up streams.

Many cell disruption techniques exist with varying success (Lee *et al.*, 2009b), however the common factor is the energy required at this point and subsequent drying steps which poses additional problems of major economic importance (Mohn, 1980). Transesterification using enzymes in the presence of water might also be a key technology to be developed. Some of the biomass residue from the cell disruption process may be anaerobically digested to produce biogas (Golueke *et al.*, 1957) which may be used to generate electricity (Chisti, 2007) and offset some of the power required for reactors, disruption and drying. This in itself presents many engineering challenges and much research and development is still required in each area of the overall process if microalgal biomass is to be used as a renewable energy source.

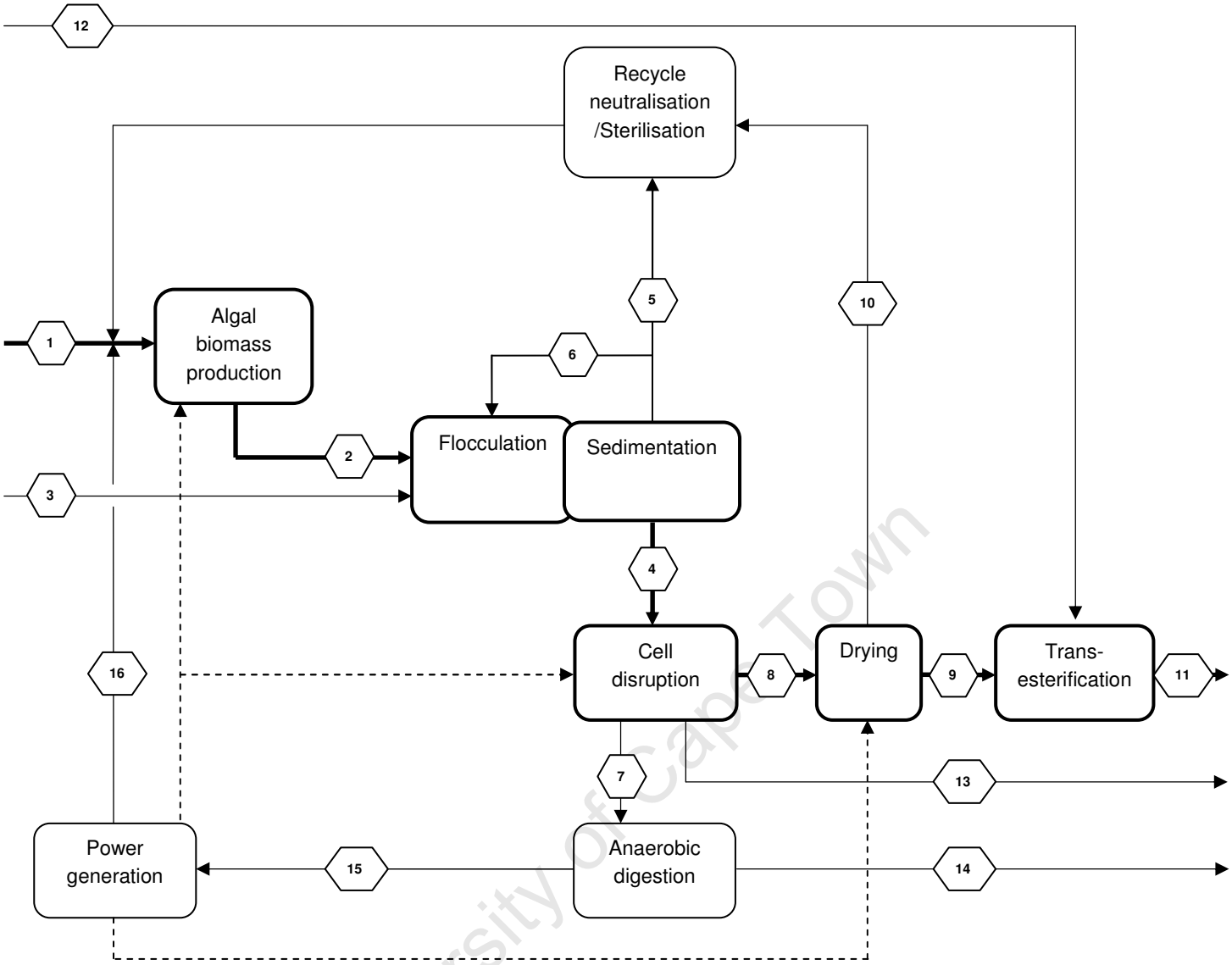

Figure 64: Revised microalgae renewable fuel block flow diagram

Table 19: Revised microalgae renewable fuel block flow diagram stream descriptions

Stream	Description	Stream	Description
1	Light, CO_2, nutrients, water, inoculum	9	Dry lipid
2	Stationary phase microalgae	10	Water
3	Acid/base/bacteria/flocculant	11	Biofuel
4	Concentrated biomass	12	Alcohol
5	Acid/base/bacteria/Water/nutrients	13	Animal feed
6	Acid/base/bacteria/Water/nutrients	14	Fertilizer
7	Biomass residue	15	Biogas
8	Wet lipid	16	CO_2

8 CONCLUSIONS AND RECOMMENDATIONS

This research has focused on the need for an effective low cost, low energy approach to the recovery of micro-algal biomass from dilute cultures for the use as an energy feedstock. A further requirement of the biomass recovery was that the quality of the residual nutrient components and water effluent streams be maintained to facilitate their recycle. This scope was motivated by the significant contribution of downstream processing to the process economics of the process for microalgal cultivation for bioenergy. In this work, the growth performance and surface properties of *Scenedesmus sp*. and *Chlorella vulgaris* were investigated throughout the growth regimes with the aim of exploiting these to assist recovery of algal biomass. While the data has been obtained specifically on these two species, many of the fundamental findings may be applied to other colloidal systems. The experimental studies reported have been conducted and analyzed within the framework of a larger critical analysis of the literature on this research topic to identify significant relationships and possible strategies to exploit naturally occurring mechanisms. It is acknowledged that this field of research is immature and lacks rigorous data and its critical assessment in the literature; hence both data analysis and postulations based upon the experimental findings are presented.

8.1 Surface properties

The surface properties of *Chlorella vulgaris* and *Scenedesmus sp.* are a function of the suspension conditions. This has been demonstrated in terms of the effect of pH and conductivity on hydrophobicity and surface charge. The relationship between suspension properties such as pH and conductivity and sedimentation behavior is expected to be mediated through surface effects. Surface properties vary with solution properties where zeta potential initially increases from a range of -27 and -58 mV to -7 and -18 mV for *Scenedesmus sp*. and *Chlorella vulgaris* respectively with an increase of 1 $S.cm^{-1}$. Zeta potential trends as a function of pH vary from species to species. The functions are largely decreasing with global maxima present between pH 0.5 and 3 as the PZC found ranged from pH 1.03 to 4.34 for *Chlorella vulgaris* and *Scenedesmus sp*. respectively, with all other tested species falling in between.

The suspension conditions are further dependent on the growth phase of the system and the reactor conditions. The suspension biomass concentration, conductivity, pH and extracellular material changed as a function of the growth phase. As a result of these changes, biomass productivity decreased (due to light limitations), cell surface charges changed (due to cell growth kinetics), average particle size changed (due to reproduction and cell surface charges), chlorophyll content changed (due to cell reproduction and metabolism), chelation increased (due to surface charges) and autoflocculation increased towards the end of the growth cycle (due to pH, surface charge and EOM). Feed CO_2 concentration also affects growth, pH and hence zeta potential and conductivity where a

feed of 2900 ppm CO_2 at 2 L.min^{-1} provided carbon sufficiency. The suspension conditions also had a major effect on the cell growth for both *Scenedesmus sp*. and *Chlorella vulgaris*.

The growth stage and environment affects the physico-chemical properties but these balance out as the growth phase does not influence the settling efficiencies directly but instead, conductivity and pH control sedimentation and flocculation rates and efficiency by directly affecting cell hydrophobicity and zeta potential. The growth phase does potentially influence zeta potential and hydrophobicity, but these are a strong function of solution properties so they may work together. The isoelectric point was however found to be independent of harvesting time, suspension conductivity and culturing CO_2 concentration. In Table 20 the zeta potential and hydrophobicity values during exponential phase (day 3) and stationary growth phase (day 9) and the PZC for *Scenedesmus sp*. and *Chlorella vulgaris* are presented.

Table 20: Zeta potential and hydrophobicity summary in standard solution conditions for *Scenedesmus sp*. and *Chlorella vulgaris* grown on 2900 ppm CO_2

Species	*Scenedesmus sp.*	*Chlorella vulgaris*
Zeta potential (day 3) (mV)	-7.3 ± 0.29	-18.7 ± 0.16
Zeta potential (day 9) (mV)	-6.3 ± 0.81	-10.8 ± 0.07
PZC (pH)	4.34 ± 0.17	1.03 ± 0.15
Hydrophobicity (day 3) (%)	5.0 ±1.5	7.6 ± 3.6
Hydrophobicity (day 9) (%)	6.5 ±0.8	6.7 ± 4.2

8.2 Rheology

Biomass concentration did not influence the rheological nature of *Chlorella vulgaris* and *Scenedesmus sp.* suspensions at concentrations of 165 g.L^{-1} and below. Under these conditions Newtonian behavior was observed for both species with a yield stress at ca. 0 Pa. The viscosity increased from 0.001 to 0.012 Pa.s across a concentration range of 0 to 205 g.L^{-1} for *Scenedesmus sp*. and viscosity increased from 0.001 to 0.004 Pa.s across a concentration range of 0 to 275 g.L^{-1} for *Chlorella vulgaris*. Deviation from Newtonian behavior can be expected at higher biomass concentrations. *Scenedesmus sp.* was found to behave as a dilatant (shear thickening) fluid when concentrated above 205 g.L^{-1} dry weight, represented by a power law function where the indices were affected by concentration (e.g. $\tau = 0.0008\gamma^{1.52}$ for 218 g.L^{-1}). *Chlorella vulgaris* remained Newtonian up to 275 g.L^{-1} dry weight ($\tau = 0.0035\gamma$ for 275 g.L^{-1}). Flocculation increased the apparent viscosity for both species of microalgae and bacteria. For industrial purposes the rheology of the two strains investigated poses no design problems as only microalgal concentrations below 200 g.L^{-1} are required for further downstream processing, where Newtonian rheology is present.

8.3 Flocculation

Flocculation can be achieved by varying pH, addition of Mg^{2+} or similar or adding specific organics. Autoflocculation occurs at pH extremes, where ionic strength is high and ionic interactions occur. Increased ionic strength increases autoflocculation efficiency by bridging

cells together by providing a positively charged intermediate for adsorption between the negative surface charges on the microalgal cell walls. Autoflocculation also occurs at PZC where there is neutral charge. Maximum hydrophobicity is observed near the PZC which is also responsible for increased efficiency in autoflocculation and therefore microalgal recovery by increasing sedimentation rates. The pH, conductivity, zeta potential and hydrophobicity were all found to have a large impact on sedimentation efficiencies with recovery efficiencies of up to 100% in 20 minutes via autoflocculation. *Scenedesmus sp*. was shown to have a faster unaided settling rate (0.187 ± 0.006 and 0.160 ± 0.004 $m.day^{-1}$ respectively) and efficiency (After 6 hours, 48 and 83% and after 10 hours, 78.9 and 91.4% of *Chlorella vulgaris* and *Scenedesmus sp*. had settled respectively) compared to *Chlorella vulgaris*; however *Chlorella vulgaris* exhibited greater flocculation abilities and efficiencies up to 100% at pH 1. Optimum autoflocculation (50 µm to 2 mm) for *Scenedesmus sp*. and *Chlorella vulgaris* was found at pH 14 and 13.5 resulting in 83 and 87% recovery efficiency respectively. Optimum chemical flocculation (50 µm to 3 mm) for *Scenedesmus sp*. and *Chlorella vulgaris* was found at pH 13 using 1 $g.L^{-1}$ $Al_2(SO_4)_3$ resulting in 47 and 100% recovery efficiency respectively.

Bacillus sp., *E. coli* BL2 (DE3), co-cultured bacteria *Nocardioides aromaticivorans* SB10005 and *Microbacterium chocolatum* RW56 successfully bioflocculated *Scenedesmus sp.* and *Chlorella vulgaris.* The co-cultured bacteria specifically showed the best bioflocculation results amongst the different bacteria used with *Nocardioides aromaticivorans* and *Microbacterium chocolatum* achieving 49 and 97% (pH 3.1 and 1) for *Scenedesmus sp.* bioflocculated and *Chlorella vulgaris* respectively. A minimum bacterial loading of 0.25 $g_{bacteria}/g_{algae}/L$ is required to achieve bioflocculation. *Scenedesmus sp.* bioflocculated with *Chlorella vulgaris* produced the most promising bioflocculation results with 81% cell recovery in 20 minutes at pH 2.55.

Bioflocculation is postulated to occur via patching of bacteria and microalgal cells at pH values where opposite surfaces charges are observed via van der Waals attractions. This patching between cells forms a large bridge network of algae-bacteria-algae. Autoflocculation near the PZC occurs via charge neutralisation and cell patching whilst autoflocculation at extreme alkaline conditions occurs via bridging adsorption of saturated cations between microalgal cells. The physico-chemical properties of microalgae, bacteria and the suspension media have direct effects on the flocculation activity and may be optimised to promote cell recoveries. Bacterial loading, flocculants and acid and base volumes required are directly proportional to algal concentration in the system and therefore the technique that requires the least amount of bioflocculant, autoflocculant or traditional flocculant would be the preferred method.

8.4 Dewatering system integration

Conductivity above 3 $S.cm^{-1}$ and extreme pH below 3 and above 12.5 was sufficient to induce flocculation and maximise settling velocities but found to inhibit growth, due to increased osmotic pressure on the cells, whilst extreme pH conditions also reduced cell metabolism performance as the microalgae spent more energy on acclimation. Recycled water after biomass flocculation would change pH and conductivity and may require effluent neutralisation processing, however this may be minimised by algal acclimatisation.

Scenedesmus sp. and *Chlorella vulgaris* showed ability to grow at extreme pH and conductivities and to re-adjust the suspension pH*. Scenedesmus sp.* and *Chlorella vulgaris* were able to grow between pH 3 and 13.

8.5 Significance of work

There is much need for efficient (low-cost and low-energy) algal dewatering techniques with concomitant water recovery and the work presented in this thesis shows some promise of developing a suitable technique. This work also investigates microalgal and bacterial surface and suspension properties which may be used in other unit operations beyond the scope of sedimentation. A greater understanding of the physical link between the physico-chemical properties and the affects and relationships with these on flocculation has been achieved. Algal suspension rheology has also been characterised which shows that pumping of concentrate is easily possible. These findings also all contribute to cell colloid science with respect to suspension effects on cells in general.

8.6 Recommendations

A “first principles” approach to understanding the effect of cell surface and suspension properties on algal separation needs to be undertaken over a range of different species to gain a better understanding of the primary parameters to be exploited. Microalgal flocculation followed by sedimentation is recommended as a viable, efficient biomass recovery technique. Recovery efficiency, biomass concentration and growth dependencies on pH, ionic strengths and other contaminations for desired products must be determined to design an optimal dewatering technique exploiting surface charge and hydrophobicity. Flocculation followed by filtration and flotation should also be investigated across a range of species to determine if these techniques efficiencies may be improved.

More intensive testing, such as atomic force microscopy and electron microscopy needs to be done to validate the postulated flocculation mechanisms and completely characterise the algal cell surface. A wider range of algal species needs to be investigated to determine whether the ideas and results presented in this thesis are largely generic across a wider species range. More bacteria should also be screened, including EPS producing bacteria to determine if improved flocculation may be obtained. In particular, an organic based polymer or bacterium with a neutral pH PZC should be tested, as this will allow for bioflocculation at pH neutral conditions (by way of opposing electrostatic charges) and hence eliminate the need for pH buffers and therefore downstream effluent processing for recycle.

The sensitivity effects of upstream processes on harvesting should be investigated, with focus on energy input required and recovery efficiencies achieved. Downstream drying and disruption techniques need further research taking preceding harvesting techniques into consideration. Biomass recovery, drying and cell disruption are closely linked processes and an optimal design of these operations is needed to make microalgal products economically feasible.

REFERENCES

Aas, E. 1996, "Refractive index of phytoplankton derived from its metabolite composition", *Journal of Plankton Research,* **18** (12):2223-2249.

Akkerman, I., Janssen, M., Rocha, J. & Wijffels, R.H. 2002, "Photobiological hydrogen production: photochemical efficiency and bioreactor design", *International Journal of Hydrogen Energy,* **27** (11):1195-1208.

Alfafara, C.G., Nakano, K., Nomura, N., Igarashi, T. & Matsumura, M. 2002, "Operating and scale-up factors for the electrolytic removal of algae from eutrophied lakewater", *Journal of Chemical Technology and Biotechnology,* **77** (8):871-876.

Anderson, R.A. 2005, *Algal culturing techniques,* First edn, Elsevier academic press: China.

Arad, S., McGowan, R.E., Friedlander, M. & Richmond, A.E. 1981, "Alkalinity -induced aggregation in *Chlorella vulgaris*. I. Changes in cell volume and cell-wall structure", *Plant Cell Physiology,* **21**:27-35.

Atkinson, B. & Mavituna, F. 1991, *Biochemical Engineering and Biotechnology Handbook,* Second edn, Macmillan Publishers: Basingstoke.

Ayoub, G.M. and Koopman, B. 1986, "Algal separation by the Lime-seawater process", *Water Pollution Control Federation,* **58**:924-931.

Azov, Y. 1982, "Effect of pH on inorganic carbon uptake by algal cultures", *Applied and Environmental Microbiology,* **43**:6.

Bache, D.H. and Rasool, E.R. 2001, "Characteristics of alumino-humic flocs in relation to DAF performance", *Water Science Technology,* **43** (8):203-208.

Bailey, J.E. & Ollis, D.F. 1986, "Product recovery operations" in *Biochemical Engineering Fundamentals*, eds. J.J. Carberry, J.R. Fair, M.S. Peters, W.R. Schowalter & J. Wei, Second edn, McGraw-Hill International, Singapore, pp. 726-796.

Bare, W.F.R., Jones, N.B. & Middlebrooks, E.J. 1975, "Algae removal using dissolved air flotation", *Water Pollution Control Federation,* **47** (1):153-169.

Barsanti, L. & Gualtieri, P. 2006, *Algae: Anatomy, Biochemistry, and Biotechnology,* First edn, Taylor & Francis Group: Boca Raton.

Becker, E.W. 1994, *Microalgae, Biotechnology and Microbiology,* First edn, Cambridge University Press: Cambridge.

Benemann, J., Koopman, B., Weissman, J., Eisenberg, D. & Gobell, R. 1980, in *Algal Biomass*, eds. G. Shelef & C.J. Soeder, Elsevier, Amsterdam, pp. 457-495.

Bernhardt, H. and Clasen, J. 1994, "Investigations into the flocculation mechanisms of small algal cells", *Journal of Water Supply: Research and Technology - AQUA,* **43** (5):222-232.

Bernhardt, H., Hoyer, O., Schell, H. & Lusse, B. 1985, "Reaction mechanisms involved in the influence of algogenic matter on flocculation", *Zeitschrift für Wasser- und Abwasser-Forschung,* **18** (1):18-30.

Bilanovic, D. and Shelef, G. 1988, "Flocculation of microalgae with cationic polymers - effects of medium salinity", *Biomass,* **17** (1):65-76.

Binova, J., Tichy, V., Livansky, K. & Zahradnik, J. 1998, "Bacterial contamination or microalgal biomass during outdoor production and downstream processing", *Algological Studies,* **89**:151-158.

Bitton, G., Fox, J.L. & Strickland, H.G. 1975, "Removal of algae from Florida lakes by magnetic filtration", *Applied Microbiology,* **30** (6):905-908.

Boone, D.R., Castenholz, R.W., De Vos, P., Garrity, G.M., Jones, D., Krieg, N.R., Ludwig, W., Rainey, F.A., Schleifer, K., Whitman, W.B., Brenner, D.J. & Staley, J.T. (eds) 2001, *Bergey's manual of systematic bacteriology*, second edn, Spinger-Verlag: New York.

Bratby, J. 2006, *Coagulation and Flocculation in Water and Wastewater Treatment,* Second edn, IWA Publishing: London.

Brennan, L. and Owende, P. 2010, "Biofuels from microalgae — A review of technologies for production, processing, and extractions of biofuels and co-products", *Renewable and Sustainable Energy Reviews,* **14** (2):557-577.

Bricaud, A., Bedhomme, A. & Morel, A. 1988, "Optical properties of diverse phytoplanktonic species: experimental results and theoretical interpretation", *Journal of Plankton Research,* **10** (5):851-873.

Buelna, G., Bhattarai, K.K., de la Noue, J. & Taiganides, E.P. 1990, "Evaluation of various flocculants for the recovery of algal biomass growth on pig-waste", *Biological Wastes,* **31**:211-222.

Castellanos, T., Ascencio, F. & Bashan, Y. 1997, "Cell-surface hydrophobicity and cell-surface charge of *Azospirillum spp.*", *FEMS Microbiology Ecology,* **24**:159-172.

Chen, C.Y. and Durbin, E.G. 1994, "Effects of pH on the growth and carbon uptake of marine phytoplankton", *Marine Ecology Progress Series,* **109**:83-94.

Chen, F., Chen, H. & Gong, X. 1997, "Mixotrophic and heterotrophic growth of *Haematococcus lacustris* and rheological behaviour of the cell suspensions", *Bioresource Technology,* **62** (1-2):19-24.

Chen, J., Yeh, H. & Tseng, I. 2009, "Effect of ozone and permanganate on algae coagulation removal - Pilot and bench scale tests", *Chemosphere,* **74** (6):840-846.

Chen, Y.M., Liu, J.C. & Ju, Y. 1998, "Flotation removal of algae from water", *Colloids and Surfaces B: Biointerfaces,* **12** (1):49-55.

Cheremisihoff & Nicholas, P. (eds) 1988, *Encyclopedia of Fluid Mechanics: Rheology and Non-Newtonian Flows*, 7th edn, Gulf Publishing Company: Houston, Texas.

Chisti, Y. 2007, "Biodiesel from microalgae", *Biotechnology Advances,* **25**:294-306.

Clesceri, L.S., Greenberg, A.E. & Eaton, A.D. 1998, *Standard methods for the examination of water and wastewater,* 20th edn, American Public Health Association: Washington DC.

Clixoo, O. 2010, *, Introduction to algae and basics*. Available: http://www.oilgae.com/algae/algae.html [2010, April] .

Conway, K. and Trainor, F.R. 1972, "*Scenedesmus* morphology and flotation", *Journal of Phycology,* **8**:138-143.

Coulson, J.M., Richardson, J.F. & Sinnott, R. 1983, "Volume 6 - Viscosity of fluids" in *Chemical Engineering*, First edn, Pergamon Press, Oxford.

Coulson, J. & Richardson, J. 2002, *Chemical Engineering Vol. 2: Particle Technology and Separation Processes,* Fifth edn, Butterworth Heinmann: Oxford.

Csordas, A. and Wang, J. 2004, "An integrated photobioreactor and foam fractionation unit for the growth and harvest of *Chaetoceros spp.* in open systems", *Aquacultural Engineering,* **30** (1):15-30.

Daffonchio, D., Thaveesri, J. & Verstraete, W. 1995, "Contact angle measurement and cell hydrophobicity of granular sludge from upflow anaerobic sludge bed reactors", *Applied and Environmental Microbiology,* **61**:3676-3680.

Danquah, M.K., Ang, L., Uduman, N., Moheimani, N. & Forde, G.M. 2009a, "Dewatering of microalgal culture for biodiesel production: exploring polymer flocculation and tangential flow filtration", *Journal of Chemical Technology and Biotechnology,* **84** (7):1078-1083.

Danquah, M.K., Gladman, B., Moheimani, N. & Forde, G.M. 2009b, "Microalgal growth characteristics and subsequent influence on dewatering efficiency", *Chemical Engineering Journal,* **151** (1-3):73-78.

de la Noue, J. and de Pauw, N. 1988, "The potential of microalgal biotechnology: a review of production and uses of microalgae", *Biotechnology Advances,* **6** (4):725-770.

Dengis, P.B., Ne´Lissen, L.R. & Rouxhet, P.G. 1995, "Mechanisms of yeast flocculation: Comparison of top and bottom-fermenting strains", *Applied and Environmental Microbiology,* **61**:718-728.

Divakaran, R. and Pillai, V.N.S. 2002, "Flocculation of algae using chitosan", *Journal of Applied Phycology,* **14** (5):419-422.

Drikas, M., Chow, C.W.K., House, J. & Burch, M.D. 2001, "Using coagulation, flocculation and settling to remove toxic cyanobacteria", *Journal of the American Water Works Association,* **93** (2):100-111.

Education committee of American Waterworks Association & U. S. Public health service 1968, *Theory and control of coagulation-flocculation,* National Center for Urban and Industrial Health: Cleveland.

Edzwald, J.K. 2010, "Dissolved air flotation and me", *Water Research,* **44**:1-30.

Edzwald, J.K. and Wingler, B.J. 1990, "Chemical and physical aspects of dissolved air-flotation for the removal of algae", *Journal of Water Supply: Research and Technology - AQUA,* **39**:24-35.

Ehimen, E.A., Sun, Z.F. & Carrington, C.G. 2010, "Variables affecting the in situ transesterification of microalgae lipids", *Fuel,* **89**:677-684.

Fattom, A. and Shilo, M. 1984, "Hydrophobicity as an adhesion mechanism of Benthic cyanobacteria", *Applied and Environmental Microbiology,* **47** (1):135-143.

Féris, L.A. and Rubio, J. 1999, "Dissolved air flotation (DAF) performance at low saturation pressures", *Filtration and Separation,* **36** (3-4):61-65.

Fisher, D., Francis, G. & Rickwood, D. 1998, "Practical Approach Series, Vol. 193" in *Cell separation; a practical approach* Oxford University Press, .

Fogg, G.E. & Thake, B. 1987, *Algal Cultures and Phytoplankton. Ecology,* Third edn, University of Wisconsin Press: Madison.

Folkman, Y. and Wachs, A.M. 1973, " Removal of algae from stabilization pond effluents by lime treatment", *Water Research,* **7**:419-435.

Golueke, C.G., Oswald, W.J. & Gotaas, H.B. 1957, "Anaerobic digestion of algae", *Applied Microbiology,* **5**:47-55.

Gordon, A.S. and Millero, F.J. 1984, "Electrolyte effects on attachment of an estuarine bacterium", *Applied and Environmental Microbiology,* **47**:495-499.

Griffin, R.A. and Jurinak, J.J. 1973, "Estimation of activity coefficients from electric conductivity of natural aquatic systems and soil extracts", *Soil Science,* **116**:26-30.

Griffiths, M.J., Dicks, R.G., Richardson, C. & Harrison, S.T.L. 2011a, "Advantages and challenges of microalgae as a source of oil for biofuel" in *Biodiesel - Feedstocks and Processing Technologies*, eds. M. Stoytcheva & G. Montero, First edn, Intech, Instituto de Ingenieria, UABC, Mexicali, Mexico.

Griffiths, M.J., Garcin, C., van Hille, R.P. & Harrison, S.T.L. 2011b, "Interference by pigment in the estimation of microalgal biomass concentration by optical density", *Journal of Microbiological Methods,* **85**:119-123.

Griffiths, M.J. and Harrison, S.T.L. 2009, "Lipid productivity as a key characteristic for choosing algal species for biodiesel production", *Journal of Applied Phycology,* **21**:493-507.

Griffiths, M.J., van Hille, R.P. & Harrison, S.T.L. 2011, "Lipid productivity, settling potential and fatty acid profile under nitrogen sufficient and deficient conditions of 11 microalgal species promising for biodiesel production", *Journal of Applied Phycology,* **In press**.

Grima, E.M., Belarbi, E., Fernandez, F.G.A., Medina, A.R. & Chisti, Y. 2003, "Recovery of microalgal biomass and metabolites: process options and economics", *Biotechnology Advances,* **20** (7-8):491-515.

Gudin, C. and Therpenier, C. 1986, "Bioconversion of solar energy into organic chemicals by microalgae", *Advanced Biotechnology Processes,* **6**:73-110.

Haesman, M., Diemar, J., O'Connor, W., Sushames, T. & Foulkes, L. 2000, "Development of extended shelf-life microalgae concentrate diets harvested by centrifugation for bivalve molluscs - a summary", *Aquaculture Research,* **31**:637-659.

Han, M.Y. and Kim, W. 2001, "A theoretical consideration of algae removal with clays", *Microchemical Journal,* **68** (2):157-161.

Harith, Z.T., Yusoff, F.M., Mohamed, M.S. & Din, M. Ariff, A. B. 2009, "Effect of different flocculants on the flocculation performance of microalgae, *Chaetoceros calcitrans*, cells", *African Journal of Biotechnology,* **8** (21):5971-5978.

Harun, R., Singh, M., Forde, G.M. & Danquah, M.K. 2010, "Bioprocess engineering of microalgae to produce a variety of consumer products", *Renewable and Sustainable Energy Reviews,* **14**:1037-1047.

Healey, F.P. 1975, *Physiological indicators of nutrient deficiency in algae,* Tech. Rep. 585 edn, Department of the Environment, Fisheries and Marine Service Research and Development Directorate: Winnipeg, Man.

Henderson, R.K., Parsons, S.A. & Jefferson, B. 2008a, "Surfactants as bubble surface modifiers in the flotation of algae: Dissolved air flotation that utilizes a chemically modified bubble surface", *Environmental Science and Technology,* **42**:4883-4888.

Henderson, R., Parsons, S.A. & Jefferson, B. 2008b, "The impact of algal properties and pre-oxidation on solid–liquid separation of algae", *Water Research,* **42**:1827-1845.

Heng, L., Yanling, Y., Weijia, G.X., L. & Guibai, L. 2008, "Effect of pretreatment by permanganate/chlorine on algae fouling control for ultrafiltration (UF) membrane system", *Desalination,* **222**:74-80.

Hermansson, I., Kjelleberg, S., Korhonen, T.K. & Stenstrom, T. 1982, "Hydrophobic and electrostatic characterization of surface structures of bacteria and its relationship to adhesion to an air-water interface", *Archives of Microbiology,* **131**:308-312.

Hiemenz, P.C. & Rajagopalan, R. 1997, *Principles of colloid and surface chemistry,* Third edn, Marcel Dekker, Inc.: New York.

Holt, P.K., Barton, G.W., Wark, M. & Mitchell, C.A. 2002, "A quantitative comparison between chemical dosing and electrocoagulation", *Colloids and Surfaces A: Physicochemical and Engineering Aspects,* **211**:233-248.

Hoyer, O., Lusse, B. & Bernhardt, H. 1985, "Isolation and characterisation of extracellular organic matter (EOM) from algae", *Zeitschrift für Wasser- und Abwasser-Forschung,* **18** (1):76-90.

Hung, M. and Liu, J. 2006, "Microfiltration for the separation of green algae from water", *Colloids and Surfaces B: Biointerfaces,* **51**:157-164.

Ives, K.J. (ed) 1978, *The Scientific Basis of Flocculation*, NATO Scientific Affairs Division: Cambridge.

Jameson, G.J. 1999, "Hydrophobicity and floc density in induced-air flotation for water treatment
", *Colloids and surfaces A: Physicochemical and engineering aspects,* **151**:269-281.

Jarvis, P., Buckingham, P., Holden, B. & Jefferson, B. 2009, "Low energy ballasted flotation", *Water Research,* **43**:3427-3434.

Jiang, J. and Graham, N.J.D. 1998, "Preliminary evaluation of the performance of new pre-polymerised inorganic coagulants for lowland surface water treatment", *Water Science Technology,* **37** (2):121-128.

Jiang, J., Graham, N.J.D. & Harward, C. 1993, "Comparison of polyferric sulphate with other coagulants for the removal of algae-derived organic matter", *Water Science Technology,* **27** (11):221-230.

Jodlowski, A. 2002, "Effect of pre-oxidation on flocculated algal cells autoflotation", *Environment Protection Engineering,* **28** (2):57-68.

Jun, H.B., Lee, Y.J., Lee, B.D. & Knappe, D.R.U. 2001, "Effectiveness of coagulants and coagulant aids for the removal of filter clogging Synedra", *Journal of Water Supply: Research and Technology - AQUA,* **50** (3):135-148.

Knuckey, R.M., Brown, M.R., Robert, R. & Frampton, D.M.F. 2006, "Production of microalgal concentrates by flocculation and their assessment as aquaculture feeds", *Aquacultural Engineering,* **35**:300-313.

Kubitschek, H.E. 1990, "Cell volume increase in *Escherichia coli* after shifts to richer media", *Journal of Bacteriology,* **172**:94-101.

Larsson, K. and Glantz, P.0. 1981, "Microbial adhesion to surfaces with different surface charges", *Acta Odontologica Scandinavica,* **39**:79-82.

Lee, A.K., Lewis, D.M. & Ashman, P.J. 2009a, "Microbial flocculation, a potentially low-cost harvesting technique for marine microalgae for the production of biodiesel", *Journal of Applied Phycology,* **21** (1):559-567.

Lee, J., Yoo, C., Jun, S., Ahn, C. & Oh, H. 2009b, "Comparison of several methods for effective lipid extraction from microalgae", *Bioresource Technology,* :1873-2976.

Lee, S.J., Kim, S., Kim, J., Kwon, G., Yoon, B. & Oh, H. 1998, "Effects of harvesting method and growth stage on the flocculation of the green alga *Botryococcus braunii*", *Letters in Applied Microbiology,* **27**:14-18.

Lee, S., Koopman, B. & Lincoln, E. 1992, "Effect of physiochemical variables on algal autoflocculation", *Water Science and Technology,* **26** (7-8):1769-1778.

Lembi, C.A. & Waaland, J.R. (eds) 1988, *Algae and Human Affairs*, First edn, Cambridge Univeristy Press: Cambridge.

Levin, G., Clendenning, J., Gibor, A. & Bogar, F. 1962, "Harvesting algae by froth flotation", *Applied Microbiology,* **10**:169-175.

Lian, B., Chen, Y., Zhao, J., Teng, H.H., Zhu, L. & Yuan, S. 2008a, "Microbial flocculation by *Bacillus mucilaginosus*: Applications and mechanisms", *Bioresource Technology,* **99**:4825-4831.

Lian, B., Chen, Y., Zhao, J., Teng, H., Zhu, L. & Yuan, S. 2008b, "Microbial flocculation by *Bacillus mucilaginosus*: Applications and mechanisms", *Bioresource Technology,* **99**:4825-4831.

Lin, C.S. and Huang, S.D. 1994, "Removal of Cu(II) from aqueous solution with high ionic strength by adsorbing colloid flotation", *Environmental Science and Technology,* **28**:474-478.

Liu, J.C., Chen, Y.M. & Ju, Y. 1999, "Separation of algal cells from water by column flotation", *Separation Science and Technology,* **34**:2259-2272.

Lyklema, J. 2000, *Fundamentals of Interface and Colloid Science,* First edn, Academic Press: London.

Ma, J. and Liu, W. 2002, "Effectiveness and mechanism of potassium ferrate (VI) preoxidation for algae removal by coagulation", *Water Research,* **36**:871-878.

Matis, K.A., Zouboulis, A.I., Grigoriadou, A.A., Lazaridis, N.K. & Ekateriniadou, L.V. 1996, "Metal biosorption - flotation. Application to cadmium removal", *Applied Microbiology and Biotechnology,* **45**:569-573.

Mayo, A.W. 1997, "Effects of temperature and pH on the kinetic growth of unialga *Chlorella vulgaris* cultures containing bacteria", *Water Environment Research,* **69**:64-72.

Mercado, J.M., Jimenez, C., Neill, F.X. & Figueroa, F.L. 1996, "Comparison of methods for measuring light absorption by algae and their application to the estimation of the package effect", *Scientia Marina,* **60**:39-45.

Mohn, F.H. 1980, "Experiences and strategies in the recovery of biomass from mass cultures of microalgae" in *Algae Biomass*, eds. G. Shelef & C.J. Soeder, Elsevier/North-Holland Biomedical press, Amsterdam, pp. 547-571.

Molina-Grima, E., Fernandez, F.G.A., Camacho, F.G. & Chisti, Y. 1999, "Photobioreactors: light regime, mass transfer, and scale up", *Journal of Biotechnology,* **70**:231-247.

Mollah, M.Y.A., Morkovsky, P., Gomes, J.A.G., Kesmez, M., Parga, J. & Cocke, D.L. 2004, "Fundamentals, present and future perspectives of electrocoagulation", *Journal of Hazardous Materials,* **114** (1-3):199-210.

Montiel, A. and Welte, B. 1998, "Preozonation coupled with flotation filtration: successful removal of algae", *Water Science Technology,* **37**:65-73.

Moraine, R., Shelef, G., Sandbank, E., Bar-Moshe, Z. & Shvartzburd, L. 1980, *Algae Biomass Production and Use,* First edn, Elsevier/North-Holland Biomedical: Amsterdam.

Mouchet, P. and Bonnelye, V. 1998, "Solving algae problems: French expertise and world-wide applications", *Journal of Water Supply: Research and Technology - AQUA,* **47** (3):125-141.

Mullin, J.W. 2001, *Crystallization,* Fourth edn, Reed Educational and Professional Publishing: Oxford.

Munoz, R. and Guieysse, B. 2006, "Algal-bacterial processes for the treatment of hazardous contaminants: a review", *Water Research,* **40** (15):2799-2815.

National Library of Medicine 2011, *, Basic Local Alignment Search Tool*. Available: http://www.ncbi.nlm.nih.gov/blast/Blast.cgi [2011, January] .

Nicholls, K.H. and Dillon, P.J. 1978, "An evaluation of phosphorus–chlorophyll–phytoplankton relationships for lakes", *International Review of Hydrobiology,* **63**:141-154.

Oh, H., Lee, S.J., Park, M., Kim, H., Kim, H., Yoon, J., Kwon, G. & Yoon, B. 2001, "Harvesting of *Chlorella vulgaris* using a bioflocculant from *Paenibacillus* sp. AM49", *Biotechnology Letters,* **23**:1229-1234.

Pedersen, L.H., Skouboe, P., Rossen, L. & Rasmussen, O.F. 1998, "Separation of *Listeria monocytogenes* and *Salmonella berta* from a complex food matrix by aqueous polymer two-phase partitioning", *Letters in Applied Microbiology,* **26**:47-50.

Peretti, S., Losordo, T. & Hobbs, A. 2007, *Algae to biodiesel conversion and scale-up*, North Carolina State University Department of Chemical Engineering, http://www.che.ncsu.edu/bullard//Senior_Design/Exemplary%20February%20Report.pdf.

Petrusevski, B., Bolier, G., van Breemen, A.N. & Alaerts, G.J. 1995, "Tangential flow filtration: A method to concentrate freshwater algae", *Water Research,* **29**:1419-1424.

Petrusevski, B., van Breemen, A.N. & Alaerts, G.J. 1996, "Effect of permanganate pre-treatment and coagulation with dual coagulants on algae removal in direct filtration", *Journal of Water Supply: Research and Technology - AQUA,* **45**:316-326.

Plummer, J.D. and Edzwald, J.K. 2002, "Effects of chlorine and ozone on algal cell properties and removal of algae by coagulation", *Journal of Water Supply: Research and Technology - AQUA,* **51**:307-318.

Pott, R. 2009, *Flotation, zeta potential and hydrophobicity of microalgae*: Cape Town.

Prasertsan, P., Wichienchot, S., Doelle, H. & Kennedy, J.F. 2008, "Optimization for biopolymer production by *Enterobacter cloacae* WD7", *Carbohydrate Polymers,* **71**:468-475.

Pushparaj, B., Pelosi, E., Torzillo, G. & Materassi, R. 1993, "Microbial biomass recovery using a synthetic cationic polymer", *Bioresource Technology,* **43**:59-62.

Rattanakawin, C. 2005, "Aggregate size distributions in sweep flocculation", *Songklanakarin Journal of Science and Technology,* **27** (5):1095-1101.

Renault, F., Sancey, B., Badot, P. & Crini, G. 2009, "Chitosan for coagulation/flocculation processes – An eco-friendly approach", *European Polymer Journal,* **45**:1337-1348.

Roh, S.H., Kwak, D.H., Jung, H.J., Hwang, K.J., Baek, I.H., Chun, Y.N., Kim, S.I. & Lee, J.W. 2008, "Simultaneous removal of algae and their secondary algal metabolites from water by hybrid system of DAF and PAC adsorption", *Separation Science and Technology,* **43**:113-131.

Rosenberg, M. 1984, "Bacterial adherence to hydrocarbons: a useful technique for studying cell surface hydrophobicity", *FEMS Microbiology Letters,* **22**:289-295.

Rossignol, N., Vandanjon, L., Jaouen, P. & Que´me´neur, F. 1999, "Membrane technology for the continuous separation microalgae: culture medium: compared performances of cross-flow microfiltration and ultrafiltration", *Aquacultural Engineering,* **20**:191-208.

Rutter, P.R. & Vincent, B. 1984, "Microbial adhesion and aggregation" in *Physicochemical interactions of the substratum, microorganisms, and the fluid phase*, ed. K.C. Marshall, Springer-Verlag AG., Berlin, pp. 21-38.

Salehizadeh, H. and Shojaosadati, S.A. 2001, "Extracellular biopolymeric flocculants. Recent trends and biotechnological importance", *Biotechnology Advances,* **19**:371-385.

Salim, S., Bosma, R. & Vermue, M.H. 2010, "Harvesting of microalgae by bio-flocculation", *Journal of Applied Phycology,* **Published Online**.

Satin, M. 2006, *, Microalgae* [Homepage of The Agro-industries and Post-harvest Management Service], [Online]. Available: http://www.fao.org/ag/ags/Agsi/MICROALG.htm [2010, April] .

Schenk, P.M., Thomas-Hall, S.R., Stephens, E., Marx, U.T., Mussgnug, J.H., Posten, C., Kruse, O. & Hankamer, B. 2008, "Second generation biofuels: High-efficiency microalgae for biodiesel production", *Bioenergy Research,* **1**:20-43.

Sheehan, J., Dunahay, T., Benemann, J. & Roessler, P. 1998, *A look back at the U.S. Department of Energy's aquatic species program — Biodiesel from algae*, National Renewable Energy Laboratory, Colorado.

Shelef, G., Sukenik, A. & Green, M. 1984, *Microalgae harvesting and processing: A literature review*, Solar Energy Research Institute, Colorado.

Sherman, P. 1970, "Industrial Rheology" in Academic Press, New York, pp. 141-151.

Shifrin, N.S. and Chisholm, S.W. 1981, "Phytoplankton lipids: Interspecific differences and effects of nitrate, silicate and light/dark cycles", *Journal of Phycology,* **17**:374-384.

Shipin, O., Meiring, P., Phaswana, R. & Kluever, H. 1999, "Integrating ponds and activated sludge process in the PETRO concept", *Water Research,* **33**:1767-1774.

Shuler, M.L. & Kargi, F. 2005, *Bioprocess Engineering: Basic Concepts,* Second edn, Pearson Education: Singapore.

Spolaore, P., Joannis-Cassan, C., Duran, E. & Isambert, A. 2006, "Commercial applications of microalgae: Review", *Journal of Bioscience and Bioengineering,* **101**:87-96.

Steynberg, M.C., Pieterse, A.J.H. & Geldenhuys, J.C. 1996, "Improved coagulation and filtration as a result of morphological and behavioural changes due to pre-oxidation", *Journal of Water Supply: Research and Technology - AQUA,* **45**:292-298.

Strand, S.P., Nordengen, T. & Østgaard, K. 2002, "Efficiency of chitosans applied for flocculation of different bacteria", *Water Research,* **36**:4745-4752.

Stumm, W. 1992, *Chemistry of the Solid-water Interface,* First edn, John Wiley and Sons, Inc.: New York.

Stutz-McDonald, S.E. and Williamson, K.J. 1979, "Settling Rates of Algae from Wastewater Lagoons", *Journal of the Environmental Engineering Division,* **105**:273-282.

Sukenik, A. and Shelef, G. 1984, "Algal autoflocculation - Verification and proposed mechanism", *Biotechnology and Bioengineering,* **26**:142-147.

Sukenik, A., Teltch, B., Wachs, A.W., Shelef, G., Nirl, G. & Levanon, D. 1987, "Effects of oxidants on microalgae flocculation", *Water Research,* **21**:533-539.

Svarovsky, L. (ed) 1985, *Solid-Liquid Separation*, Third edn, Butterworth and Company: Cambridge.

Tanford, C. 1921, *The Hydrophobic Effect: Formation of Micelles and Biological Membranes,* Second edn, John Wiley and Sons, Inc.: New York.

Teixeira, M.R. and Rosa, M.J. 2006, "Comparing dissolved air flotation and conventional sedimentation to remove cyanobacterial cells of *Microcystis aeruginosa*. Part I: The key operating conditions", *Separation and Purification Technology,* **52**:94.

Tenney, M.W., Echelberger, J., W. F., Schuessler, R.G. & Pavoni, J.L. 1969, "Algal flocculation with synthetic organic polyelectrolytes", *Applied Microbiology,* **18**:965-971.

Thapa, K.B., Qi, Y. & Hoadley, F.A. 2009, "Interaction of polyelectrolyte with digested sewage sludge and lignite in sludge dewatering", *Colloids and Surfaces A: Physiochemical and Engineering Aspects,* **334**:66-73.

Uduman, N., Qi, Y., Danquah, M.K., Forde, G.M. & Hoadley, A. 2010, "Dewatering of microalgal cultures: A major bottleneck to algae-based fuels", *Journal of Renewable and Sustainable Energy,* **2**:1-15.

Ueda, H., Otsuka, S. & Senoo, K. 2009, "Community composition of bacteria co-cultivated with microalgae in non-axenic algal cultures", *Microbial Culture Collection,* **25**:21-25.

van Loosdrecht, M., Lyklema, J., Norde, W., Schraa, G. & Zehnder, A. 1987, "Electrophoretic mobility and hydrophobicity as a measure to predict the initial steps of bacterial adhesion", *Applied and Environmental Microbiology,* **53**:1898-1901.

van Puffelen, J., Buijs, P.J., Nuhn, P. N. A. M. & Hijnen, W.A.M. 1995, "Dissolved air flotation in potable water treatment: the Dutch experience", *Water Science Technology,* **31**:149-157.

Vandamme, D., Foubert, I., Meesschaert, B. & Muylaert, K. 2010, "Flocculation of microalgae using cationic starch", *Journal of Applied Phycology,* **22**:525-530.

Vlaski, A., van Breemen, A.N. & Alaerts, G.J. 1997, "The role of particle size and density in dissolved air flotation and sedimentation", *Water Science Technology,* **36** (4):177-189.

Wedd, M.W. 2003, *, Determination of particle size distributions using laser diffraction*. Available: http://www.erpt.org/032Q/Wedd-00.htm [2011, July] .

Wills, B.A. 1985, *Mineral Processing Technology,* Third edn, Pergamon Press: Oxford.

Wu, Z. and Shi, X. 2008, "Rheological properties of *Chlorella pyrenoidosa* grown heterotrophically in a fermentor", *Journal of Applied Phycology,* **20**:279-282.

Yan, Y. and Jameson, G.J. 2004, "Application of the Jameson Cell technology for algae and phosphorous removal from maturation ponds", *International Journal of Mineral Processing,* **73**:23-28.

Zemke-White, W.L., Clements, K.D. & Harris, P.J. 2000, "Acid lysis of macroalgae by marine herbivorous fishes: effects of acid pH on cell wall porosity", *Journal of Experimental Marine Biology and Ecology,* **245**:57-68.

Zhang, X., Hu, Q., Sommerfeld, M., Puruhito, E. & Chen, Y. 2010, "Harvesting algal biomass for biofuels using untrafiltration membranes", *Bioresource Technology,* **101**:5297-5304.

Zita, A. and Hermansson, M. 1997, "Effects of bacterial cell surface structures and hydrophobicity on attachment to activated sludge flocs", *Applied and Environmental Microbiology,* **63**:1168-1170.

APPENDICES

A. 1. Literature findings

The following tables were extracted from current literature in the field of harvesting microalgae using an array of different techniques. These tables show the reader the large variances in results attained and the possible approaches and operating conditions that may be used for each technique. Their analysis has been used to support the understanding of the algal literature presented in Sections 2.4, 2.5.1, 2.5.2, 2.5.3 and 2.5.4 in the literature review.

Table 21: Summary table of flocculation efficiencies reported in the literature

Algae	Algae concentration	culture pH	Flocculant, dose (mg/l)	Initial mix time (rpm,s)	Settling time (min)	Flocculation efficiency [%], (CF)	Source
Chlorella vulgaris	62 mg/l	11	Paenibacillus sp. AM49, 1500; 0.5 mM $CaCl_2$	-,60	10	[91]	Oh et al. (2001)
Anabaena flos-aquae	-	11	Paenibacillus sp. AM49, 1500; 0.5 mM $CaCl_2$	-,60	10	[49]	Oh et al. (2001)
Microcystis aeruginosa	-	11	Paenibacillus sp. AM49, 1500; 0.5 mM $CaCl_2$	-,60	10	[38]	Oh et al. (2001)
Botryococcus braunii	-	11	Paenibacillus sp. AM49, 1500; 0.5 mM $CaCl_2$	-,60	10	[95]	Oh et al. (2001)
Scenedesmus quadricauda	-	11	Paenibacillus sp. AM49, 1500; 0.5 mM $CaCl_2$	-,60	10	[93]	Oh et al. (2001)
Selenastrum capricornutum	-	11	Paenibacillus sp. AM49, 1500; 0.5 mM $CaCl_2$	-,60	10	[91]	Oh et al. (2001)
Scenedesmus dimorphus	310 mg/l TSS	7 - 9	Autoflocculation	80, 60	15	[96]	Shelef and Sukenik (1984)
Chlorella, Monodus	480 mg/l	11	lime ($CaCO_3$), 460; 6 % seawater; $Ca(OH)_2$, 800	G=135 s^{-1}, 60	30	[99]	Ayoub and Koopman (1986)
Synechocystis minuscula	1 x 10^7 cells/ml	4	$Al_2(SO_4)_3.18H_2O$, 2	300, 10	15	[35]	Bernhardt and Clasen (1994)
Isochrysis galbana	1 x 10^6 cells/ml	7	Chitosan, Zetag 63, Zetag 92, 5-15	80, 120	30	[65-95]	Bilanovic et al. (1988)
Chlorella stimatophora	1 x 10^6 cells/ml	7	Zetag 92, 63, Chitosan, >20	80, 120	30	[<5]	Bilanovic et al. (1988)
Chlorella (fresh)	1 x 10^6 cells/ml	7	Zetag 92, 7	80, 120	30	[>90]	Bilanovic et al. (1988)
Chlorella (fresh)	1 x 10^6 cells/ml	7	Chitosan, 5	80, 120	30	[>90]	Bilanovic et al. (1988)
R. salina	1-2 x 10^6	7.5-8	NaOH (pH)	max, 5-10	5-10	[85-90]	Knuckey et al. (2006)
A. septentrionalis	1-1.5 x 10^6	7.5-8	$FeCl_3.6H_2O$, NaOH	max, 5-10	5-10	[85-95]	Knuckey et al. (2006)
C. calcitrans	1-2 x 10^7	7.5-8	NaOH (pH)	max, 5-10	5-10	[95-99]	Knuckey et al. (2006)
C. muelleri	2-3 x 10^6	7.5-8	NaOH (pH)	max, 5-10	5-10	[95-97]	Knuckey et al. (2006)
N. closterium	1-2x 10^6	7.5-8	NaOH (pH)	max, 5-10	5-10	[90-95]	Knuckey et al. (2006)
T. pseudonana	2-4 x 10^6	10.6	LT-25 & NaOH, 0.5	max, 5-10	5-10	[80-95]	Knuckey et al. (2006)
Skeletonema sp.	3-6 x 10^6	7.5-8	NaOH (pH)	max, 5-10	5-10	[95-98]	Knuckey et al. (2006)
N. oculata	1-2 x 10^7	7.5-8	NaOH (pH)	max, 5-10	5-10	[<30]	Knuckey et al. (2006)
T. suecuca	4-8 x 10^5	7.5-8	NaOH (pH)	max, 5-10	5-10	[85-95]	Knuckey et al. (2006)
Isochrysis sp.	3-4 x 10^6	7.5-8	$FeCl_3.6H_2O$, NaOH	max, 5-10	5-10	[<30]	Knuckey et al. (2006)
Pleurochrysis carterae	0.5 g/l	~8	Pseodomonas stutzeri and Bacillus cereus bacteria on 0.1 g/l substrate	-	30	[90], (226)	Lee et al. (2009)
Tertaselmis suecica	800-1000mg/l	8.2-9.4	Praestol, 1	gentle, 1	60	[70]	Pushparaj et al. (1993)
Spirulina platensis	800-1000mg/l	8.2-9.4	Praestol, 1	gentle, 1	60	[70]	Pushparaj et al. (1993)
Rhodopseudomonas	800-1000mg/l	6.8	Praestol, 1	gentle, 1	60	[86]	Pushparaj et al. (1993)
Chaetoceros meulleri	-	8.06	Chitosan, 150	1	-	[95]	Haesman et al. (2000)
Chaetoceros calcitrans	-	7.29	Chitosan, 80	1	-	[80]	Haesman et al. (2000)
Skeletonema costatum	-	8.66	Chitosan, 80	1	-	[70]	Haesman et al. (2000)
Thalassiosira pseudonana	-	8.29	Chitosan, 40	1	-	[90]	Haesman et al. (2000)
Tetreselmis chui	-	7.69	Chitosan, 40	1	-	[80]	Haesman et al. (2000)
Pavlova lutheri	-	7.28	Chitosan, 80	1	-	[80]	Haesman et al. (2000)
Tahitian isochrysis	-	7.43	Chitosan, 40	1	-	[90]	Haesman et al. (2000)

Table 22: Summary of algal concentration achieved by electrolytic coagulation or flocculation

Algal species	Anode	%TSS concentrate (CF), [removal efficiency]	Retention time (min)	Energy consumed (kWh/m^3)	Relative harvesting cost[a]	Source
Microcystis sp.	Aluminium	[100]	75	0.4	0.30	(Gao *et al.,* 2009)
Mixed	Aluminium	[96.3]	75	0.3	0.23	(Poelman *et al.,* 1997)
		[95.5]	35	1.98	1.55	(Poelman *et al,.* 1997)
Microcystis sp.	Aluminium	[100]	15	15	11.25	(Alfafara *et al.,* 2002)
	Carbon	[40-50]	15	15	25.00	(Alfafara *et al.,* 2002)
Mixed	Aluminium	[65]	10	5.2	6.00	(Azarian *et al.,* 2007)
		[100]	10	91.7	68.78	(Azarian *et al.,* 2007)

[a] Relative harvesting costs are calculated per concentrating factor achieved and relative to microstraining.

Table 23: Summary of the effect of pre-oxidation on the concentration or recovery of microalgae from suspension

Species	Cell concentration	Oxidant	Dose (mg/l)	Improvement	Source
Chlamydomonas sp.	50 µgl^{-1} as chlorophyll a	ClO_2	0.8	90% immobilisation	(Steynberg *et al.*, 1996)
		Cl_2	2	85%	
Scenedesmus	2 x 10^6 cells/ml	O_3	4.6	Coagulant demand halved	
		ClO_2	5	Coagulant demand quartered	(Sukenik *et al.*, 1987)
		Cl_2	2-20	Coagulant demand increased	
Scenedesmus quadricauda	20000 cells/ml	O_3	1.2	99%	(Plummer and Edzwald, 2002)
		Cl_2	1	10%	
Scenedesmus sp.	3.9 x 10^8 cells/ml	K_2FeO_4	5	10% enhanced removal with coagulant	(Ma and Liu, 2002)

Species	Cell concentration	Oxidant	Dose (mg/l)	Improvement	Source
Green algae mixture	70000 cells/ml	O_3	1	75 - 93%	(Montiel and Welte, 1998)
Cyclotella sp.	20000 cells/ml	O_3	0-3	no improvement	(Plummer and Edzwald, 2002)
		Cl_2	0-3	no improvement	
Euglena gracilis	50 μgl^{-1} as chlorophyll a	ClO_2	0.8	90% immobilisation	(Steynberg *et al.*, 1996)
		Cl_2	2	95%	
Chodatella sp.	4 x 10^7 cells/ml	O_3	1, 3	7%, 9%,	
		O_3	7	41% worsened removal	(Chen *et al.*, 2009)
		$KMnO_4$	0.5, 1, 1.25, 1.75	1%, 4%, 14%, 4%	
Mixed	690-1230 x 10^4 cells/l	Cl_2, MnO_2	1 and 0.5	30% increased COD removal	(Heng *et al.*, 2008)
Mixed	3 x 10^4 cells/ml	O_3	1	18% improvement	(Montiel and Welte, 1998)

Table 24: Comparison of different concentrating efficiencies with different filtration membranes and algae species

Filter type	Algal species	%TSS concentrate (CF), [removal efficiency]	Source
Pellicon filter with manifold plates	*Tetraselmis suecica*	8.88 (151)	Danquah *et al.* (2009b)
Millipore 0.45 µm	Mixed species	(5-40) [70-89]	Petrusevski *et al.* (1995)
Polyacrylamide (40kDa)	*Arthrospira platensis*	(10)	Rossi *et al.* (2004)
PVC UF (50kDa)	*Scenedesmus quadricauda*	(154)	Zhang *et al.* (2010)
-	*Thalassiosira pseudonana*	(1230)	Walsh *et al.* (1986)

Table 25: Comparison of different techniques of filtration for concentration or recovery of microalgae from suspension

Machine/type	Algal species	%TSS concentrate (CF), [removal efficiency]	Energy consumed (kWh/m^3)	Relative harvesting cost[a]	Source
Microstraining	*C. proboscideum*	1.5 (15)	0.2	1.00	Mohn (1980)
Vibrating screen	*C. proboscideum*	6 (60)	0.4	0.50	Mohn (1980)
		1-6 (15-60)	0.4	0.80	Ayoub and Semerjian (2003)
Netzch chamber filter	*Coelastrum proboscideum*	5-27 (50-245)	0.88	0.45	Ayoub and Semerjian (2003)
Bellmer belt press	*Coelastrum proboscideum*	18 (180)	0.5	0.21	Mohn (1980)
Seitz suction filter	*Coelastrum proboscideum*	16 (160)	-	-	Mohn (1980)
Engelsmann cylindrical sieve rotators	*Coelastrum proboscideum*	7.5 (75)	0.3	0.30	Mohn (1980)
Seitz Dinglinger Filter basket	*Coelastrum proboscideum*	5 (50)	0.2	0.30	Mohn (1980)
Dorr Olliver non-precoat vacuum drum filter	*Coelastrum proboscideum*	18 (180)	5.9	2.46	Mohn (1980)
Nivoba potato starch precoat vacuum drum filter	*C. proboscideum, Scenedesmus*	37 (2-18.5)	-	-	Mohn (1980)
Walther suction filter	*Coelastrum proboscideum*	8 (80)	0.1	0.09	Mohn (1980)
Dinglinger belt filter	*Coelastrum proboscideum*	9.5 (95)	0.45	0.36	Mohn (1980)
Shenck filter thickener	*C. proboscideum, Scenedesmus*	5-7 (50-70)	1.6	2.00	Mohn (1980)

Machine/type	Algal species	%TSS concentrate (CF), [removal efficiency]	Energy consumed (kWh/m^3)	Relative harvesting cost[a]	Source
Frantz ferrofilter (stainless steel wool)	*Microcystis*	[59.6]	-	-	Bitton *et al.* (1975)
	Anabaena, Aphanizomenon	[94]	-	-	Bitton *et al.* (1975)
0.22 µm Pellicon	*Tetraselmis suecica*	8.88 (151)	2.15	1.07	Danquah *et al.* (2009b)
Millipore 0.45 µm	Mixed species	(5-40) [70-89]	2.06	6.87	Petrusevski *et al.* (1995)
Polyacrylamide (40kDa)	*Spirulina*	(10)	-	-	Rossi *et al.* (2004)
PVC UF (50kDa)	*Scenedesmus quadricauda*	(154)			Zhang *et al.* (2010)
	Thalassiosira pseudonana	(1230)	-	-	Walsh *et al.* (1986)

[a] Relative harvesting costs are calculated per concentrating factor achieved and relative to microstraining

Table 26: Comparison of sedimentation techniques for concentration or recovery of microalgae from suspension

Algal species	Machine/type	%TSS concentrate (CF), [removal efficiency]	Energy consumed (kWh/m^3)	Relative harvesting cost[a]	Source
Scenedesmus, Coelastrum	Lamella separator	1.6 (16)	0.1	0.47	Mohn (1980)
Scenedesmus, Coelastrum	Sedimentation tank	1.5 (15)	0.1	0.50	Mohn (1980)
Monodus subterraneus	Ultrasound chamber	(20.8) [54.4]	300	1082	Bosma *et al.* (2003)

[a] Relative harvesting costs are calculated per concentrating factor achieved and relative to microstraining

Table 27: Comparison of sedimentation techniques for concentration or recovery of microalgae from suspension continued

Algae	Algae concentration (cells/ml)	Flocculant, dose (mg/l)	Flocculation (rpm; min)	Cell removal (%)	Source
Microcystis aeruginosa	1.5×10^6	$Al_2(SO_4)_3$, 10.3	25,14	75	(Drikas *et al.*, 2001)
Microcystis aeruginosa	1×10^4	Fe, 10; superfloc C-573, 1	$G=30s^{-1}$, >30	98.9	(Vlaski *et al.*, 1997)
Microcystis aeruginosa	5.8×10^4	$Fe_2(SO_4)_3$, 5	35,20	62	(Jiang and Graham, 1998)
Microcystis aeruginosa	5.8×10^4	PFS, 5	35,20	81.6	(Jiang and Graham, 1998)
Microcystis aeruginosa	1×10^5	Al_2O_3, 2-20	$24s^{-1}$, 15	69-94	(Teixeira and Rosa, 2006)
Anabaena flosaquae	2×10^5	$Fe_2(SO_4)_3$, 11.2	35,25	74	(Jiang *et al.*, 1993)
Anabaena flosaquae	2×10^5	$Al_2(SO_4)_3$, 5.4	35,25	78	(Jiang *et al.*, 1993)
Anabaena flosaquae	2×10^5	PFS, 11.2	35,25	94	(Jiang *et al.*, 1993)
Anabaena flosaquae	2×10^5	PAC, 5.4	35,25	68	(Jiang *et al.*, 1993)
Asterionella formosa	2×10^5	$Fe_2(SO_4)_3$, 11.2	35,25	63	(Jiang *et al.*, 1993)
Asterionella formosa	2×10^5	$Al_2(SO_4)_3$, 5.4	35,25	79	(Jiang *et al.*, 1993)
Asterionella formosa	2×10^5	PAC, 5.4	35,25	68	(Jiang *et al.*, 1993)
Asterionella formosa	2×10^5	PFS, 11.2	35,25	87	(Jiang *et al.*, 1993)
Synedra acus/melosira	1500	$Al_2(SO_4)_3$, 1.62	45,10	88	(Jun *et al.*, 2001)
Synedra acus	1040	PAC, 2.16	45,10	76	(Jun *et al.*, 2001)
Synedra acus	760	PAHCS, 2.16	45,10	54	(Jun *et al.*, 2001)
Synedra acus	1040	$FeCl_3$, 14	45,10	74	(Jun *et al.*, 2001)
Synedra acus	1480	$Al_2(SO_4)_3$, 2.16; C-599A polymer, 0.25	45,10	99	(Jun *et al.*, 2001)
Chlorella sp.	6.8×10^5	$Al_2(SO_4)_3$, 8	25,20	80	(Liu *et al.*, 1999)
Chlorella sp.	6.8×10^5	PAC, 8	25,20	85	(Liu *et al.*, 1999)
Mixture	55 NTU	Chitosan, 5	60,30	90	(Divakaran and Pillai, 2002)
Mixture	3×10^4	Al, 9.5	-	70-80	(Mouchet and Bonnelye, 1998)

Table 28: Comparison of different techniques of centrifugation for concentration or recovery of microalgae from suspension

Machine/type	Algal species	%TSS concentrate (CF), [removal efficiency]	Energy consumed (kWh/m^3)	Relative harvesting cost[a]	Source
Self cleaning plate separator	*Scenedesmus, Coelastrum*	12, (120)	1	0.63	Mohn (1980)
Nozzle centrifuge	*Scenedesmus, Coelastrum*	2-15 (20-150)	0.9	0.79	Mohn (1980)
Screw centrifuge	*Scenedesmus, Coelastrum*	22 (11)	8	54.55	Mohn (1980)
Hydrocyclone	*Coelastrum*	0.4 (4)	0.3	5.63	Mohn (1980)
Supercentrifuge	9 different strains	[94-100]	-	-	Haesman *et al.* (2000)
Cream separator	9 different strains	[46-96]	-	-	Haesman *et al.* (2000)
Bucket Centrifuge	9 different strains	[5-66]	-	-	Haesman *et al.* (2000)
Zonal rotor	*Dunaliella, Pyramimonas, Thalassiosira, Synechoccus*	[99, 99, 99, 78]	-	-	Price *et al.* (1974)

[a] Relative harvesting costs are calculated per concentrating factor achieved and relative to microstraining

Table 29: Summary of flotation literature for concentration or recovery of microalgae from suspension

Machine/type	Algal species	%TSS concentrate (CF), [removal efficiency]	Energy consumed (kWh/m^3)	Relative harvesting cost[a]	Source
Ballasted	*Microcystis*	[97]	-	-	Jarvis *et al.* (2009)
Ballasted	*Chlorella*	[86]	-	-	Jarvis *et al.* (2009)
Standard DAF	*Melosira*	[76]	10-20[b]	14.80	Jarvis *et al.* (2009)
Electro	Mixed	[96]	0.3	0.23	Poelman *et al.* (1997)

[b] Feris *et al.* (2000) [a]Relative harvesting costs are calculated per concentrating factor achieved and relative to microstraining

Table 30: Summary of flotation results using flocculants for concentration or recovery of microalgae from suspension

Algae	Concentration (cells/ml)	Floc, dose (mg/l)	Flotation/R/bubble conc. (min, %, ppm)	Removal efficiency (%)	Source
Chlorella vulgaris	1.3 x 10^5	PAC, 0.5	10, 8, 4600	97-99	Edzwald and Wingler (1990)
Chlorella vulgaris	1.3 x 10^5	$Al_2(SO_4)_3$, 1.6	10, 8, 4600	96.8	Edzwald and Wingler (1990)
Cyclotella sp.	5.3 x 10^4	PAC, 1	10, 8, 4600	97-99	Edzwald and Wingler (1990)
Cyclotella sp.	5.3 x 104	$Al_2(SO_4)_3$, 1.6	10, 8, 4600	99.8	Edzwald and Wingler (1990)
Mixture	1.5 x 10^5	PAC, 1.3	9.5, 6, -	80	Kempeneers *et al.* (2001)
Synedra	1.2 x 10^6	PAC, 1.3	9.5, 6, -	76	Kempeneers *et al.* (2001)
Asterionella	4 x 10^4	PAC, 1.3	9.5, 6, -	58	Kempeneers *et al.* (2001)
Chlamydomonas	3.4 x 10^4	PAC, 1.3	9.5, 6, -	66	Kempeneers *et al.* (2001)
Scenedesmus	2.6 x 10^4	PAC, 1.3	9.5, 6, -	71	Kempeneers *et al.* (2001)
Scenedesmus quadricauda	7.4 x 10^4	CTAB, 40	20, -, 114ml/min	90	Chen *et al.* (1998)
Scenedesmus quadricauda	7.4 x 10^4	SDS, 20; Chitosan, 10	20, -, 114ml/min	95	Chen *et al.* (1998)
Chlorella sp.	6.8 x 10^5	SDS, 20; Chitosan, 10	20, -, 114ml/min	90	Liu *et al.* (1999)
Chlorella sp.	6.8 x 10^5	CTAB, 40	20, -, 114ml/min	86	Liu *et al.* (1999)

A. 2. Experimental

Bacteria and microalgae cell counts were done using an Olympus BX40 microscope with a built in Colourview digital camera and Hawksley Thoma counting chamber shown hereafter in Figure 65.

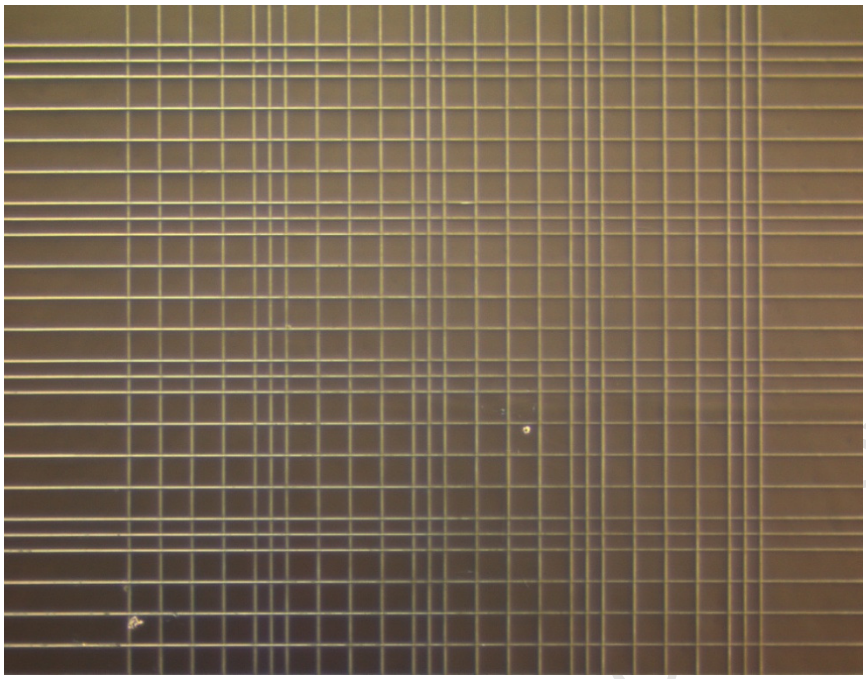

Figure 65: Counting grid of Hawksley Thoma counting chamber with area of one large square = 0.04 mm^2, area of one smallest square = 0.0025 mm^2, depth = 0.02 mm

8.6.1 Bacteria isolation and identification

The co-cultured bacteria within the *Scenedesmus sp*. and *Chlorella vulgaris* airlift photobioreactors were analysed and sequenced (Section 4.1.2) and the samples were identified as follows:

Sample 1: *Nocardioides aromaticivorans* SB10005 16S ribosomal RNA gene, partial sequence.

CCGCCATGGCGGCCGCGGGAATTCGATTTTGTGCGGGCCCCCGTCAATTCCTTTGAG
TTTTAGCCTTGCGGCCGTACTCCCCAGGCGGGGCGCTTAATGCGTTAGCTACGGCAC
GGAGTCCGTGGAAAGGACCCCACACCTAGCGCCCAACGTTTACGGTGTGGTCTACCA
GGGTATCTAATCCTGTTCGCTCACCACACTTTCGCTCCTCAGCGTCAGGTAATGCCCA
GAGAACCGCCTTCGCCACCGGTGTTCCTCCTGATATCTGCGCATTTCACCGCTACACC
AGGAATTCCATTCTCCCCTGCATACCTCTAGTCTGCCCGTATCGAAAGCAAGCAACGA
GTTAAGCCCGCTGTTTTCACTCCCGACGCGACAAACCGCCTACGAGCCCTTTACGCCC
AATAATTCCGGACAACGCTCGGACCCTACGTATTACCGCGGCTGCTGGCACGTAGTTG
GCCGGTCCTTCTTCTGTACCTACCGTCACTTTCGCTTCGTCGGTACTGAAAGAGGTTTA
CAACCCGAAGGCCGTCGTCCCTCACGCGGCGTTGCTGGATCAGGCTTCCGCCCATTG
TCCAATATTCCCCACTGCTGCCTCCCGTAGGAGTCAATCACTAGTGAATTCGCGGCCG
CCTGCAGGTCGACCATATGGGAGAGCTCC

Sample 2: *Microbacterium chocolatum* RW56 16S ribosomal RNA gene, partial sequence.

GCTCCCGGCCGCCATGGCGGCCGCGGGAATTCGATTTTGTGCGGGCCCCCGTCAATT
CCTTTGAGTTTTAGCCTTGCGGCCGTACTCCCCAGGCGGGGAACTTAATGCGTTAGCT
GCGTCACGGAATCCGTGGAATGGACCCCACAACTAGTTCCCAACGTTTACGGGGTGG
ACTACCAGGGTATCTAAGCCTGTTTGCTCCCCACCCTTTCGCTCCTCAGCGTCAGTTAC
GGCCCAGAGATCTGCCTTCGCCATCGGTGTTCCTCCTGATATCTGCGCATTCCACCGC
TACACCAGGAATTCCAATCTCCCCTACCGCACCCTAGTCTGCCCGTACCCACTGCAGG
CCCGAGGTTGAGCCTCGGGTTTTCACAGCAGACGCGACAAACCGCCTACGAGCTCTTT
ACGCCCAATAATTCCAGATAATGCTTGCGCCCTACGTATTACCGCGGCTGCTGGCACG
TAGTTAGCCGGCGCTTTTTCTGCAGGTGCCGTCACTTTCGCTTCTTCCCTGCTAAAAGA
GGTTTACAACCCGAAGGCCGTCATCCCTCACGCGGCGTTGCTGCATCAGGCTTCCGC
CCATTGTGCGATATTCCCCACTGCTGCCTCCCGTAGGAGTCAATCACTAGTGAATTCG
CGGCCGCCTGCAGGTCGACCATATGGGAGAGCTC

Sample 3: *Stenotrophomonas maltophilia*

CWATGCATCCAACGCGTTGGGAGCTCTCCCATATGGTCGACCTGCAGGCGGCCGCGA
ATTCACTAGTGATTCCGGATCCGTCGACAGAGTTTGATCGTGGCTCAGTTCCAGTGTG
GCTGATCATCCTCTCAGACCAGCTACGGATCGTCGCCTTGGTGGGCCTTTACCCCGCC
AACTAGCTAATCCGACATCGGCTCATTCAATCGCGCAAGGTCCGAAGATCCCCTGCTT
TCACCCGTAGGTCGTATGCGGTATTAGCGTAAGTTACCCTACGTTATCCCCCACGACA
GAGTAGATTCCGATGTATTCCTCACCCGTCCGCCACTCGCCACCCAAGGAGCAAGCTC
CTCTGTGCTGCCGTTCGACTTGCATGTGTTAGGCCTACCGCCAGCGTTCACTCTGAGC
CACGATCAAACTCTGTCGACGACCGAATCGAATTCCCGCGGCCGCCATGGCGGCCGN
GAGCANG

Sample 4: *Acenitobacter*

NNCAAGCTATGCATCCANCGCGTTGGGAGCTCTCCCATATGGTCGACCTGCAGGCGG
CCGCGAATTCACTAGTGATTCCGGACCGTCGACAGAGTTTGATCGTGGCTCAGTCCCA
GTGTGGCGGATCATCCTCTCAGACCCGCTACAGATCGTCGCCTTGGTAGGCCTTTACC
CCACCAACTAGCTAATCCGACTTAGGCTCATCTATTAACGCAAGGTCACAAGTGATCCC
CTGCTTTCCCCCGTAGGGCGTATGCGGTATTAGCATCCCTTTCGAGATGTTGTCCCCC
ATTAATAGGCAGATTCCTAAGTATTACTCACCCGTCCGCCGCTAGGTCAGTTACCGAAG
CAACCTCCCCCGCTCGACTTGCATGTGTTAAGCCTGCCGCCAGCGTTCAATCTGAGCC
AGATCAAACTCTGTCGACGGATCCGGAATCGAATTCCCGCGGCCGCCATGGCGGCCN
GGA

Sample 5: *Azospirillum*

NCAAGCTATGCATCCANCGCGTTGGGAGCTCTCCCATATGGTCGACCTGCAGGCGGC
CGCGAATTCACTAGTGATTCCGACCGTCGACAGAGTTTGATCGTGGCTCAGAACGAAC
GCCGGCGGCATGCCTAACACATGCAAGTCGAACGAAGGCTTCGGCCTTAGTGACGCA
CGGGTGAGTAACACGTGGGAACCTGCCTTATGGTTCGGAATAACGTCTGGTAACGGAC
GCTAACACCGGATGTGCCCTTCGGGGGAAAGTTTACGCCATGAGAGGGGCCCGCGTC
GGAGTAGGTAGATGGTGTGGTAACGGCGCACCAAGCCGACGATCCGTAGCTGGTCTG
AGAGGATGATCAGCCACACTGGGACTGAGCCACGATCAAACTCTGTCGACGGATCCG
GAATCGAATTCCCGCGGCCGCCATGGCGGCCGGNAGCATGCGA

Sample 6: *Chryseobacterium*

CCMACGCGTTGGGAGCTCTCCCATATGGTCGACCTGCAGGCGGCCGCGAATTCACTA
GTGATTCCGGATCCGTCGACAGAGTTTGATCGTGGCTCAGTACCAGTGTGGGGGATCA
CCCTCTCAGGCCCCCTAAAGATCATCGACTTGGTGAGCCGTTACCTCACCAACTATCT
AATCTTGCGCGTGCCCATCTTTATCCACCTCAGTTTTCAATATAAAGTGATGCCACTCTA
TATATTATGGGGTATTAATCTTCCTTTCGAAAGGCTATCCCCCCGATAAAGGCAGGTTG
CACACGTGTTCCGCACCCGTACGCCGCTCTCAAGTCTCCGAAGAAACTCTACCGCTCA
GCTTGCATGTGTTAGGCCTCCCGCTAGCGTTCATCCTGAGCCACGATCAAACTCTGTC
GGGATCCGGAATCGAATTCCCGCGGCCGCCATGGCGGCCGGNAGCATG

Sample 7: *Rhizobium gallicum*

CGTTGGGAGCTCTCCCATATGGTCGACCTGCAGGCGGCCGCGAATTCACTAGTGATTC
GGATCCGCGACAGAGTTTGATCGTGGCTCAGAACGAACGCTGGCGGCAGGCTTAACA
CATGCAAGTCGAACGCCCCGCAAGGGGAGTGGCAGACGGGTGAGTACGCGTGGGAA
CGTACCCTTTACTACGGAATAACTCAGGGAAACTTGTGCTAATACCGTATGTGCCCTTC
GGGGGAAAGATTTATCGGTAAAGGATCGGCCCGCGTTGGATTAGCTAGTTGGTGGGG
TAAAGGCCTACCAAGGCGACGATCCATAGCTGGTCTGAGAGGGTGATCAGCCACATTG
GGACTGACCCACGATCAAACTCTGTCGACGGATCCGGAATCGAATTCCCGCGGCCGC
CATGGCGGCCGGNAGCATGCGA

8.6.2 Growth characteristics

To allow for ease of concentration determination, the following assays were constructed to relate optical, cell number and dry biomass concentrations at different conditions.

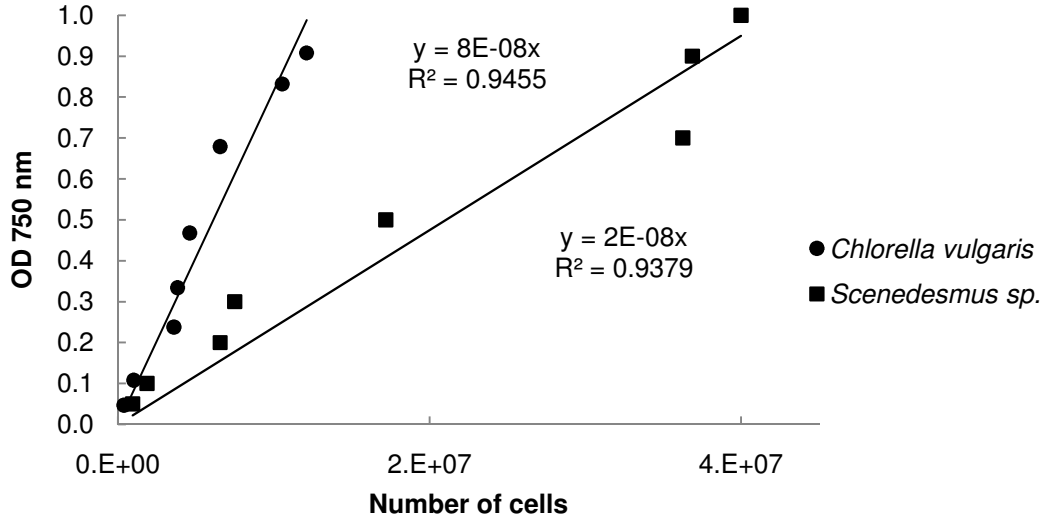

Figure 66: Optical density and cell number assays for *Chlorella vulgaris* and *Scenedesmus sp.*

Growth assays for *Chlorella vulgaris* on 2 L.min^{-1} air:

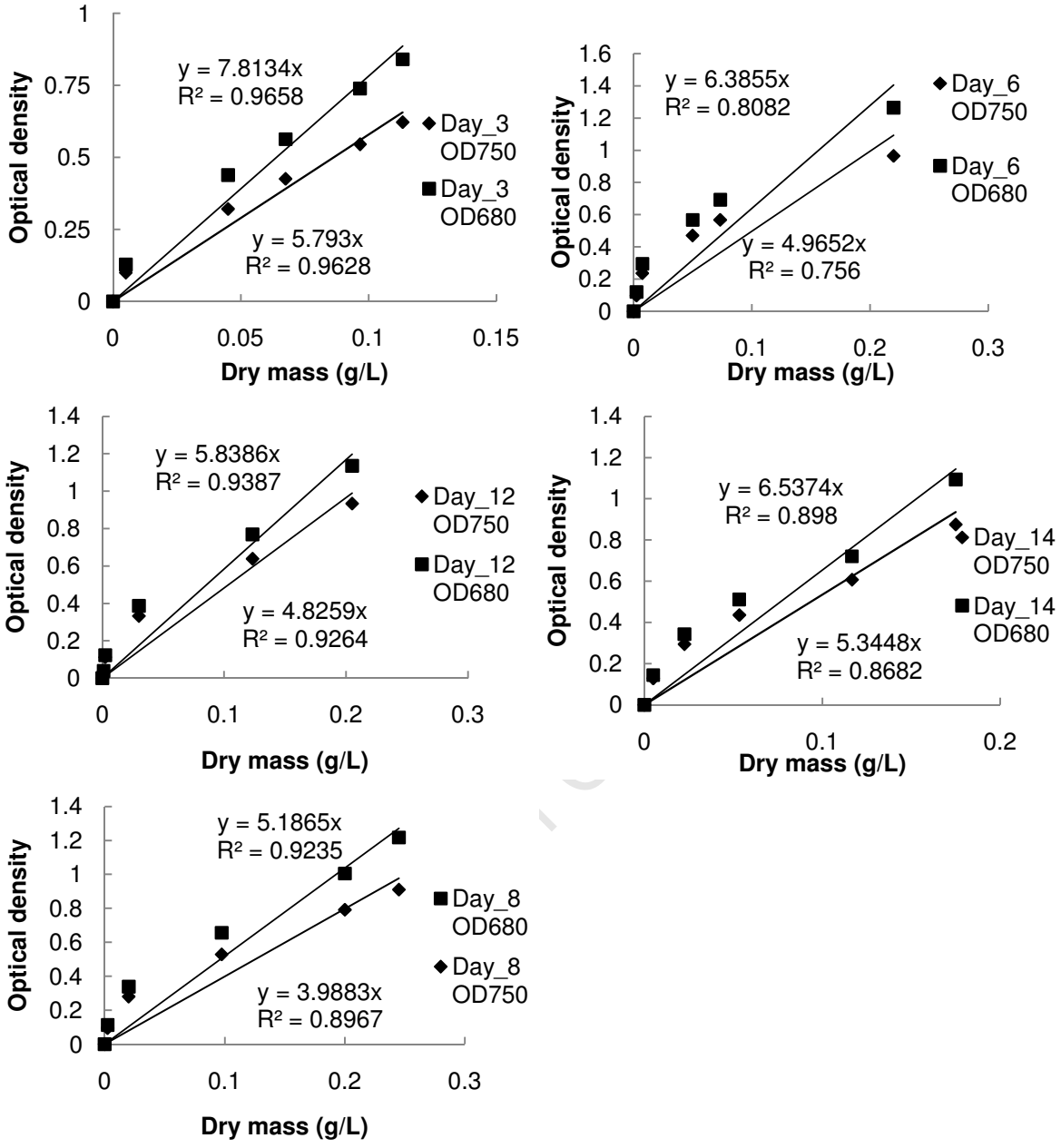

Figure 67: Day 3, 6, 8, 12 and 14 growth phase assays for *Chlorella vulgaris* grown on 2 L.min^{-1} air in an airlift photobioreactor

Growth assays for *Chlorella vulgaris* on 2 L.min^{-1} 2900 ppm CO_2:

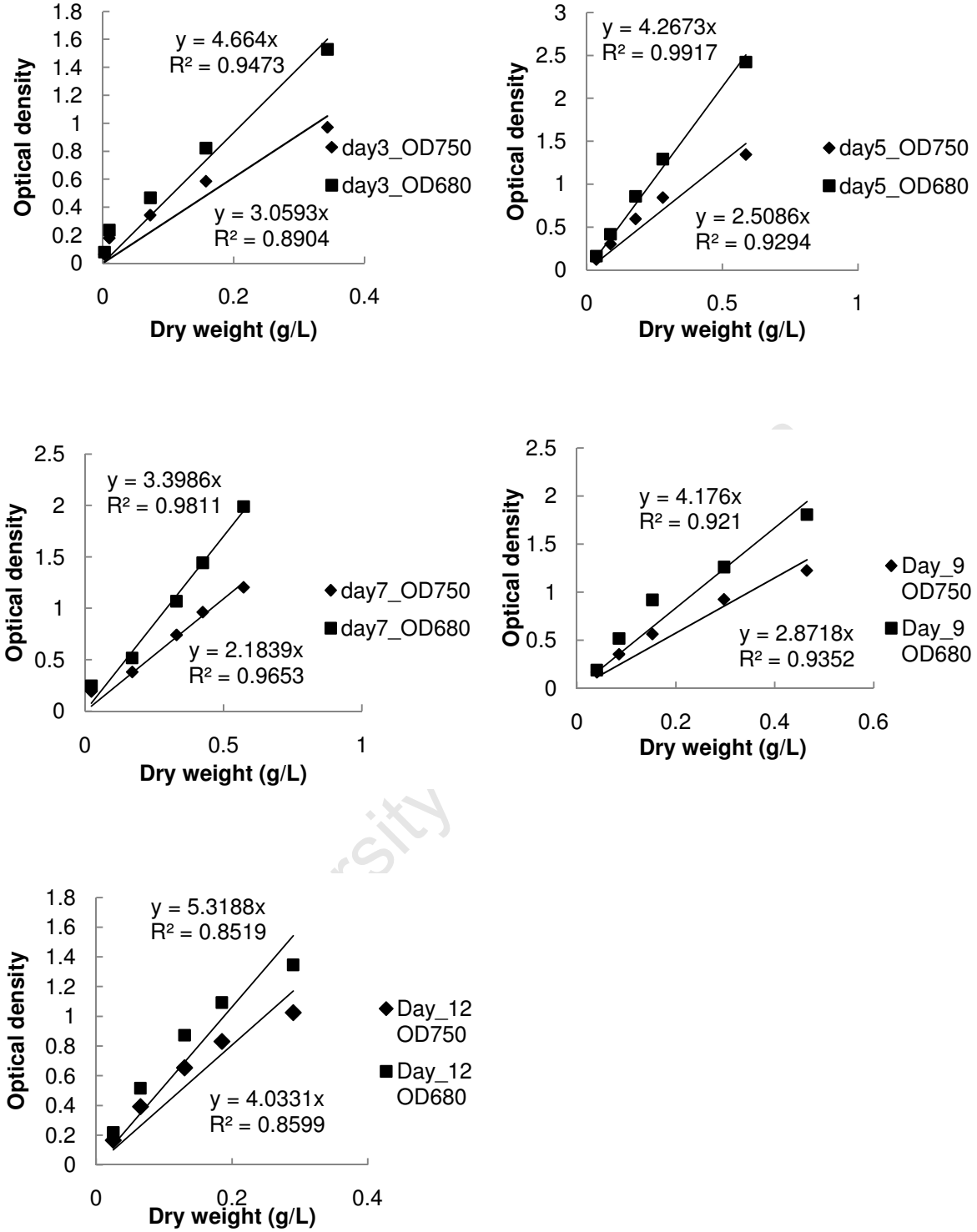

Figure 68: Day 3, 5, 7, 9 and 12 growth phase assays for *Chlorella vulgaris* grown on 2 L.min^{-1} 2900 ppm CO_2 in an airlift photobioreactor

Growth assays for *Scenedesmus sp.* on 2 L.min^{-1} air:

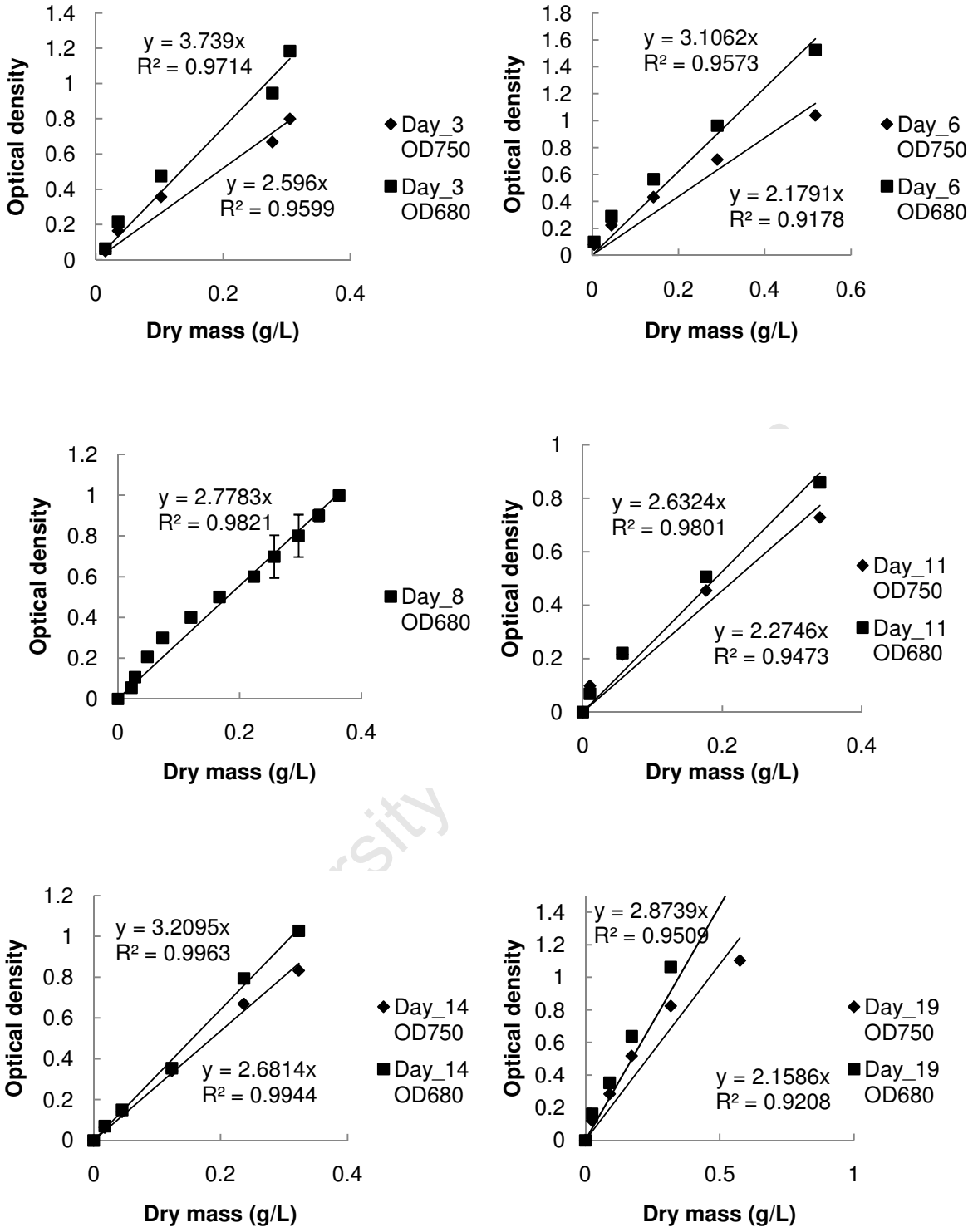

Figure 69: Day 3, 6, 8, 11, 14 and 19 growth phase assay for *Scenedesmus sp.* grown on 2 L.min^{-1} air

Growth assays for *Scenedesmus sp.* on 2 L.min^{-1} 2900 ppm CO_2:

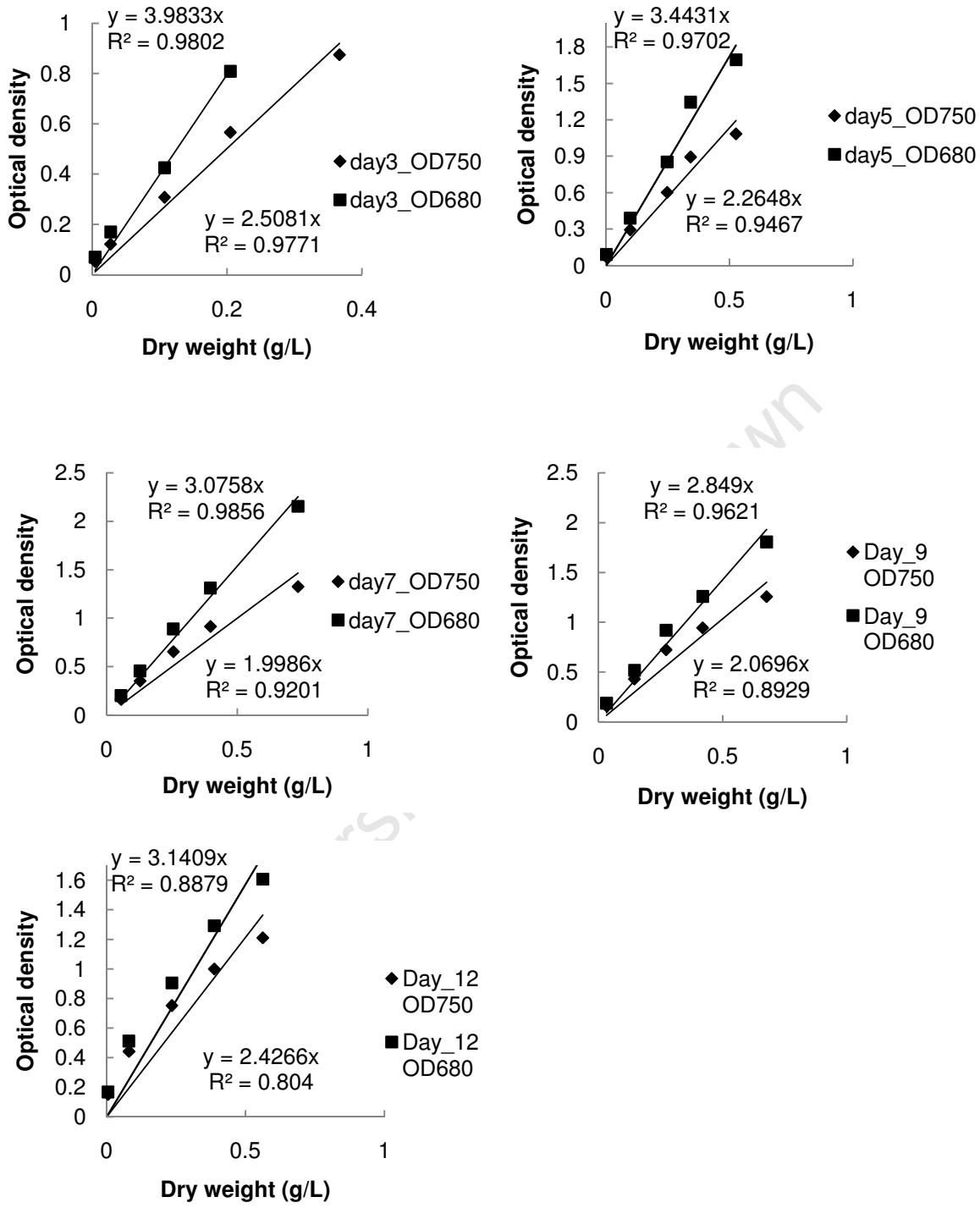

Figure 70: Day 3, 5, 7, 9, and 12 growth phase assay for *Scenedesmus sp.* grown on 2 L.min^{-1} 2900 ppm CO_2

Bacterial bioassays for *Microbacterium chocolatum* RW56 and *Nocardioides aromaticivorans* SB10005 respectively:

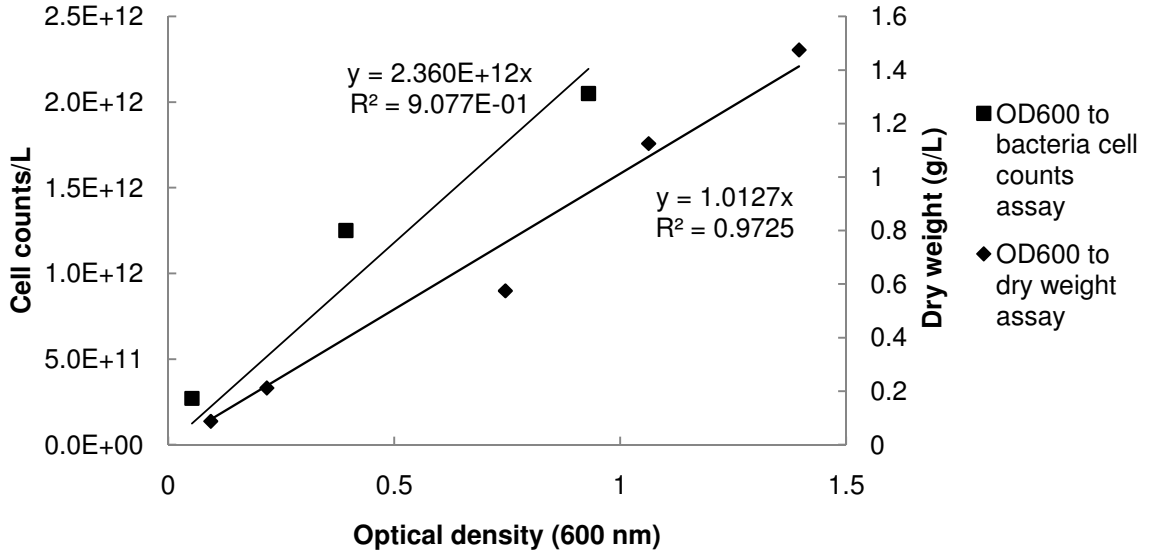

Figure 71: Cell concentration and optical density assay for *Microbacterium chocolatum* RW56

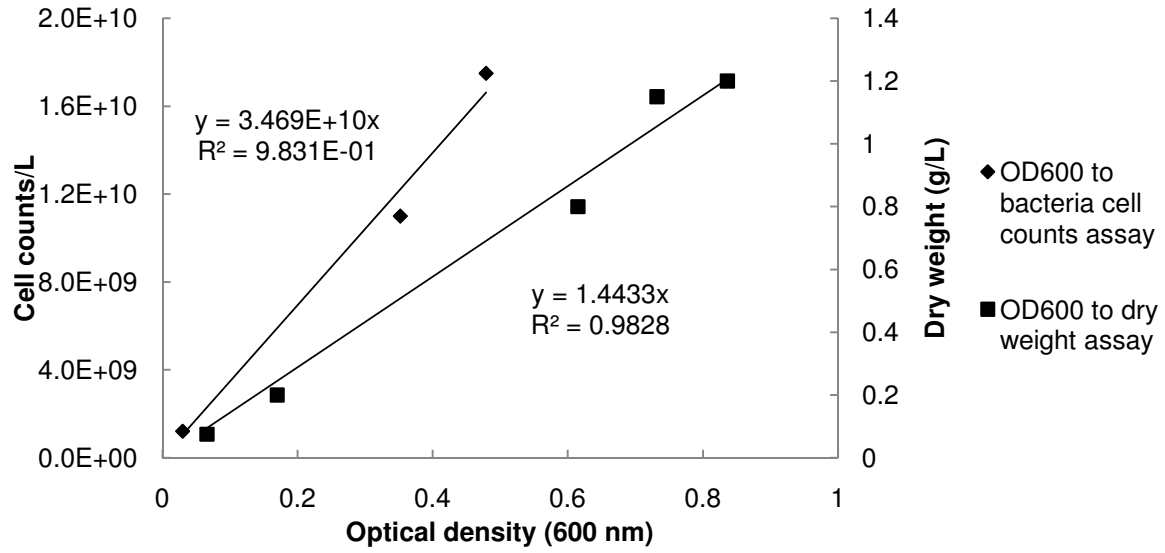

Figure 72: Cell concentration and optical density assay for *Nocardioides aromaticivorans* SB10005

8.6.3 *Algal characterisation*

To determine whether chelation could be proved, relationships between proton concentration, conductivity and biomass productivity within the airlift photobioreactors were investigated in Figure 73.

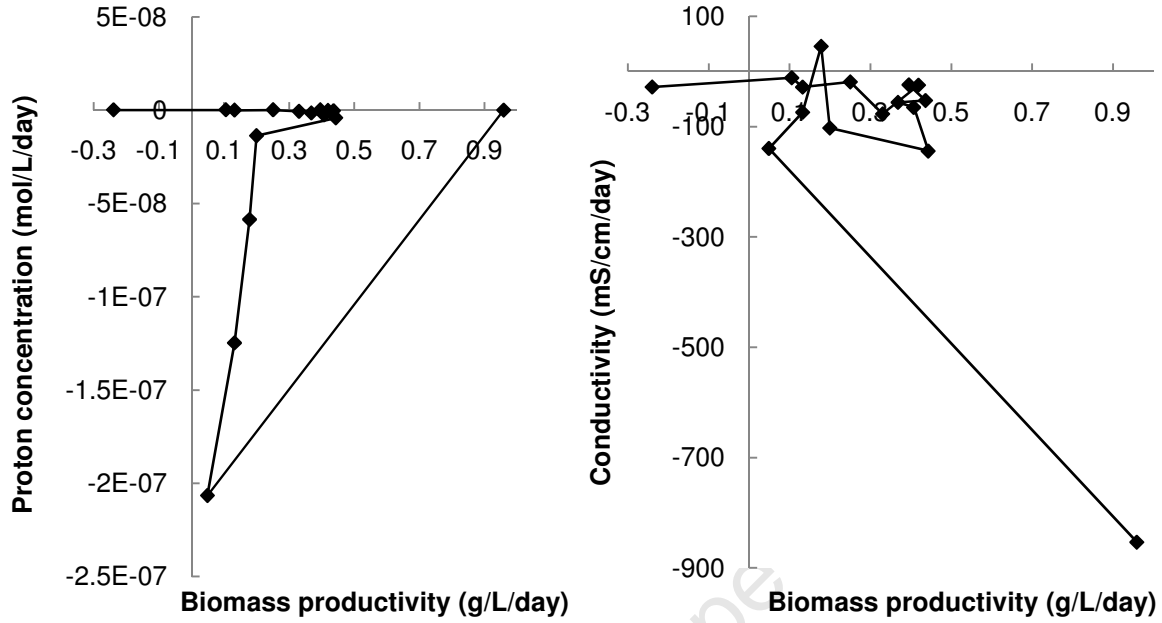

Figure 73: Changes in *Scenedesmus sp*. suspension proton concentration and conductivity as a function of biomass productivity in the airlift photobioreactors sparged with 2 L.min^{-1} 2900 ppm CO_2

The effective particle diameter distributions during growth for *Chlorella vulgaris* and *Scenedesmus sp*. are shown following in Figure 75 and Figure 74 respectively.

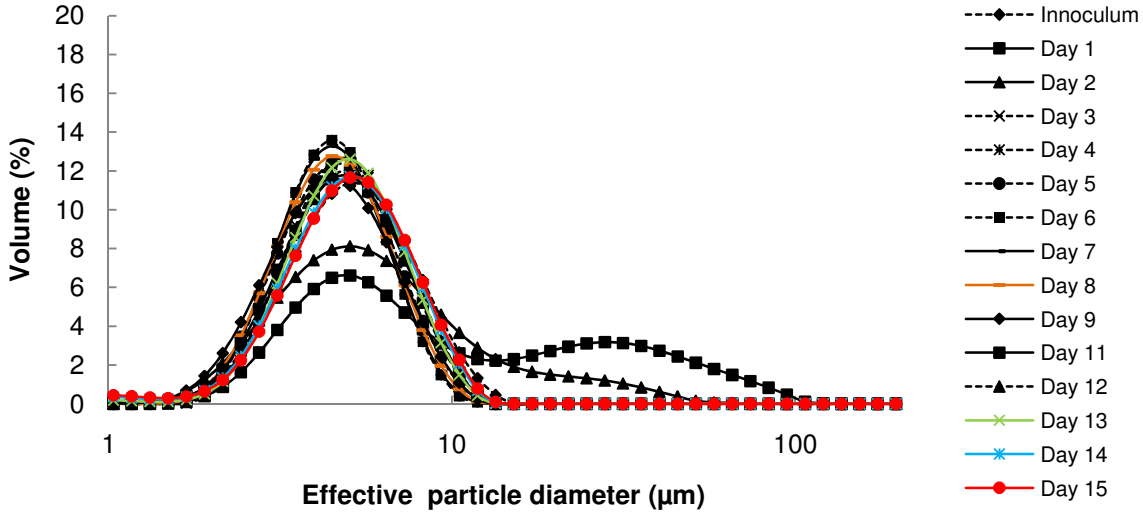

Figure 74: Effective particle diameter distribution during growth for *Scenedesmus sp.*

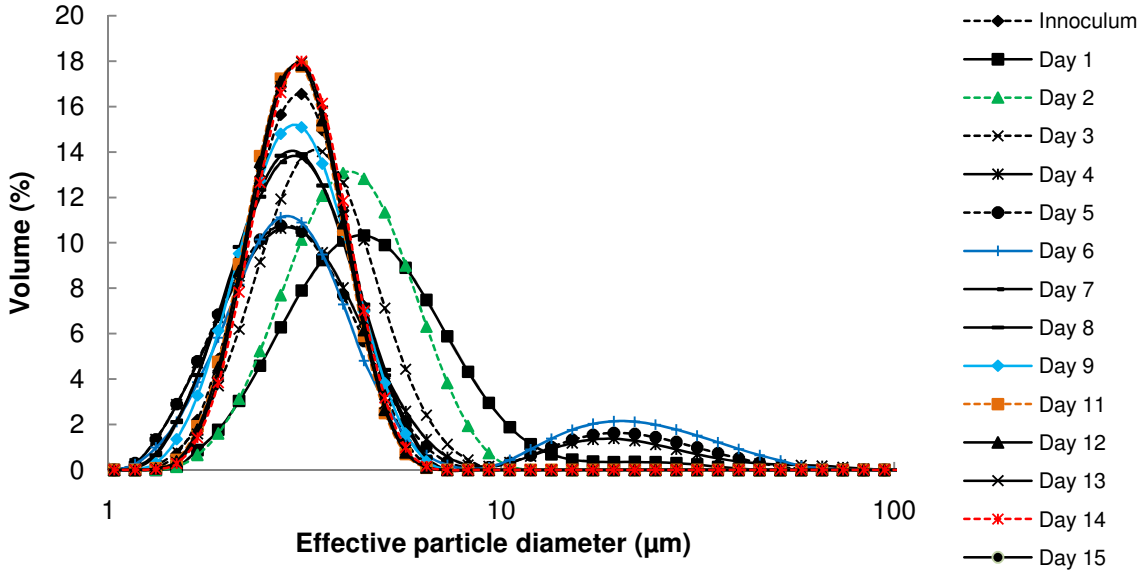

Figure 75: Effective particle diameter distribution during growth for *Chlorella vulgaris*

8.6.4 *Surface properties*

Zetasizer machine measurement inaccuracies with respect to optical density at 750 nm are shown in Figure 76 and the respective relationships for electrophoretic mobility, conductivity and zeta potential for *Scenedesmus sp.* and *Chlorella vulgaris* in Figure 77. The approximate relationship between conductivity and pH is also present in Figure 78.

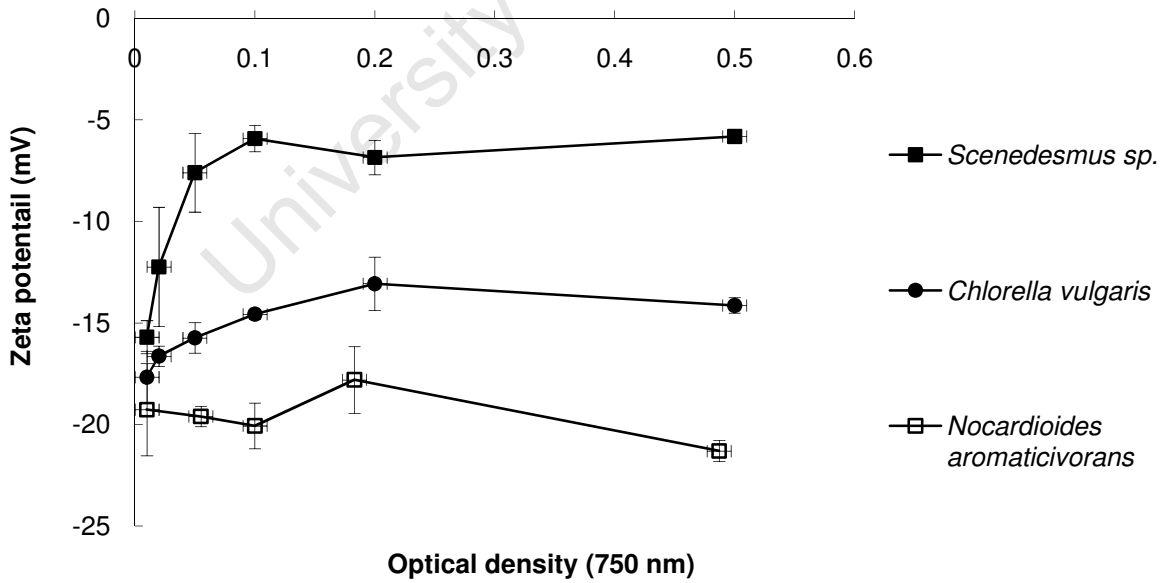

Figure 76: Malvern Zetasizer dependency of zeta potential on concentration for different microorganisms

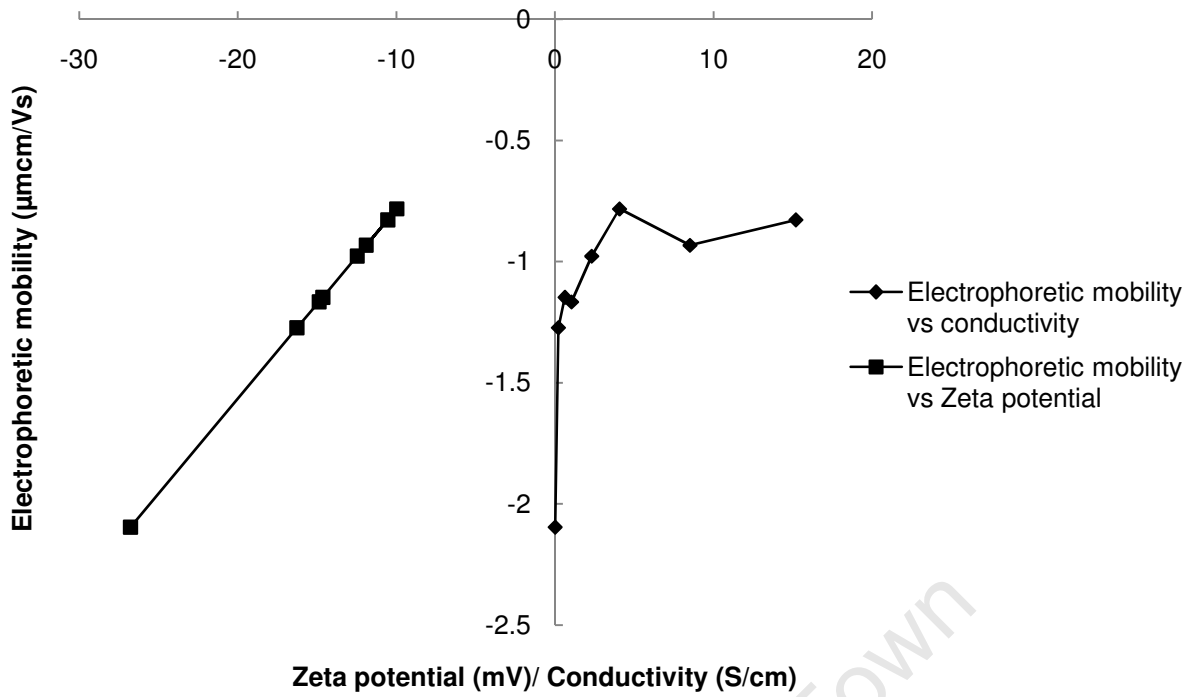

Figure 77: Electrophoretic mobility, conductivity and zeta potential relationships for *Scenedesmus sp.* and *Chlorella vulgaris*

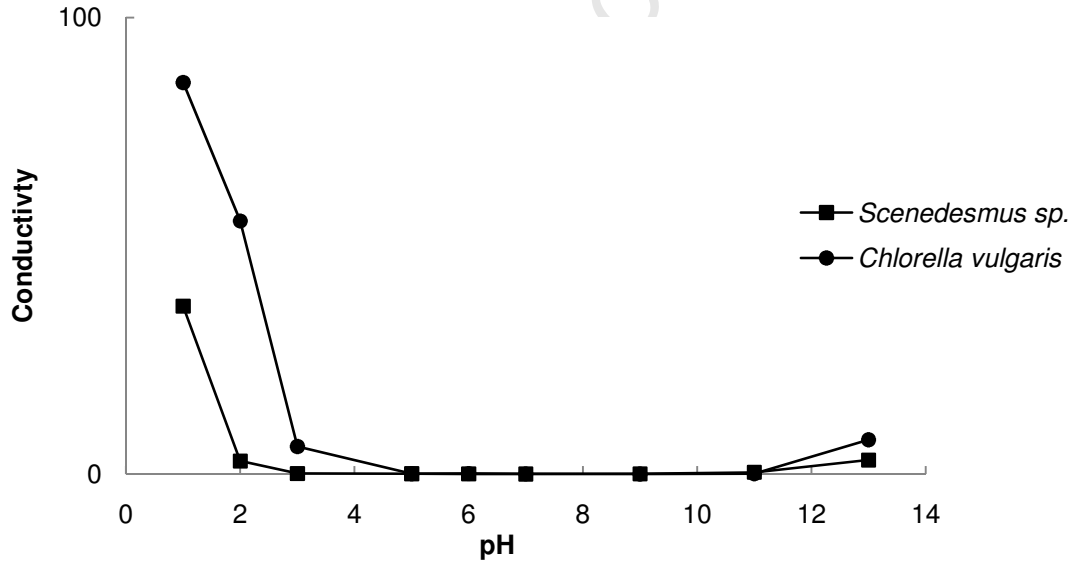

Figure 78: Relationship between pH and ionic strength (conductivity) for *Scenedesmus sp.* and *Chlorella vulgaris*

8.6.5 *Rheology*

Matlab cftool was used to fit curves onto the apparent viscosity data for *Scenedesmus sp.* and *Chlorella vulgaris* and samples of these fits are shown hereafter in Figure 79, Figure 80 and Figure 81.

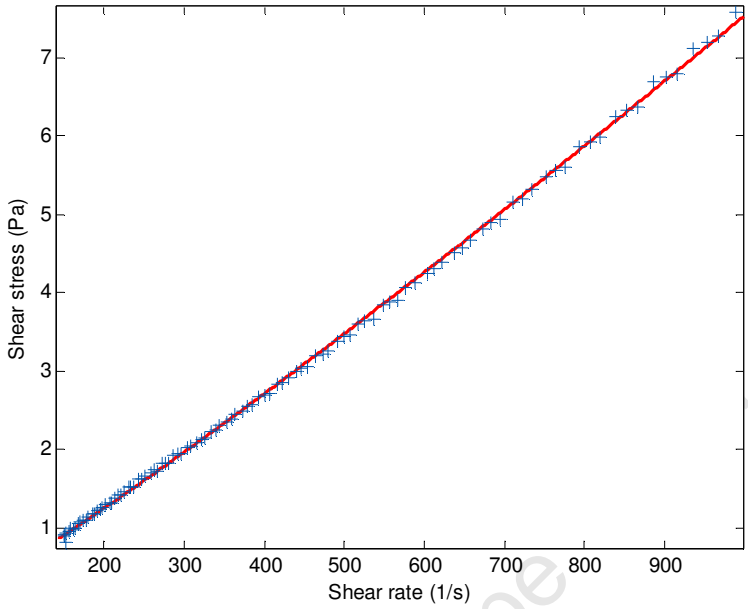

Figure 79: 172.1 g.L^{-1} *Scenedesmus sp.* at 25°C dilatants fit

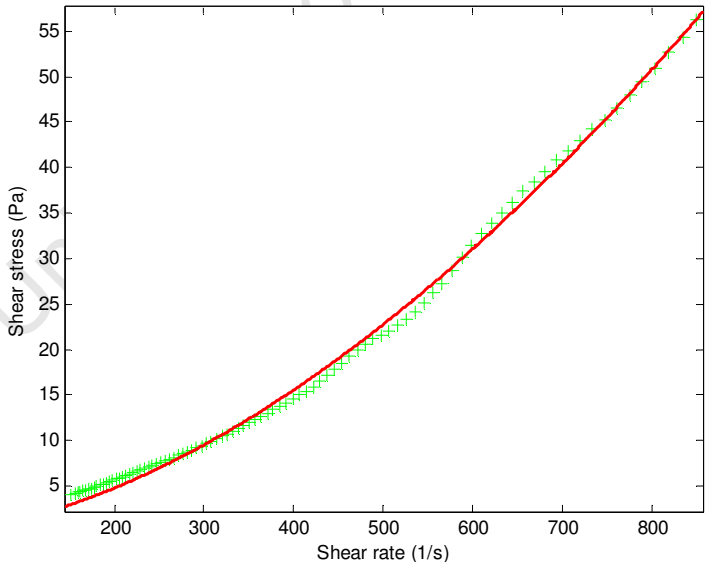

Figure 80: 217.8 g.L^{-1} *Scenedesmus sp.* at 25°C dilatants fit

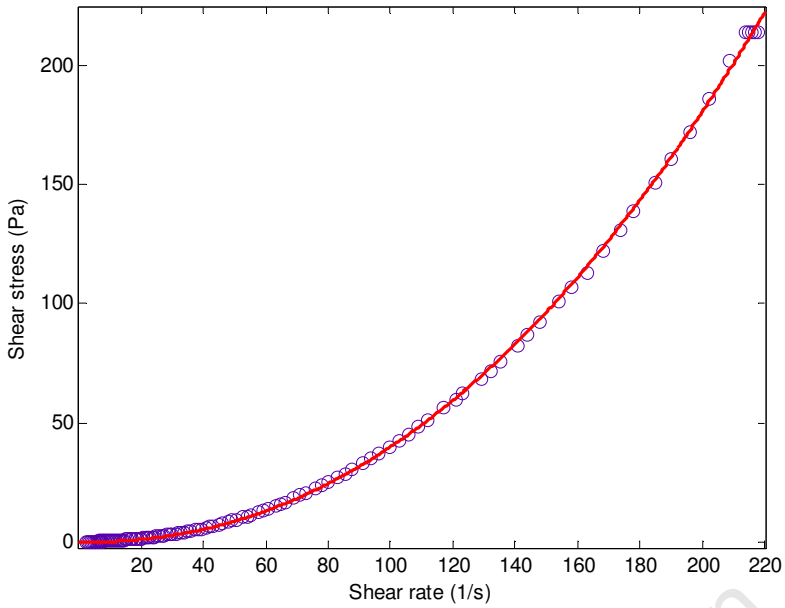

Figure 81: 369.8 g.L^{-1} *Scenedesmus sp.* at 25°C dilatants fit

8.6.6 Flocculation

Due to the nature of spectrophotometric readings the settling results portrayed varying amounts of instability initially depicted by the fluctuations in optical density. Figure 82 shows the repeated runs of *Scenedesmus sp*. autoflocculation.

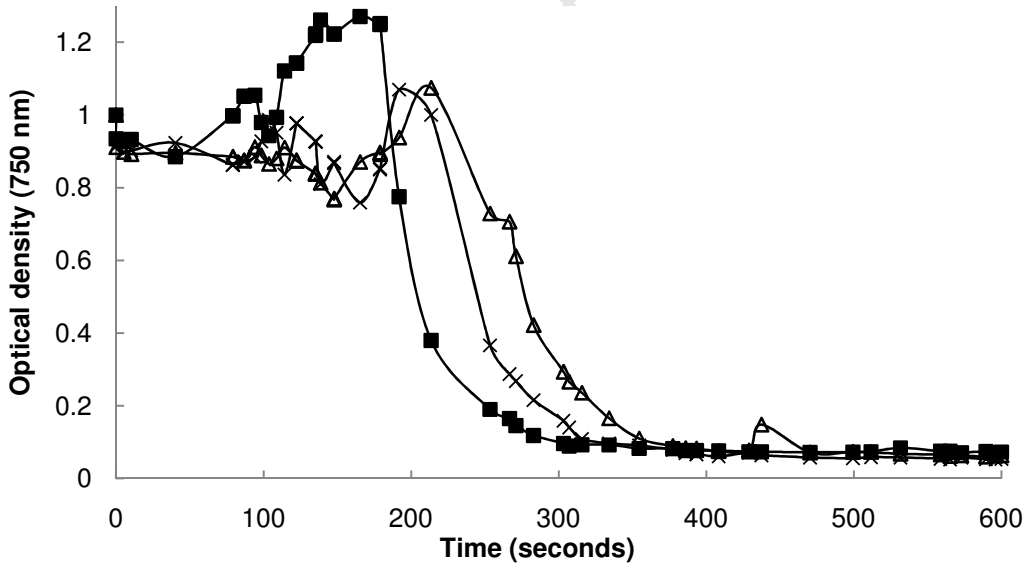

Figure 82: Repeated runs of *Scenedesmus sp*. autoflocculation real time settling from spectrometry at pH 4.6. All samples started at an optical density of 1

Figure 83 and Figure 84 shows the decrease in floc size at different pump speeds for *Chlorella vulgaris* and *Scenedesmus sp*. respectively. The correlation from pump speed to shear stress is seen in Figure 85.

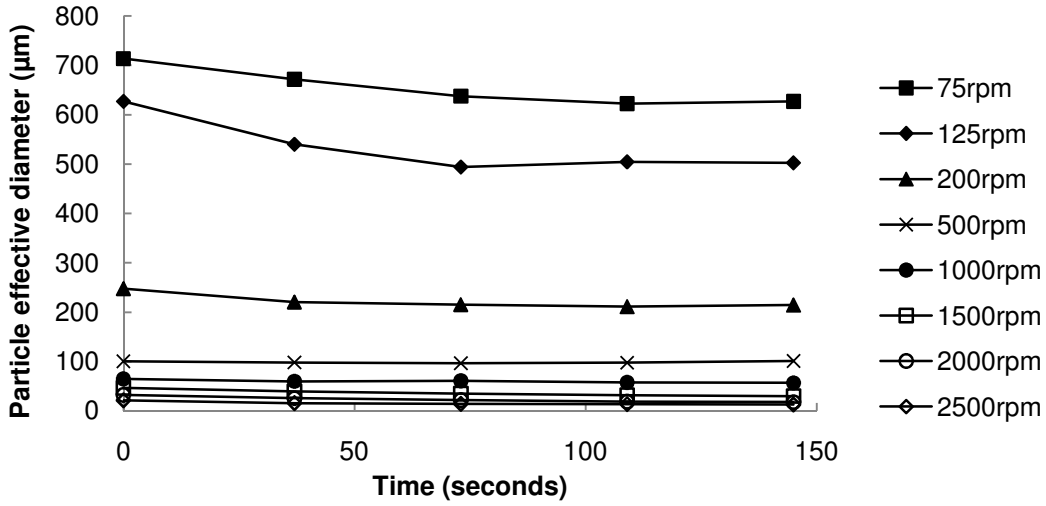

Figure 83: *Chlorella vulgaris* flocculated by 1 g.L^{-1} $MgSO_4$ and constant 30 rpm agitation

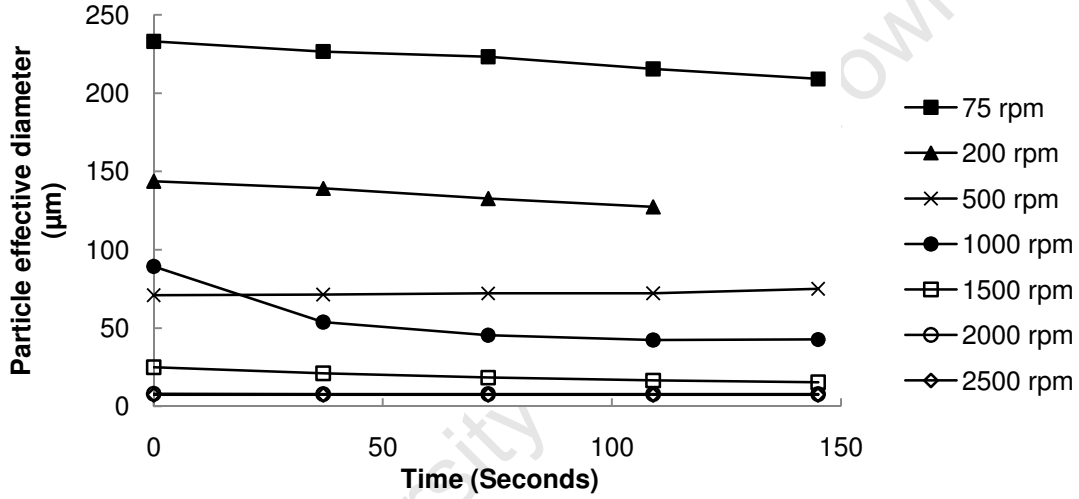

Figure 84: *Scenedesmus sp.* flocculated by 1 g.L^{-1} $MgSO_4$ and constant 30 rpm agitation

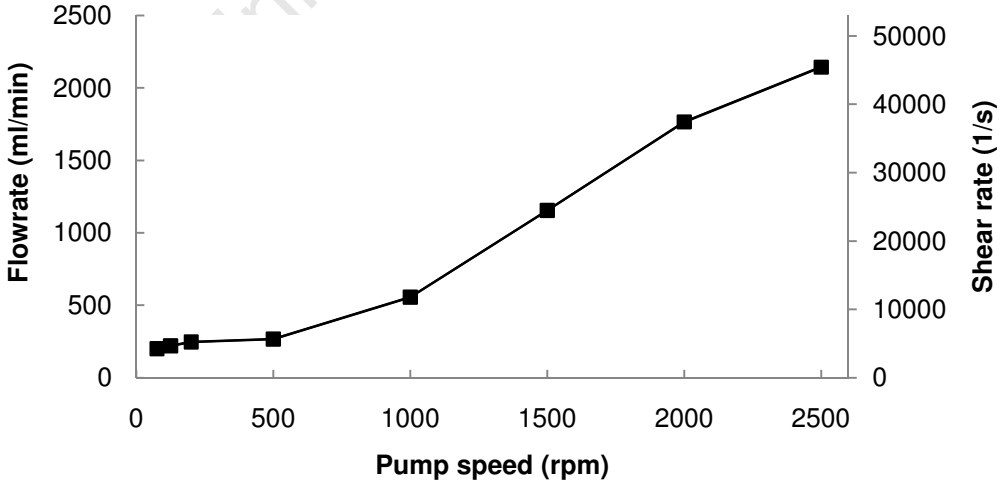

Figure 85: Pump speed correlation to shear stress at 1 cm diameter for the Malvern Hydro 2000G mastersizer instrument

EBE Faculty: Assessment of Ethics in Research Projects

Any person planning to undertake research in the Faculty of Engineering and the Built Environment at the University of Cape Town is required to complete this form before collecting or analysing data. When completed it should be submitted to the supervisor (where applicable) and from there to the Head of Department. If any of the questions below have been answered YES, and the applicant is NOT a fourth year student, the Head should forward this form for approval by the Faculty EIR committee: submit to Ms Zulpha Geyer (Zulpha.Geyer@uct.ac.za; Chem Eng Building, Ph 021 650 4791). Students must include a copy of the completed form with the thesis when it is submitted for examination.

Name of Principal Researcher/Student: REAY DICKS Department: CHEMICAL ENGINEERING

If a Student: Degree: MSc Supervisor: PROF. SUE HARRISON

If a Research Contract indicate source of funding/sponsorship: DST/NRF

Research Project Title: MICROALGAE FLOCCULATION AND SEDIMENTATION BY PHYSICO-CHEMICAL PROPERTY EXPLOITATION

Overview of ethics issues in your research project:

Question 1: Is there a possibility that your research could cause harm to a third party (i.e. a person not involved in your project)?	YES	(NO)
Question 2: Is your research making use of human subjects as sources of data? If your answer is YES, please complete Addendum 2.	YES	(NO)
Question 3: Does your research involve the participation of or provision of services to communities? If your answer is YES, please complete Addendum 3.	YES	(NO)
Question 4: If your research is sponsored, is there any potential for conflicts of interest? If your answer is YES, please complete Addendum 4.	YES	(NO)

If you have answered YES to any of the above questions, please append a copy of your research proposal, as well as any interview schedules or questionnaires (Addendum 1) and please complete further addenda as appropriate.

I hereby undertake to carry out my research in such a way that

- there is no apparent legal objection to the nature or the method of research; and
- the research will not compromise staff or students or the other responsibilities of the University;
- the stated objective will be achieved, and the findings will have a high degree of validity;
- limitations and alternative interpretations will be considered;
- the findings could be subject to peer review and publicly available; and
- I will comply with the conventions of copyright and avoid any practice that would constitute plagiarism.

Signed by:

	Full name and signature	Date
Principal Researcher/Student:	Signed by candidate	3/3/2010

This application is approved by:

Supervisor (if applicable):	Signed by candidate	4/3/2010
HOD (or delegated nominee): Final authority for all assessments with NO to all questions and for all undergraduate research.	Signed by candidate	05/03/2010
Chair : Faculty EIR Committee For applicants other than undergraduate students who have answered YES to any of the above questions.		